The spectral problem of spin chains in $\mathcal{N} = 2$ quiver gauge theories

by
Randle Rabe

Submitted in partial fulfillment of the requirements for the
degree of
Doctor of Philosophy

IN THE FACULTY OF NATURAL & AGRICULTURAL SCIENCES
UNIVERSITY OF PRETORIA
Pretoria

2021
December

Randle Rabe
ORCID: 0000-0001-5292-8896

Dedicated to my parents,
Shawn and Petro

DECLARATION

I, Randle Rabe declare that the thesis, which I hereby submit for the degree *Doctor of Philosophy* at the University of Pretoria, is my own work and has not previously been submitted by me for a degree at this or any other tertiary institution.

Signature: .....

Date: .....

ACKNOWLEDGEMENTS

First and foremost, I would like to express my deepest gratitude to my supervisor, Professor Konstantinos Zoubos. In particular, I have benefited greatly from his deep knowledge and experience in this research area. Additionally, I also thank him for his patience when explaining difficult aspects of the project, as well as always being willing to help in supporting me for bursaries and attending conferences/workshops, where I have had the opportunity to meet many amazing people from the integrability community.

Secondly, I also wish to express much gratitude to Dr. Elli Pomoni, who often felt like a second supervisor during this project. I thank her for many useful discussions and explanations to my questions and ideas.

I also acknowledge the generous funding support from the National Institute of Theoretical Physics (NITheP), now called the National Institute for Theoretical and Computational Sciences (NITheCS), and their exciting bursary/associate workshops at the Stellenbosch Institute for Advanced Studies (STIAS). In addition, I also acknowledge the generous funding support from the University of Pretoria.

Finally, I would like to express gratitude to my family (in particular, Shawn & Petro Rabe, Johan & Ina Kruger, Petrus & Elana Treurnicht) and friends (in particular, Franz & Maresia Bruwer, Towan Nothling, Joshua Botha, Yannick Mvondo-She, Hector Dlamini, Mathys Snyman, Willem Barnard, Prof. Rocco Duvenhage) who have supported me during this degree.

Most notably, I wish to express the highest gratitude to my wife, Irma Rabe, who has been incredibly patient and supportive during this entire journey. Without her, the many late nights and weekends working would have been much more difficult. I am truly fortunate to have someone like her by my side.

ABSTRACT

We investigate the spectral problem of spin chain models in a family of $4D$ $\mathcal{N} = 2$ superconformal quiver gauge theories, constructed as an orbifold of $\mathcal{N} = 4$ super Yang-Mills theory, in the planar limit. We consider two scalar subsectors, namely, the dense XY sector (constructed out of scalar fields in the bifundamental representation of the gauge groups) and the dilute XZ sector (constructed out of scalar fields in the bifundamental and adjoint representations of the gauge groups). At one-loop level, we show that the XY sector can be mapped to an alternating-bond spin chain model and that the XZ sector can be mapped to a dynamical Temperley-Lieb spin chain model. Using the coordinate Bethe ansatz and techniques from alternating-bond spin chains, we are able to solve the eigenvalue problem for both sectors up to the two magnon level by enhancing the usual Bethe wavefunctions with an extra set of momenta that is not a permutation of the original set of momenta. Thus, the two magnon sector already exhibits diffractive scattering. The solutions exhibit rich physics and properties, such as two scattering matrices and a ratio function, which we study in detail. The dispersion relation, which is shared by both scalar subsectors, can be naturally parametrised using elliptic functions. Finally, given our solution for the two magnon problem, we discuss the challenges that arise in attempting to extend the construction of the wavefunctions to the three magnon problem, as well as the notion of quantum integrability within our scalar subsectors.

PUBLISHED CONTENT AND CONTRIBUTIONS

[1] E. Pomoni, R. Rabe, and K. Zoubos. "Dynamical spin chains in 4D $\mathcal{N} = 2$ SCFTs". In: *Journal of High Energy Physics* 2021.8 (Aug. 2021), p. 127. ISSN: 1029-8479. DOI: 10.1007/JHEP08(2021)127. arXiv: 2106.08449 [hep-th].

TABLE OF CONTENTS

LIST OF ILLUSTRATIONS

LIST OF TABLES

Chapter 1

INTRODUCTION

Superconformal gauge theories are marvellous theoretical laboratories to study different aspects of gauge theories. Due to the high amount of symmetry present in these theories, they admit exact computations which may not be achievable in less symmetric theories such as quantum chromodynamics (QCD).

The canonical example of a superconformal gauge theory is the non-abelian maximally symmetric $\mathcal{N} = 4$ super Yang-Mills theory (SYM) in flat $4D$ spacetime with gauge group $U(N)$ and Yang-Mills coupling g_{YM}. The theory shows many remarkable properties such as a vanishing beta function $\beta(g_{YM})$ to all loop orders, which means its conformal symmetry is not broken by anomalous effects (equivalently, it has a zero conformal anomaly to all loop orders) [1, 2, 3]. In addition, in the planar limit where $N \to \infty$ and the 't Hooft coupling $\lambda = g_{YM}^2 N$ is kept fixed, it is the dual theory to Type IIb string theory on an $AdS_5 \times S^5$ background. This is an example of the celebrated AdS/CFT correspondence [4]. However, for this thesis, its most important feature is the fact that it is integrable in the planar limit since its dilatation operator can be mapped to an integrable spin chain Hamiltonian with spin chain states corresponding to single trace operators. This was discovered for a small $\mathfrak{su}(2) \subset \mathfrak{su}(4)_R$ closed scalar subsector of the R-symmetry at one-loop order, where the dilatation operator was mapped to the integrable ferromagnetic Heisenberg model [5], and with the full one-loop Hamiltonian being determined in [6]. The details of this theory have been studied in great detail to higher loops using spin chain techniques such as the coordinate Bethe ansatz, algebraic Bethe ansatz, and the nested algebraic Bethe ansatz [7]. We note that the higher loop dispersion relation is given by [8, 9, 10, 11]

$$E(p) = \sqrt{1 + 4g_{YM}^2 \sin^2(\frac{p}{2})}, \tag{1.1}$$

which, as we will see, has a resemblance to the one-loop dispersion relation that we find in this thesis.

In terms of the amount of symmetry present in the theory, however, $\mathcal{N} = 4$ SYM is an unrealistic theory compared to experimentally-tested gauge theories such as QCD. It is therefore of physical interest to try to study less supersymmetric theories. From

a practical point of view, it is highly favourable to approach this in a systematic and controlled manner. More precisely, we would like to reduce the amount of supersymmetry in the theory but keep other useful symmetries intact, such as conformal symmetry. Such theories can be elegantly constructed using an orbifold construction. On the gravity side of the correspondence, given by Type IIb string theory, the $R-$symmetry of $\mathcal{N} = 4$ SYM is matched with the isometry group $SO(6) \sim SU(4)_R$ of the 5-sphere S^5, which is generated by 16 supergenerators. One can remove some of the supergenerators by forming an orbifold space. The construction, outlined in [12, 13, 14, 15, 16], is achieved by acting non-freely with a discrete abelian subgroup $\Gamma \subset SO(6)$ on the S^5 manifold. There is also a corresponding action on the Chan-Paton indices that label the N stack of $D3-$branes. This deforms S^5 into an orbifold space where all points in the orbit, generated by the discrete group Γ, are identified. Points invariant under Γ become singular points (and therefore, S^5/Γ is no longer a topological space). The AdS_5 space is left untouched thus its isometry group, the conformal group $SO(4, 2)$, is left intact. The resulting orbifold theory is given by $AdS_5 \times S^5/\Gamma$ with a quiver gauge group.

In this thesis, focusing on the gauge theory side, we will consider the simplest orbifold theory which is determined by $\Gamma = \mathbb{Z}_2$ [1]. The resulting supersymmetry is reduced from $\mathcal{N} = 4$ to $\mathcal{N} = 2$ (in other words, 8 of the 16 supergenerators survive the orbifold construction) and the gauge group is given by a $\mathbb{Z}_2$ quiver product of gauge groups. Consequently for the field content, one finds fields that are either in the adjoint representation of one of the two gauge groups or fields that are in the bifundamental representation of each gauge group. There is also an overall $SU(2)_L$ flavour symmetry left over from the construction. Furthermore, we also obtain a family of one-parameter $\mathcal{N} = 2$ superconformal theories specified by a parameter $\kappa = g_2/g_1$ where $g_i,\ i = 1, 2$, are the two gauge couplings of the $\mathcal{N} = 2$ quiver theory. We can vary this parameter to marginally deform the theory away from the orbifold point $\kappa = 1$, keeping the conformal symmetry intact. In this thesis, we will study these family of theories by using spin chain models and techniques.

The orbifold point $\kappa = 1$, where the $\mathcal{N} = 2$ quiver theory is undeformed, has been studied using the algebraic Bethe ansatz [14] (see also [13][12][17]). In particular, one can again use a spin chain picture by mapping the dilatation operator to a spin chain model but with the addition of the orbifold twist appearing as an extra

[1] As standard in the literature, we will also refer to the gauge theory side as an orbifold theory, even though we technically use an algebra quotient to reduce the supersymmetry from $\mathcal{N} = 4$ to $\mathcal{N} = 2$.

excitation. The spin chain model is the Heisenberg ferromagnetic model, similar to the $\mathcal{N} = 4$ case and, therefore, the theory remains integrable after performing the orbifold. On the other hand, the limit $\kappa \to 0$ in a small scalar subsector, consisting of scalar fields from the $\mathcal{N} = 2$ vector multiplet in the adjoint and scalar fields from the $\mathcal{N} = 2$ hypermultiplet in the bifundamental of the theory, has also been studied [18] [2]. Unlike the closed $\mathfrak{su}(2)$ subsector studied in the $\mathcal{N} = 4$ SYM case, there is no R-symmetry that rotates the scalar fields from the two $\mathcal{N} = 2$ multiplets into each other since they are in different representations of the gauge groups of the quiver theory. In this limit, one of the gauge groups decouples from the theory and the remaining field content matches that of $\mathcal{N} = 2$ superconformal QCD (SCQCD) with fields transforming in the fundamental of the remaining gauge group. The uncoupled gauge group becomes a global symmetry of the theory, combined with the $SU(2)_L$ flavour symmetry from the orbifold construction. Using the coordinate Bethe ansatz and checking the Yang-Baxter equation, one can show that $\mathcal{N} = 2$ SCQCD is integrable in the mentioned scalar subsector.

Fascinatingly, for the interpolating theory $\kappa \in (0, 1)$, the S-matrix in the same scalar subsector violates the Yang-Baxter equation and would, therefore, not be expected to be integrable [18]. In particular, using the coordinate Bethe ansatz, one finds two XXZ spin chains that are $\mathbb{Z}_2$ conjugate but mix with each other due to constraints imposed by the gauge indices. This leads to two $\mathbb{Z}_2$ conjugate $S-$matrices that, together, do not satisfy the Yang-Baxter equation for the interpolating theory. However, integrability is a subtle concept in quantum mechanics [20] and is not yet as well defined as its classical counterpart. Apart from the usual Yang-Baxter equation tested by [18], there are more exotic versions such as the quasi-Hopf version of the quantum Yang-Baxter equation [21, 22, 23] or the dynamical Yang-Baxter equation [24, 25] realized through elliptic quantum groups [3].

For this thesis, our motivation is to continue and expand on the study of the scalar sector of [18] using spin chain models and techniques. We will use the coordinate Bethe ansatz to solve two closed scalar subsectors up to the two magnon level. Despite working at first loop order, we find the dispersion relation

$$E(p;\kappa) = \frac{1}{\kappa} + \kappa \pm \frac{1}{\kappa}\sqrt{(1+\kappa^2)^2 - 4\kappa^2 \sin^2 p}, \tag{1.2}$$

[2] The full Hamiltonian in the flavour-singlet sector was determined in [19].

[3] It is also worth noting that there is always an integrable $SU(2,1|2)$ sector inherited by the daughter $\mathcal{N} = 2$ theories from the $\mathcal{N} = 4$ mother theory [26].

which, due to the square root, bears resemblance to the higher loop dispersion relation given in equation (1.1). We will show that the two magnon problem for both sectors can be solved using techniques from alternating-bond spin chains. This is achieved by enhancing the usual Bethe ansatz with an extra set of momenta, and its permutation, that is generically complex-valued. The resulting two magnon wavefunctions for each of our sectors, which are characterised by a ratio function, have rich properties. Due to the extra set of momenta, we find two S-matrices for two different scattering channels. We study these S-matrices and their properties in detail. Finally, we will provide some comments about the technical difficulties in constructing the three magnon wavefunctions and the question of quantum integrability for our sectors. There is convincing evidence that the interpolating theory has a deformed symmetry algebra that is realized by an elliptic quantum group [27] and a dynamical Yang-Baxter equation. In this regard, the results in this thesis may help to illuminate the construction of an elliptic R-matrix using the algebraic Bethe ansatz.

Furthermore, we hope that the program started in this thesis work may ultimately lead to deeper insights to $\mathcal{N} = 2$ SCFTs as a whole. There are still interesting open questions regarding $\mathcal{N} = 2$ theories. For example, the classification or landscape of possible $\mathcal{N} = 2$ theories has been broadened due to the discovery of $\mathcal{N} = 2$ theories with no lagrangian description [28] such as the T_n trinion theories [29, 30] and Argyres-Douglas theories [31].

The outline for this thesis is as follows:

In Chapter 2 we discuss the background theory which supports the later results chapters. We start by discussing the relevant $\mathcal{N} = 2$ and $\mathcal{N} = 4$ supermultiplets in Section 2.1.1 and their shortening conditions. The superconformal algebra is stated in Appendix A. In Section 2.2, we setup our spin chain formalism. We demonstrate the formalism on two spin chain models given by the integrable Heisenberg ferromagnetic spin chain and the non-integrable spin-1 model that exhibits diffractive scattering. These examples also allows us to demonstrate the coordinate Bethe ansatz technique first used in [32]. We conclude the spin chain section by discussing the alternating-bond/alternating-spin model. Then, in Section 2.3, we derive the one-loop dilatation operator for $\mathcal{N} = 4$ SYM in the scalar sector of the theory. Looking at a small closed subsector, we argue that it can be mapped to the integrable Heisenberg spin chain model. Finally, in Section 2.4, we construct the $\mathcal{N} = 2$ quiver gauge theory and derive its one-loop planar dilatation operator in a

scalar subsector. More precisely, we argue the $\mathcal{N} = 2$ one-loop Hamiltonian in the "upstairs" $\mathcal{N} = 4$ picture for our scalar sectors and, in Appendix B, we derive the form for the scalar Hamiltonian in the "downstairs" $\mathcal{N} = 2$ picture. In Appendix B, we show that the two pictures are in agreement with each other. Finally, we discuss a useful notation for the Hamiltonian which makes use of a dynamical parameter in Section 2.4.3.

In Chapters 3 and 4, we study two closed scalar subsectors which we call the dense XY sector and the dilute XZ sector, respectively. In Section 3.1, we solve the one magnon problem for the XY sector. In Section 3.2, we solve the two magnon problem. We first solve it for the special centre-of-mass (CoM) case using contact terms. Next, we solve the two magnon problem in general using alternating-bond spin chain techniques. Using the dispersion relation, we show that there exists an extra set of momenta that needs to be added to the Bethe wavefunctions to solve the two magnon problem. In Appendix C, we study the two magnon continuum by deriving the boundaries of the continua. We next discuss the effects of boundary conditions for an infinite length spin chain or the CoM case which leads us to the restricted solution. It turns out that this restricted solution is the one which is most appropriate for taking the CoM limit. We discuss this limit, including the subtleties that arise, and show how the contact terms of the CoM solution are recovered from the restricted solution. Finally, in Section 3.3, we formulate the Bethe ansatz for a closed spin chain for the XY sector in both the twisted and the untwisted case.

Despite having different Hamiltonians, the XY sector and XZ sector share the same dispersion relation. Thus, the procedure described above is also used for the dilute XZ sector and the overall features of the solutions is therefore very similar. The one magnon case is solved in Section 4.1 and the two magnon case is solved in Section 4.2. The Bethe ansatz for a closed spin chain for the XZ sector is stated in Section 4.3.

In Chapter 5, we argue that the dispersion relation and the ratio functions, computed for each sector, can be naturally parametrised using elliptic functions. We show an interesting relation for the two ratio functions which can be related by a modular transformation. In Chapter 6, we discuss some of the technical details towards constructing the three magnon wavefunctions. We also discuss the notion of quantum integrability for our scalar subsectors based on the two magnon data.

Finally, in Chapter 7, we provide our conclusion based on the results for this thesis.

Chapter 2

THEORY

In this chapter, we will develop the theory that supports the later results sections of this thesis.

2.1 Supersymmetry

In this section, we describe the relevant supermultiplets for the $\mathcal{N} = 2$ and $\mathcal{N} = 4$ cases. Following [33, 28, 34, 18], we will describe the BPS (shortening) conditions imposed on the highest weight states and the unitarity constraints on the conformal dimension Δ. In Section 2.3 and Section 2.4, we will give explicit examples of single trace operators that are part of the short supermultiplets. Using the BPS and unitarity conditions, we can then identify spin chain vacua which will be used in the results section of this thesis.

Following [33], the full $\mathcal{N}$-extended superconformal algebra $\mathfrak{su}(2,2|\mathcal{N})$ in 4-dimensions is given in Appendix A. Since we are discussing supermultiplets, the important algebra relations for this section are

$$\begin{aligned}
&\{Q^A_{\ \alpha}, \mathcal{S}_B^{\ \beta}\} = 4\left(\delta^A_{\ B}\left(M_\alpha^{\ \beta} - \frac{1}{2}i\delta_\alpha^{\ \beta}D\right) - \delta_\alpha^{\ \beta}R^A_{\ \beta}\right),\\
&\{Q^A_{\ \alpha}, \bar{\mathcal{S}}^{A\dot{\alpha}}\} = 0, \quad \{\mathcal{S}_A^{\ \alpha}, \bar{Q}_{B\dot{\alpha}}\} = 0,\\
&\left[D, Q^A_{\ \alpha}\right] = \frac{i}{2}Q^A_{\ \alpha}, \quad \left[D, \bar{Q}_{A\dot{\alpha}}\right] = \frac{i}{2}\bar{Q}_{A\dot{\alpha}},\\
&\left[D, \mathcal{S}_A^{\ \alpha}\right] = -\frac{i}{2}\mathcal{S}_A^{\ \alpha}, \quad \left[D, \bar{\mathcal{S}}^{A\dot{\alpha}}\right] = -\frac{i}{2}\bar{\mathcal{S}}^{A\dot{\alpha}}.
\end{aligned} \tag{2.1}$$

Note in particular that the commutators with the generator D imply that the conformal dimension of states in a multiplet get raised (by the supergenerators $Q, \bar{Q}$) or lowered (by the supergenerators $\mathcal{S}, \bar{\mathcal{S}}$) by $1/2$ [28].

2.1.1 Supermultiplets

In this subsection, we describe the relevant supermultiplets and important shortening conditions. We will consider two specific shortening conditions which will be used for constructing the highest weight state (or ground state) of our spin chain picture (see Section 2.4).

A state in a supermultiplet carries the following labels: $|\Delta, [R]\rangle_{(j,\bar{j})}$. The charge

Δ (or the conformal dimension) is the eigenvalue of an operator measured by the dilatation operator D and $(j, \bar{j})$ are the Lorentz charges for $\mathfrak{sl}(2) \oplus \mathfrak{sl}(2)$. The label $[R]$ is the R-symmetry representation and depends on which case we are considering. For the $\mathcal{N} = 2$ case (with R-symmetry given by $\mathfrak{su}(2)_R \oplus \mathfrak{u}(1)_r$), the R-symmetry charge $[R]$ is given by (R, r) where R is the Cartan charge for $\mathfrak{su}(2)_R$ (which can be integer or half-integer valued) and r is the $\mathfrak{u}(1)_r$ charge. For the case $\mathcal{N} = 4$ (with R-symmetry given by $\mathfrak{su}(4)_R$, which is rank 3 and therefore contains three copies of $\mathfrak{sl}(2)$), we will use the Dynkin labels $[q, p, s]$ (which are integer valued [35, 36]) for $[R]$.

The *highest weight state* (also called the *superconformal primary state*) of a supermultiplet will be denoted as $|\Delta, [R]\rangle^{\text{hw}}_{(j,\bar{j})}$. It is the state annihilated by the following generators

$$K^{\dot{\alpha}\alpha}|\Delta, [R]\rangle^{\text{hw}}_{(j,\bar{j})} = 0, \quad \mathcal{S}_A^{\ \alpha}|\Delta, [R]\rangle^{\text{hw}}_{(j,\bar{j})} = 0, \quad \bar{\mathcal{S}}^{A\dot{\alpha}}|\Delta, [R]\rangle^{\text{hw}}_{(j,\bar{j})} = 0, \tag{2.2}$$

for all $A = 1, .., \mathcal{N}$ and $\alpha, \dot{\alpha} = \pm$. Starting with the highest weight state, one may generate the descendant states in the supermultiplet by acting with the supergenerators Q^A_α, $\bar{Q}_{B\dot{\alpha}}$ (see Appendix (A) for their charges). The supermultiplets are generically denoted as $\chi_{[R](j,\bar{j})}$.

As determined in [33] (see also [28, 18]), one may ensure unitary representations by imposing BPS conditions which leads to unitarity constraints in terms of the labels $(\Delta, [R], j, \bar{j})$ for the highest weight state. For the $\mathcal{N} = 2$ case, there are three types of conditions:

- $\mathcal{A}$-type: These are generic long multiplets and with no shortening conditions.
- $\mathcal{B}$-type: These are called 1/4-BPS since $1/4$ of the supercharges annihilate the highest weight state.
- C-type: These are called 1/8-BPS since $1/8$ of the supercharges annihilate the highest weight state.

In addition, one may combine these supermultiplets to obtain 1/2-BPS multiplets. For this thesis, we will only need to consider the $\mathcal{B}$-type supermultiplets as well as their combinations.

$\mathcal{N} = 2$ Shortening conditions

There are two important shortening conditions that we will consider. Following [28, 18, 33], we will consider the $\mathcal{B}$-type BPS condition with $j = 0$ (and $\bar{j} = 0$ for the conjugate case)

- Type $\mathcal{B}^1$: $Q^1{}_\alpha|\Delta, R, r\rangle^{\rm hw}_{(0,\bar{j})} = 0$ $\big($or $\bar{\mathcal{B}}_1$: $\bar{Q}_{1\dot{\alpha}}|\Delta, R, r\rangle^{\rm hw}_{(j,0)} = 0\big)$, $\quad \alpha, \dot{\alpha} = \pm$
- Type $\mathcal{B}^2$: $Q^2{}_\alpha|\Delta, R, r\rangle^{\rm hw}_{(0,\bar{j})} = 0$ $\big($ or $\bar{\mathcal{B}}_2$: $\bar{Q}_{2\dot{\alpha}}|\Delta, R, r\rangle^{\rm hw}_{(j,0)} = 0\big)$, $\quad \alpha, \dot{\alpha} = \pm$

Recall for the $\mathcal{N} = 2$ case, $[R]$ is given by (R, r). As mentioned above, two (out of the eight) generators annihilate the highest weight state and, thus, this condition is 1/4-BPS. This leads to the following unitarity constraints for the highest weight states [33] (conjugation reverses the signs of r and $(j, \bar{j})$)

- For $\mathcal{B}^1, \mathcal{B}^2$: $\Delta = 2R + r$
- For $\bar{\mathcal{B}}_1, \bar{\mathcal{B}}_2$: $\Delta = 2R - r$

Following [33, 28, 18], the supermultiplets are denoted as $\mathcal{B}_{R,r(0,\bar{j})}$ and $\bar{\mathcal{B}}_{R,r(0,\bar{j})}$.

Furthermore, we may combine these short supermultiplets to form 1/2-BPS multiplets. We will consider two types of combinations, namely, the $\mathcal{E}$-type and the $\hat{\mathcal{B}}$-type. In particular, with $R = 0$ and $j = 0$, we have [33, 28, 18]

- Type $\mathcal{E}$ $(\mathcal{B}_1 \cap \mathcal{B}_2)$: $Q^1{}_\alpha|\Delta, 0, r\rangle^{\rm hw}_{(0,\bar{j})} = 0$ and $Q^2{}_\alpha|\Delta, 0, r\rangle^{\rm hw}_{(0,\bar{j})} = 0$

There is also of course the conjugate case $\bar{\mathcal{E}}$ which is the combination of the conditions for $\bar{\mathcal{B}}_1$ and $\bar{\mathcal{B}}_2$. Finally, with $r = 0$ and $j = \bar{j} = 0$, we have the $\hat{\mathcal{B}}$-type case

- Type $\hat{\mathcal{B}}$ $(\mathcal{B}_1 \cap \bar{\mathcal{B}}_2)$: $Q^1{}_\alpha|\Delta, R, 0\rangle^{\rm hw}_{(0,0)} = 0$ and $\bar{Q}_{2\dot{\alpha}}|\Delta, R, 0\rangle^{\rm hw}_{(0,0)} = 0$

Under these conditions, one finds the following unitarity constraints for the highest weight state [33]

- For $\mathcal{E}$: $\Delta = r$ (and $\Delta = -r$ for the conjugate $\bar{\mathcal{E}}$)
- For $\hat{\mathcal{B}}$: $\Delta = 2R$

The corresponding supermultiplets are denoted as $\mathcal{E}_{r(0,\bar{j})}$, $\bar{\mathcal{E}}_{-r(j,0)}$ and $\hat{\mathcal{B}}_R$. These multiplets are special since they are protected by representation theory from recombination [33, 28, 18]. Thus, any operators that belong to these supermultiplets are protected from receiving corrections (or anomalous dimensions) to their conformal dimension Δ. These operators will therefore be candidates for vacua (lowest energy states) when we consider the spin chain formalism later in this thesis (see Section 2.4).

Finally, we mention two special cases for the multiplets $\mathcal{E}_{r(0,\bar{j})}$ (the case for the conjugate is similar) and $\hat{\mathcal{B}}_R$. For $\hat{\mathcal{B}}_R$, we consider the case when $R = 1/2$ which means that $\Delta = 2R = 1$. Using the compact notation $R_{(j,\bar{j})}$ from [33], we can start with the highest weight state $\frac{1}{2}{}_{(0,0)}$ (with $\Delta = 1$) and can act with $Q^2{}_\alpha$ and $\bar{Q}_{1\dot{\alpha}}$ to generate the descendent states (see Appendix A for their charges). Imposing the equations of motion (which sets states with negative contributions to zero, see page 35 of [33]), we find the states given in Figure 2.1. Note that we follow the

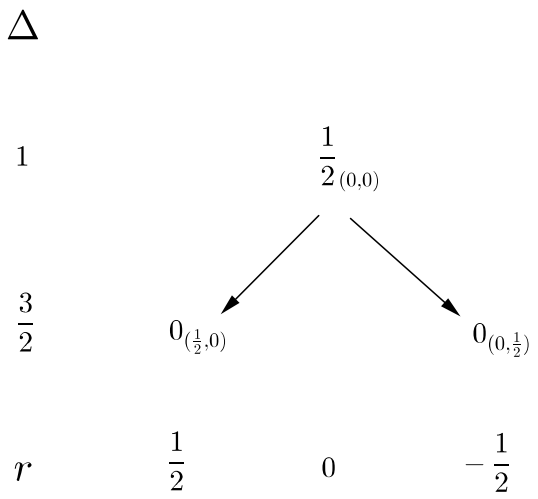

Figure 2.1: *The $\mathcal{N} = 2$ half hypermultiplet contained in the supermultiplet $\hat{\mathcal{B}}_{\frac{1}{2}}$.*

conventions of [33] where a $\swarrow$-arrow indicates the action of Q and a $\searrow$-arrow indicates the action of $\bar{Q}$. This yields the $\mathcal{N} = 2$ half *hypermultiplet* [33, 28, 34]. CPT invariance of this multiplet depends on the choice of gauge group: if the gauge group is $\mathfrak{su}(2)$, then the doublet of scalars transform in a pseudo-real representation (of the R-symmetry algebra and the gauge algebra) and the half hypermultiplet is CPT invariant. For higher rank gauge groups, one must include the CPT conjugate states to construct the full $\mathcal{N} = 2$ hypermultiplet [28, 34]. The full hypermultiplet consists of two Weyl spinors and a $\mathfrak{su}(2)_R$-doublet of complex scalars.

The case $\mathcal{E}_{r(0,0)}$ (with $r = 1, \bar{j} = 0$) gives the $\mathcal{N} = 2$ *vector multiplet* with its equations of motion and an auxiliary field [28] (which contributes null states). After removing these null states, the standard $\mathcal{N} = 2$ vector multiplet is given by $\mathcal{D}_{0(0,0)}$ (see page 20 of [33]). The states are shown in Figure 2.2 where both $\mathcal{D}_{0(0,0)}$ and

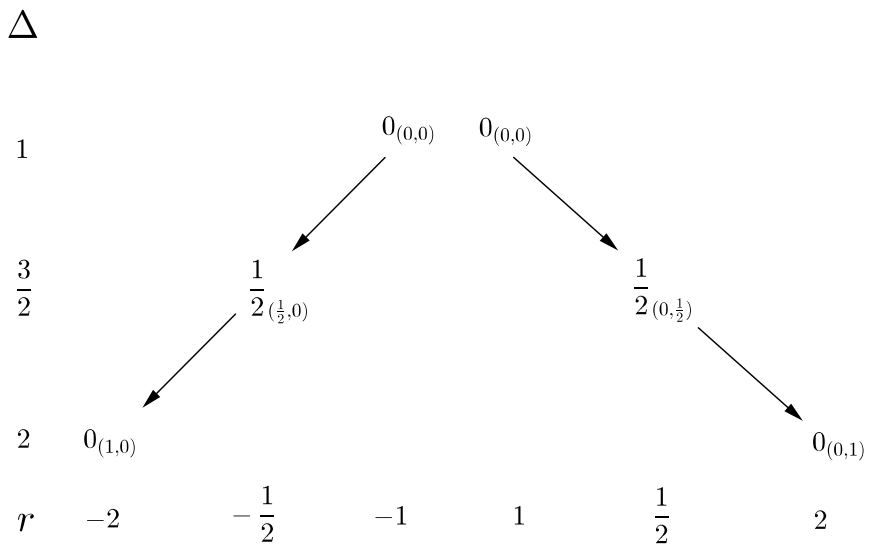

Figure 2.2: *The $\mathcal{N} = 2$ vector multiplet contained in the supermultiplets $\mathcal{D}_{0(0,0)}$ and $\bar{\mathcal{D}}_{0(0,0)}$.*

its conjugate $\bar{\mathcal{D}}_{0(0,0)}$ is shown. The vector multiplet consists of a complex scalar, a doublet of Weyl spinors and a vector gauge field.

$\mathcal{N} = 4$ Shortening Conditions

For the $\mathcal{N} = 4$ case, we only consider one shortening condition. In this case, states and supermultiplets are dressed with the following labels: $\Delta, [q, p, s]$, and $(j, \bar{j})$. The symbols $[q, p, s]$ are the Dynkin labels for the R-symmetry $\mathfrak{su}(4)_R$ (see for example Appendix B in [35]). The other labels are the same as in the $\mathcal{N} = 2$ case.

Following the notation of [33, 28, 18], the 1/2-BPS short supermultiplet that we will consider is $\mathcal{B}^{\frac{1}{2},\frac{1}{2}}_{[0,p,0]}$ with $j = \bar{j} = 0$ (the $\frac{1}{2}, \frac{1}{2}$ labels mean 1/2-BPS). The unitarity constraint for the highest weight state is given by $\Delta = p$. This supermultiplet is also protected from recombination and thus states belonging to this supermultiplet are candidates for spin chain vacua (see Section 2.3).

As in the $\mathcal{N} = 2$ case, we mention a special case given by $\mathcal{B}^{\frac{1}{2},\frac{1}{2}}_{[0,1,0]}$. This is the $\mathcal{N} = 4$ vector multiplet [33, 28]. It consists of one vector gauge field, four Weyl fermions in the **4** of $\mathfrak{su}(4)_R$ and six real scalar fields in the antisymmetric **6** of $\mathfrak{su}(4)_R$ (or the fundamental of $\mathfrak{so}(6)$).

2.2 Spin Chains

In this section, we develop the theory behind spin chain models with an $\mathfrak{su}(2)$ symmetry. In terms of a physical system, a spin chain is quite simple. It has a single spatial dimension which consists of discrete lattice points or sites that is occupied by a particle in a representation of some Lie algebra. Adding a temporal dimension, they are examples of a $(1+1)$-dimensional lattice model. The particles only have internal degrees of freedom and are fixed in space. Interactions are mediated through the coupling of these internal degrees of freedom which, for this thesis, will be the spin of each particle. The strength of the spin coupling (or bond strength) is determined by a constant parameter $J > 0$. The choice of parameter $-J$ leads to ferromagnetic behaviour while J leads to antiferromagnetic behaviour. Furthermore, these interactions can be nearest-neighbour or long range. Finally, one may impose boundary conditions such as periodic conditions (in other words, putting the lattice on a circle) and open boundary conditions. As we will show, despite spin chain models having a relatively simple setup, they are models with rich physics exhibiting excitations, scattering and, sometimes, deep algebraic structures such as integrability to quantum groups (which can arise as deformations of a symmetry given by a Lie algebra).

In this section, we will first develop the theory behind a general ferromagnetic spin-S model by motivating the form for the Hamiltonian. This section will also set the formalism for spin chains. We will then consider two examples to demonstrate the formalism, namely, the isotropic Heisenberg spin-1/2 chain and a spin-1 model. These examples also serve a further purpose: the Heisenberg model can be shown to be quantum integrable. In addition, this model appears in the $\mathfrak{su}(2)$ subsector in planar $\mathcal{N} = 4$ super Yang-Mills theory (see Section 2.3). On the other hand, the spin-1 model is not integrable for general values of the coupling constant but can still be solved up to the three spin deviation case. The form of the three spin deviation wavefunctions bears remarkable similarity to the wavefunctions computed for the $\mathcal{N} = 2$ quiver Hamiltonians in our results section. Finally, we will briefly mention the alternating-spin/alternating-bond chain which is a generalization of the ferromagnetic spin-S model. Our results section will serve as a demonstration of a special case of this model.

2.2.1 Setup

We consider a lattice of L-sites. For this thesis, we will assume that each lattice site hosts a particle in a spin-S representation of $\mathfrak{su}(2)$ where S can be integer or

half-integer valued and $S \geq 1/2$. Then, the local Hilbert space $\mathcal{H}_\ell$ at each site ℓ is spanned by the basis states $\{|S, j\rangle\}$, $j \in \{-S, -S+1, ..., S-1, S\}$ and is $(2S+1)$-dimensional (as will be discussed below, the basis states are eigenvectors of the S^z spin operator). The first label S is the total spin and the second label j is the z-spin projection. If it is clear from the context, we will drop the first label for a spin state and simply write $|j\rangle$. The total Hilbert space of the spin chain is therefore given by a tensor product

$$\mathcal{H} = \bigotimes_{\ell=1}^{L} \mathcal{H}_\ell, \tag{2.3}$$

where $\ell \in \mathbb{Z}$ labels the lattice coordinate. It is clearly $(2S+1)^L$-dimensional.

The observables of the spin chain are given by spin operators. Concretely, let S^i be a representation of the $\mathfrak{su}(2)$ algebra (in what follows, we set $\hbar = 1$) [37]

$$\left[S^i, S^j\right] = i\epsilon^{ijk} S^k, \quad ij, k = \{x, y, z\}, \tag{2.4}$$

where the structure constant ϵ^{ijk} is fixed as $\epsilon^{xyz} = 1$ and is totally antisymmetric. The basis states $\{|j\rangle\}$, $j \in \{-S, -S+1, ..., S-1, S\}$ discussed above are eigenvectors of the spin operator S^z

$$S^z|j\rangle = j|j\rangle, \quad j \in \{-S, -S+1, ..., S-1, S\}. \tag{2.5}$$

For example, the spin-1/2 representation is given by (2×2)-matrices, that can be written in terms of the Pauli matrices $S^i = (1/2)\sigma^i$, and act on a 2-dimensional Hilbert space spanned by basis eigenstates $\{|-1/2\rangle, |1/2\rangle\}$. Furthermore, we can use the Cartan algebra formalism [38] to define raising and lowering operators that will move us between states in the multiplet $\{|j\rangle\}$. This is achieved by complexifying $\mathfrak{su}(2) \to \mathfrak{su}(2)_{\mathbb{C}} \cong \mathfrak{sl}(2)$. More precisely, we define

$$S^\pm := S^x \pm iS^y, \quad (S^\pm)^\dagger = S^\mp, \tag{2.6}$$

which gives the $\mathfrak{sl}(2)$ algebra

$$\left[S^z, S^\pm\right] = \pm S^\pm, \quad \left[S^+, S^-\right] = 2S^z, \quad \left[S^\pm, S^\pm\right] = 0. \tag{2.7}$$

For a state $|j\rangle$, the operators $S^\pm$ shift the eigenstates as follows (see page 79 of [38])

$$S^\pm|j\rangle = \sqrt{S(S+1) - j(j \pm 1)}|j \pm 1\rangle. \tag{2.8}$$

There exist two special states called the *highest weight state*, which is annihilated by S^+, and the *lowest weight state*, which is annihilated by S^- [38]. In our setup, these states are $|j = S\rangle$ and $|j = -S\rangle$, respectively

$$S^+|S\rangle = 0, \quad S^-|-S\rangle = 0. \tag{2.9}$$

Thus, starting from the highest weight state, we can apply the lowering operator 2S-times to find (up to some constant factor depending on the spin representation S of the system - see equation (2.8))

$$(S^-)^{2S}|j = S\rangle \sim |j = -S\rangle. \tag{2.10}$$

To lift the action of these operators to the entire spin chain, we define the lattice spin operator S^i_ℓ

$$S^i_\ell = \underset{1}{\mathbb{1}} \otimes \cdots \otimes \underset{\ell-1}{\mathbb{1}} \otimes \underset{\ell}{S^i} \otimes \underset{\ell+1}{\mathbb{1}} \otimes \cdots \otimes \underset{L}{\mathbb{1}}, \tag{2.11}$$

where the labels underneath indicate the lattice coordinate. In other words, S^i_ℓ acts non-trivially on site ℓ and trivially elsewhere. This is also a representation of the $\mathfrak{su}(2)$ algebra [37]

$$\left[S^i_m, S^j_n\right] = i\delta_{mn}\epsilon^{ijk}S^k, \quad i, j, k = \{x, y, z\}, \tag{2.12}$$

which is said to be *ultralocal* since the operators at different sites commute. In exactly the same manner, we can lift the raising/lowering operators to the full spin chain [37]

$$\left[S^z_m, S^\pm_n\right] = \pm\delta_{mn}S^\pm_n, \quad \left[S^+_m, S^-_n\right] = 2\delta_{mn}S^z_n, \quad \left[S^\pm_m, S^\pm_n\right] = 0. \tag{2.13}$$

Generalised Spin-S Hamiltonian

We are interested in the energy spectrum of the spin chain. The corresponding operator is, of course, the Hamiltonian H. Similar to the discussion in [37], the Hamiltonian will be constructed to be

- isotropic or rotationally invariant: $[S^z, H] = 0$
- homogeneous or translationally invariant
- nearest-neighbour interactions

For the last point, nearest-neighbour interactions are implemented by two sites m, n constrained to $|m - n| = 1$. Thus, our Hamiltonian will be dressed with subscripts $H_{\ell,\ell+1}$. The first point implies that H is a rank-0 tensor or scalar constructed out of the spin operators $\mathbf{S}_\ell = (S^x_\ell, S^y_\ell, S^z_\ell)$; in other words, terms of the form $(\mathbf{S}_\ell \cdot \mathbf{S}_{\ell+1})$

since $[S^z, \mathbf{S}\cdot\mathbf{S}] = 0$. Now, since we are considering generalised spin-S spin chains, the Hamiltonian can be expanded in terms of $(\mathbf{S}_\ell \cdot \mathbf{S}_{\ell+1})$ as a polynomial of degree d

$$H_{\ell,\ell+1} = -J^{(0)} - J^{(1)}(\mathbf{S}_\ell \cdot \mathbf{S}_{\ell+1}) - J^{(2)}(\mathbf{S}_\ell \cdot \mathbf{S}_{\ell+1})^2 - ... - J^{(d)}(\mathbf{S}_\ell \cdot \mathbf{S}_{\ell+1})^d. \quad (2.14)$$

The parameters $J^{(i)},\ i = \{1, ..., d\}$, set the bond strength and, since we only consider the ferromagnetic regime in this thesis, will always be assumed to be $J^{(i)} \geq 0$. The term with the parameter $J^{(0)}$ is the identity operator. Terms proportional to the identity operator only shift the energy eigenvalues and do not affect the physics of the system. We can thus add or subtract these terms as needed. Next, we use the well-known expansion

$$\begin{aligned} \mathbf{S}_\ell \cdot \mathbf{S}_{\ell+1} &= S^x_\ell S^x_{\ell+1} + S^y_\ell S^y_{\ell+1} + S^z_\ell S^z_{\ell+1} \\ &= S^z_\ell S^z_{\ell+1} + \frac{1}{2}\left(S^+_\ell S^-_{\ell+1} + S^-_\ell S^+_{\ell+1}\right). \end{aligned} \quad (2.15)$$

From equation (2.10), for a highest weight state say, we can act up to $d = 2S$ after which all terms $d > 2S$ in the expansion acting on a state $|j\rangle$ vanishes (see also [39] and page 84 of [40]). Therefore,

$$H_{\ell,\ell+1} = -\sum_{p=1}^{2S} J^{(p)}(\mathbf{S}_\ell \cdot \mathbf{S}_{\ell+1})^p. \quad (2.16)$$

The total Hamiltonian is therefore given by

$$\begin{aligned} H &= \sum_{\ell=1}^{L} H_{\ell,\ell+1} \\ &= -\sum_{\ell=1}^{L}\sum_{p=1}^{2S} J^{(p)}(\mathbf{S}_\ell \cdot \mathbf{S}_{\ell+1})^p. \end{aligned} \quad (2.17)$$

Finally, to implement translational invariance, let $U = \exp(iT)$ be the unitary hermitian operator that shifts each site of the chain by one site ℓ to $\ell - 1$. Lattice translations are generated by the momentum operator T with eigenvalue $K \in \mathbb{R}$, which is the total momentum (for U, the eigenvalue is exp(iK)). Translational invariance of the Hamiltonian is then implemented by [37, 40]

$$[U, H] = 0. \quad (2.18)$$

If the spin chain is periodic, then the total momentum is quantised since $U^L = 1 \implies K \in 2\pi c/L$ where $c \in \{0, 1, ..., L-1\}$ (see the example of the Heisenberg ferromagnetic model in Section 2.2.2) and

$$H = -\sum_{\ell=1}^{L}\sum_{p=1}^{2S} J^{(p)}(\mathbf{S}_\ell \cdot \mathbf{S}_{\ell+1})^p, \quad S_{\ell+L} = S_\ell. \quad (2.19)$$

In Section 2.2.4, we will generalize the above Hamiltonian further to include alternating-bonds and alternating-spins.

Spin Chain States

For the ground state of the model, we use the highest weight state. Physically, we take this to be the state with all particle spins aligned with the positive z-axis. More precisely, for general spin-S, the ground state is the state with all j set to $j = S$

$$|0\rangle = |S\rangle_1 \otimes |S\rangle_2 \otimes \cdots \otimes |S\rangle_\ell \otimes \cdots \otimes |S\rangle_L, \tag{2.20}$$

where as before, the subscripts indicate lattice coordinates. As a shorthand notation, we will suppress the tensor symbols and simply write

$$|0\rangle = |\underset{1}{S}\,\underset{2}{S}\cdots\underset{\ell}{S}\cdots\underset{L}{S}\rangle. \tag{2.21}$$

Looking at equation (2.15) and equation (2.19), we note that each term in the polynomial has a raising operator S^+ which annihilates $|0\rangle$ (see equation (2.9)) except for the term proportional to $(S^z_\ell S^z_{\ell+1})^p$. Thus, using equation (2.5) (lifted to the full lattice similar to equation (2.11)), we find the ground state energy (we assume periodic boundary conditions)

$$\begin{aligned} H|0\rangle &= -\sum_{\ell=1}^{L}\sum_{p=1}^{2S} J^{(p)}(\mathbf{S}_\ell \cdot \mathbf{S}_{\ell+1})^p \; |\underset{1}{S}\,\underset{2}{S}\cdots\underset{\ell}{S}\cdots\underset{L}{S}\rangle \\ &= -\sum_{\ell=1}^{L}\sum_{p=1}^{2S} J^{(p)}(S^z_\ell S^z_{\ell+1})^p \; |\underset{1}{S}\,\underset{2}{S}\cdots\underset{\ell}{S}\cdots\underset{L}{S}\rangle \\ &= E_0|0\rangle, \end{aligned} \tag{2.22}$$

where

$$E_0 = -L\sum_{p=1}^{2S} J^{(p)} S^{2p}. \tag{2.23}$$

For example, for $S = 1/2$, $E_0 = -J^{(1)}L/4$ which matches [41].

A *spin deviation* is created by acting with the lowering operator at site ℓ on $|0\rangle$. A single spin deviation at site ℓ is

$$S^-_\ell \; |\underset{1}{S}\,\underset{2}{S}\cdots\underset{\ell}{S}\cdots\underset{L}{S}\rangle = \sqrt{2S}\; |\underset{1}{S}\,\underset{2}{S}\cdots\underset{\ell}{S-1}\cdots\underset{L}{S}\rangle, \tag{2.24}$$

where we used equation (2.8). Two spin deviations at sites ℓ_1, ℓ_2 can be created by acting twice with the lowering operator

$$S^-_{\ell_1} S^-_{\ell_2} \; |\underset{1}{S}\cdots\underset{\ell_1}{S}\cdots\underset{\ell_2}{S}\cdots\underset{L}{S}\rangle = 2S\; |\underset{1}{S}\cdots\underset{\ell_1}{S-1}\cdots\underset{\ell_2}{S-1}\cdots\underset{L}{S}\rangle. \tag{2.25}$$

If $S > 1/2$, then we can act at least twice with the lowering operator on the same site ℓ

$$(S^-_\ell)^2 \, |\underset{1}{S}\, \underset{2}{S} \cdots \underset{\ell}{S} \cdots \underset{L}{S}\rangle = 2\sqrt{S(2S-1)} \, |\underset{1}{S}\, \underset{2}{S} \cdots S \underset{\ell}{-} 2 \cdots \underset{L}{S}\rangle. \tag{2.26}$$

One may continue in this manner and create more spin deviations.

These states are not eigenstates of the Hamiltonian. Instead, the action of the Hamiltonian on a state with spin deviation on site ℓ is a mixture or linear combination of states with spin deviations shifted by a single site. The diagonalisation problem of the Hamiltonian, however, is greatly simplified by the fact that H commutes with the total z-spin operator

$$S^{z,\text{tot}} = \sum_{\ell=1}^{L} S^z_\ell, \quad \left[S^{z,\text{tot}}, H\right] = 0. \tag{2.27}$$

This relation implies that, given r spin deviations, the Hamiltonian preserves r. The approach to diagonalizing the Hamiltonian is to solve it in sectors for a given value of r.

The Hamiltonian, which can be represented as a $(2S+1)^L \times (2S+1)^L$-matrix, can grow rapidly in size as L grows. Thus, the problem of diagonalising the Hamiltonian is a formidable linear algebra problem. Despite this complexity, there exist exactly solvable models, of which the Heisenberg model is perhaps the most well-known. In the next subsection, we will solve this model using the celebrated coordinate Bethe ansatz [32]. As we will discuss, the solvability displayed in this model is due to integrability.

2.2.2 Example I: Integrable Heisenberg Ferromagnetic Spin Chain

For this example, we look at the following special case of the Hamiltonian (2.17) where $S = 1/2$. Following the discussion in [41], we will assume periodic equations and set $J^{(1)} = J$. The local two-site Hamiltonian is therefore given by

$$\begin{aligned} H &= -J \sum_{\ell=1}^{L} \left(\mathbf{S}_\ell \cdot \mathbf{S}_{\ell+1} - \frac{1}{4} \mathbb{1}_{2\times 2} \otimes \mathbb{1}_{2\times 2} \right) \\ &= -J \sum_{\ell=1}^{L} \left(S^z_\ell S^z_{\ell+1} + \frac{1}{2} \left(S^+_\ell S^-_{\ell+1} + S^-_\ell S^+_{\ell+1} \right) - \frac{1}{4} \mathbb{1}_{2\times 2} \otimes \mathbb{1}_{2\times 2} \right), \end{aligned} \tag{2.28}$$

where $\mathbb{1}_{2\times 2} \otimes \mathbb{1}_{2\times 2}$ is the two-site identity (as discussed, this shifts all the eigenvalues; in particular, we will show that the ground state is shifted to $E_0 = 0$). This is the famous isotropic Heisenberg model for a one-dimensional ferromagnet. Perhaps even

more famously, Hans Bethe was able to solve the model exactly using the *coordinate Bethe ansatz* [32] (as we will show, this is due to the model exhibiting *integrability*). In this approach, each sector with r spin deviations can be solved by taking a linear combination of all the states and introducing spin wave coefficients. These spin waves are complex plane waves dependent on a set of numbers $\{p_1, p_2, ..., p_r\}$ (subject to constraints introduced by conserved charges) and are referred to as *magnons*. In this section, we will demonstrate the approach which will be useful to compare to when we consider more general spin models later. In addition, as we will argue later, the one-loop mixing matrix for the anomalous dimensions of scalar fields in the closed $\mathfrak{su}(2)$-subsector of $\mathcal{N} = 4$ super Yang-Mills can be mapped exactly to this model.

As mentioned in the previous section, the spin-1/2 representation is a 2-dimensional representation of the $\mathfrak{su}(2)$-algebra called the *fundamental representation*. It can therefore be represented by (2×2)-matrices acting on a complex 2-dimensional Hilbert space $\mathcal{H}$ spanned by the basis states

$$\mathcal{H} = \text{span}_{\mathbb{C}}\{|\frac{1}{2}, \frac{1}{2}\rangle, |\frac{1}{2}, -\frac{1}{2}\rangle\} \cong \mathbb{C}^2. \tag{2.29}$$

The spin operators are given by the (2×2)-Pauli matrices

$$S^i = \frac{1}{2}\sigma^i, \quad i = x, y, z \tag{2.30}$$

where

$$\sigma^x = \begin{pmatrix} 0 & 1 \\ 1 & 0 \end{pmatrix}, \ \sigma^y = \begin{pmatrix} 0 & -i \\ i & 0 \end{pmatrix}, \ \sigma^z = \begin{pmatrix} 1 & 0 \\ 0 & -1 \end{pmatrix}. \tag{2.31}$$

As is often conventional in the literature (see for example [41, 42, 43]), we will use the notation $|\frac{1}{2}, \frac{1}{2}\rangle = |\uparrow\rangle$ and $|\frac{1}{2}, -\frac{1}{2}\rangle = |\downarrow\rangle$. For a length-$L$ spin chain, the ground state is given by equation (2.21)

$$|0\rangle = |\underset{1}{\uparrow}\underset{2}{\uparrow}\cdots\underset{\ell}{\uparrow}\cdots\underset{L}{\uparrow}\rangle, \tag{2.32}$$

and we have

$$\begin{aligned}
&S^+_\ell|\underset{1}{\uparrow}\underset{2}{\uparrow}\cdots\underset{\ell}{\uparrow}\cdots\underset{L}{\uparrow}\rangle = 0, \quad S^-_\ell|\underset{1}{\uparrow}\underset{2}{\uparrow}\cdots\underset{\ell}{\uparrow}\cdots\underset{L}{\uparrow}\rangle = |\underset{1}{\uparrow}\underset{2}{\uparrow}\cdots\underset{\ell}{\downarrow}\cdots\underset{L}{\uparrow}\rangle, \\
&S^z_\ell|\underset{1}{\uparrow}\underset{2}{\uparrow}\cdots\underset{\ell}{\uparrow}\cdots\underset{L}{\uparrow}\rangle = \frac{1}{2}|\underset{1}{\uparrow}\underset{2}{\uparrow}\cdots\underset{\ell}{\uparrow}\cdots\underset{L}{\uparrow}\rangle, \\
&S^z_\ell|\underset{1}{\uparrow}\underset{2}{\uparrow}\cdots\underset{\ell}{\downarrow}\cdots\underset{L}{\uparrow}\rangle = -\frac{1}{2}|\underset{1}{\uparrow}\underset{2}{\uparrow}\cdots\underset{\ell}{\downarrow}\cdots\underset{L}{\uparrow}\rangle.
\end{aligned} \tag{2.33}$$

The unshifted ground state energy is given by equation (2.23) $E_0 = -JL/4$, however, since we shifted by $(1/4)\mathbb{1}$, this shifts E_0 to $E_0 = 0$ (we shift by the identity since this is how it appears in the context of $\mathcal{N} = 4$ super Yang-Mills theory).

One Magnon

A single spin deviation is introduced using equation (2.24). We will first solve the one magnon system for an infinite length spin chain and, at the end, we will implement periodic boundary conditions. Physically, one may think of this as solving the bulk equations on a long spin chain while first ignoring the sites at the boundaries of the spin chain. Following [32, 41], we take a linear combination of these states by Fourier expanding in a coordinate basis

$$|p\rangle = \sum_{\ell\in\mathbb{Z}} \psi(\ell)|\ell\rangle, \tag{2.34}$$

where

$$\begin{aligned} |\ell\rangle &= S^-_\ell |\underset{1}{\uparrow}\underset{2}{\uparrow}\cdots\underset{\ell}{\uparrow}\cdots\underset{L}{\uparrow}\rangle \\ &= |\underset{1}{\uparrow}\underset{2}{\uparrow}\cdots\underset{\ell}{\downarrow}\cdots\underset{L}{\uparrow}\rangle, \end{aligned} \tag{2.35}$$

and

$$\psi(\ell) = e^{ip\ell}. \tag{2.36}$$

Consider the action of each term in the Hamiltonian for two sites $(\ell-1,\ell)$ and $(\ell,\ell+1)$. First,

$$\begin{aligned} S^z_{\ell-1}S^z_\ell\,|\underset{1}{\uparrow}\cdots\underset{\ell-1}{\uparrow}\underset{\ell}{\downarrow}\underset{\ell+1}{\uparrow}\cdots\underset{L}{\uparrow}\rangle &= -\frac{1}{4}\,|\underset{1}{\uparrow}\cdots\underset{\ell-1}{\uparrow}\underset{\ell}{\downarrow}\underset{\ell+1}{\uparrow}\cdots\underset{L}{\uparrow}\rangle, \\ S^z_{\ell}S^z_{\ell+1}\,|\underset{1}{\uparrow}\cdots\underset{\ell-1}{\uparrow}\underset{\ell}{\downarrow}\underset{\ell+1}{\uparrow}\cdots\underset{L}{\uparrow}\rangle &= -\frac{1}{4}\,|\underset{1}{\uparrow}\cdots\underset{\ell-1}{\uparrow}\underset{\ell}{\downarrow}\underset{\ell+1}{\uparrow}\cdots\underset{L}{\uparrow}\rangle, \end{aligned} \tag{2.37}$$

which we observe acts like an identity term. Next,

$$\begin{aligned} S^-_{\ell-1}S^+_\ell\,|\underset{1}{\uparrow}\cdots\underset{\ell-1}{\uparrow}\underset{\ell}{\downarrow}\underset{\ell+1}{\uparrow}\cdots\underset{L}{\uparrow}\rangle &= |\underset{1}{\uparrow}\cdots\underset{\ell-1}{\downarrow}\underset{\ell}{\uparrow}\underset{\ell+1}{\uparrow}\cdots\underset{L}{\uparrow}\rangle, \\ S^+_{\ell}S^-_{\ell+1}\,|\underset{1}{\uparrow}\cdots\underset{\ell-1}{\uparrow}\underset{\ell}{\downarrow}\underset{\ell+1}{\uparrow}\cdots\underset{L}{\uparrow}\rangle &= |\underset{1}{\uparrow}\cdots\underset{\ell-1}{\uparrow}\underset{\ell}{\uparrow}\underset{\ell+1}{\downarrow}\cdots\underset{L}{\uparrow}\rangle, \end{aligned} \tag{2.38}$$

which we observe acts as permutation terms (the other combinations of the raising/lowering terms vanish). In fact, we may write the Hamiltonian for two sites $(\ell,\ell+1)$ as [44]

$$\begin{aligned} H_{\ell,\ell+1} &= -J\left(S^z_\ell S^z_{\ell+1} + \frac{1}{2}\left(S^+_\ell S^-_{\ell+1} + S^-_\ell S^+_{\ell+1}\right) - \frac{1}{4}\mathbb{1}_{2\times2}\otimes\mathbb{1}_{2\times2}\right) \\ &= -\frac{J}{2}\left(P_{\ell,\ell+1} - \mathbb{1}_{2\times2}\otimes\mathbb{1}_{2\times2}\right), \end{aligned} \tag{2.39}$$

where $P_{\ell,\ell+1}$ is the permutation matrix

$$P_{\ell,\ell+1} = \begin{pmatrix} 1 & 0 & 0 & 0 \\ 0 & 0 & 1 & 0 \\ 0 & 1 & 0 & 0 \\ 0 & 0 & 0 & 1 \end{pmatrix}_{\ell,\ell+1} . \tag{2.40}$$

In matrix notation, the single site states are represented by column matrices $|\uparrow\rangle = (1,0)^T$, $|\downarrow\rangle = (0,1)^T$ and the two site states $\{|\uparrow\uparrow\rangle, |\uparrow\downarrow\rangle, |\downarrow\uparrow\rangle, |\downarrow\downarrow\rangle\}$ are constructed by the Kronecker product. The two site Hamiltonian is represented in matrix form as

$$H_{\ell,\ell+1} = \begin{pmatrix} 0 & 0 & 0 & 0 \\ 0 & \frac{J}{2} & -\frac{J}{2} & 0 \\ 0 & -\frac{J}{2} & \frac{J}{2} & 0 \\ 0 & 0 & 0 & 0 \end{pmatrix}_{\ell,\ell+1} . \tag{2.41}$$

We will refer to the above matrix for $H_{\ell,\ell+1}$, up to possible shifts by the identity, as *Heisenberg-type*.

To solve the eigenvalue equation

$$H|p\rangle = E_1(p)|p\rangle, \tag{2.42}$$

we consider a single arbitrary site ℓ. Using the form given by equation (2.39), the terms that contribute to this site yield the following equation

$$J\psi(\ell) - \frac{J}{2}\psi(\ell-1) - \frac{J}{2}\psi(\ell+1) = E_1(p)\psi(\ell). \tag{2.43}$$

This equation is easily solved by equation (2.34) with eigenvalue

$$E_1(p) = 2J\ \sin^2\left(\frac{p}{2}\right). \tag{2.44}$$

The energy is a conserved charge. The total momentum K, the eigenvalue of the lattice translation operator U (see the discussion around equation (2.18)), is another conserved charge

$$\begin{aligned} U|p\rangle &= \sum_{\ell\in\mathbb{Z}} e^{ip\ell} U|\ell\rangle \\ &= \sum_{\ell\in\mathbb{Z}} e^{ip\ell}|\ell-1\rangle \\ &= e^{ip}\sum_{\ell'\in\mathbb{Z}} e^{ip\ell'}|\ell'\rangle, \quad \ell' = \ell - 1 \\ &= e^{ip}|p\rangle, \end{aligned} \tag{2.45}$$

where we clearly have $K = p$.

Finally, we implement periodicity by placing the spin chain on a circle with L lattice sites. Then, using the above result, we find [32, 41]

$$\begin{aligned} & U^L|p\rangle = |p\rangle \\ & \Rightarrow \psi(\ell + L) = \psi(\ell) \\ & \Rightarrow \ e^{ipL} = 1. \end{aligned} \tag{2.46}$$

This is an L-th root of unity equation which is solved by

$$p = \frac{2\pi c}{L}, \quad c = 0, 1, ..., L-1. \tag{2.47}$$

In other words, p is quantised.

Finally, we briefly mention that the system can be parametrised by uniformising momentum space. We first rewrite E_1 in terms of the coupling $J/2$

$$E_1(p) = \frac{J}{2}E(p), \quad E(p) = 4\sin^2\left(\frac{p}{2}\right). \tag{2.48}$$

Then, using the condition [43, 42] (see also equation (4.42) in [5] and the discussions in [45])

$$du = -\frac{dp}{E} \quad \Rightarrow \quad u = \frac{1}{2}\cot\left(\frac{p}{2}\right), \tag{2.49}$$

from which it follows that

$$p(u) = -i\,\ln\frac{u+\frac{i}{2}}{u-\frac{i}{2}}, \quad e^{ip(u)} = \frac{u+\frac{i}{2}}{u-\frac{i}{2}}. \tag{2.50}$$

The energy eigenvalue then becomes

$$E_1(u) = \frac{J}{2}\frac{1}{u^2+\frac{1}{4}}. \tag{2.51}$$

Two Magnons

We next consider two spin deviations. As for the one magnon case, we start by first assuming an infinite length spin chain and then solving the system's equations. At the end, we implement periodic boundary conditions on the wavefunction, which will give the well-known *Bethe quantum numbers*. Following the same arguments as for the one magnon case, we start with the following ansatz for the wavefunction

$$|p_1, p_2\rangle = \sum_{\substack{\ell_1,\ell_2\in\mathbb{Z} \\ \ell_1<\ell_2}} \psi(\ell_1, \ell_2)\ |\ell_1, \ell_2\rangle, \tag{2.52}$$

where

$$\psi(\ell_1, \ell_2) = e^{ip_1\ell_1 + ip_2\ell_2}. \tag{2.53}$$

One may think of $\psi(\ell_1, \ell_2)$ as the product of two one-particle states. Note the sum over the set of integers with the ordering $\ell_1 < \ell_2$.

There are two sets of equations: first, the *non-interacting* equation given by $\ell_2 - \ell_1 > 1$

$$\begin{aligned} &2J\psi(\ell_1, \ell_2) - \frac{J}{2}\psi(\ell_1 - 1, \ell_2) - \frac{J}{2}\psi(\ell_1 + 1, \ell_2) - \frac{J}{2}\psi(\ell_1, \ell_2 - 1) - \frac{J}{2}\psi(\ell_1, \ell_2 + 1) \\ &= E_2(p_1, p_2)\psi(\ell_1, \ell_2), \end{aligned} \tag{2.54}$$

and, secondly, the *interacting* equation given by $\ell_2 - \ell_1 = 1$

$$J\psi(\ell, \ell + 1) - \frac{J}{2}\psi(\ell - 1, \ell + 1) - \frac{J}{2}\psi(\ell, \ell + 2) = E_2(p_1, p_2)\psi(\ell, \ell + 1). \tag{2.55}$$

The non-interacting equation is solved by $\psi(\ell_1, \ell_2)$ if

$$E_2(p_1, p_2) = E_1(p_1) + E_1(p_2). \tag{2.56}$$

However, for this expression for the dispersion relation, $\psi(\ell_1, \ell_2)$ is not a solution of the interacting equation.

As an observation, one notices immediately a symmetry of E_2 under the permutation from $\{p_1, p_2\} \to \{p_2, p_1\}$. In other words, the term $\exp(ip_2\ell_1 + ip_1\ell_2)$ is also a solution of the non-interacting equation. Since each of the terms (the original momenta and the permuted momenta) are a solution of the non-interacting equation, their sum is also a solution. This is one of the key insights of [32] and we therefore update the wavefunction to a linear combination of these solutions [32, 41]

$$\psi(\ell_1, \ell_2) = A(p_1, p_2)e^{ip_1\ell_1 + ip_2\ell_2} + A(p_2, p_1)e^{ip_2\ell_1 + ip_1\ell_2}. \tag{2.57}$$

This linear combination is a solution of the interacting equation if the general coefficients satisfy

$$S(p_1, p_2) := \frac{A(p_2, p_1)}{A(p_1, p_2)} = -\frac{e^{i(p_1+p_2)} - 2e^{ip_2} + 1}{e^{i(p_1+p_2)} - 2e^{ip_1} + 1}. \tag{2.58}$$

The ratio S is called the *scattering matrix* (even though it is a scalar quantity (or (1×1)-matrix), we will continue to refer to it as a matrix). The scattering matrix is a phase

$$|S(p_1, p_2)| = 1, \tag{2.59}$$

and it obeys physical unitarity

$$S(p_1, p_2)^\dagger = S(p_2, p_1) = 1/S(p_1, p_2). \tag{2.60}$$

Physically, this result is interpreted as spin wave scattering: we start with two incoming spin waves with momenta $\{p_1, p_2\}$ and these states scatter with outgoing momenta $\{p_2, p_1\}$, with the outgoing wavefunction picking up a phase given by $S(p_1, p_2)$. Consequently, by introducing $\Theta(p_1, p_2)$ as (see for example [41]; note that our S-matrix is defined as the inverse of their S-matrix)

$$\Theta(p_1, p_2) := -i \ln\left(S(p_1, p_2)\right), \tag{2.61}$$

one may rewrite the wavefunction as

$$\psi(\ell_1, \ell_2) = e^{ip_1\ell_1 + ip_2\ell_2 + \frac{1}{2}\Theta(p_2,p_1)} + e^{ip_2\ell_1 + ip_1\ell_2 + \frac{1}{2}\Theta(p_1,p_2)}. \tag{2.62}$$

Finally, similar to the one magnon case, the total momentum eigenvalue is given by $K = p_1 + p_2 \in \mathbb{R}$. Note that p_1, p_2 are not true momenta but merely a labeling device (as conventional in the literature, however, we will continue to refer to p_1, p_2 as momenta); rather, it is their sum that gives the eigenvalue. In fact, as will discuss, p_1, p_2 can be complex valued as well. The lattice momentum is, as always in quantum mechanics, given by the real-valued eigenvalue of a hermitian operator.

We now implement periodic boundary conditions. Since we have the ordering $\ell_1 < \ell_2$, periodicity implies the following constraint

$$\begin{aligned} &\psi(\ell_1, \ell_2) = \psi(\ell_2, \ell_1 + L) \\ &\implies e^{ip_1 L} = e^{-i\Theta(p_1,p_2)} = S(p_1, p_2)^{-1}, \quad e^{ip_2 L} = e^{i\Theta(p_1,p_2)} = S(p_1, p_2). \end{aligned} \tag{2.63}$$

Physically, one can think about this result as follows [42, 43]: the magnon p_1 at site ℓ_1 say, is transported once around the circle. As it does so, it scatters through the second magnon p_2 and picks up a phase before returning to the same site ℓ on the circle. Solving the L-th root of unity equations: $\exp(iL(p_1 + \frac{1}{L}\Theta) = 1$, $\exp(iL(p_2 - \frac{1}{L}\Theta) = 1$, one finds that [41, 32]

$$Lp_1 = 2\pi\lambda_1 - \Theta(p_1, p_2), \quad Lp_2 = 2\pi\lambda_2 + \Theta(p_1, p_2) \tag{2.64}$$

where $\lambda_i \in \{0, 1, ..., L-1\}$, $i = 1, 2$. The integers λ_i are called the *Bethe quantum numbers*. Equation (2.63) is called the *Bethe ansatz equation*. This, of course, quantises the total momentum to be [41]

$$K = p_1 + p_2 = \frac{2\pi}{L}\left(\lambda_1 + \lambda_2\right), \ \lambda_i \in \{0, 1, ..., L-1\}, \ i = 1, 2. \tag{2.65}$$

The remaining task is to determine the pairs (λ_1, λ_2) subject to Bethe ansatz equation.

The pairs have real-valued solutions leading to $\{p_1, p_2\}$ that satisfy energy and momentum conservation. In addition, the pairs also have complex-valued solutions. The complex-valued solutions yield $\{p_1, p_2\}$ which must be of the form $p_1 = K/2+iv,\ p_2 = K/2-iv,\ v > 0$, because $K = p_1+p_2 \in \mathbb{R}$. These complex solutions are *bound states* of the spin waves since the the probability distribution $|\psi|^2$ favours the spin deviations being nearest-neighbour. They are also zeroes or poles of the S-matrix. For a detailed study, see Hans Bethe's original paper [32] as well as [41].

Finally, we can use the parametrisation from the one magnon section to write the dispersion relation as (with $p_1 = p_1(u_1),\ p_2 = p_2(u_2)$)

$$E_2(u_1, u_2) = \sum_{i=1}^{2} E_1(u_i), \quad E_1(u_i) = \frac{J}{2}\frac{1}{u_i^2 + \frac{1}{4}}, \tag{2.66}$$

and the Bethe ansatz equation as

$$\left(\frac{u_1 + \frac{i}{2}}{u_1 - \frac{i}{2}}\right)^L = \frac{u_1 - u_2 + i}{u_1 - u_2 - i}, \quad \left(\frac{u_2 + \frac{i}{2}}{u_2 - \frac{i}{2}}\right)^L = \frac{u_1 - u_2 - i}{u_1 - u_2 + i}. \tag{2.67}$$

Three Magnons and Integrability

In solving the two magnon problem, Hans Bethe [32] showed that the r magnon problem was automatically solved. This astonishing result is due to this model exhibiting quantum integrability (see the definition in equation (2.75). In the next section, we will consider a spin-1 model that is non-integrable.

Inspired by the two magnon wavefunction, we start by making the following ansatz for an infinite length spin chain

$$|p_1, p_2, p_3\rangle = \sum_{\substack{\ell_1,\ell_2,\ell_3 \in \mathbb{Z} \\ \ell_1 < \ell_2 < \ell_3}} \sum_{\sigma \in S_3} A(p_{\sigma(1)}, p_{\sigma(2)}, p_{\sigma(3)}) e^{ip_{\sigma(1)}\ell_1 + ip_{\sigma(2)}\ell_2 + ip_{\sigma(3)}\ell_3}. \tag{2.68}$$

As in the two magnon case, there are three systems of equations: for arbitrary sites ℓ_1, ℓ_2, ℓ_3 with $\ell_2 - \ell_1 > 1, \ell_3 - \ell_2 > 1$, we have the non-interacting equation

$$\begin{aligned} &3J\psi(\ell_1, \ell_2, \ell_3) - \frac{J}{2}\psi(\ell_1 - 1, \ell_2, \ell_3) - \frac{J}{2}\psi(\ell_1 + 1, \ell_2, \ell_3) - \frac{J}{2}\psi(\ell_1, \ell_2 - 1, \ell_3) \\ &- \frac{J}{2}\psi(\ell_1, \ell_2 + 1, \ell_3) - \frac{J}{2}\psi(\ell_1, \ell_2, \ell_3 - 1) - \frac{J}{2}\psi(\ell_1, \ell_2, \ell_3 + 1) \\ &= E_3(p_1, p_2, p_3)\psi(\ell_1, \ell_2, \ell_3). \end{aligned} \tag{2.69}$$

For $\ell_2 - \ell_1 = 1$ or $\ell_3 - \ell_2 = 1$, we have two interacting equations for two magnons (the third magnon being a distance greater than one site away)

$$\begin{aligned}
&2J\psi(\ell,\ell+1,\ell_3) - \frac{J}{2}\psi(\ell-1,\ell+1,\ell_3) - \frac{J}{2}\psi(\ell,\ell+2,\ell_3) - \frac{J}{2}\psi(\ell,\ell+1,\ell_3-1) \\
&- \frac{J}{2}\psi(\ell,\ell+1,\ell_3+1) = E_3(p_1,p_2,p_3)\psi(\ell,\ell+1,\ell_3) \\
&2J\psi(\ell_1,\ell,\ell+1) - \frac{J}{2}\psi(\ell_1-1,\ell,\ell+1) - \frac{J}{2}\psi(\ell_1+1,\ell,\ell+1) - \frac{J}{2}\psi(\ell_1,\ell-1,\ell+1) \\
&- \frac{J}{2}\psi(\ell_1,\ell,\ell+2) = E_3(p_1,p_2,p_3)\psi(\ell_1,\ell,\ell+1).
\end{aligned} \tag{2.70}$$

Finally, there is the three particle interacting equation

$$J\psi(\ell{-}1,\ell,\ell{+}1){-}\frac{J}{2}\psi(\ell{-}2,\ell,\ell{+}1){-}\frac{J}{2}\psi(\ell{-}1,\ell,\ell{+}2) = E_3(p_1,p_2,p_3)\psi(\ell{-}1,\ell,\ell{+}1). \tag{2.71}$$

Each term in the ansatz is a solution of equation (2.69) and, therefore, the sum is also a solution with energy eigenvalue $E_3(p_1,p_2,p_3) = E_1(p_1) + E_1(p_2) + E_1(p_3)$.

Next, we solve equation (2.70). Noting that these equations involve two-body scattering, there are two routes one my travel by starting with the initial set of momenta $\{p_1,p_2,p_3\}$ and ending with the maximally permuted set of momenta $\{p_3,p_2,p_1\}$. The first route, through two body scattering, is given by the $(12)-(13)-(23)$ sequence of permutations: $\{p_1,p_2,p_3\} \to \{p_2,p_1,p_3\} \to \{p_2,p_3,p_1\} \to \{p_3,p_2,p_1\}$. The second route is given by the sequence $(23)-(13)-(12)$: $\{p_1,p_2,p_3\} \to \{p_1,p_3,p_2\} \to \{p_3,p_1,p_2\} \to \{p_3,p_2,p_1\}$. In terms of the coefficient $A(p_1,p_2,p_3)$ and using the solution from the two magnon system, the first route gives

$$\begin{aligned}
\frac{A(p_2,p_1,p_3)}{A(p_1,p_2,p_3)} &= S(p_1,p_2), \\
\frac{A(p_2,p_3,p_1)}{A(p_1,p_2,p_3)} &= \frac{A(p_2,p_3,p_1)}{A(p_2,p_1,p_3)}\frac{A(p_2,p_1,p_3)}{A(p_1,p_2,p_3)} \\
&= S(p_1,p_3)S(p_1,p_2), \\
\frac{A(p_3,p_2,p_1)}{A(p_1,p_2,p_3)} &= \frac{A(p_3,p_2,p_1)}{A(p_2,p_3,p_1)}\frac{A(p_2,p_3,p_1)}{A(p_2,p_1,p_3)}\frac{A(p_2,p_1,p_3)}{A(p_1,p_2,p_3)} \\
&= S(p_2,p_3)S(p_1,p_3)S(p_1,p_2).
\end{aligned} \tag{2.72}$$

In exactly the same manner, the second route gives

$$\begin{aligned}
\frac{A(p_1,p_3,p_2)}{A(p_1,p_2,p_3)} &= S(p_2,p_3),\\
\frac{A(p_3,p_1,p_2)}{A(p_1,p_2,p_3)} &= \frac{A(p_3,p_1,p_2)}{A(p_1,p_3,p_2)}\frac{A(p_1,p_3,p_2)}{A(p_1,p_2,p_3)}\\
&= S(p_1,p_3)S(p_2,p_3),\\
\frac{A(p_3,p_2,p_1)}{A(p_1,p_2,p_3)} &= \frac{A(p_3,p_2,p_1)}{A(p_3,p_1,p_2)}\frac{A(p_3,p_1,p_2)}{A(p_1,p_3,p_2)}\frac{A(p_1,p_3,p_2)}{A(p_1,p_2,p_3)}\\
&= S(p_1,p_2)S(p_1,p_3)S(p_2,p_3).
\end{aligned} \tag{2.73}$$

Notice that the ratios for the amplitudes appear as products of the two magnon S-matrices. This property is called *factorization*. The above forms for the coefficients solves equations (2.70). In addition, we find an example of the celebrated Yang-Baxter equation (although for this case, it is trivial because the S-matrices are 1×1-matrices)

$$S(p_2,p_3)S(p_1,p_3)S(p_1,p_2) = S(p_1,p_2)S(p_1,p_3)S(p_2,p_3), \tag{2.74}$$

which is graphically shown in Figure 2.3 (we used the shorthand notation $S(p_i,p_j) = S_{ij}$).

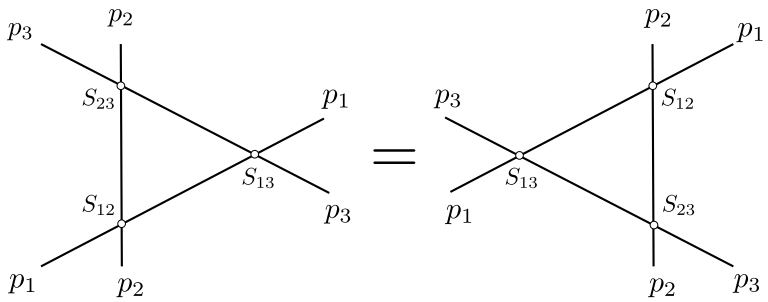

Figure 2.3: *Yang-Baxter equation*

Fascinatingly, the solution for the two-magnon/one-free interacting equation is also a solution of the three-magnon interacting equation (2.71). Thus, the system for three magnons is completely solved by two magnon processes.

The fact that we can use two magnon data to completely solve the three magnon case is strong evidence that the model is quantum integrable. As a practical definition for quantum integrability, we will use the definition from [46]:

Definition (Quantum Integrability): A quantum system is said to be *quantum integrable* if the system exhibits *non-diffractive scattering*. More concretely, if the three magnon wavefunction $\psi(\ell_1, \ell_2, \ell_3)$ contains a diffractive term and is, therefore, of the form [47, 48, 46]

$$\begin{aligned}\psi(\ell_1, \ell_2, \ell_3) = &\sum_{\substack{\ell_1,\ell_2,\ell_3\in\mathbb{Z}\\ \ell_1<\ell_2<\ell_3}} \sum_{\sigma\in S_3} A(p_{\sigma(1)}, p_{\sigma(2)}, p_{\sigma(3)}) e^{ip_{\sigma(1)}\ell_1 + ip_{\sigma(2)}\ell_2 + ip_{\sigma(3)}\ell_3} \\ &+ \int_{K,E_3 \text{ fixed}} dk_1 dk_2 dk_3 \; A_{\text{diff}}(k_1, k_2, k_3) e^{ik_1\ell_1 + ik_2\ell_2 + ik_3\ell_3},\end{aligned} \tag{2.75}$$

where "K, E_3 fixed" means that the integral is constrained to the manifolds in momentum space given by $K = p_1 + p_2 + p_3 = k_1 + k_2 + k_3$, and $E_3 = E_1(p_1) + E_1(p_2) + E_1(p_3) = E_1(k_1) + E_1(k_2) + E_1(k_3)$, then the system exhibits diffractive scattering and is non-integrable. The first term is the usual Bethe ansatz that accounts for pure two body scattering. The second term accounts for diffractive scattering processes which are true three-body scattering processes (in the sense that it cannot be decomposed to two-body scattering processes).

For the above definition, we note that the test for integrability is at the three spin deviation level since we are testing for true three-body scattering. The two spin deviation problem is therefore insensitive to integrability and can always be solved regardless of whether integrability is present. The three spin deviation problem for the Heisenberg model is completely solved by the ansatz (2.68). It clearly does not have a diffractive term and is, according to the above definition, quantum integrable. In addition, note that scattering its incoming set of momenta $\{p_1, p_2, p_3\}$ yields an outgoing set of momenta that is a permutation of the original set (for example, $\{p_3, p_2, p_1\}$). This is due to the existence of a tower of higher conserved charges (for an explicit construction of these charges, see [49])[1]. In contrast, a non-integrable system will have three-body scattering processes that lead to a new set of momenta $\{k_1, k_2, k_3\}$ (subject to energy and momentum conservation). Note also that the S-matrices computed using the diffractive coefficient A_{diff} will not decompose into two-body S-matrices (when solving in terms of $A(p_1, p_2, p_3)$) so that a non-integrable system will not have S-matrix factorization. Finally, we briefly mention that the question of quantum integrability is more subtle than the classical counterpart. A detailed discussion on the various definitions for quantum integrability (including the definition we use for this thesis) is discussed in [20].

[1] This is also commonly used as a definition of quantum integrability, although one needs to be careful about the subtleties which are discussed in [20].

General Solution

Due to the model being integrable, the solution for three magnons generalizes to r magnons. The wavefunction is given by [32, 5, 42, 37]

$$|p_1, p_2, ..., p_r\rangle = \sum_{\substack{\ell_1,\ell_2,..,\ell_r\in\mathbb{Z} \\ \ell_1<\ell_2<\cdots<\ell_r}} \sum_{\sigma\in S_r} A(p_{\sigma(1)}, p_{\sigma(2)}, ..., p_{\sigma(r)}) e^{ip_{\sigma(1)}\ell_1+ip_{\sigma(2)}\ell_2+...+ip_{\sigma(r)}\ell_r}. \tag{2.76}$$

The system is solved by the Bethe equations with S-matrix factorization

$$\left(\frac{u_j+\frac{i}{2}}{u_j-\frac{i}{2}}\right)^L = \prod_{k\neq j}^{r} \frac{u_j-u_k+i}{u_j-u_k-i}, \tag{2.77}$$

and with energy eigenvalue

$$E(u_1, ..., u_r) = \sum_{i=1}^{r} E(u_i). \tag{2.78}$$

2.2.3 Example II: Solvable Spin-1 Chain with Diffractive Scattering

In the previous section, we discussed an example of an integrable spin chain model. In particular, once the two magnon solution was found, integrability implied that the r-magnon solution was solved using only two magnon data. In this section, we study a spin-1 model that, except for two special values of the coupling constant, is not integrable. Despite the absence of integrability, we can still solve the three magnon case using the method in [47].

The model

For this section, we will only consider an infinite length spin chain (in other words, we ignore boundary conditions). The spin-1 Hamiltonian we will consider is given by [47]

$$H = \sum_{\ell\in\mathbb{Z}} H_{\ell,\ell+1}, \tag{2.79}$$

where the two site Hamiltonian is given by

$$H_{\ell,\ell+1} = \mathbb{1} - (\mathbf{S}_\ell \cdot \mathbf{S}_{\ell+1}) + J\left(\mathbb{1} - (\mathbf{S}_\ell \cdot \mathbf{S}_{\ell+1})^2\right). \tag{2.80}$$

This is an example of the Hamiltonian (2.17), where we have again shifted by the identity so that the ground state is $E_0 = 0$. The term linear in $(\mathbf{S}_\ell \cdot \mathbf{S}_{\ell+1})$ is called *dipolar* and the quadratic term is called *quadrupolar*. For $J = 1$, the Hamiltonian

has an enhanced $\mathfrak{su}(3)$ symmetry (in addition to the $\mathfrak{su}(2)$ symmetry) [47] (see especially the discussion in [50]).

We again expand in terms of equation (2.15). Then, using our labeling in terms of the z-axis spin $j = 1, 0, -1$ and looking at two arbitrary sites $(\ell, \ell+1)$, we have the basis states

$$|j_1\rangle_\ell \otimes |j_2\rangle_{\ell+1}, \quad j_i \in \{1, 0, -1\},\ i = 1, 2, \tag{2.81}$$

with ground state $j_i = 1,\ i = 1, 2$. Notice that we can have two spin deviations on a single site, unlike the Heisenberg spin chain studied in the previous section. More precisely, the action of the spin operators S^+_ℓ, S^-_ℓ on the ground state is given by equations (2.24), (2.25) and (2.26)

$$S^+|1\rangle = 0, \quad S^-|1\rangle = \sqrt{2}|0\rangle, \quad (S^-)^2|1\rangle = 2|-1\rangle, \tag{2.82}$$

together with

$$S^z_\ell|j\rangle_\ell = j|j\rangle_\ell, \quad j = 1, 0, -1. \tag{2.83}$$

Then, the two-site Hamiltonian gives [47]

$$\begin{aligned}
H_{\ell,\ell+1}\ |\pm 1\rangle_\ell \otimes |\pm 1\rangle_{\ell+1} \quad &= 0, \\
H_{\ell,\ell+1}\ |\pm 1\rangle_\ell \otimes |0\rangle_{\ell+1} \quad &= |\pm 1\rangle_\ell \otimes |0\rangle_{\ell+1} - |0\rangle_\ell \otimes |\pm 1\rangle_{\ell+1}, \\
H_{\ell,\ell+1}\ |0\rangle_\ell \otimes |\pm 1\rangle_{\ell+1} \quad &= |0\rangle_\ell \otimes |\pm 1\rangle_{\ell+1} - |\pm 1\rangle_\ell \otimes |0\rangle_{\ell+1}, \\
H_{\ell,\ell+1}\ |0\rangle_\ell \otimes |0\rangle_{\ell+1} \quad &= (1-J)\left(|0\rangle_\ell \otimes |0\rangle_{\ell+1} - |1\rangle_\ell \otimes |-1\rangle_{\ell+1}\right. \\
&\quad \left. - |-1\rangle_\ell \otimes |1\rangle_{\ell+1}\right), \\
H_{\ell,\ell+1}\ |\pm 1\rangle_\ell \otimes |\mp 1\rangle_{\ell+1} \quad &= (2-J)\,|\pm 1\rangle_\ell \otimes |\mp 1\rangle_{\ell+1} + (J-1)\,|0\rangle_\ell \otimes |0\rangle_{\ell+1} \\
&\quad - J\,|\mp 1\rangle_\ell \otimes |\pm 1\rangle_{\ell+1}.
\end{aligned} \tag{2.84}$$

One Spin Deviation

Similar to the Heisenberg spin chain, we solve the one magnon problem by Fourier expanding in a coordinate basis. The state is given by [47]

$$|p\rangle = \sum_{\ell \in \mathbb{Z}} e^{ip\ell}|\ell\rangle, \tag{2.85}$$

where $|\ell\rangle = S^-_\ell|0\rangle$. The one magnon energy is given by

$$E_1(p) = 4\sin^2(p/2). \tag{2.86}$$

This energy closely matches the Heisenberg spin chain since only the linear term for $\mathbf{S}_\ell \cdot \mathbf{S}_{\ell+1}$ contributes in the one magnon case (see the second and third equations in equation (2.84) which closely resemble the analogous equations for the Heisenberg system).

Two Spin Deviations

For this case, we observe the first significant difference between the spin-1 system and the spin-1/2 system, namely, the fact that we can have two spin deviations on the same site ℓ. The ansatz for the wavefunction is [47]

$$|p_1, p_2\rangle = \sum_{\substack{\ell_1,\ell_2\in\mathbb{Z} \\ \ell_1<\ell_2}} \alpha(\ell_1, \ell_2)|\ell_1, \ell_2\rangle + \sum_{\ell\in\mathbb{Z}} \beta(\ell)|\ell, \ell\rangle, \tag{2.87}$$

where $|\ell, \ell\rangle = (S^-_\ell)^2|0\rangle$. This is a state called a *quadruplon* [47].

The non-interacting equations for $\ell_2 - \ell_1 > 1$ are given by

$$\begin{aligned} &4\alpha(\ell_1, \ell_2) - \alpha(\ell_1 - 1, \ell_2) - \alpha(\ell_1 + 1, \ell_2) - \alpha(\ell_1, \ell_2 - 1) - \alpha(\ell_1, \ell_2 + 1) \\ &= E_2(p_1, p_2)\ \alpha(\ell_1, \ell_2) \end{aligned} \tag{2.88}$$

For the interacting equations $\ell_2 - \ell_1 = 1$ and $\ell_2 - \ell_1 = 0$, we have

$$\begin{aligned} &(3 - J)\alpha(\ell, \ell + 1) - \alpha(\ell - 1, \ell + 1) - \alpha(\ell, \ell + 2) + (J - 1)\ (\beta(\ell) + \beta(\ell + 1)) \\ &= E_2(p_1, p_2)\ \alpha(\ell, \ell + 1), \\ &2(2 - J)\beta(\ell) - J\ (\beta(\ell - 1) + \beta(\ell + 1)) + (J - 1)\ (\alpha(\ell - 1, \ell) + \alpha(\ell, \ell + 1)) \\ &= E_2(p_1, p_2)\ \beta(\ell). \end{aligned} \tag{2.89}$$

For the special value $J = 1$, which is the special point where H has an extra $\mathfrak{su}(3)$ invariance, notice that the system of interacting equations decouple into two independent systems. The quadruplon state, referred to in [50] as a *quadrupole wave*, becomes an eigenstate of the Hamiltonian with $\beta(p) = \exp(iK)$, $K = p_1 + p_2$, and energy degenerate with the energy for the one magnon state [47]. For $J \neq 1$, the quadruplon is a resonant state.

For $J \neq 1$, the system of equations can be solved with the ansatz [47]

$$\begin{aligned} \alpha(\ell_1, \ell_2) &= A(p_1, p_2)e^{ip_1\ell_1 + ip_2\ell_2} - A(p_2, p_1)e^{ip_2\ell_1 + ip_1\ell_2} \\ \beta(p_1, p_2) &= B(p_1, p_2)e^{i(p_1+p_2)\ell} \end{aligned} \tag{2.90}$$

with energy $E_2(p_1, p_2) = E_1(p_1) + E_1(p_2)$ and

$$\begin{aligned} A(x,y) &= e^{iy} + e^{i(x+2y)} - (1+J)e^{2ix} - (1+3J)e^{i(x+y)} \\ &\quad + J\left(3e^{ix} + 3e^{i(2x+y)} - 1 - e^{2i(x+y)}\right), \\ B(x,y) &= (1-J)\left(e^{iy} - e^{ix}\right)\left(1 + e^{i(x+y)}\right). \end{aligned} \tag{2.91}$$

Following the discussion around quantum integrability (see equation (2.75)), we note that the two spin deviation case can be solved despite the system not being integrable (in other words, the two spin deviation case is insensitive to integrability) [47].

Three Spin Deviations

Due to the quadruplon excitation being a resonance, the quadruplon is unstable. In particular, it leads to diffractive scattering in the three magnon case (see page 3 of [47]) which means the model is non-integrable according to the definition in equation (2.75), for which the wavefunction for a general non-integable spin chain is given by

$$\begin{aligned} \psi(\ell_1, \ell_2, \ell_3) = &\sum_{\substack{\ell_1,\ell_2,\ell_3 \in \mathbb{Z} \\ \ell_1 < \ell_2 < \ell_3}} \sum_{\sigma \in S_3} A(p_{\sigma(1)}, p_{\sigma(2)}, p_{\sigma(3)}) e^{ip_{\sigma(1)}\ell_1 + ip_{\sigma(2)}\ell_2 + ip_{\sigma(3)}\ell_3} \\ &+ \int_{K,E_3 \text{ fixed}} dk_1 dk_2 dk_3 \; A_{\text{diff}}(k_1, k_2, k_3) e^{ik_1\ell_1 + ik_2\ell_2 + ik_3\ell_3}. \end{aligned} \tag{2.92}$$

Interestingly, using the *degenerative discrete-diffractive* wavefunctions given in [47] (which is a special case of the non-integable wavefunction above for this spin-1 model), we can still solve the three magnon problem using a discrete and finite set of terms. In this approach, the above wavefunction can be reduced to the discrete form

$$\psi(\ell_1, \ell_2, \ell_3) = \sum_{m=1}^{M} \sum_{\substack{\ell_1,\ell_2,\ell_3 \in \mathbb{Z} \\ \ell_1 < \ell_2 < \ell_3}} \sum_{\sigma \in S_3} A^{(m)}_{\sigma(1)\sigma(2)\sigma(3)} e^{ip^{(m)}_{\sigma(1)}\ell_1 + ip^{(m)}_{\sigma(2)}\ell_2 + ip^{(m)}_{\sigma(3)}\ell_3}, \tag{2.93}$$

where we have introduced the compact notation

$$A^{(m)}_{ijk} = A^{(m)}(p^{(m)}_i, p^{(m)}_j, p^{(m)}_k). \tag{2.94}$$

The parameter m labels a set of momenta (that is not a permutation of the original set of momenta) of which there is a finite number $1 < M < \infty$ (the $M = 1$ case would

of course give the original integrable Bethe ansatz). In other words, by adding finite sets of extra momenta and using the same discrete form for the usual Bethe ansatz, the three spin deviation case for this system can be solved. Following [47], we will show that we only need one extra set of momenta to solve the system of equations; in other words, the total sets of momenta are $M = 2$.

Starting first with an initial set of momenta $\{p_1, p_2, p_3\}$, the initial ansatz is given by [47]

$$\begin{aligned} |p_1, p_2, p_3\rangle = & \sum_{\substack{\ell_1,\ell_2,\ell_3\in\mathbb{Z} \\ \ell_1<\ell_2<\ell_3}} \alpha(\ell_1,\ell_2,\ell_3)|\ell_1,\ell_2,\ell_3\rangle \\ & + \sum_{\substack{\ell_1,\ell_2\in\mathbb{Z} \\ \ell_1<\ell_2}} \left[\beta^{(1)}(\ell_1,\ell_2)|\ell_1,\ell_1,\ell_2\rangle + \beta^{(2)}(\ell_1,\ell_2)|\ell_1,\ell_2,\ell_2\rangle\right]. \end{aligned} \tag{2.95}$$

Using the compact notation introduced above, the non-interacting equations for $\ell_2 - \ell_1 > 1,\ \ell_3 - \ell_2 > 1$ are given by

$$\begin{aligned} & 6\alpha_{\ell_1,\ell_2,\ell_3} - \alpha_{\ell_1-1,\ell_2,\ell_3} - \alpha_{\ell_1+1,\ell_2,\ell_3} - \alpha_{\ell_1,\ell_2-1,\ell_3} - \alpha_{\ell_1,\ell_2+1,\ell_3} - \alpha_{\ell_1,\ell_2,\ell_3-1} - \alpha_{\ell_1,\ell_2,\ell_3+1} \\ & = E_3\ \alpha_{\ell_1,\ell_2,\ell_3}, \end{aligned} \tag{2.96}$$

the two particle interacting equations for $|\ell_3 - \ell| > 1,\ |\ell_2 - \ell| > 1$ are given by

$$\begin{aligned} & (5-J)\,\alpha_{\ell-1,\ell,\ell_3} - \alpha_{\ell-2,\ell,\ell_3} - \alpha_{\ell-1,\ell+1,\ell_3} - \alpha_{\ell-1,\ell,\ell_3-1} - \alpha_{\ell-1,\ell,\ell_3+1} \\ & + (J-1)\left(\beta^{(1)}_{\ell-1,\ell_3} + \beta^{(1)}_{\ell,\ell_3}\right) = E_3\ \alpha_{\ell-1,\ell,\ell_3}, \\ & (5-J)\,\alpha_{\ell_1,\ell,\ell+1} - \alpha_{\ell_1-1,\ell,\ell+1} - \alpha_{\ell_1+1,\ell,\ell+1} - \alpha_{\ell_1,\ell-1,\ell+1} - \alpha_{\ell_1,\ell,\ell+2}, \\ & + (J-1)\left(\beta^{(2)}_{\ell_1,\ell} + \beta^{(2)}_{\ell_1,\ell+1}\right) = E_3\ \alpha_{\ell_1,\ell,\ell+1}, \\ & 2\,(3-J)\,\beta^{(1)}_{\ell,\ell_3} - \beta^{(1)}_{\ell,\ell_3+1} - \beta^{(1)}_{\ell,\ell_3-1} - J\left(\beta^{(1)}_{\ell-1,\ell_3} + \beta^{(1)}_{\ell+1,\ell_3}\right) \\ & + (J-1)\left(\alpha_{\ell,\ell+1,\ell_3} + \alpha_{\ell-1,\ell,\ell_3}\right) = E_3\ \beta^{(1)}_{\ell,\ell_3}, \\ & 2\,(3-J)\,\beta^{(2)}_{\ell_1,\ell} - \beta^{(2)}_{\ell_1-1,\ell} - \beta^{(2)}_{\ell_1+1,\ell} - J\left(\beta^{(2)}_{\ell_1,\ell-1} + \beta^{(2)}_{\ell_1,\ell+1}\right) \\ & + (J-1)\left(\alpha_{\ell_1,\ell-1,\ell} + \alpha_{\ell_1,\ell,\ell+1}\right) = E_3\ \beta^{(2)}_{\ell_1,\ell}, \end{aligned} \tag{2.97}$$

and, finally, the three particle interacting equations are given by

$$\begin{aligned} & 2\,(2-J)\,\alpha_{\ell-1,\ell,\ell+1} - \alpha_{\ell-2,\ell,\ell+1} - \alpha_{\ell-1,\ell,\ell+2} \\ & + (J-1)\left(\beta^{(1)}_{\ell-1,\ell+1} + \beta^{(1)}_{\ell,\ell+1} + \beta^{(2)}_{\ell-1,\ell} + \beta^{(2)}_{\ell-1,\ell+1}\right) = E_3\ \alpha_{\ell-1,\ell,\ell+1}, \end{aligned} \tag{2.98}$$

and

$$(4-J)\,\beta^{(1)}_{\ell,\ell+1} - \beta^{(1)}_{\ell,\ell+2} - J\beta^{(1)}_{\ell-1,\ell+1} - \beta^{(2)}_{\ell,\ell+1} + (J-1)\,\alpha_{\ell-1,\ell,\ell+1} = E_3\,\beta^{(1)}_{\ell,\ell+1},$$
$$(4-J)\,\beta^{(2)}_{\ell-1,\ell} - \beta^{(2)}_{\ell-2,\ell} - J\beta^{(2)}_{\ell-1,\ell+1} - \beta^{(1)}_{\ell-1,\ell} + (J-1)\,\alpha_{\ell-1,\ell,\ell+1} = E_3\,\beta^{(2)}_{\ell-1,\ell}. \tag{2.99}$$

We will use the more compact notation in [47] for the terms generated by the action of the permutation group S_3: we use the completely antisymmetric symbol $\epsilon_{abc} = 1$. Then, using equation (2.91) and assuming only two-body scattering for the moment (so that the coefficients factorize), we make the ansatz [47]

$$\alpha(\ell_1,\ell_2,\ell_3) = \sum_{a,b,c=1}^{3} \epsilon_{abc} A(p_a,p_b)A(p_a,p_c)A(p_b,p_c)e^{ip_a\ell_1+ip_b\ell_2+ip_c\ell_3},$$
$$\beta^{(1)}(\ell_1,\ell_2) = \frac{1}{2}\sum_{a,b,c=1}^{3} \epsilon_{abc} B(p_a,p_b)A(p_a,p_c)A(p_b,p_c)e^{i(p_a+p_b)\ell_1+ip_c\ell_2},$$
$$\beta^{(2)}(\ell_1,\ell_2) = \frac{1}{2}\sum_{a,b,c=1}^{3} \epsilon_{abc} A(p_a,p_b)A(p_a,p_c)B(p_b,p_c)e^{ip_a\ell_1+i(p_b+p_c)\ell_2}. \tag{2.100}$$

This solves equations (2.96) - (2.98) with energy eigenvalue $E_3(p_1,p_2,p_3) = E_1(p_1)+E_1(p_2)+E_1(p_3)$. However, the ansatz is not a solution of equation (2.99) as (for $J \neq 1$) the quadruplons are unstable resonant states that produce diffractive scattering processes (which are three-body processes).

Despite this, [47] found that one can manipulate equation (2.99) (after substituting equation (2.100)) to find the equations

$$X^{(1)}(p_1,p_2,p_3) = \left(1-J^2\right)\phi(p_1,p_2,p_3)\left[\,(E_3-5)\,e^{iK} - 1 + J\left(2+3e^{iK}+e^{2iK}\right)\right],$$
$$X^{(2)}(p_1,p_2,p_3) = \left(1-J^2\right)\phi(p_1,p_2,p_3)\left[e^{iK} - E_3 + 5 - J\left(3+2e^{iK}+e^{-iK}\right)\right], \tag{2.101}$$

where $K = p_1+p_2+p_3$ and

$$\phi(p_1,p_2,p_3) = \left(e^{ip_1}-e^{ip_2}\right)\left(e^{ip_2}-e^{ip_3}\right)\left(e^{ip_3}-e^{ip_1}\right)\prod_{j=1}^{3}\left(1-e^{ip_j}\right). \tag{2.102}$$

Analysing $X^{(i)}$, $i = 1,2$, we note that for $J = 1$ the equations vanish and thus we have no diffractive scattering. For $J \neq 1$, note that the terms in square brackets consist of conserved charges K, E_3. The coefficient ϕ, however, contains no conserved charges. By using an extra set of momenta $\{k_1,k_2,k_3\}$ subject to the same energy/momentum constraints and multiplying the Bethe ansatz by an overall factor $\phi(k_1,k_2,k_3)$ (the

wavefunctions will still satisfy the other equations), one finds the new equations for $X^{(i)}$

$$\begin{aligned}
&X^{(1)}(p_1,p_2,p_3)\\
&=\left(1-J^2\right)\phi(k_1,k_2,k_3)\phi(p_1,p_2,p_3)\big[\,(E_3-5)\,e^{iK}-1+J\left(2+3e^{iK}+e^{2iK}\right)\big],\\
&X^{(2)}(p_1,p_2,p_3)\\
&=\left(1-J^2\right)\phi(k_1,k_2,k_3)\phi(p_1,p_2,p_3)\big[e^{iK}-E_3+5-J\left(3+2e^{iK}+e^{-iK}\right)\big].
\end{aligned} \tag{2.103}$$

Noticing that the two sets of momenta appear symmetrically, we find that the $X^{(i)},\ i=1,2$ equations vanish if we update the wavefunctions to

$$\begin{aligned}
\alpha(\ell_1,\ell_2,\ell_3)&=\phi(k_1,k_2,k_3)\alpha_{p_1,p_2,p_3}(\ell_1,\ell_2,\ell_3)-\phi(p_1,p_2,p_3)\alpha_{k_1,k_2,k_3}(\ell_1,\ell_2,\ell_3),\\
\beta^{(1)}(\ell_1,\ell_2)&=\phi(k_1,k_2,k_3)\beta^{(1)}_{p_1,p_2,p_3}(\ell_1,\ell_2)-\phi(p_1,p_2,p_3)\beta^{(1)}_{k_1,k_2,k_3}(\ell_1,\ell_2),\\
\beta^{(2)}(\ell_1,\ell_2)&=\phi(k_1,k_2,k_3)\beta^{(2)}_{p_1,p_2,p_3}(\ell_1,\ell_2)-\phi(p_1,p_2,p_3)\beta^{(2)}_{k_1,k_2,k_3}(\ell_1,\ell_2),
\end{aligned} \tag{2.104}$$

where the subscripts on α,β mean equation (2.100) with the indicated set of momenta.

Thus, despite the absence of integrability, we can solve the system of equations for three spin deviations. However, unlike the integrable Heisenberg model which is completely solved using two magnon data, the four spin deviation problem (and the more general r spin deviation problem) will need to be solved in its own right (see the discussion in [47]).

2.2.4 Alternating-Spin/Alternating-Bond Spin Chains

In this section, we state the alternating-spin/alternating-bond chain model, which is a generalization of the Hamiltonian in equation (2.17). The models we consider were studied in [51, 52] (see also [53, 54]).

We start by dividing the spin chain into even and odd-valued sublattices. To introduce alternating spin representations, we assume that even-valued sites host the spin-S' representation and odd-valued sites host the spin-S representation. In this case, the polynomial can be expanded to order $d=\min(S',S)$. Similar to [51], we will assume without loss of generality that $S'\leq S$. Then, depending on whether the sites are even-odd (eo) or odd-even (oe), the two site Hamiltonian becomes

$$H^{\text{eo}}_{2\ell,2\ell+1}=-\sum_{p=1}^{2S'}J^{(p)}(\mathbf{S'}_{2\ell}\cdot\mathbf{S}_{2\ell+1})^p,\quad H^{\text{oe}}_{2\ell+1,2\ell+2}=-\sum_{p=1}^{2S'}J^{(p)}(\mathbf{S}_{2\ell+1}\cdot\mathbf{S'}_{2\ell+2})^p, \tag{2.105}$$

where we have emphasised the even/odd sublattices in the lattice coordinates. Furthermore, one may deform the spin chain through the spin couplings by introducing couplings $J_1^{(p)}$ and $J_2^{(p)}$, thus leading to an alternating-spin/alternating-bond spin chain

$$H^{\text{eo}}_{2\ell,2\ell+1} = -\sum_{p=1}^{2S'} J_1^{(p)} (\mathbf{S'}_{2\ell} \cdot \mathbf{S}_{2\ell+1})^p, \quad H^{\text{oe}}_{2\ell+1,2\ell+2} = -\sum_{p=1}^{2S'} J_2^{(p)} (\mathbf{S}_{2\ell+1} \cdot \mathbf{S'}_{2\ell+2})^p. \tag{2.106}$$

Assuming the length L of the spin chain to be an even integer $L \in 2\mathbb{Z}$, the total Hamiltonian for the model is given by

$$\begin{aligned} H &= \sum_{\ell=1}^{L/2} \left[H^{\text{eo}}_{2\ell,2\ell+1} + H^{\text{oe}}_{2\ell+1,2\ell+2} \right] \\ &= -\sum_{\ell=1}^{L/2} \sum_{p=1}^{2S'} \left[J_1^{(p)} (\mathbf{S'}_{2\ell} \cdot \mathbf{S}_{2\ell+1})^p + J_2^{(p)} (\mathbf{S}_{2\ell+1} \cdot \mathbf{S'}_{2\ell+2})^p \right]. \end{aligned} \tag{2.107}$$

In Chapter 3,4 of this thesis, we will solve this type of model up to the two magnon case using the methods of [51, 52].

2.3 Integrable Spin Chains in Planar $\mathcal{N} = 4$ Super Yang-Mills Theory

In this section, we briefly demonstrate how spin chains arise in planar $\mathcal{N} = 4$ super Yang-Mills (SYM) theory. We only consider single trace operators constructed out of scalar fields in the $\mathcal{N} = 4$ supermultiplet in the large-N (planar) limit.

As we will argue, the problem of computing anomalous dimensions is transformed to the problem of diagonalising a mixing matrix (with eigenvalues being the anomalous dimensions). The problem is considerably complicated by the fact that the operators mix under the action of the mixing matrix and the space of operators grows very large. However, the discovery of integrability in [5] (through mapping the mixing matrix to the integrable Heisenberg ferromagnetic Hamiltonian) for a small closed subsector of the theory, made the problem solvable by spin chain methods.

Field Content

The field content of $\mathcal{N} = 4$ SYM belongs to the vector supermultiplet $\mathcal{B}^{\frac{1}{2},\frac{1}{2}}_{[0,1,0]}$ described in Section 2.1.1. Using the notation $[p, q, r]_{(j,\bar{j})}$ (recall that $[p, q, r]$ is the $\mathfrak{su}(4)_R$ Dynkin labels), the highest weight state has labels $[0, 1, 0]_{(0,0)}$. The Dynkin label $[0, 1, 0]$ is the antisymmetric selfdual $\mathbf{6}$ of $\mathfrak{su}(4)_R$ or the fundamental of $\mathfrak{so}(6)$. Thus, the highest weight state is given by six real scalars ϕ^I, $I = 4, ..., 9$

(we choose this numbering to align with [18] and the discussion in Section 2.4). Acting with the supergenerators $Q, \bar{Q}$, one may generate the remaining states in the supermultiplet (see page 37-38 of [33]). Acting once with the supergenerators yields the two descendant states $[1,0,0]_{(\frac{1}{2},0)}$ and $[0,0,1]_{(0,\frac{1}{2})}$. The Dynkin label $[1,0,0]$ is the fundamental $\mathbf{4}$ of $\mathfrak{su}(4)_R$ and $[0,0,1]$ is the antifundamental $\bar{\mathbf{4}}$ of $\mathfrak{su}(4)_R$. Thus, $[1,0,0]_{(\frac{1}{2},0)}$ is a left-moving Weyl fermion $\psi^A_{\ \alpha}$ and $[0,0,1]_{(0,\frac{1}{2})}$ is a right-moving Weyl fermion $\bar{\psi}_{A\dot{\alpha}}$, where $A = 1,..,4$. Finally, acting once more with the supergenerators, one obtains the descendants $[0,0,0]_{(1,0)}$ and $[0,0,0]_{(0,1)}$. This is the well-known decomposition of the antisymmetric field strength tensor $F_{\mu\nu}$ into its selfdual and anti-selfdual parts $F_{\alpha\beta}$ and $\bar{F}_{\dot{\alpha}\dot{\beta}}$ (see, for example, the discussion on page 41 of [55]). It is a scalar field with respect to the R-symmetry and contains the gauge field A_μ. Finally, although not needed for this thesis, we mention that $\mathcal{B}^{\frac{1}{2},\frac{1}{2}}_{[0,1,0]}$ also includes an arbitrary number of covariant derivatives $\mathcal{D}_{\alpha\dot{\alpha}}$ [28]. In summary, the field content for $\mathcal{N} = 4$ SYM is given by the set

$$V_{\mathcal{N}=4} = \{\phi^I, \psi^A_{\ \alpha}, \bar{\psi}_{A\dot{\alpha}}, F_{\alpha\beta}, \bar{F}_{\dot{\alpha}\dot{\beta}}\}, \qquad I = 4,...,9,\ A = 1,...,4, \tag{2.108}$$

and one may act with an arbitrary number $n \in \mathbb{N}$ covariant derivatives $\mathcal{D}^n\,[V_{\mathcal{N}=4}]$. All fields in the supermultiplet are in the adjoint representation of the gauge group $SU(N)$; in other words, for any field $\chi \in V_{\mathcal{N}=4}$,

$$\chi = \chi^a_{\ b} = \chi^m (T^m)^a_{\ b}, \quad a,b = 1,...,N,\ \chi^m \in \mathbb{C}, \tag{2.109}$$

where $T^m,\ m = 1,...,N^2-1$, are the traceless hermitian generators of $\mathfrak{su}(N)$. In particular, note that

$$(\chi^a_{\ b})^\dagger = \bar{\chi}^b_{\ a} = \bar{\chi}^m (T^m)^b_{\ a}. \tag{2.110}$$

Correlation Functions of Scalar Operators

We consider the problem of computing the anomalous dimensions of scalar operators in the theory. Observables are constructed out of single or multitrace trace operators (the trace is taken over the gauge indices and ensures gauge invariance) through the fields in $V_{\mathcal{N}=4}$. For example, one may construct the following single trace scalar operator consisting of a linear combination of L scalar fields inserted at a spacetime point x as follows

$$\mathcal{O}_{I_1 I_2 \cdots I_L}(x) = \chi_{I_1 I_2 \cdots I_L} \mathrm{Tr}(\phi^{I_1}\phi^{I_2}\cdots\phi^{I_L})(x), \tag{2.111}$$

where the coefficient $\chi_{I_1 I_2 \cdots I_L}$ is a totally symmetric traceless rank-L tensor of $\mathfrak{so}(6)$. Multitrace operators are constructed through products of traces but, since we are

considering the planar (large-N) limit, these multitrace sectors decouple from the theory and therefore do not contribute to single trace operator correlators.

To compute the conformal dimension Δ of $\mathcal{O}_{I_1 I_2 \cdots I_L}$, we observe that it appears explicitly in the two-point correlator of the single trace operator with itself (the spacetime dependence part is completely fixed by conformal symmetry, see [56])

$$\langle \mathcal{O}_{I_1 I_2 \cdots I_L}(x) \bar{\mathcal{O}}^{J_1 J_2 \cdots J_L}(y) \rangle \sim \frac{1}{|x-y|^{2\Delta}}, \tag{2.112}$$

where we have used $(\mathcal{O}_{J_1 J_2 \cdots J_L})^\dagger = \bar{\mathcal{O}}^{J_1 J_2 \cdots J_L}$ with the gauge indices transforming as in equation (2.110).

The scaling dimension Δ picks up corrective terms when quantum interactions are turned on; more precisely, $\Delta = \Delta_0 + \gamma(\lambda)$ where Δ_0 is the *classical* (non-quantum) scaling dimension of the field and $\gamma(\lambda)$ is the corrective factor called the *anomalous dimension*. The coupling λ is the well-known *'t Hooft coupling* [57]

$$\lambda = g_{YM}^2 N, \tag{2.113}$$

which is kept fixed for

$$N \to \infty, \quad g_{\mathrm{YM}} \to 0. \tag{2.114}$$

Here, g_{YM} is the Yang-Mills coupling. For $\lambda << 1$, the anomalous dimension can be determined perturbatively. In this section, we will determine $\gamma(\lambda)$ to first (one-loop) order.

It is insightful to first consider an example (we will follow [43, 35, 58, 7]). This example also allows us to introduce a convenient Feynman diagram approach for the large-N limit in which only planar diagrams survive. We start by combining the six scalar fields ϕ^I in the vector supermultiplet of $\mathcal{N} = 4$ into the following scalar fields (and their complex conjugates) [43]

$$Z = \frac{1}{\sqrt{2}}\left(\phi^4 + i\phi^5\right), \; X = \frac{1}{\sqrt{2}}\left(\phi^6 + i\phi^7\right), \; Y = \frac{1}{\sqrt{2}}\left(\phi^8 + i\phi^9\right). \tag{2.115}$$

In $d = 4$, each scalar field has $\Delta = 1$ and is, of course, spinless. In terms of the Cartan charges $(\Delta, j, \bar{j}; J_1, J_2, J_3)$ (Δ is the scaling dimension, $j, \bar{j}$ is the Lorentz charges and (J_1, J_2, J_3) is the R-charges of the Cartan subalgebra of $\mathfrak{su}(4)_R$ [2]). Thus, Z has

[2] To be explicitly clear, we will use parentheses for the Cartan charges (which can be half-integer valued) and brackets for the Dynkin labels (which are integer valued)

labels $(1,0,0;1,0,0)$, X has labels $(1,0,0;0,1,0)$ and Y has labels $(1,0,0;0,0,1)$. Then, the length L single trace operator ($L \geq 2$ since $\mathrm{Tr}(Z) = 0$)

$$\mathcal{O}(x) = \mathrm{Tr}\left(ZZ\cdots Z\right)(x), \tag{2.116}$$

has Cartan labels $(L,0,0;L,0,0)$ or, equivalently, $\Delta = J_1 = L$. It is an example of a *chiral operator* or 1/2-BPS operator as it is the highest weight state in the supermultiplet $\mathcal{B}^{\frac{1}{2},\frac{1}{2}}_{[0,p,0]}$ with $p = L$. As mentioned in Section 2.1.1, its conformal dimension Δ is fixed by supersymmetry to be $\Delta = p$ and thus, when considering the interacting theory, does not receive corrective terms (anomalous dimensions).

We will use the following two-point correlator [43] (see also [56])

$$\langle Z^a{}_b(x)\bar{Z}^c{}_d(y)\rangle = \frac{\delta^a{}_d\,\delta_b{}^c}{4\pi^2|x-y|^2}, \tag{2.117}$$

with spatial dependence determined completely by conformal symmetry. We normalize the above chiral operator as follows

$$\mathcal{O}_C(x) = \frac{(4\pi^2)^{L/2}}{\sqrt{L}N^{L/2}}\,\mathrm{Tr}(Z^L). \tag{2.118}$$

We consider the case when $L = 3$ (the following arguments can easily be generalized to L). We find the following correlator

$$\begin{aligned}\langle \mathcal{O}_C(x)\mathcal{O}_C(y)^\dagger\rangle &= \frac{(4\pi^2)^3}{3N^3}\,\langle\left(Z^a{}_bZ^b{}_cZ^c{}_a\right)(x)\left(Z^{a'}{}_{b'}Z^{b'}{}_{c'}Z^{c'}{}_{a'}\right)^\dagger(y)\rangle \\ &= \frac{(4\pi^2)^3}{3N^3}\,\langle Z^a{}_bZ^b{}_cZ^c{}_a\;\bar{Z}^{a'}{}_{c'}\bar{Z}^{c'}{}_{b'}\bar{Z}^{b'}{}_{a'}\rangle,\end{aligned} \tag{2.119}$$

where in the last line we suppressed the spacetime dependence. The correlator can be decomposed into two-point correlators using Wick contractions. However, in the large-N limit, not all of these terms will survive.

A useful diagrammatic approach is to use fat Feynman graphs where the gauge indices for the matrix fields are made explicit in the Feynman diagram (similar to [57]). The two-point correlator in equation (2.117) is represented by Figure 2.4 below.

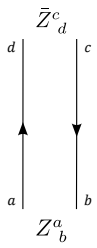

Figure 2.4: *The two-point correlator. The upper index flows away from the operator and the lower index flows towards the operator.*

There are six diagrams since there are 3! Wick contractions. Two of these diagrams are presented in Figure 2.5. Observe that Figure 2.5(a) has three closed loops. This translates to the following terms for the gauge indices

$$\begin{aligned}\langle Z^a{}_b Z^b{}_c Z^c{}_a \bar{Z}^{a'}{}_{c'} \bar{Z}^{c'}{}_{b'} \bar{Z}^{b'}{}_{a'} \rangle &\to \delta^a{}_{a'} \delta_b{}^{b'} \delta^b{}_{b'} \delta_c{}^{c'} \delta^c{}_{c'} \delta_a{}^{a'} \\ &= N^3.\end{aligned} \tag{2.120}$$

In other words, each closed loop contributes a factor of N. In contrast, Figure 2.5(b) only has one closed loop which matches the Wick contraction

$$\begin{aligned}\langle Z^a{}_b Z^b{}_c Z^c{}_a \bar{Z}^{a'}{}_{c'} \bar{Z}^{c'}{}_{b'} \bar{Z}^{b'}{}_{a'} \rangle &\to \delta^a{}_{a'} \delta_b{}^{b'} \delta^b{}_{c'} \delta_c{}^{a'} \delta^c{}_{b'} \delta_a{}^{c'} \\ &= N.\end{aligned} \tag{2.121}$$

Observe that Figure 2.5(a) is *planar* and Figure 2.5(b) is *non-planar*.

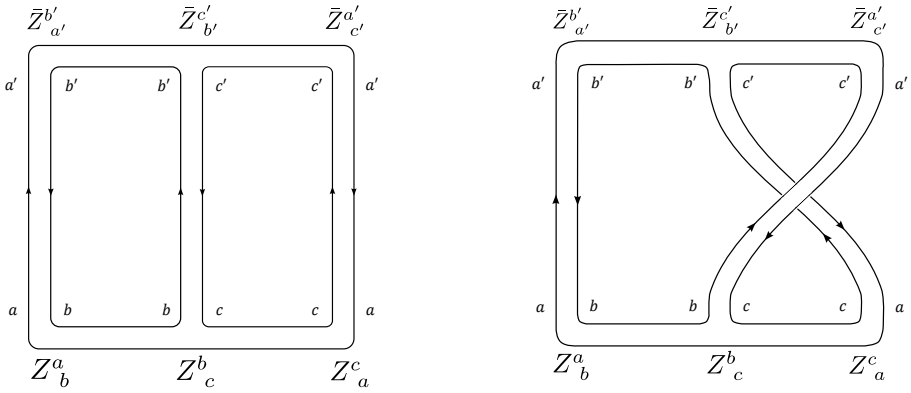

Figure 2.5: *Examples of Feynman graphs for the case L=3. (a) Planar diagram, (b) non-planar diagram.*

The non-planar diagram contributes to the overall correlator a term with $1/N^2$ which is subleading in the large-N limit. Thus, we ignore all non-planar diagrams. In total,

by shifting each connecting arm in the diagram by one site, there are three planar diagrams of order N^3. Inserting these results back into the correlator and adding the spacetime dependence (see equation (2.117)), we find that the correlator reduces to

$$\langle \mathcal{O}_C(x)\mathcal{O}_C(y)^\dagger\rangle = \frac{1}{|x-y|^6}, \quad \text{for } N \longrightarrow \infty. \tag{2.122}$$

The result easily generalizes to a string of L Z-fields [43]

$$\begin{aligned}\langle \mathcal{O}_C(x)\mathcal{O}_C(y)^\dagger\rangle &= \frac{LN^L}{(\sqrt{L}N^{L/2})^2|x-y|^{2L}} \\ &= \frac{1}{|x-y|^{2L}}.\end{aligned} \tag{2.123}$$

We note that the factor $\sqrt{L}$ in equation (2.118) counts the number of planar diagrams (which was 3 in the $L = 3$ example). Importantly, note that supersymmetry protects the conformal dimension of this special operator to all loop orders in the perturbative analysis.

We return to the general operator written in equation (2.111) but we normalize it as follows

$$\mathcal{O}_{I_1 I_2 \cdots I_L}(x) = \frac{(4\pi)^{L/2}}{\sqrt{C_{I_1 I_2 \cdots I_L}}N^{L/2}}\mathrm{Tr}(\phi^{I_1}\phi^{I_2}\cdots\phi^{I_L})(x), \tag{2.124}$$

where the $\mathfrak{so}(6)$ tensor $C_{I_1 I_2 \cdots I_L}$ is totally symmetric and traceless (it generalizes the factor $\sqrt{L}$ in equation (2.118)). It takes the maximal value n if the indices are invariant under shifts by L/n; in particular, if all the indices satisfy $I_1 = I_2 = \cdots = I_L$ and are invariant under shifts by 1, so that $n = L$, we recover the normalization in equation (2.118) [43, 35]. Generally, these operators do have anomalous dimensions added to their classical conformal dimensions. We therefore consider the problem of computing the anomalous dimension. Since we are only considering scalar operators, we only need to consider the bosonic part of the $\mathcal{N} = 4$ SYM action, which is given by [43]

$$\begin{aligned}S_{\mathcal{N}=4} = \frac{1}{2g_{YM}^2}\int d^4x\Big(&-\frac{1}{2}\mathrm{Tr}F^2 + \mathrm{Tr}\mathcal{D}_\mu\phi_I\mathcal{D}^\mu\phi^I - \frac{1}{2}\mathrm{Tr}[\phi_I,\phi_J]^2 \\ &+ \text{fermions}\Big).\end{aligned} \tag{2.125}$$

We examine, in particular, the quartic scalar interaction term (in terms of the R-symmetry, we will argue that the other interaction terms only contribute terms proportional to the identity; the proportionality constant can be fixed by using our knowledge of representation theory). Rescaling the fields by absorbing a factor of

g_{YM}, the quartic interaction term (which we represent with the symbol $\mathcal{K}$) can be expanded as

$$\mathcal{K}(x) = \frac{g_{\mathrm{YM}}^2}{4} \sum_{I,J} \left(\mathrm{Tr}(\phi_I \phi_I \phi_J \phi_J)(x) - \mathrm{Tr}(\phi_I \phi_J \phi_I \phi_J)(x)\right). \tag{2.126}$$

We can represent these interaction terms as a vertex with four connections. For example, the first term in $\mathcal{K}(x)$ can be represented as in Figure 2.6.

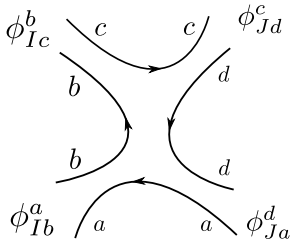

Figure 2.6: *Four vertex diagram for the first term in $\mathcal{K}$ (the second term is similar).*

Then, inserting these terms into the correlator, we can use the Feynman diagram approach from our example to compute the Wick contractions in the planar limit. We will calculate the one-loop (first order) correction to the two-point correlator in the planar limit

$$\begin{aligned} &\langle \mathcal{O}_{I_1 I_2 \cdots I_L}(x) \bar{\mathcal{O}}^{J_1 J_2 \cdots J_L}(y) \rangle \\ &\approx \langle \mathcal{O}_{I_1 I_2 \cdots I_L}(x) \bar{\mathcal{O}}^{J_1 J_2 \cdots J_L}(y) \rangle_{(0)} + \langle \mathcal{O}_{I_1 I_2 \cdots I_L}(x) \bar{\mathcal{O}}^{J_1 J_2 \cdots J_L}(y) \rangle_{(1)}, \end{aligned} \tag{2.127}$$

where the subscript (0) indicates zero-order/tree-level and (1) indicates the first-order/one-loop correction. The tree-level correlator is given by

$$\begin{aligned} &\langle \mathcal{O}_{I_1 I_2 \cdots I_L}(x) \bar{\mathcal{O}}^{J_1 J_2 \cdots J_L}(y) \rangle_{(0)} \\ &= \frac{1}{C_{I_1 I_2 \cdots I_L}} \left(\delta_{I_1}^{J_1} \delta_{I_2}^{J_2} \cdots \delta_{I_L}^{J_L} + \text{cycles} \right) \frac{1}{|x-y|^{2L}}. \end{aligned} \tag{2.128}$$

The first term with the delta symbols is the generalized version of Figure 2.5. The term *cycles* means all shifts of the connecting arms by one site (which is the other possible planar diagrams). This will, for example, give the term $\delta_{I_1}^{J_2} \delta_{I_2}^{J_3} \cdots \delta_{I_L}^{J_1}$ (and similar for the other terms).

The one-loop correlator is computed the same as the tree level correlator, except for the insertion of the two vertices given by $\mathcal{K}(z)$

$$\begin{aligned} &\langle \mathcal{O}_{I_1 I_2 \cdots I_L}(x) \bar{\mathcal{O}}^{J_1 J_2 \cdots J_L}(y) \rangle_{(1)} \\ &= \langle \mathcal{O}_{I_1 I_2 \cdots I_L}(x) \left(i \int d^4 z \, \mathcal{K}(z) \right) \bar{\mathcal{O}}^{J_1 J_2 \cdots J_L}(y) \rangle_{(0)}. \end{aligned} \tag{2.129}$$

Following [43], we consider the subcorrelator

$$\langle (\phi_{I_k}\phi_{I_{k+1}})^a{}_c(x)\; i\int d^4z\,\mathcal{K}(z)\;(\phi^{J_{k+1}}\phi^{J_k})^{c'}{}_{a'}(y)\rangle. \tag{2.130}$$

In Figure 2.7, we show the Feynman diagram with one of the terms from the scalar vertex $\mathcal{K}$ inserted (we suppressed the gauge indices).

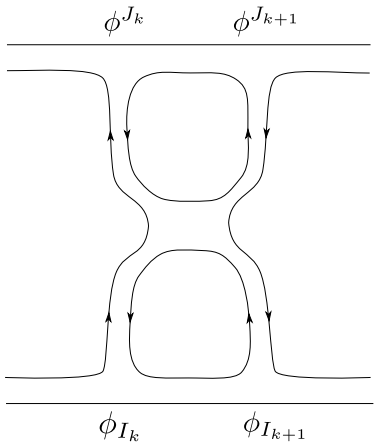

Figure 2.7: *A term from the scalar vertex $\mathcal{K}$ inserted into the subcorrelator. The open ends of the diagram illustrate the fact that we are only considering a section of the entire Feynman diagram.*

For both terms in $\mathcal{K}$, there are two closed color loops in each diagram which therefore contributes a factor of N^2. For the first term, given by the vertex in Figure 2.6, the R-symmetry indices flow as $\delta_{I_kI}\delta_{I_{k+1}I}\delta^{J_k}_J\delta^{J_{k+1}}_J = \delta_{I_kI_{k+1}}\delta^{J_kJ_{k+1}}$. In the same manner and by rotating the vertex, we obtain three more terms to find a total contribution

$$2N^2\delta^a{}_{a'}\delta_c{}^{c'}\;\delta_{I_kI_{k+1}}\delta^{J_kJ_{k+1}} + 2N^2\delta^a{}_{a'}\delta_c{}^{c'}\;\delta_{I_k}{}^{J_k}\delta_{I_{k+1}}{}^{J_{k+1}}. \tag{2.131}$$

The vertex for the second term (which has the same diagram as Figure 2.6 except for the R-symmetry indices) works identically the same and gives the total contribution

$$4N^2\delta^a{}_{a'}\delta_c{}^{c'}\;\delta_{I_kI}\delta_{I_{k+1}J}\delta^{J_k}_J\delta^{J_{k+1}}_I = 4N^2\delta^a{}_{a'}\delta_c{}^{c'}\;\delta_{I_k}{}^{J_{k+1}}\delta_{I_{k+1}}{}^{J_k}. \tag{2.132}$$

Importantly, notice that the scalar vertex can only connect nearest-neighbour sites since next-to-nearest-neighbour sites, say, will lead to a non-planar diagram.

Using equation (2.117) (there are four propagators in Figure 2.7), the subcorrelator

is thus given by [43]

$$\begin{aligned}
&\langle(\phi_{I_k}\phi_{I_{k+1}})^a_{\ c}(x)\; i\int d^4z\,\mathcal{K}(z)\;(\phi^{J_{k+1}}\phi^{J_k})^{c'}_{\ a'}(y)\rangle \\
&= i\frac{N}{(4\pi^2)^4}\,\delta^a_{\ a'}\delta_c^{\ c'}\frac{g_{YM}^2N}{4}\left(2\delta_{I_kI_{k+1}}\delta^{J_kJ_{k+1}}+2\delta_{I_k}^{\ J_k}\delta_{I_{k+1}}^{\ J_{k+1}}-4\delta_{I_k}^{\ J_{k+1}}\delta_{I_{k+1}}^{\ J_k}\right) \\
&\times\int\frac{d^4z}{|z-x|^4|z-y|^4}.
\end{aligned}\tag{2.133}$$

The integral over z remains to be determined for the subcorrelator. Following [43], we note that the integral is logarithmically divergent for $z\to x$ and $z\to y$ and it is therefore required to regularize the integral by adding a UV cutoff Λ (for long range $z\to\infty$, the integral is well behaved and therefore free of IR divergences). We also Wick rotate from Minkowski space to Euclidean space $d^4z\to id^4z_E$. The integral is restricted to $|z_E-x|\le\Lambda^{-1},\ |z_E-y|\le\Lambda^{-1}$ and is dominated by regions near the cutoff Λ. It can be approximated to [43]

$$\begin{aligned}
i\int\frac{d^4z_E}{|z-x|^4|z-y|^4}&\approx\frac{2i}{|x-y|^4}\int_{\Lambda^{-1}}^{|x-y|}\frac{d^4\rho\;d\Omega_3}{\rho} \\
&=\frac{2\pi^2i}{|x-y|^4}\ln\left(\Lambda^2|x-y|^2\right).
\end{aligned}\tag{2.134}$$

Thus, using the 't Hooft coupling λ, the subcorrelator reduces to

$$\begin{aligned}
&\langle(\phi_{I_k}\phi_{I_{k+1}})^a_{\ c}(x)\; i\int d^4z\,\mathcal{K}(z)\;(\phi^{J_{k+1}}\phi^{J_k})^{c'}_{\ a'}(y)\rangle \\
&=\frac{N\delta^a_{\ a'}\delta_c^{\ c'}}{(4\pi^2)^2|x-y|^4}\;\frac{\lambda}{16\pi^2}\left(2\delta_{I_k}^{\ J_{k+1}}\delta_{I_{k+1}}^{\ J_k}-\delta_{I_kI_{k+1}}\delta^{J_kJ_{k+1}}-\delta_{I_k}^{\ J_k}\delta_{I_{k+1}}^{\ J_{k+1}}\right) \\
&\times\;\ln\left(\Lambda^2|x-y|^2\right).
\end{aligned}\tag{2.135}$$

Notice that the first term with delta symbols is a permutation term and the second term is a trace term (the third term is, of course, an identity term). As in [43], we therefore find the one-loop correlator contribution

$$\begin{aligned}
&\langle O_{I_1I_2\cdots I_L}(x)\bar{O}^{J_1J_2\cdots J_L}(y)\rangle_{(1)}=\frac{\lambda}{16\pi^2}\frac{\ln\left(\Lambda^2|x-y|^2\right)}{|x-y|^{2L}} \\
&\times\sum_{\ell=1}^{L}\left(2P_{\ell,\ell+1}-K_{\ell,\ell+1}-1+C\right)\frac{1}{\sqrt{C_{I_1I_2\cdots I_L}C_{J_1J_2\cdots J_L}}}\,\delta_{I_1}^{\ J_1}\delta_{I_2}^{\ J_2}\cdots\delta_{I_L}^{\ J_L} \\
&+\text{cycles},
\end{aligned}\tag{2.136}$$

where we have defined the nearest-neighbour permutation operator $P_{\ell,\ell+1}$ which acts on sites $\ell,\ell+1$ and trivially elsewhere [43]

$$P_{\ell,\ell+1}\delta_{I_1}^{\ J_1}\delta_{I_2}^{\ J_2}\cdots\delta_{I_\ell}^{\ J_\ell}\delta_{I_{\ell+1}}^{\ J_{\ell+1}}\cdots\delta_{I_L}^{\ J_L}=\delta_{I_1}^{\ J_1}\delta_{I_2}^{\ J_2}\cdots\delta_{I_\ell}^{\ J_{\ell+1}}\delta_{I_{\ell+1}}^{\ J_\ell}\cdots\delta_{I_L}^{\ J_L},\tag{2.137}$$

and the nearest-neighbour trace operator $K_{\ell,\ell+1}$ as [43]

$$K_{\ell,\ell+1}\delta_{I_1}^{J_1}\delta_{I_2}^{J_2}\cdots\delta_{I_\ell}^{J_\ell}\delta_{I_{\ell+1}}^{J_{\ell+1}}\cdots\delta_{I_L}^{J_L} = \delta_{I_1}^{J_1}\delta_{I_2}^{J_2}\cdots\delta_{I_\ell I_{\ell+1}}\delta^{J_\ell J_{\ell+1}}\cdots\delta_{I_L}^{J_L}. \tag{2.138}$$

As in [43], we have added an extra constant term C (in other words, a term proportional to the identity). This accounts for the other interacting terms from the action that contribute and is shown in Diagram (2.8) (we have suppressed the double-line notation).

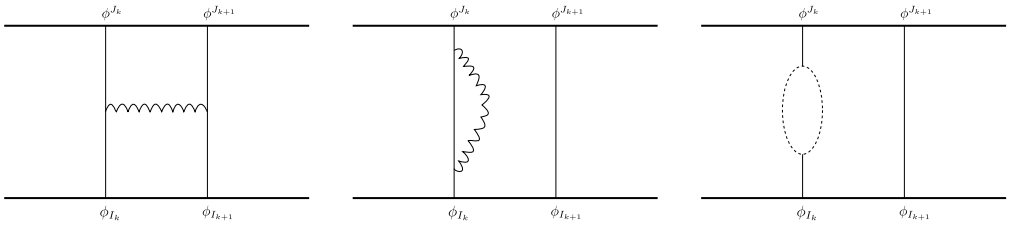

(a) *(b)* (c)

Figure 2.8: *The remaining one-loop contributions from the $\mathcal{N} = 4$ SYM action. (a) Gluon exchange, (b) scalar self-energy from a gluon and (c) scalar self-energy from a fermion loop.*

For (a) and (b) (which displays gluon exchange and scalar self-energy from a gluon, respectively), we know that the gauge field A_μ is not charged under $\mathfrak{su}(4)_R$ (see the discussion about the field content at the beginning of this section) and thus does not affect the incoming-to-outgoing R-symmetry indices (in other words, it contributes a term proportional to the identity). Finally, for (c) (which displays scalar self-energy from a fermion loop), the contribution is again proportional to the identity since the fermion loop involves only one scalar and R-charge conservation (thus, leading to the contribution $\delta_{I_k}^{J_k}$ for site k). The constant C will be fixed when we consider the $\mathfrak{su}(2)$ closed subsector (see equation (2.141)).

In total, adding the tree-level correlator and the one-loop correlator, we find [43]

$$\begin{aligned}
&\langle \mathcal{O}_{I_1 I_2\cdots I_L}(x)\bar{\mathcal{O}}^{J_1 J_2\cdots J_L}(y)\rangle \\
&\approx \langle \mathcal{O}_{I_1 I_2\cdots I_L}(x)\bar{\mathcal{O}}^{J_1 J_2\cdots J_L}(y)\rangle_{(0)} + \langle \mathcal{O}_{I_1 I_2\cdots I_L}(x)\bar{\mathcal{O}}^{J_1 J_2\cdots J_L}(y)\rangle_{(1)} \\
&= \frac{1}{|x-y|^{2L}}\left(1 - \frac{\lambda}{16\pi^2}\ln\left(\Lambda^2|x-y|^2\right)\right. \\
&\left.\times \sum_{\ell=1}^{L}\left(C - 1 - 2P_{\ell,\ell+1} + K_{\ell,\ell+1}\right)\ \delta_{I_1}^{J_1}\delta_{I_2}^{J_2}\cdots\delta_{I_L}^{J_L}\right) + \text{cycles} \\
&= \frac{1}{|x-y|^{2L}}\left(1 - \ln\left(\Lambda^2|x-y|^2\right)\Gamma\ \delta_{I_1}^{J_1}\delta_{I_2}^{J_2}\cdots\delta_{I_L}^{J_L}\right) + \text{cycles},
\end{aligned} \tag{2.139}$$

where we have defined the one-loop *mixing matrix* Γ [43]

$$\Gamma = \frac{\lambda}{16\pi^2}\sum_{\ell=1}^{L}\left(C - 1 - 2P_{\ell,\ell+1} + K_{\ell,\ell+1}\right), \tag{2.140}$$

with the constant C to still be determined. The anomalous dimensions at one-loop are determined by diagonalizing the mixing matrix Γ.

Closed $\mathfrak{su}(2)$ Subsector and Spin Chain Identification

For a given length L spin chain, the vector space spanned by basis states that diagonalise Γ can be enormous (due to operator mixing) and, thus, a difficult linear algebra problem. However, starting with the insights of [5] and the discovery of integrability, the diagonalisation problem becomes much more tractable.

We consider a closed subsector $\mathfrak{su}(2) \subset \mathfrak{su}(4)_R$ which is constructed out of the doublet $\{Z, X\}$. By closed, we mean the following: we consider single trace operators constructed out of strings of Z and X fields. For a single trace operator $\mathrm{Tr}(Z^{L-M}X^M)$, we have the Cartan charges $(L, 0, 0; L-M, M, 0)$ (see the discussion around equation (2.115)). The action of Γ preserves these charges and can only mix single trace operators constructed out of Z, X fields, up to reshuffled combinations, with the same charges.

We consider again a length L single trace chiral operator $\mathcal{O}_C$ made out of a string of Z-fields as in equation (2.118). From our previous arguments, we know that this operator's scalar dimension $\Delta = L$ is protected by supersymmetry from correction terms (since it is the highest weight state of $\mathcal{B}^{\frac{1}{2},\frac{1}{2}}_{[0,L,0]}$); in other words, this operator does not have an anomalous dimension and is, therefore, an eigenstate of Γ (with eigenvalue 0). For a string of Z-fields, the action of the permutation operator is $P_{\ell,\ell+1}\mathcal{O}_C = \mathcal{O}_C$ and the action of the trace operator is $K_{\ell,\ell+1}\mathcal{O}_C = 0$ (since there are no conjugate fields in this subsector). Thus,

$$\begin{aligned}\Gamma\,\mathcal{O}_C &= \frac{\lambda}{16\pi^2}\sum_{\ell=1}^{L}(1 - C - 2)\,\mathcal{O}_C = 0\\ \Rightarrow\ C &= -1.\end{aligned} \tag{2.141}$$

This fixes C in equation (2.140). For this subsector then, the mixing matrix reduces to [5, 43]

$$\Gamma = \frac{\lambda}{8\pi^2}\sum_{\ell=1}^{L}\left(1 - P_{\ell,\ell+1}\right). \tag{2.142}$$

The insight from [5] is that we can precisely match this with the spin-1/2 Heisenberg ferromagnetic spin chain model; more precisely, we identify Γ with the Hamiltonian in equation (2.28) (see in particular equation (2.39)) with $J/2 = \lambda/(8\pi^2) \Rightarrow J = \lambda/(4\pi^2)$.

For the spin deviations, we identify the chiral primary operator $\mathcal{O}_C$ with the spin-1/2 ground state in equation (2.32) and $Z = \uparrow$. Spin deviations are introduced by $X = \downarrow$. For example,

$$\mathrm{Tr}(ZZZXZZZXZ) \mapsto |\uparrow\uparrow\uparrow\downarrow\uparrow\uparrow\uparrow\downarrow\uparrow\rangle. \tag{2.143}$$

The r-spin deviation problem for this model is solved using the methods shown in Section 2.2.2. The $\mathfrak{su}(2)$ subsector is thus planar integrable at one-loop.

In fact, for $\mathcal{N} = 4$ SYM, planar integrability extends to the full scalar sector [6] as well as to higher loop orders [7, 59, 60]. From this viewpoint, it is interesting to understand what happens in more general theories, especially theories with less supersymmetry.

2.4 $\mathcal{N} = 2$ Quiver Gauge Theory

In this section, we discuss the class of $\mathcal{N} = 2$ theories which arise as an orbifold of $\mathcal{N} = 4$ SYM. In particular, we will use the discrete abelian group $\mathbb{Z}_2$ to reduce the supersymmetry from $\mathcal{N} = 4$ to $\mathcal{N} = 2$. The orbifold procedure also has an action inside the gauge group which leads to a product of gauge groups [12]. Furthermore, the corresponding two gauge couplings, which can be collected into a deformation parameter κ, can be deformed without breaking the conformal symmetry of the theory. We thus obtain a one-parameter family of $\mathcal{N} = 2$ theories that can be marginally deformed.

We also derive the one-loop Hamiltonian for two closed scalar subsectors. For the spin chains studied in this thesis, it will be most convenient to work in the "upstairs" picture using the $\mathcal{N} = 4$ chiral fields. The Hamiltonian in the "downstairs" picture using the $\mathcal{N} = 2$ orbifold projected fields is discussed in detail in Appendix B.

2.4.1 $\mathcal{N} = 2$ Quiver Theory from $\mathbb{Z}_2$ Orbifold of $\mathcal{N} = 4$ SYM

In Section 2.3, we discussed the field content for $\mathcal{N} = 4$ SYM. For this section, we will follow the discussion in [18, 61]. We will also use their notation X_I, $I = 4, ..., 9$ to represent the six real scalar fields. The symbol ϕ will be used for the orbifold projected scalar fields.

From Section 2.3, the field content of $\mathcal{N} = 4$ SYM consists of a gauge field A_μ, four Weyl fermions λ^A_α and real scalar fields X_I. The fermions λ^A_α transform in the fundamental **4** of $\mathfrak{su}(4)_R$ and the scalars X_I transform in the vector representation **6** of $\mathfrak{so}(6)$, which is the antisymmetric selfdual **6** of $\mathfrak{su}(4)_R$. The gauge field is scalar with respect to the R-symmetry. All fields transform in the adjoint of the gauge group $SU(N)$. For the scalars, we can make the $\mathfrak{su}(4)_R$ symmetry more manifest by combining the six real scalars into a selfdual antisymmetric matrix X_{AB}, $A, B = 1, ..., 4$, where the reality (selfdual) condition is given by

$$(X_{AB})^\dagger = \frac{1}{2}\epsilon^{ABCD}X_{CD}. \tag{2.144}$$

Hermitian conjugation is performed in color space. Explicitly, the matrix X_{AB} is given by [18]

$$X_{AB} = \frac{1}{\sqrt{2}}\left(\begin{array}{cc|cc} 0 & X_4 + iX_5 & X_7 + iX_6 & X_8 + iX_9 \\ -X_4 - iX_5 & 0 & X_8 - iX_9 & -X_7 + iX_6 \\ \hline -X_7 - iX_6 & -X_8 + iX_9 & 0 & X_4 - iX_5 \\ -X_8 - iX_9 & X_7 - iX_6 & -X_4 + iX_5 & 0 \end{array}\right) \tag{2.145}$$

The construction of the matrix can be found in [62, 63]. As in [18, 61], the matrix is divided into four quadrants which is useful for the discussion below.

Using the conventions in [18, 61], we pick out a $SU(2)_L \times SU(2)_R \times U(1)_r \subset SU(4)_R$. In particular, for the orbifold theory, we will choose $SU(2)_R \times U(1)_r$ as the $\mathcal{N} = 2$ R-symmetry group with an additional global flavour symmetry given by $SU(2)_L$. Define submatrices $\mathcal{Z}_{\mathcal{I}\mathcal{J}}$ and $\mathcal{X}_{\mathcal{I}\hat{\mathcal{I}}}, \mathcal{I}, \mathcal{I} = \pm, \hat{\mathcal{I}} = \hat{\pm}$, as

$$\mathcal{Z}_{\mathcal{I}\mathcal{J}} = \begin{pmatrix} 0 & Z \\ -Z & 0 \end{pmatrix}, \qquad \mathcal{X}_{\mathcal{I}\hat{\mathcal{I}}} = \frac{1}{\sqrt{2}}\begin{pmatrix} X_7 + iX_6 & X_8 + iX_9 \\ X_8 - iX_9 & -X_7 + iX_6 \end{pmatrix}, \tag{2.146}$$

where $Z = \frac{1}{\sqrt{2}}(X_4 + iX_5)$ and $\mathcal{X}_{\mathcal{I}\hat{\mathcal{I}}}$ obeys the reality condition $(\chi_{\mathcal{I}\hat{\mathcal{I}}})^\dagger = -\epsilon^{\mathcal{I}\mathcal{J}}\epsilon^{\hat{\mathcal{I}}\hat{\mathcal{J}}}\chi_{\mathcal{J}\hat{\mathcal{J}}}$. An index $\mathcal{I}$ will transform under $SU(2)_R$ and an index $\hat{\mathcal{I}}$ will transform under $SU(2)_L$. This divides X_{AB} into

$$X_{AB} = \left(\begin{array}{c|c} \mathcal{Z}_{\mathcal{I}\mathcal{J}} & \mathcal{X}_{\mathcal{I}\hat{\mathcal{I}}} \\ \hline (\mathcal{X}_{\mathcal{I}\hat{\mathcal{I}}})^\dagger & \bar{\mathcal{Z}}_{\hat{\mathcal{I}}\hat{\mathcal{J}}} \end{array}\right). \tag{2.147}$$

Schematically,

$$X_{AB} = \left(\begin{array}{c|c} SU(2)_R \times U(1)_r & \\ \hline & SU(2)_L \times U(1)_r^* \end{array}\right). \tag{2.148}$$

Note that the first quadrant in the above matrix has labels I, J and the fourth quadrant has labels $\hat{I}, \hat{J}$; the second and third quadrants have mixed labels $I, \hat{I}$.

Using the conventions in [18, 61], Z transforms under $U(1)_r$ with charge -1; the total symmetry group for $\mathcal{Z}_{\mathcal{I}\mathcal{J}}$ is $SU(2)_R \times U(1)_r$. The matrix $\mathcal{X}_{I\hat{I}}$ is in the bifundamental of $SU(2)_L \times SU(2)_R$ and is neutral with respect to $U(1)_r$.

We note, as in [18, 61], that $SU(2)_L \times SU(2)_R \simeq SO(4)$ rotates the fields 6789 into one another and $U(1)_r \simeq SO(2)$ rotates the fields 45 into one another. Furthermore, diagonal $SU(2)$ transformations preserve $\mathrm{Tr}(\mathcal{X}_{I\hat{I}}) = 2iX_6$ and thus correspond to 789 rotations.

$\mathbb{Z}_2$ Orbifold

To reduce the amount of supersymmetry, we use an abelian finite discrete group $\Gamma = \mathbb{Z}_p$ that is embedded into both the gauge group and the R-symmetry group [12]. For $\Gamma \subset SU(pN)$, the subgroup is generated by the block diagonal $(pN \times pN)$-generator [62, 12, 14, 13]

$$\gamma = \begin{pmatrix} \mathbb{1}_{N\times N} & & & \\ & \omega\mathbb{1}_{N\times N} & & \\ & & \ddots & \\ & & & \omega^{p-1}\mathbb{1}_{N\times N} \end{pmatrix}, \quad \omega = e^{\frac{2\pi i}{p}}. \tag{2.149}$$

For the R-symmetry group $SU(4)_R$, the generator is given by four phases specified by a set of four integers $q_A,\ A = 1, ..., 4$, with the condition $q_1 + q_2 + q_3 + q_4 = 0 \bmod p$ [62, 14]. The action on the Weyl fermions is given by

$$\lambda^A \to e^{\frac{2\pi i q_A}{p}} \lambda^A, \tag{2.150}$$

and the action on the scalar fields is given by

$$X_{AB} \to e^{\frac{2\pi i (q_A + q_B)}{p}} X_{AB}. \tag{2.151}$$

The gauge field A_μ is, of course, scalar with respect to the R-symmetry. Then, the orbifold gauge theory is specified by the constraint [14, 62]

$$A_\mu = \gamma A_\mu \gamma^{-1}, \quad \lambda^A = \omega^{q_A} \gamma \lambda^A \gamma^{-1}, \quad X_{AB} = \omega^{q_A + q_B} \gamma X_{AB} \gamma^{-1}. \tag{2.152}$$

Written slightly differently, we have

$$A_\mu \gamma = \gamma A_\mu, \quad \lambda^A \gamma = \omega^{q_A} \gamma \lambda^A, \quad X_{AB}\gamma = \omega^{q_A + q_B} \gamma X_{AB}. \tag{2.153}$$

Fields that exchange with γ are referred to as the *untwisted* sector while fields that pick up an additional phase when exchanged with γ are referred to as the *twisted* sector [28, 14, 13]. These sectors will play a role in Section 3.3.

We specialize to $p = 2$ so that $\Gamma = \mathbb{Z}_2$. Without loss of generality, we take $q_1 = q_2 = 0$ and $q_3 = -q_4 = 1$. The subgroup embedded inside the gauge group $SU(2N)$ is then generated by

$$\gamma = \begin{pmatrix} \mathbb{1}_{N\times N} & 0 \\ 0 & -\mathbb{1}_{N\times N} \end{pmatrix}. \tag{2.154}$$

Defining

$$\lambda^A = \begin{pmatrix} \lambda_I \\ \lambda_{\hat{I}} \end{pmatrix}, \tag{2.155}$$

and using equation (2.147), the action of $\mathbb{Z}_2$ on the fields is then given by

$$A_\mu \mapsto \gamma A_\mu \gamma, \quad \mathcal{Z}_{IJ} \mapsto \gamma \mathcal{Z}_{IJ}\gamma, \quad \mathcal{X}_{I\hat{I}} \mapsto -\gamma \mathcal{X}_{I\hat{I}}\gamma, \quad \lambda_I \mapsto \gamma\lambda_I\gamma, \quad \lambda_{\hat{I}} \mapsto -\gamma\lambda_{\hat{I}}\gamma. \tag{2.156}$$

Under the constraint in equation (2.152), we find the $\mathbb{Z}_2$-invariant fields stated in[3] [18, 61]

$$A_\mu = \begin{pmatrix} A_{\mu\ b}^{a} & 0 \\ 0 & \check{A}_{\mu\ \check{b}}^{\check{a}} \end{pmatrix}, \quad Z = \begin{pmatrix} \phi^a_{\ b} & 0 \\ 0 & \check{\phi}^{\check{a}}_{\ \check{b}} \end{pmatrix}, \quad \lambda_I = \begin{pmatrix} \lambda^a_{I\ b} & 0 \\ 0 & \check{\lambda}^{\check{a}}_{I\ \check{b}} \end{pmatrix}, \quad \lambda_{\hat{I}} = \begin{pmatrix} 0 & \psi^a_{\hat{I}\ \check{a}} \\ \tilde{\psi}^{\check{b}}_{\hat{I}\ b} & 0 \end{pmatrix},$$
$$\mathcal{X}_{I\hat{I}} = \begin{pmatrix} 0 & Q^a_{I\hat{I}\ \check{a}} \\ -\epsilon_{I\mathcal{J}}\epsilon_{\hat{I}\hat{\mathcal{J}}}\tilde{Q}^{\check{b}\hat{\mathcal{J}}\mathcal{J}}_{\ \ b} & 0 \end{pmatrix}. \tag{2.157}$$

The $\mathbb{Z}_2$ projection factors the gauge group $SU(2N)$ into a product $SU(N_1)\times SU(N_2)$. An index a will transform under $SU(N_1)$ and an index $\check{a}$ will transform under $SU(N_2)$. In addition, the R-symmetry $SU(4)_R$ is broken to $SU(2)_R \times U(1)_r$. The supergenerators for $SU(2)_L$ are projected out and, thus, $SU(2)_L$ becomes a global bosonic flavour symmetry. In $\mathcal{N} = 2$ language, we have [18, 1]

- Two $\mathcal{N} = 2$ vector multiplets in the adjoint of each gauge group: $\{\phi, \lambda_\mathcal{I}, A_\mu\}$ and $\{\check{\phi}, \check{\lambda}_\mathcal{I}, \check{A}_\mu\}$, $\quad \mathcal{I} = \pm$,
- Two hypermultiplets in the bifundamental of the gauge groups: $\{Q_{\mathcal{I}\dot{+}}, \psi_{\dot{+}}, \tilde{\psi}_{\dot{+}}\}$, $\{Q_{\mathcal{I}\dot{-}}, \psi_{\dot{-}}, \tilde{\psi}_{\dot{-}}\}$, $\quad \mathcal{I} = \pm$.

[3] Any field with a single $\hat{I}$ index will pick up a factor of -1. For example, $\chi_{-\dot{-}} = X_{13} \mapsto e^{i(q_1+q_3)\pi}X_{13} = -X_{13} = -\chi_{-\dot{-}}$.

The $\mathcal{N} = 2$ vector multiplets belong to the $\mathcal{D}_{0(0,0)}$ supermultiplet discussed in Section 2.1.1. The hypermultiplets belongs to the $\hat{\mathcal{B}}_{\frac{1}{2}}$ supermultiplet. Following the conventions of [18], the R-symmetry charges are listed in table (2.1) together with the product gauge group representations and the $SU(2)_L$ flavour symmetry.

$\mathcal{N} = 2$ **Quiver Symmetries**					
	$SU(N)$	$SU(\check{N})$	$SU(2)_R$	$SU(2)_L$	$U(1)_r$
A_μ	adj	**1**	**1**	**1**	0
$\check{A}_\mu$	**1**	adj	**1**	**1**	0
ϕ	adj	**1**	**1**	**1**	-1
$\check{\phi}$	**1**	adj	**1**	**1**	-1
$\lambda^{\mathcal{I}}$	adj	**1**	**2**	**1**	-1/2
$\hat{\lambda}^{\mathcal{I}}$	**1**	adj	**2**	**1**	-1/2
$Q_{\mathcal{I}\hat{\mathcal{I}}}$	$\square$	$\overline{\square}$	**2**	**2**	0
$\psi^{\hat{\mathcal{I}}}$	$\square$	$\overline{\square}$	**1**	**2**	+1/2
$\check{\psi}^{\hat{\mathcal{I}}}$	$\overline{\square}$	$\square$	**1**	**2**	+1/2

Table 2.1: *The $\mathcal{N} = 2$ orbifold fields and their symmetries [18].* For the conjugate fields, the results are similar except for conjugating the gauge group representations and the $U(1)_r$ charge.

We will focus on the $\mathcal{N} = 2$ SCFT which interpolates between the $\mathbb{Z}_2$ orbifold of $\mathcal{N} = 4$ SYM and $\mathcal{N} = 2$ superconformal QCD (SCQCD). Starting from the $\mathbb{Z}_2$ orbifold where the couplings of the two gauge groups are equal, $g_1 = g_2$, also known as the orbifold point, we will be interested in the marginally deformed theory with $g_1 \neq g_2$. The marginal deformation introduces an one parameter family of theories parametrised by the ratio $\kappa = g_2/g_1$. Without loss of generality, we will take $\kappa \leq 1$. For all allowed values of $\kappa \in [0, 1]$ this one parameter family of theories enjoys the full $\mathcal{N} = 2$ superconformal algebra (SCA) including the $SU(2)_R \times U(1)_r$ R-symmetries but also an extra $SU(2)_L$ global symmetry which is special for the $\mathbb{Z}_2$ quiver.

The edge of the conformal manifold where $g_2 \to 0$ or equivalently $\kappa \to 0$ is special. In this limit, the second gauge group gets ungauged and becomes a global symmetry, which combines with the extra $SU(2)_L$ to give the $U(N_f) = U(2N)$ flavour symmetry of SCQCD; more precisely, the ungauged index $\check{a}$ and the flavour symmetry $SU(2)_L$ can be combined into a single enhanced index $i = (\check{a}, \mathcal{I}) = 1, ..., N_f$ with $N_f = 2N$ [18, 28].[4]

[4]In the limit $\kappa \to 0$ the spin chain states (single trace local operators) which are not in a $SU(2)_L$

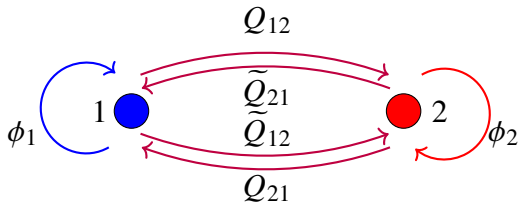

Figure 2.9: *The $\mathbb{Z}_2$ quiver. The color groups are denoted by blobs representing the field content of the $\mathcal{N}=1$ vector multiplets inside the $\mathcal{N}=2$ vector multiplets. We use $\mathcal{N}=1$ language for the hypermultiplets. The arrow to the right is $Q^{\hat{I}}$ while the arrow to the left is $\tilde{Q}^{\hat{I}}$.*

For the results in this thesis, however, it is most convenient to work with the $2N\times 2N$ color matrices in the mother $\mathcal{N}=4$ theory, which, in $\mathcal{N}=1$ language, contains the three chiral superfields which were defined in Section 2.3 as $Z=\frac{1}{\sqrt{2}}(X_4+iX_5)$, $X=\frac{1}{\sqrt{2}}(X_6+iX_7)$, $Y=\frac{1}{\sqrt{2}}(X_8+iX_9)$ in the adjoint of the $SU(2N)$ gauge group (see [28]). In this picture, the orbifold projected $\mathcal{N}=2$ scalar fields can be arranged as[5]

$$X=\begin{pmatrix} & Q_{12} \\ Q_{21} & \end{pmatrix}, \quad Y=\begin{pmatrix} & \tilde{Q}_{12} \\ \tilde{Q}_{21} & \end{pmatrix}, \quad Z=\begin{pmatrix} \phi_1 & \\ & \phi_2 \end{pmatrix}. \tag{2.158}$$

In terms of equation (2.157), $\phi_1=\phi$, $\phi_2=\check{\phi}$, $Q_{12}=\tilde{Q}_{12}=Q$ and $Q_{21}=\tilde{Q}_{21}=\tilde{Q}$. The $\mathbb{Z}_2$ quiver diagram is shown in Figure 2.9. We see that while Z acts diagonally and thus keeps us on the same node of the quiver, X takes us clockwise around the quiver while Y takes us anticlockwise.[6] From the surviving $N\times N$ blocks, Q_{12} and $\tilde{Q}_{12}$ have the same bifundamental color structure $\square_1\times\overline{\square}_2$, and similarly for the case for Q_{21} and $\tilde{Q}_{21}$ but with the opposite orientation $\overline{\square}_1\times\square_2$. Thus, we can put them together in a doublet of an extra $SU(2)_L$ with index $\hat{I}$, as follows (see also the hypermultiplet described earlier in this section)

$$Q_{\hat{I}}=\left(Q_{12}\,,\,\tilde{Q}_{12}\right)^T \qquad \text{and} \qquad \tilde{Q}_{\hat{I}}=\left(\tilde{Q}_{21}\,,\,Q_{21}\right)^T. \tag{2.159}$$

The superpotential is explicitly invariant under the extra $SU(2)_L$ rotating the doublets of $SU(2)_L$ in (2.159) and can be written as [28]

$$\mathcal{W}_{\mathbb{Z}_2}=ig_1\,\mathrm{tr}_2\left(\tilde{Q}^{\hat{I}}\phi_1 Q_{\hat{I}}\right)-ig_2\,\mathrm{tr}_1\left(Q_{\hat{I}}\phi_2\tilde{Q}^{\hat{I}}\right), \tag{2.160}$$

singlet representation break. What is more, the bifundamental hypermultiplet fields stick together forming dimers which are much more difficult to treat. In this thesis we will not consider this limit, but rather the spin chain at generic values of κ, which can be thought of as a regularisation of the SCQCD spin chain.

[5]Despite the notation $\tilde{Q}$, the fields are all holomorphic.

[6]This distinction is not very important here as there are only two nodes, but it becomes more relevant for $\mathbb{Z}_k$ quivers. The quiver for the $\mathcal{N}=2$ preserving $\mathbb{Z}_3$ orbifold is displayed in [27].

or more explicitly as

$$\mathcal{W}_{\mathbb{Z}_2} = ig_1 \,\mathrm{tr}_2(\widetilde{Q}_{21}\phi_1 Q_{12} - Q_{21}\phi_1\widetilde{Q}_{12}) - ig_2 \,\mathrm{tr}_1(Q_{12}\phi_2\widetilde{Q}_{21} - \widetilde{Q}_{12}\phi_2 Q_{21})\,. \quad (2.161)$$

This second more explicit form may be more intuitive as it is easy to remember that the bifundamental fields Q_{ij} and $\tilde{Q}_{ij}$ are labelled according to the direction of the arrows. For instance, Q_{12} transforms in the fundamental of gauge group 1 and the antifundamental of gauge group 2 ($\square_1 \times \overline{\square}_2$).

As already mentioned, we have the choice of working in the daughter $\mathcal{N} = 2$ SCFT picture (with our single letter basis composed of the six fields ϕ_i and $Q_{ij}, \tilde{Q}_{ij}$) or in the mother $\mathcal{N} = 4$ SYM picture where the single site basis is made out of X, Y, Z . We will mostly use the latter as it allows us to simplify the discussion. As we will see, the information of whether we are working with the upper or lower component of a given field in the $\mathcal{N} = 4$ picture will be provided by a dynamical parameter λ.

2.4.2 One-Loop Hamiltonian for the Interpolating Theory

In this thesis, we will focus on the one-loop holomorphic SU(3) sector of the $\mathbb{Z}_2$ quiver. In the mother $\mathcal{N} = 4$ SYM this sector is made up of three complex scalar fields X, Y, Z in the adjoint of the SU($2N$) gauge group. The planar Hamiltonian of this theory has been derived, for the full scalar sector, in [18] and discussed in Appendix B. We begin by visually rederiving the Hamiltonian in two SU(2)-like sectors, the one sector formed by the fields X and Y and the other sector formed by X and Z, so that we can highlight the difference between these sectors. We refer to these sectors as $SU(2)$-like because, although they resemble the $\mathfrak{su}(2) \subset \mathfrak{su}(4)_R$ sector discussed in Section 2.3, there is no symmetry that rotates the fields into each other since they have different gauge structures.

The XY sector

In Section 2.3 for the $\mathcal{N} = 4$ theory, we considered the closed $\mathfrak{su}(2) \subset \mathfrak{su}(4)_R$ subsector that is constructed out of Z, Y chiral fields. In this section, we consider the $\mathcal{N} = 2$ orbifold projected Z, Y fields which constitutes a $SU(2)$-like closed subsector. This is the sector which includes all the (holomorphic) bifundamental fields. To derive the Hamiltonian, we start by considering the ϕ_i F-terms

$$F_{\phi_1} = ig_1(Q_{12}\widetilde{Q}_{21} - \widetilde{Q}_{12}Q_{21}) \quad , \quad F_{\phi_2} = ig_2(Q_{21}\widetilde{Q}_{12} - \widetilde{Q}_{21}Q_{12}). \quad (2.162)$$

From the potential $F\bar{F}$ and following the treatment in [64], we can immediately draw the vertices contributing to the one-loop Hamiltonian. These are shown in Figure 2.10.

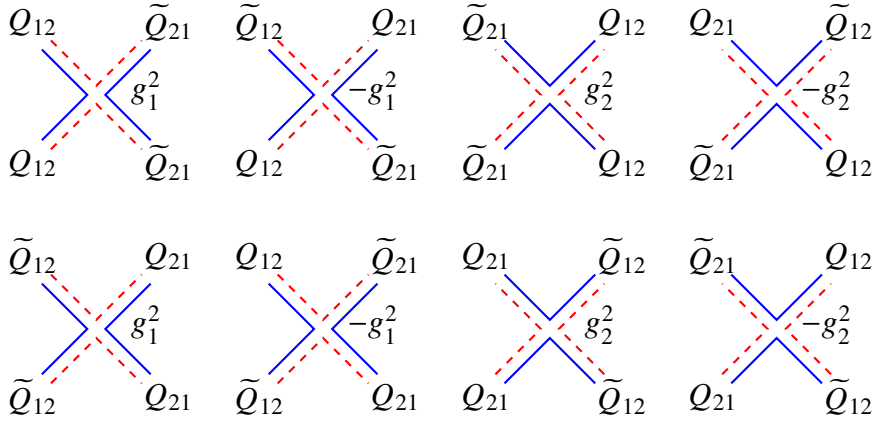

Figure 2.10: *The vertices contributing to the Hamiltonian in the XY sector. A solid blue line denotes the first gauge group and a dashed red line denotes the second gauge group. Time moves upwards. Here we have already performed the Wick contractions of the conjugate fields with the second gauge invariant operator to write the vertices directly as spin chain interactions.*

After taking out an overall factor of $g_1 g_2$ and defining $\kappa = g_2/g_1$, we find the Hamiltonian:

$$H_{\ell,\ell+1} = \begin{pmatrix} 0 & 0 & 0 & 0 & 0 & 0 & 0 & 0 \\ 0 & \kappa^{-1} & -\kappa^{-1} & 0 & 0 & 0 & 0 & 0 \\ 0 & -\kappa^{-1} & \kappa^{-1} & 0 & 0 & 0 & 0 & 0 \\ 0 & 0 & 0 & 0 & 0 & 0 & 0 & 0 \\ 0 & 0 & 0 & 0 & 0 & 0 & 0 & 0 \\ 0 & 0 & 0 & 0 & 0 & \kappa & -\kappa & 0 \\ 0 & 0 & 0 & 0 & 0 & -\kappa & \kappa & 0 \\ 0 & 0 & 0 & 0 & 0 & 0 & 0 & 0 \end{pmatrix}, \qquad \text{in the basis} \quad \begin{pmatrix} Q_{12}Q_{21} \\ Q_{12}\tilde{Q}_{21} \\ \tilde{Q}_{12}Q_{21} \\ \tilde{Q}_{12}\tilde{Q}_{21} \\ Q_{21}Q_{12} \\ Q_{21}\tilde{Q}_{12} \\ \tilde{Q}_{21}Q_{12} \\ \tilde{Q}_{21}\tilde{Q}_{12} \end{pmatrix}, \tag{2.163}$$

where the indices $\ell, \ell+1$ denote the nearest-neighbour sites of the spin chain. Note that the basis is 8-dimensional instead of 16-dimensional as one would expect given our four fields. The remaining combinations of fields cannot occur, as they are not allowed by the gauge structure (for example, a Q_{12} cannot be followed by a Q_{12} or $\tilde{Q}_{12}$). We have chosen this truncated basis such that the upper left

block of the Hamiltonian corresponds to the first gauge group to the left of the first site where the Hamiltonian acts. In other words, the upper left block acts on two bifundamental squarks which are contracted or in the singlet representation of the second gauge group and, with their indices open, means that they are in the bifundamental representation of the first color group ($\square_1 \times \overline{\square}_1$). On the other hand, the lower right block of the Hamiltonian acts on two squarks which have open color indices from the second gauge group ($\square_2 \times \overline{\square}_2$) and are color contracted with respect to the first color group. We emphasise that, although the Hamiltonian looks block-diagonal, this is an artifact of the notation. The same fields appear in both blocks, and thus the upper and lower blocks of the Hamiltonian will mix when acting on a spin chain configuration.

For this and other reasons to become clear later, we will prefer to work in the mother $\mathcal{N} = 4$ picture, where we only deal with the $2N \times 2N$ fields X, Y instead of their component fields. A spin chain state such as $|XYXYYX\cdots\rangle$ in the $\mathcal{N} = 4$ picture can be decomposed into two states, in this case $\left|Q_{12}\tilde{Q}_{21}Q_{12}\tilde{Q}_{21}\tilde{Q}_{12}Q_{21}\cdots\right\rangle$ and $\left|Q_{21}\tilde{Q}_{12}Q_{21}\tilde{Q}_{12}\tilde{Q}_{21}Q_{12}\cdots\right\rangle$ in the $\mathcal{N} = 2$ picture. These states can of course be mapped to each other by exchanging the gauge groups. In the XY picture, which of the two chains we are considering is uniquely defined by specifying the gauge group to the left of a given site of the chain (meaning the first index of the bifundamental field at that site). Without loss of generality we can take this reference site to be the first site of the chain.

Similarly, the above action of the Hamiltonian is decomposed into an action of *two* Hamiltonians in the XY basis. Whether we are on the upper or lower block again depends on which gauge group is to the left of the first site we are acting on. We call these Hamiltonians $\mathcal{H}_1$ and $\mathcal{H}_2$, with

$$\mathcal{H}_1 = \begin{pmatrix} 0 & 0 & 0 & 0 \\ 0 & \kappa^{-1} & -\kappa^{-1} & 0 \\ 0 & -\kappa^{-1} & \kappa^{-1} & 0 \\ 0 & 0 & 0 & 0 \end{pmatrix}, \quad \mathcal{H}_2 = \begin{pmatrix} 0 & 0 & 0 & 0 \\ 0 & \kappa & -\kappa & 0 \\ 0 & -\kappa & \kappa & 0 \\ 0 & 0 & 0 & 0 \end{pmatrix}, \text{ in the basis } \begin{pmatrix} XX \\ XY \\ YX \\ YY \end{pmatrix}_{i=1,2} \tag{2.164}$$

where the notation is that $\mathcal{H}_1$ acts on the basis labelled by $i = 1$ in the representation $\square_1 \times \overline{\square}_1$ of the color group, while $\mathcal{H}_2$ acts on the basis with $i = 2$ in the representation $\square_2 \times \overline{\square}_2$. In other words, by $\mathcal{H}_1$ we denote the Hamiltonian which is applicable when the gauge group to the left of a site ℓ along the chain is the first one, while $\mathcal{H}_2$ is the corresponding Hamiltonian when the gauge group to the left of a site ℓ is the

second one. Both Hamiltonians are of XXX-type but with different (ferromagnetic) couplings given by κ^{-1} and κ, respectively. We will refer to the Hamiltonians as *Heisenberg-type*.

Given that the XY sector is only made up of bifundamentals, which means that the gauge group alternates at consecutive sites (regardless of whether the field at that site is an X or a Y), we conclude that the Hamiltonian of this sector alternates between $\mathcal{H}_1$ and $\mathcal{H}_2$. If, for instance, we fix the gauge group to the left of the first site to be the first one, we will have $\mathcal{H}_1$ acting on odd-even sites and $\mathcal{H}_2$ acting on even-odd sites.

We conclude that the XY sector of the interpolating theory is governed by an alternating-bond XXX-model Hamiltonian, as described in Section 2.2.4. In Chapter 3 we will study this alternating spin chain in more detail using the coordinate Bethe ansatz.

From the Hamiltonian derived in (2.164) from [18], which is also discussed in Appendix B, we can start with the form of the Hamiltonian given in equation (B.43). Firstly, we note that $\mathbb{K}$ is zero on our sector as we look only at the upper components ($\mathcal{I}\mathcal{J} = ++$) of the $SU(2)_R$ triplet $Q\tilde{Q}$ or $\tilde{Q}Q$. Then the only contributions that are left in our sector are

$$\mathcal{H}_1|Q\tilde{Q}\rangle = 2\hat{\mathbb{K}}|Q\tilde{Q}\rangle\,, \quad \mathcal{H}_2|\tilde{Q}Q\rangle = 2\kappa^2\hat{\mathbb{K}}|\tilde{Q}Q\rangle \tag{2.165}$$

Rescaling the Hamiltonian by an overall 2κ and choosing the basis (2.163) we get (2.164).

XZ sector

In this sector we will consider operators composed of the bifundamental field X and the adjoint field Z. To find the Hamiltonian we will need the $\tilde{Q}_{ij}$ F-terms

$$F_{\tilde{Q}_{12}} = i(g_2\phi_2 Q_{21} - g_1 Q_{21}\phi_1)\,, \quad F_{\tilde{Q}_{21}} = i(g_1\phi_1 Q_{12} - g_2 Q_{12}\phi_2), \tag{2.166}$$

which lead to the interactions shown in Figure 2.11.

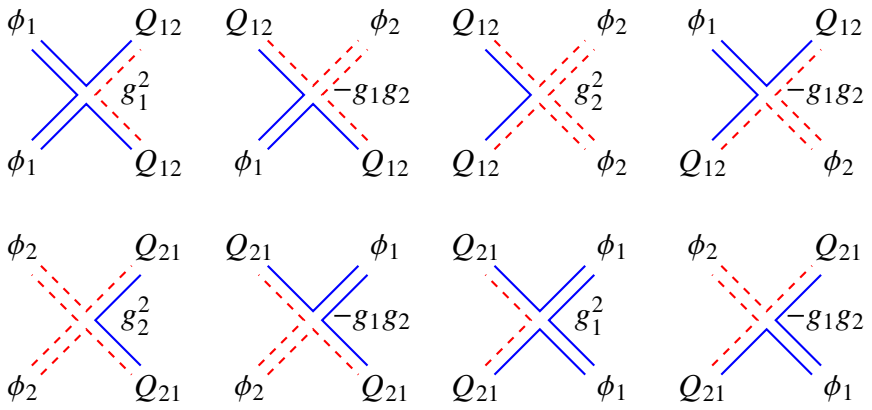

Figure 2.11: *The vertices contributing to the Hamiltonian in the XZ sector. A solid blue line denotes the first and a dashed red line denotes the second gauge group. Time moves upwards. Here we have already performed the Wick contractions of the conjugate fields with the second gauge invariant operator to write the vertices directly as spin chain interactions.*

We will again divide by an overall factor of g_1g_2, resulting in the Hamiltonian:

$$H_{i,i+1} = \begin{pmatrix} 0 & 0 & 0 & 0 & 0 & 0 & 0 & 0 \\ 0 & \kappa & -1 & 0 & 0 & 0 & 0 & 0 \\ 0 & -1 & \kappa^{-1} & 0 & 0 & 0 & 0 & 0 \\ 0 & 0 & 0 & 0 & 0 & 0 & 0 & 0 \\ 0 & 0 & 0 & 0 & 0 & 0 & 0 & 0 \\ 0 & 0 & 0 & 0 & 0 & \kappa^{-1} & -1 & 0 \\ 0 & 0 & 0 & 0 & 0 & -1 & \kappa & 0 \\ 0 & 0 & 0 & 0 & 0 & 0 & 0 & 0 \end{pmatrix}, \qquad \text{in the basis} \quad \begin{pmatrix} Q_{12}Q_{21} \\ Q_{12}\phi_2 \\ \phi_1 Q_{12} \\ \phi_1\phi_1 \\ Q_{21}Q_{12} \\ Q_{21}\phi_1 \\ \phi_2 Q_{21} \\ \phi_2\phi_2 \end{pmatrix}. \tag{2.167}$$

As before, the upper left block contains the interactions with the first gauge group on the left, while the lower right block the opposite. The state space is again truncated as some combinations of fields (e.g. $\phi_1\phi_2$) cannot occur due to the gauge index structure. The Hamiltonian (2.167) can of course also be reproduced from the more general scalar Hamiltonian in [18] (see also Appendix B).

As in the XY sector, we will again prefer to use the Hamiltonian for the $\mathcal{N} = 4$ X and Z fields rather than their $\mathcal{N} = 2$ component fields. For instance, a state like $|XXZXZZ\cdots\rangle$ will correspond to two states $|Q_{12}Q_{21}\phi_1 Q_{12}\phi_2\phi_2\cdots\rangle$ and its $\mathbb{Z}_2$ conjugate $|Q_{21}Q_{12}\phi_2 Q_{21}\phi_1\phi_1\cdots\rangle$ depending on the gauge group at a given reference site. To act with the Hamiltonian on the X, Z basis, we again need to specify whether the gauge group is 1 or 2 to the left of the first site where the

Hamiltonian acts. The major difference from the XY sector is that the gauge group does not change on crossing a Z field. We write:

$$\mathcal{H}_1 = \begin{pmatrix} 0 & 0 & 0 & 0 \\ 0 & \kappa & -1 & 0 \\ 0 & -1 & \kappa^{-1} & 0 \\ 0 & 0 & 0 & 0 \end{pmatrix}, \quad \mathcal{H}_2 = \begin{pmatrix} 0 & 0 & 0 & 0 \\ 0 & \kappa^{-1} & -1 & 0 \\ 0 & -1 & \kappa & 0 \\ 0 & 0 & 0 & 0 \end{pmatrix}, \quad \text{in the basis} \begin{pmatrix} XX \\ XZ \\ ZX \\ ZZ \end{pmatrix}_{i=1,2}, \tag{2.168}$$

where the notation is that $\mathcal{H}_i$ acts on the basis in the gauge group representation $\square_i \times \overline{\square}_j$ where j is not correlated to i as above and can take both 1,2 values. More explicitly, $\mathcal{H}_1$ is the Hamiltonian acting on two sites where the gauge group to the left of the first site is the first one, while $\mathcal{H}_2$ acts when the gauge group to the left is the second one. Unlike the XY sector, where each Hamiltonian was of Heisenberg-type, in the XZ sector the Hamiltonians are of *Temperley-Lieb type* [40]. This immediately brings to mind the XXZ model[7] whose quantum-group invariant Hamiltonian (obtained by adding an appropriate boundary term to the open chain) is of Temperley-Lieb type. However, unlike the XXZ case, this Hamiltonian changes dynamically along the chain, since $\mathcal{H}_1$ is exchanged with $\mathcal{H}_2$ (and vice versa) every time one crosses an X field. We will see in Chapter 4 that Z excitations around the vacuum formed by the X fields behave very similarly to those of the alternating XY sector. On the other hand, as the Hamiltonian does not change when crossing a Z field, X excitations around the Z vacuum can be expected to behave similarly to those of the XXZ model. This is precisely what was found in the study of this case in [18], where the S-matrix for two-X magnon scattering in the Z vacuum was found to be of XXZ-type. More appropriately, using the language of the current thesis, the S-matrix for two-X magnon scattering in the Z vacuum was found to be a dynamical XXZ S-matrix.

There is of course a third SU(2)-like sector formed by the Y and Z fields but it is equivalent to the XZ sector by exchanging the Q_{ij} fields with the $\tilde{Q}_{ij}$ ones. We will therefore not consider this sector separately.

2.4.3 The dynamical Hamiltonian

A very useful concept is the introduction of a *dynamical parameter* λ. A more complete motivation is given in [27] where λ is an additional parameter in the R-matrix that leads to a dynamical Yang-Baxter equation. For this thesis, however,

[7] This model is an integrable deformation of the model studied in Section 2.2.2 by deforming the coupling constant in front of the $\sigma^z_\ell \sigma^z_{\ell+1}$ term in the Hamiltonian (2.28). See [40][37].

the motivation for introducing the dynamical parameter is simply that it provides us with a very natural language with which to describe the spin chains under study, and, we expect, similar spin chains one might want to consider for larger sectors in the $\mathbb{Z}_2$ quiver or for more general quivers.

The dynamical parameter naturally divides the lattice up for each sector. For an arbitrary site ℓ on the spin chain, we place the dynamical parameter to its left. Then, a dynamical Hamiltonian $H(\lambda)$ acting on sites $(\ell, \ell+1)$ will "see" the parameter λ and this will determine how $H(\lambda)$ acts on the two sites. With motivation from [27], we impose the following rule: if the field at site ℓ is X or Y, then crossing these fields to site $\ell+1$ shifts the dynamical parameter to λ' (in other words, site $\ell+1$ will "see" the dynamical parameter λ'); and if the field at site ℓ is Z, then crossing the field to site $\ell+1$ does not shift the dynamical parameter (in other words, site $\ell+1$ will "see" the dynamical parameter λ). Thus, for the XY sector, we will have an alternating sequence of dynamical parameters since every time we cross an X or Y field, the dynamical parameter is shifted. Due to this fact, we will refer to the XY sector as the "dense" XY sector. For the XZ sector, the dynamical parameter only shifts when we cross an X field but not a Z field. We will refer to the XZ sector as the "dilute" XZ sector. For both these sectors, there are only two dynamical parameters λ, λ'. Thus, crossing an X or Y field twice returns us to the same parameter. In terms of the deformation parameter κ, shifting the dynamical parameter captures the effect of $\kappa \to 1/\kappa$ (see the Hamiltonians below).

For alternating chains such as the XY sector, one can of course assign different Hamiltonians on even-odd and odd-even sites and study them without needing the dynamical parameter. But for dilute-type sectors where different fields affect the Hamiltonian in different ways (e.g. as in the XZ sector where crossing a Z field leaves κ invariant while crossing an X field takes $\kappa \to 1/\kappa$), the dynamical parameter appears to be very helpful in organising the computation. There is always the alternative of working in the $\mathcal{N}=2$ picture, with the 8×8 Hamiltonians (2.163) and (2.167) but this carries its own problems as the multiparticle basis is not a direct product of the single-particle basis (e.g. combinations such as $Q_{12}\tilde{Q}_{12}$ are not allowed by the gauge indices). Working in what we call the dynamical $\mathcal{N}=4$ picture, with the dynamical parameter tracking the gauge group at each site of the chain, any combination one writes is automatically correct.

We can now summarise the Hamiltonians in the two sectors of relevance as follows:

XY sector:

$$\mathcal{H}(\lambda) = \begin{pmatrix} 0 & 0 & 0 & 0 \\ 0 & \kappa^{-1} & -\kappa^{-1} & 0 \\ 0 & -\kappa^{-1} & \kappa^{-1} & 0 \\ 0 & 0 & 0 & 0 \end{pmatrix} \quad \text{and} \quad \mathcal{H}(\lambda') = \begin{pmatrix} 0 & 0 & 0 & 0 \\ 0 & \kappa & -\kappa & 0 \\ 0 & -\kappa & \kappa & 0 \\ 0 & 0 & 0 & 0 \end{pmatrix}. \quad (2.169)$$

XZ sector:

$$\mathcal{H}(\lambda) = \begin{pmatrix} 0 & 0 & 0 & 0 \\ 0 & \kappa & -1 & 0 \\ 0 & -1 & \kappa^{-1} & 0 \\ 0 & 0 & 0 & 0 \end{pmatrix} \quad \text{and} \quad \mathcal{H}(\lambda') = \begin{pmatrix} 0 & 0 & 0 & 0 \\ 0 & \kappa^{-1} & -1 & 0 \\ 0 & -1 & \kappa & 0 \\ 0 & 0 & 0 & 0 \end{pmatrix}. \quad (2.170)$$

In the next chapter, we will study the two magnon problem for the XY sector Hamiltonian, and in Chapter 4 that of the XZ sector Hamiltonian above.

Chapter 3

SPIN CHAINS IN THE DENSE XY SECTOR

We focus on the Heisenberg-type Hamiltonian (2.169) which describes the XY sector. As discussed, we characterise this sector as "dense" since the dynamical parameter shifts every time we cross a field. Since the shift is the same regardless of whether the field is an X or a Y, the dynamical parameter will alternate between two values λ and λ', and thus the Hamiltonian will be alternately $\mathcal{H}(\lambda)$ or $\mathcal{H}(\lambda')$ given in (2.169).[1] So the net effect is that of an alternating bond Hamiltonian.

Choosing the convention that λ' is on even sites and λ on odd sites, $\mathcal{H}_{\lambda'}$ will act on even-odd sites while $\mathcal{H}_{\lambda}$ will act on odd-even sites (see Figure 3.1). We can make this explicit by writing the Hamiltonian as

$$\mathcal{H}_{eo} = \begin{pmatrix} 0 & 0 & 0 & 0 \\ 0 & \kappa & -\kappa & 0 \\ 0 & -\kappa & \kappa & 0 \\ 0 & 0 & 0 & 0 \end{pmatrix}, \quad \mathcal{H}_{oe} = \begin{pmatrix} 0 & 0 & 0 & 0 \\ 0 & 1/\kappa & -1/\kappa & 0 \\ 0 & -1/\kappa & 1/\kappa & 0 \\ 0 & 0 & 0 & 0 \end{pmatrix}. \tag{3.1}$$

Since the Hamiltonian is invariant under $\kappa \to 1/\kappa$, without loss of generality we can take $\kappa \leq 1$. Alternating nearest-neighbour chains such as this have been studied in [52, 51] and discussed in Section 2.2.4. The dispersion relations and overall treatment of the chains are similar in both the bond and spin alternation case. There are also known materials which exhibit such alternating ferromagnetic behaviour, see e.g. [65] for an example with bond alternation and [66] for a case with spin alternation.[2]

The works of [52, 51] mostly studied the two magnon problem. The three- and multi-magnon problems were considered in [67, 68], without, however, making use of a Bethe-type approach but rather the recursion method (e.g. [69]) which is applicable regardless of integrability. A long-wavelength approximation to this chain, which might be relevant for comparisons to the string sigma model side, is discussed in [70].

[1] This behaviour is specific for the $\mathbb{Z}_2$ quiver case. For $\mathbb{Z}_k$ quivers, where we would expect $k-1$ parameters λ_i, the X and Y field would shift them differently.

[2] Let us remark that the literature on *antiferromagnetic* alternating chains is much more extensive, as well as that on chains with alternating antiferromagnetic/ferromagnetic bonds.

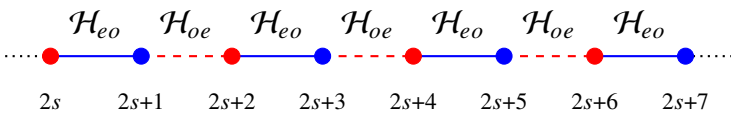

Figure 3.1: *A section of the alternating bond spin chain for the XY sector. We emphasise the alternating nature by showing the bonds between lattice sites as a dashed line or a thick line.*

For this sector, we note that there are two equivalent pseudovacua, $|\cdots XXXXX\cdots\rangle$ and $|\cdots YYYYY\cdots\rangle$ which belong to the $1/2-$BPS supermultiplet $\hat{\mathcal{B}}_R$ discussed in Section 2.1.1 with $\Delta = 2R$ [3]. Thus, since these are protected, they have zero energy. We will choose the X vacuum as a reference and consider Y spin deviations on top of this reference state. Following in large part the techniques outlined in [52, 51], we will study the diagonalisation of the one and two magnon Hamiltonian for this alternating chain.

Finally, we can of course explicitly relate these Hamiltonians to the alternating model stated in Section 2.2.4. Note that we can have only one spin deviation from a X at some site ℓ. Thus, we have $S = S' = 1/2$ (consequently, $p = 1$) and therefore we use the spin-1/2 Pauli matrices $S^i = 1/2\ \sigma^i,\ i = \{x, y, z\}$. Setting $J_1 = 2g_2^2$ and $J_2 = 2g_1^2$, we find for equation (2.107)

$$\begin{aligned} H &= -g_1 g_2 \sum_{\ell=1}^{L/2} \left[2\frac{g_2}{g_1} \left(\mathbf{S}'_{2\ell} \cdot \mathbf{S}_{2\ell+1}\right) + 2\frac{g_1}{g_2} \left(\mathbf{S}_{2\ell+1} \cdot \mathbf{S}'_{2\ell+2}\right) \right] \\ &= -g_1 g_2 \sum_{\ell=1}^{L/2} \left[2\kappa \left(\mathbf{S}'_{2\ell} \cdot \mathbf{S}_{2\ell+1}\right) + \frac{2}{\kappa} \left(\mathbf{S}_{2\ell+1} \cdot \mathbf{S}'_{2\ell+2}\right) \right], \end{aligned} \tag{3.2}$$

where we have used the deformation parameter $\kappa = g_2/g_1$. Thus far, we have (looking at local sites $(2\ell, 2\ell+1)$ and $(2\ell+1, 2\ell+2)$)

$$-2\kappa \left(\mathbf{S}_{2\ell} \cdot \mathbf{S}_{2\ell+1}\right) = \begin{pmatrix} -\frac{\kappa}{2} & 0 & 0 & 0 \\ 0 & \frac{\kappa}{2} & -\kappa & 0 \\ 0 & -\kappa & \frac{\kappa}{2} & 0 \\ 0 & 0 & 0 & -\frac{\kappa}{2} \end{pmatrix}_{2\ell,2\ell+1} , \tag{3.3}$$

[3] In terms of the $\mathcal{N} = 2$ fields in the downstairs picture and written in terms of single trace operators, these are the operators $\mathrm{Tr}\left[(Q_{12}Q_{21})^R\right]$ and $\mathrm{Tr}\left[(Q_{21}Q_{12})^R\right]$.

and

$$-\frac{2}{\kappa}\left(\mathbf{S}_{2\ell+1}\cdot\mathbf{S}_{2\ell+2}\right)=\begin{pmatrix}-\frac{1}{2\kappa} & 0 & 0 & 0\\ 0 & \frac{1}{2\kappa} & -\frac{1}{\kappa} & 0\\ 0 & -\frac{1}{\kappa} & \frac{1}{2\kappa} & 0\\ 0 & 0 & 0 & -\frac{1}{2\kappa}\end{pmatrix}_{2\ell+1,2\ell+2} \quad . \tag{3.4}$$

These are precisely our two Hamiltonians up to a shift by the identity operator which does not affect the physics of the system. Upon shifting by the identity[4] $(1/4)\mathbb{1}\otimes\mathbb{1}$ and setting $S^i=(1/2)\,\sigma^i,\ i=\{x,y,z\}$, we find

$$-\frac{\kappa}{2}\left(\sigma^i_{2\ell}\otimes\sigma^i_{2\ell+1}-\mathbb{1}_{2\ell}\otimes\mathbb{1}_{2\ell+1}\right)=\begin{pmatrix}0 & 0 & 0 & 0\\ 0 & \kappa & -\kappa & 0\\ 0 & -\kappa & \kappa & 0\\ 0 & 0 & 0 & 0\end{pmatrix}_{2\ell,2\ell+1} \quad , \tag{3.5}$$

and

$$-\frac{1}{2\kappa}\left(\sigma^i_{2\ell+1}\otimes\sigma^i_{2\ell+2}-\mathbb{1}_{2\ell+1}\otimes\mathbb{1}_{2\ell+2}\right)=\begin{pmatrix}0 & 0 & 0 & 0\\ 0 & \frac{1}{\kappa} & -\frac{1}{\kappa} & 0\\ 0 & -\frac{1}{\kappa} & \frac{1}{\kappa} & 0\\ 0 & 0 & 0 & 0\end{pmatrix}_{2\ell+1,2\ell+2} \quad . \tag{3.6}$$

Note that there is a summation on the i index above. Rescaling $H\mapsto(1/g_1g_2)H$, we thus conclude that our system is an alternating-bond spin chain with Hamiltonian (we suppress the tensor notation)

$$H=-\sum_{\ell=1}^{L/2}\left[\frac{\kappa}{2}\left(\sigma^i_{2\ell}\sigma^i_{2\ell+1}-\mathbb{1}_{2\ell}\mathbb{1}_{2\ell+1}\right)+\frac{1}{2\kappa}\left(\sigma^i_{2\ell+1}\sigma^i_{2\ell+2}-\mathbb{1}_{2\ell+1}\mathbb{1}_{2\ell+2}\right)\right], \tag{3.7}$$

where $i=\{x,y,z\}$.

3.1 One magnon

Let us start by considering a single Y magnon in the X vacuum and proceed to solve the one magnon problem $H|p\rangle=E_1(p)|p\rangle$. Due to the alternating-bond nature of the spin chain, there will be two equations to solve, namely, for Y on even sites and for Y on odd sites. Denoting these states by $|2r\rangle$ and $|2s+1\rangle$, the equations are

$$\begin{aligned}&\left(\kappa+\kappa^{-1}\right)|2r\rangle-\kappa^{-1}|2r-1\rangle-\kappa|2r+1\rangle=E_1|2r\rangle \ \text{ and}\\ &\left(\kappa+\kappa^{-1}\right)|2s+1\rangle-\kappa|2s\rangle-\kappa^{-1}|2s+2\rangle=E_1|2s+1\rangle\ .\end{aligned} \tag{3.8}$$

[4]The vacuum energy is simply shifted to $E_0=0$; the energy of a spin deviation, shifted by the same amount, is measured relative to the ground state and thus does not change.

We will therefore take for our ansatz a superposition of a single Y excitation on odd and even sites

$$|p\rangle = \sum_{\ell\in 2\mathbb{Z}} \psi_e(\ell)|\ell\rangle + \sum_{\ell\in 2\mathbb{Z}+1} \psi_o(\ell)|\ell\rangle. \tag{3.9}$$

This leads to the following equations:

$$\kappa^{-1}\big(\psi_e(2r) - \psi_o(2r-1)\big) + \kappa\big(\psi_e(2r) - \psi_o(2r+1)\big) = E_1(p)\psi_e(2r), \tag{3.10}$$

and

$$\kappa\big(\psi_o(2s+1) - \psi_e(2s)\big) + \kappa^{-1}\big(\psi_o(2s+1) - \psi_e(2s+2)\big) = E_1(p)\psi_o(2s+1)\,, \tag{3.11}$$

which can be solved easily by the Bethe-type ansatz

$$\psi_e(\ell) = A_e(p)e^{ip\ell}, \quad \psi_o(\ell) = A_o(p)e^{ip\ell}\,, \tag{3.12}$$

where the ratio between the even and odd amplitudes is fixed to be

$$r(p;\kappa) = \frac{A_o(p)}{A_e(p)} = \mp\frac{e^{ip}\sqrt{1+\kappa^2e^{-2ip}}}{\sqrt{1+\kappa^2e^{2ip}}}\,. \tag{3.13}$$

The eigenvalue of the eigenvector (3.9) is

$$E_1(p) = E_1(p;\kappa) = \frac{1}{\kappa} + \kappa \pm \frac{1}{\kappa}\sqrt{(1+\kappa^2)^2 - 4\kappa^2\sin^2 p}\,. \tag{3.14}$$

Similarly to [52, 51], we will call the negative branch of the square root the *acoustic branch* and the positive branch the *optical branch*. The acoustic branch is the one which includes the zero-energy state $E_1(0) = 0$. As can be seen in Figure 3.2, as κ is tuned away from 1, a gap of magnitude $2(1/\kappa - \kappa)$ develops between the branches at the boundary of the Brillouin zone, which is at $p = \pi/2$. Therefore, scattering states are confined either to the lower ("acoustic") or upper ("optical") branch.

Note that by a choice of branch cut we can also bring the energy eigenvalue to the form

$$E_1(p;\kappa) = \kappa + \frac{1}{\kappa} \pm \frac{1}{\kappa}\sqrt{1+\kappa^2e^{-2ip}}\sqrt{1+\kappa^2e^{2ip}}\,. \tag{3.15}$$

In this section we will choose to use the dispersion relation in this form. Some motivation for this will be discussed in Chapter 5. Without loss of generality, we will work with the acoustic branch; however, when considering specific solutions (such as in section 3.3), magnons belonging to both branches need to be considered (as well as solutions with complex momenta which can lead to energies between the branches.)

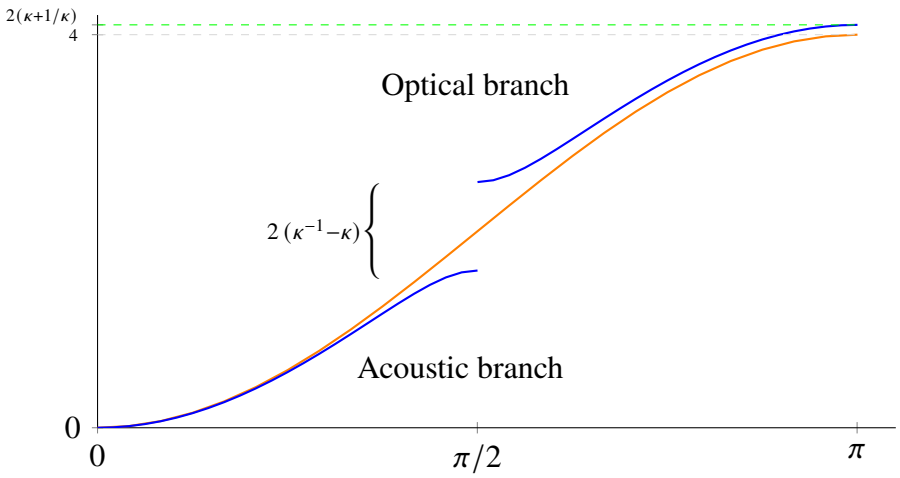

Figure 3.2: *A plot of the 1-magnon energy E_1 (blue line) for $\kappa < 1$, as compared to the XXX energy $E_1^{XXX} = 2(1 - \cos p)$ at $\kappa = 1$. The gap between the branches is $2(1/\kappa - \kappa)$, and the maximum of the energy is $2(\kappa + \kappa^{-1})$.*

We observe that the energy is even under reflection of the momentum, while the ratio function is inverted

$$E_1(-p;\kappa) = E_1(p;\kappa) \quad , \quad r(-p;\kappa) = \frac{1}{r(p;\kappa)}. \tag{3.16}$$

Similarly, the energy is invariant under the $\mathbb{Z}_2$ transformation $\kappa \to 1/\kappa$, while the ratio is again inverted

$$E_1(p;1/\kappa) = E_1(p;\kappa) \quad , \quad r(p;1/\kappa) = \frac{1}{r(p;\kappa)} \, . \tag{3.17}$$

This behaviour of the ratio function is natural, since the $\mathbb{Z}_2$ transformation exchanges the gauge groups and thus the even and odd sites of the chain. Thus, the energy eigenfunction is also an eigenfunction of the $\mathbb{Z}_2$ symmetry $\kappa \to 1/\kappa$

$$\mathbb{Z}_2|p\rangle = \frac{1}{r(p;\kappa)}|p\rangle \, . \tag{3.18}$$

In the following, we will work with a fixed value of κ, so where no confusion can arise, we will simply write $r(p) = r(p;\kappa)$.

In the orbifold limit $\kappa \to 1$, the alternating-bond behaviour disappears, as both Hamiltonians reduce to the well-known ferromagnetic XXX Hamiltonian. This fact is also reflected in the dispersion relation reducing to the standard XXX form and the ratio between even and odd sites becoming trivial

$$E_1(p;1) = 2(1 - \cos(p)) = 4\sin^2(p/2) \, , \quad r(p;1) = 1 \, . \tag{3.19}$$

Note, however, that even though the Hamiltonian is that of the XXX model, the orbifold limit is not equivalent to $\mathcal{N} = 4$ SYM as one also needs to include the twisted sector. The orbifold limit and the corresponding Bethe ansatz have been discussed in detail in [14, 13, 71, 17].

We will now proceed to the two magnon problem which, as we will see, exhibits several novel features compared to the XXX case.

3.2 Two magnons

Following the treatment of [52, 51] and similar to Section 2.2.2, we will organise the eigenvalue problem for two magnons into *non-interacting* and *interacting equations*. The difference from the standard analysis of Section 2.2.2 is that the equations depend on whether the magnons are at even-even, even-odd, odd-even or odd-odd sites. The non-interacting equations for even-even and even-odd sites are

$$\begin{aligned}
&2(\kappa+\kappa^{-1})\,|2r,2s\rangle - \kappa^{-1}(|2r-1,2s\rangle + |2r,2s-1\rangle) - \kappa(|2r+1,2s\rangle + |2r,2s+1\rangle)\\
&= E_2\,|2r,2s\rangle\\
&\text{and}\\
&2(\kappa+\kappa^{-1})\,|2r,2s+1\rangle - \kappa^{-1}(|2r-1,2s+1\rangle + |2r,2s+2\rangle) - \kappa(|2r+1,2s+1\rangle + |2r,2s\rangle)\\
&= E_2\,|2r,2s+1\rangle\,,
\end{aligned} \tag{3.20}$$

and the odd-even and odd-odd cases can be obtained from these by taking $\kappa \to \kappa^{-1}$. There are two interacting equations, depending on whether the neighbouring magnons are at even-odd or odd-even sites

$$\begin{aligned}
&2\kappa^{-1}\,|2r,2r+1\rangle - \kappa^{-1}\,|2r-1,2r+1\rangle - \kappa^{-1}\,|2r,2r+2\rangle = E_2\,|2r,2r+1\rangle \ \text{ and}\\
&2\kappa\,|2r-1,2r\rangle - \kappa\,|2r-2,2r\rangle - \kappa\,|2r-1,2r+1\rangle = E_2\,|2r-1,2r\rangle
\end{aligned} \tag{3.21}$$

Since the non-interacting equations are simply sums of the 1-magnon equations, it is easy to check that an ansatz of the type

$$\begin{aligned}
|p_1,p_2\rangle = &\sum_{r<s}\psi_{ee}(2r,2s)\,|2r,2s\rangle + \sum_{r<s+1}\psi_{eo}(2r,2s+1)\,|2r,2s+1\rangle\\
&+\sum_{r<s+1}\psi_{oe}(2r-1,2s)\,|2r-1,2s\rangle + \sum_{r<s}\psi_{oo}(2r+1,2s+1)\,|2r+1,2s+1\rangle\,,
\end{aligned} \tag{3.22}$$

where (with ℓ_1, ℓ_2 being even or odd as specified by the indices on ψ)

$$\begin{aligned}
\psi_{ee}(\ell_1, \ell_2) &= A_{ee}(p_1, p_2) e^{ip_1\ell_1 + ip_2\ell_2}, \\
\psi_{eo}(\ell_1, \ell_2) &= A_{eo}(p_1, p_2) e^{ip_1\ell_1 + ip_2\ell_2}, \\
\psi_{oe}(\ell_1, \ell_2) &= A_{oe}(p_1, p_2) e^{ip_1\ell_1 + ip_2\ell_2}, \\
\psi_{oo}(\ell_1, \ell_2) &= A_{oo}(p_1, p_2) e^{ip_1\ell_1 + ip_2\ell_2} \ ,
\end{aligned} \tag{3.23}$$

and where the coefficients are fixed in terms of $A_{ee}(p_1, p_2)$ as

$$\begin{aligned}
A_{eo}(p_1, p_2) &= r(p_2) A_{ee}(p_1, p_2) \ , \\
A_{oe}(p_1, p_2) &= r(p_1) A_{ee}(p_1, p_2) \ , \\
A_{oo}(p_1, p_2) &= r(p_1) r(p_2) A_{ee}(p_1, p_2) \ ,
\end{aligned} \tag{3.24}$$

solves the non-interacting equations, with the additive eigenvalue $E_2(p_1, p_2) = E_1(p_1) + E_1(p_2)$. To solve the interacting equations, the usual Bethe approach would be to add terms with swapped momenta to the wavefunctions (see Section 2.2.2), i.e. with $e^{i\ell_1 p_2 + i\ell_2 p_1}$ in the exponent. However, in this case this does not lead to a solution, thus we will need to enhance the Bethe ansatz (3.22) to obtain a solution.

3.2.1 Centre-of-mass solution

One way to improve on (3.22) is by adding, apart from swapped terms, also *contact terms* to the wavefunction. As we will see, this will indeed provide a solution, but only in the centre-of-mass frame where $p_1 + p_2 = 0$. The origin of these contact terms will become clearer in the next section, after we solve the more general case of $p_1 + p_2 \neq 0$.

We will now write

$$\begin{aligned}
|p_1, p_2\rangle = &\sum_{r<s} \psi_{ee}(2r, 2s) \, |2r, 2s\rangle + \sum_{r<s+1} \psi_{eo}(2r, 2s+1) \, |2r, 2s+1\rangle \\
&+ \sum_{r<s+1} \psi_{oe}(2r-1, 2s) \, |2r-1, 2s\rangle + \sum_{r<s} \psi_{oo}(2r+1, 2s+1) \, |2r+1, 2s+1\rangle \ ,
\end{aligned} \tag{3.25}$$

where

$$\begin{aligned}
\psi_{ee}(\ell_1,\ell_2) &= A_{ee}(p_1,p_2)e^{ip_1\ell_1+ip_2\ell_2} + A_{ee}(p_2,p_1)e^{ip_2\ell_1+ip_1\ell_2},\\
\psi_{oo}(\ell_1,\ell_2) &= A_{oo}(p_1,p_2)e^{ip_1\ell_1+ip_2\ell_2} + A_{oo}(p_2,p_1)e^{ip_2\ell_1+ip_1\ell_2},\\
\psi_{eo}(\ell_1,\ell_2) &= A_{eo}(p_1,p_2)e^{ip_1\ell_1+ip_2\ell_2}(1+\delta_{\ell_1+1,\ell_2}\mathcal{A}(p_1,p_2))\\
&\quad + A_{eo}(p_2,p_1)e^{ip_2\ell_1+ip_1\ell_2}(1+\delta_{\ell_1+1,\ell_2}\mathcal{A}(p_2,p_1)),\\
\psi_{oe}(\ell_1,\ell_2) &= A_{oe}(p_1,p_2)e^{ip_1\ell_1+ip_2\ell_2}(1+\delta_{\ell_1+1,\ell_2}\mathcal{B}(p_1,p_2))\\
&\quad + A_{oe}(p_2,p_1)e^{ip_2\ell_1+ip_1\ell_2}(1+\delta_{\ell_1+1,\ell_2}\mathcal{B}(p_2,p_1)).
\end{aligned} \tag{3.26}$$

We have locally enhanced the wavefunctions for ψ_{eo}, ψ_{oe} for nearest-neighbour terms by adding general coefficients $\mathcal{A}, \mathcal{B}$ which play the role of contact terms. Note that we are not assuming that $\mathcal{A}(p_2,p_1), \mathcal{B}(p_2,p_1)$ are related to $\mathcal{A}(p_1,p_2), \mathcal{B}(p_1,p_2)$ by permuting the momenta, so we have four independent contact terms. At this stage we have not imposed the CoM frame yet (so we keep p_2 in the notation for now) but we will soon see that the condition $p_2 = -p_1$ is required for consistency of the ansatz.

Factoring out the overall coefficient $A_{ee}(p_1,p_2)$, we can write the wavefunctions as

$$\begin{aligned}
\psi_{ee}(\ell_1,\ell_2) &= e^{ip_1\ell_1+ip_2\ell_2} + S(p_1,p_2)e^{ip_2\ell_1+ip_1\ell_2}\\
\psi_{oo}(\ell_1,\ell_2) &= r(p_1)r(p_2)e^{ip_1\ell_1+ip_2\ell_2} + r(p_1)r(p_2)S(p_1,p_2)e^{ip_2\ell_1+ip_1\ell_2}\\
\psi_{eo}(\ell_1,\ell_2) &= r(p_2)e^{ip_1\ell_1+ip_2\ell_2}(1+\delta_{\ell_1+1,\ell_2}\mathcal{A}(p_1,p_2))\\
&\quad + r(p_1)S(p_1,p_2)e^{ip_2\ell_1+ip_1\ell_2}(1+\delta_{\ell_1+1,\ell_2}\mathcal{A}(p_2,p_1))\\
\psi_{oe}(\ell_1,\ell_2) &= r(p_1)e^{ip_1\ell_1+ip_2\ell_2}(1+\delta_{\ell_1+1,\ell_2}\mathcal{B}(p_1,p_2))\\
&\quad + r(p_2)S(p_1,p_2)e^{ip_2\ell_1+ip_1\ell_2}(1+\delta_{\ell_1+1,\ell_2}\mathcal{B}(p_2,p_1)).
\end{aligned} \tag{3.27}$$

where we have defined $S(p_1,p_2) = A_{ee}(p_2,p_1)/A_{ee}(p_1,p_2)$. We thus need to determine $S(p_1,p_2)$ and the four contact terms $\mathcal{A}(p_1,p_2), \mathcal{A}(p_2,p_1), \mathcal{B}(p_1,p_2), \mathcal{B}(p_2,p_1)$ in order to obtain a solution.

Next-to-nearest neighbour magnons

The first thing to consider when adding contact terms that only arise at nearest-neighbour sites, is that they will jump out to the next-to-nearest neighbour terms and enter the even-even and odd-odd non-interacting equations (3.20) when $s = r+1$. However, we have already computed the eigenvalue for the non-interacting equations, which of course includes this case. To not spoil the eigenvalue that we found, we will need to constrain the contact terms. Looking at the $(2r, 2r+2)$ equation, we

find the constraint

$$\mathcal{A}(p_1, p_2) = -\kappa^2 \frac{r(p_1)}{r(p_2)} e^{i(p_1+p_2)} \mathcal{B}(p_1, p_2) \ . \tag{3.28}$$

Similarly, from the $(2r+1, 2r+3)$ equation, we have

$$\mathcal{A}(p_1, p_2) = -\kappa^2 \frac{r(p_1)}{r(p_2)} e^{-i(p_1+p_2)} \mathcal{B}(p_1, p_2) \ . \tag{3.29}$$

These equations can only agree if $K = p_1 + p_2 = n\pi,\ n \in \mathbb{Z}$. We will choose $n = 0$ to keep K in the first Brillouin zone $K \in (-\pi/2, \pi/2]$. This leads to a single constraint

$$\mathcal{A}(p, -p) = -\kappa^2 \frac{r(p)}{r(-p)} \mathcal{B}(p, -p). \tag{3.30}$$

We will thus restrict to the centre-of-mass case for the rest of this section.

Interacting Equations

Substituting the ansatz (3.26) together with (3.30) in the interacting equations (3.21), we can solve for $A_{ee}(-p, p)$ in terms of $A_{ee}(p, -p)$ in each case to find an expression for the S-matrix $S(p, -p)$. We find

$$S^{(eo)}(p, -p) = \frac{e^{-2ip}\left(\mathcal{B}(p,-p)\kappa^2(2 - E_2\kappa) - (\mathcal{B}(p,-p) - 1)e^{2ip}(E_2\kappa - 2) + 2\right)}{\mathcal{B}(-p,p)(E_2\kappa - 2)\left(1 + \kappa^2 e^{2ip}\right) - E_2\kappa - 2e^{2ip} + 2} \ , \tag{3.31}$$

from the even-odd equation, while the odd-even equation gives

$$S^{(oe)}(p, -p) = \frac{e^{-2ip}\left(-(1 + \mathcal{B}(p,-p))e^{2ip}(E_2 - 2\kappa) + \kappa(-2 + \mathcal{B}(p,-p)\kappa(2\kappa - E_2))\right)}{E_2\left(1 + \mathcal{B}(-p,p)(1 + e^{2ip}\kappa^2) - 2\kappa(1 - e^{2ip} + \mathcal{B}(-p,p)(1 + e^{2ip}\kappa^2))\right)} \ . \tag{3.32}$$

To keep the expressions compact we write E_2 for the centre-of-mass energy $E_2 = 2(\kappa + 1/\kappa) - 2\sqrt{1 + \kappa^2 e^{2ip}}\sqrt{1 + \kappa^2 e^{-2ip}}$.

Of course, the two expressions for the S-matrix need to agree. Setting them equal we can solve for $\mathcal{B}(-p, p)$ to find

$$\mathcal{B}(-p, p) = F(p)\mathcal{B}(p, -p) + \mathcal{G}(p), \tag{3.33}$$

where

$$F(p) = -\frac{\left(\kappa^2 + e^{2ip}\right)\left(E_2^2\kappa + E_2\left(\kappa^2 + 1\right)\left(-2 + e^{2ip}\right) - 4\kappa\left(-1 + e^{2ip}\right)\right)}{\left(1 + \kappa^2 e^{2ip}\right)\left(E_2^2\kappa\left(-e^{2ip}\right) + E_2\left(\kappa^2 + 1\right)\left(-1 + 2e^{2ip}\right) - 4\kappa\left(-1 + e^{2ip}\right)\right)}, \tag{3.34}$$

and

$$\mathcal{G}(p) = \frac{E_2\left(\kappa^2-1\right)\left(-1+e^{4ip}\right)}{\left(1+\kappa^2 e^{2ip}\right)\left(E_2^2\kappa e^{2ip} - E_2\left(\kappa^2+1\right)\left(-1+2e^{2ip}\right)+4\kappa\left(-1+e^{2ip}\right)\right)}. \tag{3.35}$$

Substituting this solution for $\mathcal{B}(-p,p)$ into either of the S-matrices above we find that the dependence on $\mathcal{B}(p,-p)$ cancels out and we obtain our final S-matrix in the centre-of-mass frame

$$S_{\text{CoM}}(p,-p) = \frac{e^{-2ip}\left(E_2^2\kappa\left(-e^{2ip}\right)+E_2\left(\kappa^2+1\right)\left(-1+2e^{2ip}\right)-4\kappa\left(-1+e^{2ip}\right)\right)}{E_2^2\kappa+E_2\left(\kappa^2+1\right)\left(-2+e^{2ip}\right)-4\kappa\left(-1+e^{2ip}\right)}. \tag{3.36}$$

Final form of the contact terms

At this stage, looking at our ansatz (3.27) evaluated in the $K=0$ frame, the only term left to determine is $\mathcal{B}(p,-p)$ which appears in the direct even-odd (after using (3.30)) and odd-even terms, as everything else is expressed in terms of it (and $\mathcal{G}(p)$ which was fixed above). However, now that we have $S_{\text{CoM}}(p,-p)$, we can check that $F(p)$ factors as

$$F(p) = -r(p)^2 e^{-2ip} S_{\text{CoM}}(p,-p)^{-1}, \tag{3.37}$$

and therefore,

$$\mathcal{B}(-p,p) = -\frac{1+\kappa^2 e^{-2ip}}{1+\kappa^2 e^{2ip}} S(p,-p)^{-1}_{\text{CoM}} \mathcal{B}(p,-p) + \mathcal{G}(p). \tag{3.38}$$

Noting that the ratio between the swapped and direct terms, for $\ell_2 = \ell_1 + 1$, is

$$\frac{r(p_2)S_{\text{CoM}}(p_1,p_2)e^{ip_2\ell_1+ip_1\ell_2}}{r(p_1)e^{ip_1\ell_1+ip_2\ell 2}} \to \frac{1+\kappa^2 e^{2ip}}{1+\kappa^2 e^{-2ip}} S_{\text{CoM}}(p,-p) \text{ as } p_1 \to p,\ p_2 \to -p, \tag{3.39}$$

we find that the $\mathcal{B}(p,-p)$ term coming from (3.38) precisely cancels the $\mathcal{B}(p,-p)$ term in both the even-odd and odd-even wavefunctions.[5] We are then left with only the $\mathcal{G}(p)$ contact term. Recalling also that $r(-p) = 1/r(p)$, we can write the final

[5] Of course, this cancellation means that the ansatz (3.27) was too permissive and we could have started with a more restrictive ansatz, with a contact term only in the direct or only in the swapped wavefunctions.

solution of the XY-sector 2-magnon problem in the centre-of-mass frame as

$$\begin{aligned}
\psi_{ee}(\ell_1,\ell_2) &= e^{ip\ell_1+i(-p)\ell_2} + S(p,-p)e^{i(-p)\ell_1+ip\ell_2},\\
\psi_{oo}(\ell_1,\ell_2) &= e^{ip\ell_1+i(-p)\ell_2} + S(p,-p)e^{i(-p)\ell_1+ip\ell_2)},\\
\psi_{oe}(\ell_1,\ell_2) &= r(p)e^{ip\ell_1+i(-p)\ell_2} + \frac{1}{r(p)}S(p,-p)e^{i(-p)\ell_1+ip\ell_2}(1+\delta_{\ell_1+1,\ell_2}\mathcal{G}(p)),\\
\psi_{eo}(\ell_1,\ell_2) &= \frac{1}{r(p)}e^{ip\ell_1+i(-p)\ell_2} + r(p)S(p,-p)e^{i(-p)\ell_1+ip\ell_2}(1-\delta_{\ell_1+1,\ell_2}\frac{\kappa^2}{r(p)^2}\mathcal{G}(p))\ .
\end{aligned} \tag{3.40}$$

Note that we now have a contact term only in the swapped parts of ψ_{oe} and ψ_{eo}. However, by their nature, the placement of contact terms is ambiguous and we could for instance move them to the direct terms. Sending $p \mapsto -p$, we find

$$\begin{aligned}
&\mathcal{B}(p,-p) = F(-p)\mathcal{B}(-p,p) + \mathcal{G}(-p)\\
&\Rightarrow\ \mathcal{B}(-p,p) = \frac{1}{F(-p)}\mathcal{B}(p,-p) - \frac{\mathcal{G}(-p)}{F(-p)}\\
&\Rightarrow\ F(-p) = \frac{1}{F(p)},\quad \mathcal{G}(-p) = -F(-p)\mathcal{G}(p).
\end{aligned} \tag{3.41}$$

The identity for F is expected given the form in equation (3.37). The identity for $\mathcal{G}$ can be written as

$$S(p,-p)\mathcal{G}(p)/r(p) = \mathcal{G}(-p)e^{-2ip}r(p)\ , \tag{3.42}$$

which leads to an equivalent form of writing the solution as follows

$$\begin{aligned}
\psi_{ee}(\ell_1,\ell_2) &= e^{ip\ell_1+i(-p)\ell_2} + S(p,-p)e^{i(-p)\ell_1+ip\ell_2}\\
\psi_{oo}(\ell_1,\ell_2) &= e^{ip\ell_1+i(-p)\ell_2} + S(p,-p)e^{i(-p)\ell_1+ip\ell_2)}\\
\psi_{oe}(\ell_1,\ell_2) &= r(p)e^{ip\ell_1+i(-p)\ell_2}(1+\delta_{\ell_1+1,\ell_2}\mathcal{G}(-p)) + \frac{1}{r(p)}S(p,-p)e^{i(-p)\ell_1+ip\ell_2}\\
\psi_{eo}(\ell_1,\ell_2) &= \frac{1}{r(p)}e^{ip\ell_1+i(-p)\ell_2}(1-\delta_{\ell_1+1,\ell_2}\,\kappa^2 r(p)^2\mathcal{G}(-p)) + r(p)S(p,-p)e^{i(-p)\ell_1+ip\ell_2}\ .
\end{aligned} \tag{3.43}$$

Note that we distribute the term $\exp(-2ip)$ into the overall exponent as $\exp(i(-p)(2\ell-1)-ip+ip(2\ell)-ip) = \exp(i(-p)(2\ell)+ip(2\ell-1))$. This is because the $\exp(-2ip)$ term comes from contributions of p_1 and p_2: $\exp(-i(p_1-p_2))$. In turn, this has the effect of exchanging p_1 and p_2 to give the direct momenta[6] exponential term. The above final form will be useful when recovering the contact terms from the general solution in Section 3.2.4.

[6]By direct momenta, we mean the unpermuted incoming set of momenta $\{p_1, p_2\}$.

At this point, if we were only interested in two magnon excitations we would be done, since in string theory we need to impose the zero momentum condition. However, we wish to solve the chain for arbitrary two magnon centre-of-mass momentum K, as that would be necessary if we were to feed the solution into the three-magnon problem at a later stage. Therefore, starting from the next section we will study how to solve the two magnon problem for $K \neq 0$. Apart from exhibiting several interesting features, our solution will also shed light on the origin of the centre-of-mass contact terms, which were introduced by hand.

3.2.2 General solution

To solve the 2-magnon problem beyond the CoM frame we will follow the work of [51, 52] on alternating chains (see also Section 2.2.4). As usual for the coordinate Bethe ansatz, one starts by splitting the eigenvalue equations into non-interacting and interacting ones. The non-interacting ones are those involving states where no two magnons are next to each other. First one finds all solutions of the non-interacting equations (all the values of the momenta p_1 and p_2 that solve all those equations with given energy E and total momentum K). One then combines them appropriately to solve the interacting equations. The new feature in [51, 52], compared to more standard spin chains, is that there is more than one set of momenta $\{p_1, p_2\}$ giving the same E_2 and K. These additional momenta also need to be added in order to obtain a solution of the interacting equations.

One can also think of the above in terms of the formalism of [47], where apart from the usual Bethe swap of momenta one allows a discrete number of additional momenta (see Section 2.2.3). In that work, the additional momenta were needed for the three magnon problem, but in our case we see the need already at the two magnon level.

For the non-interacting equations (3.20) we make the same ansatz as (3.25), including the relations (3.24). The difference is in treating the interacting equations (3.21). Following the treatment in [51, 52], instead of contact terms as in (3.26), we will add an extra set of momenta $\{k_1, k_2\}$ which also correspond to the same total momentum K and energy E_2. By adding these terms (and their permutations) to our ansatz, we will show that the interacting equations are satisfied without any constraints on the momenta.

The additional momenta

The main important feature of the type of dispersion relation (3.14) is that one can achieve the same two magnon energy with more than one set of momenta. To see this, let us consider the solutions of the equations

$$K = p_1 + p_2 \quad \text{and} \quad E_2(p_1, p_2) = E_1(p_1) + E_2(p_2) \ , \tag{3.44}$$

for given total momentum K and total energy E_2. Rewriting (3.14) slightly, we have

$$E_2(p_1, p_2) = 2(\kappa + 1/\kappa) + \frac{1}{\kappa}\gamma_1\sqrt{A} + \frac{1}{\kappa}\gamma_2\sqrt{B}, \quad \gamma_1 = \gamma_2 = \pm 1, \tag{3.45}$$

where $A = \kappa^4 + 1 + 2\kappa^2\cos(2p_1)$, $B = \kappa^4 + 1 + 2\kappa^2\cos(2p_2)$. We switch to new variables $K = p_1 + p_2$ and $2q = p_1 - p_2$ so that $p_1 = (1/2)K + q$ and $p_2 = (1/2)K - q$. Then, defining $\Omega = E_2\kappa - 2\kappa(\kappa + 1/\kappa)$, we find that

$$\begin{aligned}
&\Omega = \gamma_1\sqrt{A} + \gamma_2\sqrt{B} \\
&\Rightarrow\ A = \Omega^2 - 2\gamma_2\Omega\sqrt{B} + B \\
&\Rightarrow\ 4\Omega^2 B = \Omega^4 - \Omega^2 A + \Omega^2 B - \Omega^2 A + A^2 - AB + \Omega^2 B - AB + B^2 \\
&\Rightarrow\ \Omega^4 - 2\Omega^2 A - 2\Omega^2 B + A^2 - 2AB + B^2 = 0.
\end{aligned} \tag{3.46}$$

Substituting

$$\begin{aligned}
A &= \kappa^4 + 1 + 2\kappa^2\cos(K)\cos(2q) - 2\kappa^2\sin(K)\sin(2q), \\
B &= \kappa^4 + 1 + 2\kappa^2\cos(K)\cos(2q) + 2\kappa^2\sin(K)\sin(2q),
\end{aligned} \tag{3.47}$$

into the above equation, one can solve for $\cos(2q)$ to find [7]

$$\cos(2q) = \frac{T_1}{32\kappa^4} \pm \frac{\sqrt{T_2}}{32\kappa^4}, \tag{3.48}$$

where

$$\begin{aligned}
T_1 &= -8\kappa^2\,\cot(K)\csc(K)\,\Omega^2, \\
T_2 &= 64\kappa^4\,\sin^2(K)\,(-4\kappa^4\Omega^2 + \Omega^4 - 4\Omega^2 + 16\kappa^4\sin^2(K)) + 64\kappa^4\Omega^4\cos^2(K).
\end{aligned} \tag{3.49}$$

One of the signs for the square root gives back our first momenta $\{p_1, p_2\}$ as well as $\{p_2, p_1\}$ (since cos is an even function). The other sign gives a new set of momenta $\{k_1, k_2\}$ (as well as $\{k_2, k_1\}$) for the same (K, E_2). This new set of momenta is generally complex valued with equal but opposite imaginary parts (since K is always real valued). The real parts also have the interesting feature that they differ by π. This makes them different from a bound state which has equal real parts given by $K/2$. In addition, bound states can also be determined by looking for zeroes and poles of the S-matrix [8]. It can be checked that these new momenta are neither zeroes

[7] Observe that the signs γ_1, γ_2 have been squared out of the final expression.

[8] As a practical example of this, see the spin chain computations performed in [18].

nor poles of the S-matrix determined later in this section. Rather, the new set of momenta are *resonances* [72][73] [9].

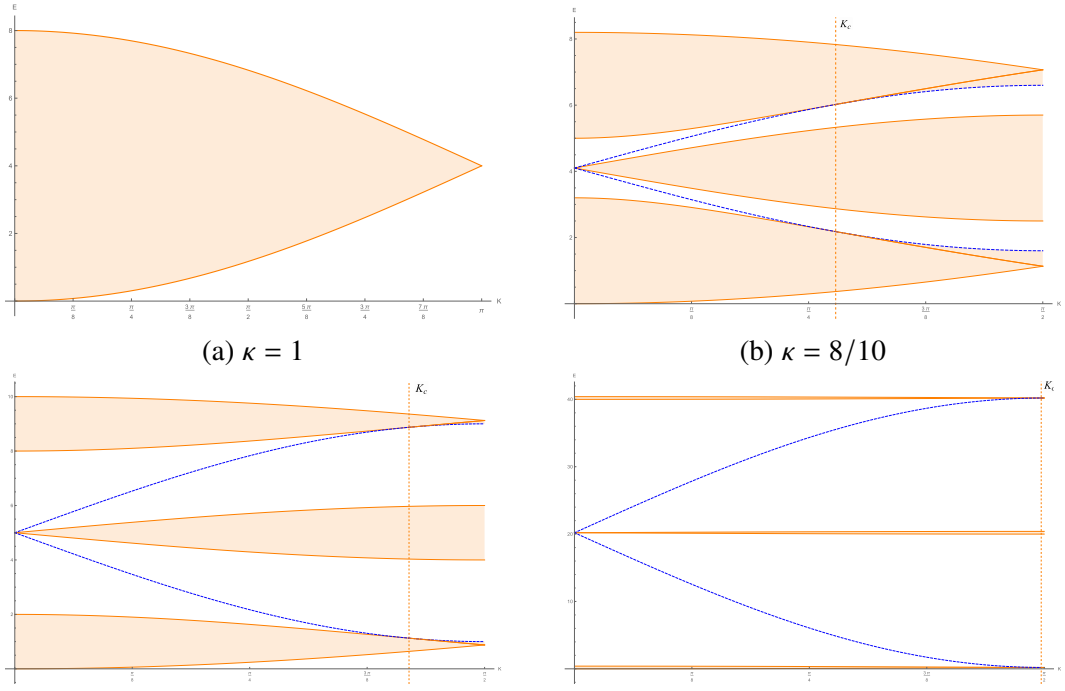

(a) $\kappa = 1$ (b) $\kappa = 8/10$

(c) $\kappa = 5/10$ (d) $\kappa = 1/10$

Figure 3.3: *E-K graphs for various values of κ. The y-axis is the energy E and the x-axis is the total momentum K. We show half of the Brillouin zones. The shaded regions are the scattering continua. The vertical dashed line denotes K_c. After K_c, the blue dashed line becomes a true boundary for the upper and lower continua. Note that the y-axis does change drastically from $\kappa = 5/10$ to $\kappa = 1/10$.*

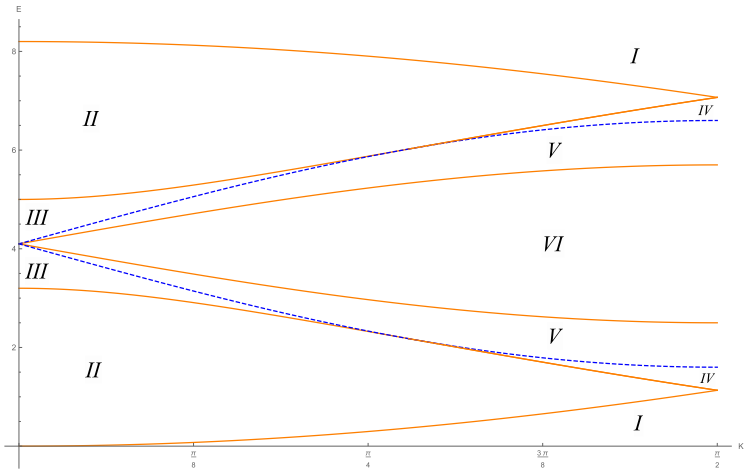

Figure 3.4: *Krupennikov zones*

[9] See especially the discussion on page 99 of [72] for resonances that do not appear as poles or zeroes of the S-matrix.

In Figure 3.3, we have plotted the E-K graphs for various values of κ. The derivation of continua boundaries is performed in Appendix C. The orbifold case, $\kappa = 1$, is shown in Figure 3.3a. It has a single scattering continuum which reflects the fact that the orbifold point is described by the XXX Heisenberg model (see, for example, Figure 2 of [41]). The Brillouin zone, of which we show half in the figures, extends to π.

Tuning away from the orbifold point to $\kappa = 8/10$, the scattering continuum splits into three distinct scattering continua in Figure 3.3b with the Brillouin zone now extending to $\pi/2$ (see also Figure 3.2). These continua are labeled as in Figure 3.4 using the Krupennikov zones described in [52][51]. Regions II, IV and VI label the three scattering continua which are combinations of acoustic-acoustic (AA, the lower region II and IV), optic-optic (OO, the upper region II and IV) and mixed acoustic-optic (AO, region VI). In these regions and before the critical point $K = K_c = \cos^{-1}(\kappa^2)$, the solutions for q consist of two real q solutions and two complex q solutions. After K_c and as discussed in Appendix C, the blue dashed line becomes a true continuum boundary and is given by the curves Z_a for the AA region and Z_d for the OO region. For the AA region (the argument is identical for the OO case), the upper orange curve W_b (which is a true continuum boundary for $K \leq K_c$) traces into the continuum below Z_a and, together, these curves define region IV. The curve W_b, now being inside the continuum, forms internal van Hove singularities. Crossing over this curve, from region II to region IV, changes the nature of the q solutions such that all solutions are real-valued. Outside of the scattering continua, given by regions III and V, all the q solutions are complex-valued. Bound state solutions exist in these regions and were studied in [52][51].

Tuning κ further away from the orbifold point, as shown in Figure 3.3c and most notably in 3.3d, the continua start to flatten and the gaps between the continua start increasing. Notice also that the critical points $K = K_c$ shift towards the end of the first Brillouin zone, which starts to shrink region IV. The collapsing of the continua matches the results shown in Figure 2 of [18] which also exhibits flattening continua as κ approaches zero (in their case, they were studying spin chains in the XZ sector, which we will also study later in Chapter 4 (although, for a different choice of vacuum)).

Thus, in summary, there are four solutions given by $\{q_1, q_2\}$ and their negatives.

Note that the we can add the solutions together to give

$$\boxed{\cos(2q_1)+\cos(2q_2) = -\frac{(E_2-2(\kappa+1/\kappa))^2\cos K}{2\sin^2 K}}\,. \tag{3.50}$$

To translate this new set of momenta back into the form $\{k_1, k_2\}$, let us assume an initial set of momenta $\{p_1, p_2\}$ with sum $K = p_1 + p_2$ and difference $2q_1 = p_1 - p_2$. Then, with the same $K = k_1 + k_2$ but with difference $2q_2 = k_1 - k_2$, we find

$$k_{1,2} = \frac{K}{2} \pm \frac{\pi}{2} \mp \frac{1}{2}\arccos\left(\cos(p_1-p_2) + \frac{(E_2-2(\kappa+1/\kappa))^2\cos K}{2\sin^2 K}\right), \tag{3.51}$$

where we used that $\arccos(-x) = \pi - \arccos(x)$.

Let us remark that the possibility of additional momenta is not there for the XXX dispersion relation $E_2 = 2(1-\cos(p_1)) + 2(1-\cos(p_2))$, where the only solutions (up to periodicity) are the original p_1, p_2 and their permutation p_2, p_1. This feature is characteristic of staggered-type chains such as the one under study (see e.g. a comment in [74], p.137). Of course, the swapped solutions $q_1 \to -q_1$ and $q_2 \to -q_2$ are still there in (3.50), so we find a total of four solutions of our two magnon dispersion relation:

Direct p	Swapped p	Direct k	Swapped k
$\{p_1, p_2\}$	$\{p_2, p_1\}$	$\{k_1, k_2\}$	$\{k_2, k_1\}$

As all these momenta have the same total energy and momentum, the most general wavefunction for fixed K and E_2 will be a superposition of all of them. As expected from the discussion in [52, 51], generalising the Bethe ansatz to include the k momenta will indeed lead to a solution of the interacting equations.

Generalised Bethe ansatz

Given the above discussion, we will now update the wavefunction (3.22) to include all the four sets of momenta. We have:

$$\begin{aligned}|p_1,p_2,k_1,k_2\rangle = &\sum_{r<s}\Big(\psi_{ee}(2r,2s)\,|2r,2s\rangle + \psi_{oo}(2r+1,2s+1)\,|2r+1,2s+1\rangle\Big)\\ &+\sum_{r<s+1}\Big(\psi_{oe}(2r-1,2s)\,|2r-1,2s\rangle + \psi_{eo}(2r,2s+1)\,|2r,2s+1\rangle\Big)\,,\end{aligned} \tag{3.52}$$

with

$$\begin{aligned}
\psi_{ee}(\ell_1,\ell_2) &= A_{ee}(p_1,p_2)e^{ip_1\ell_1+ip_2\ell_2} + A_{ee}(p_2,p_1)e^{ip_2\ell_1+ip_1\ell_2} \\
&\quad + A_{ee}(k_1,k_2)e^{ik_1\ell_1+ik_2\ell_2} + A_{ee}(k_2,k_1)e^{ik_2\ell_1+ik_1\ell_2}, \\
\psi_{eo}(\ell_1,\ell_2) &= A_{eo}(p_1,p_2)e^{ip_1\ell_1+ip_2\ell_2} + A_{eo}(p_2,p_1)e^{ip_2\ell_1+ip_1\ell_2} \\
&\quad + A_{eo}(k_1,k_2)e^{ik_1\ell_1+ik_2\ell_2} + A_{eo}(k_2,k_1)e^{ik_2\ell_1+ik_1\ell_2}, \\
\psi_{oe}(\ell_1,\ell_2) &= A_{oe}(p_1,p_2)e^{ip_1\ell_1+ip_2\ell_2} + A_{oe}(p_2,p_1)e^{ip_2\ell_1+ip_1\ell_2} \\
&\quad + A_{oe}(k_1,k_2)e^{ik_1\ell_1+ik_2\ell_2} + A_{oe}(k_2,k_1)e^{ik_2\ell_1+ik_1\ell_2}, \\
\psi_{oo}(\ell_1,\ell_2) &= A_{oo}(p_1,p_2)e^{ip_1\ell_1+ip_2\ell_2} + A_{oo}(p_2,p_1)e^{ip_2\ell_1+ip_1\ell_2} \\
&\quad + A_{oo}(k_1,k_2)e^{ik_1\ell_1+ik_2\ell_2} + A_{oo}(k_2,k_1)e^{ik_2\ell_1+ik_1\ell_2}.
\end{aligned} \tag{3.53}$$

Each of these extra terms are solutions of the non-interacting equations and therefore their sum is also a solution of the non-interacting equations. From the non-interacting equations, the coefficients for the direct and swapped p momenta are fixed in terms of $A_{ee}(p_1,p_2)$and $A_{ee}(p_2,p_1)$ as in equation (3.24), of course with $p_1 \leftrightarrow p_2$ in the swapped case. In exactly the same manner, the coefficients for the direct k momenta and swapped k momenta are fixed, through the appropriate replacements in equation (3.24), in terms of the coefficients $A_{ee}(k_1,k_2)$ and $A_{ee}(k_2,k_1)$, respectively. Explicitly, we have (with ℓ_1,ℓ_2 even or odd as required by the labels)

$$\begin{aligned}
\psi_{ee}(\ell_1,\ell_2) &= A_{ee}(p_1,p_2)e^{ip_1\ell_1+ip_2\ell_2} + A_{ee}(p_2,p_1)e^{ip_2\ell_1+ip_1\ell_2} \\
&\quad + A_{ee}(k_1,k_2)e^{ik_1\ell_1+ik_2\ell_2} + A_{ee}(k_2,k_1)e^{ik_2\ell_1+ik_1\ell_2}, \\
\psi_{eo}(\ell_1,\ell_2) &= r(p_2)\,A_{ee}(p_1,p_2)e^{ip_1\ell_1+ip_2\ell_2} + r(p_1)\,A_{ee}(p_2,p_1)e^{ip_2\ell_1+ip_1\ell_2} \\
&\quad + r(k_2)\,A_{ee}(k_1,k_2)e^{ik_1\ell_1+ik_2\ell_2} + r(k_1)\,A_{ee}(k_2,k_1)e^{ik_2\ell_1+ik_1\ell_2}, \\
\psi_{oe}(\ell_1,\ell_2) &= r(p_1)\,A_{ee}(p_1,p_2)e^{ip_1\ell_1+ip_2\ell_2} + r(p_2)\,A_{ee}(p_2,p_1)e^{ip_2\ell_1+ip_1\ell_2} \\
&\quad + r(k_1)\,A_{ee}(k_1,k_2)e^{ik_1\ell_1+ik_2\ell_2} + r(k_2)\,A_{ee}(k_2,k_1)e^{ik_2\ell_1+ik_1\ell_2}, \\
\psi_{oo}(\ell_1,\ell_2) &= r(p_1)r(p_2)\,A_{ee}(p_1,p_2)e^{ip_1\ell_1+ip_2\ell_2} + r(p_1)r(p_2)\,A_{ee}(p_2,p_1)e^{ip_2\ell_1+ip_1\ell_2} \\
&\quad + r(k_1)r(k_2)\,A_{ee}(k_1,k_2)e^{ik_1\ell_1+ik_2\ell_2} + r(k_1)r(k_2)\,A_{ee}(k_2,k_1)e^{ik_2\ell_1+ik_1\ell_2}\ .
\end{aligned} \tag{3.54}$$

Imposing the non-interacting equations has left us with four remaining coefficients: $A_{ee}(p_1,p_2)$, $A_{ee}(p_2,p_1)$, $A_{ee}(k_1,k_2)$ and $A_{ee}(k_2,k_1)$. These coefficients will be fixed in terms of $A_{ee}(p_1,p_2)$ through the interacting equations and will give us our final S-matrices.

Interacting equations

It is useful to simplify the interacting equations (3.21) by noting the fact that the even-odd and odd-even non-interacting equations (3.20) also hold if we set $r = s$ (even though these equations are unphysical). We can subtract the even-odd interacting equation in (3.21) from the corresponding one in (3.20) and similarly for the odd-even one, to obtain the two equations

$$\frac{1}{\kappa}\psi_{ee}(2r, 2r) - \frac{2}{\kappa}\psi_{oe}(2r-1, 2r) + \frac{1}{\kappa}\psi_{oo}(2r-1, 2r-1) = 0 \,, \tag{3.55}$$

and

$$\kappa\, \psi_{ee}(2s, 2s) - 2\kappa\, \psi_{eo}(2s, 2s+1) + \kappa\, \psi_{oo}(2s+1, 2s+1) = 0 \,. \tag{3.56}$$

Now we apply the following procedure to solve these equations[10]:

- We take equation (3.55) and disregard the coefficients $A_{ee}(k_1, k_2)$ and $A_{ee}(k_2, k_1)$ momentarily. We then solve equation (3.55) for $A_{ee}(p_2, p_1)$ in terms of $A_{ee}(p_1, p_2)$. This gives us the S-matrix for $\{p_1, p_2\} \to \{p_2, p_1\}$ scattering.
- Next, we disregard the coefficients $A_{ee}(p_1, p_2)$ and $A_{ee}(p_2, p_1)$ momentarily and solve again equation (3.55) but this time for $A_{ee}(k_2, k_1)$ in terms of $A_{ee}(k_1, k_2)$. This gives us the S-matrix for $\{k_1, k_2\} \to \{k_2, k_1\}$ scattering.
- Since each scattering sector is solved, their sum also solves equation (3.55). It does not however solve equation (3.56), but we still have two coefficients remaining: $A_{ee}(p_1, p_2)$ and $A_{ee}(k_1, k_2)$ (after substituting the results from the previous points). We can therefore solve for $A_{ee}(k_1, k_2)$ in terms of $A_{ee}(p_1, p_2)$ which gives us the S-matrix for $\{p_1, p_2\} \to \{k_1, k_2\}$ scattering. Thus, equation (3.56) is also solved.

It should be noted that we could also start this procedure with equation (3.56) first and then end with equation (3.55). The S-matrices will be different to the first procedure but are related by inversion of κ, except for the S-matrices where we go from p's to k's.

[10] As we will later show, this procedure results in two magnon wavefunctions with exactly the same form as the three spin deviation wavefunctions (2.104) in Section 2.2.3.

Following the above procedure, in the end we find two $\mathbb{Z}_2$-conjugate solutions for the remaining coefficients. The first solution is given by

$$\begin{aligned}
A_{ee}(p_1,p_2) &= \big(a(k_2,k_1)b(k_1,k_2) - b(k_2,k_1)a(k_1,k_2)\big)a(p_1,p_2)\\
A_{ee}(p_2,p_1) &= -\big(a(k_2,k_1)b(k_1,k_2) - b(k_2,k_1)a(k_1,k_2)\big)a(p_2,p_1)\\
A_{ee}(k_1,k_2) &= -\big(a(p_2,p_1)b(p_1,p_2) - b(p_2,p_1)a(p_1,p_2)\big)a(k_1,k_2)\\
A_{ee}(k_2,k_1) &= -\big(a(p_1,p_2)b(p_2,p_1) - b(p_1,p_2)a(p_2,p_1)\big)a(k_2,k_1)\ ,
\end{aligned} \tag{3.57}$$

and the second solution (for which we will use the letter B) is given by

$$\begin{aligned}
B_{ee}(p_1,p_2) &= \big(a(k_2,k_1)b(k_1,k_2) - b(k_2,k_1)a(k_1,k_2)\big)b(p_1,p_2)\\
B_{ee}(p_2,p_1) &= -\big(a(k_2,k_1)b(k_1,k_2) - b(k_2,k_1)a(k_1,k_2)\big)b(p_2,p_1)\\
B_{ee}(k_1,k_2) &= -\big(a(p_2,p_1)b(p_1,p_2) - b(p_2,p_1)a(p_1,p_2)\big)b(k_1,k_2)\\
B_{ee}(k_2,k_1) &= -\big(a(p_1,p_2)b(p_2,p_1) - b(p_1,p_2)a(p_2,p_1)\big)b(k_2,k_1)\ ,
\end{aligned} \tag{3.58}$$

where the coefficients a, b are

$$\boxed{\begin{aligned}
a(p_1,p_2,\kappa) &= e^{i(p_1+p_2)} - 2e^{ip_1}r(p_2,\kappa) + r(p_1,\kappa)r(p_2,\kappa)\ ,\\
b(p_1,p_2,\kappa) &= 1 - 2e^{ip_1}r(p_1,\kappa) + r(p_1,\kappa)r(p_2,\kappa)e^{i(p_1+p_2)}\ ,
\end{aligned}} \tag{3.59}$$

where the ratio $r(p,\kappa)$ is defined in equation (3.13). Clearly, these coefficients are deformations of the terms appearing in the XXX S-matrix, to which they reduce in the $\kappa = 1$ limit. That is, $a(p_1,p_2,1) = b(p_1,p_2,1) = 1 - 2e^{ip_1} + e^{i(p_1+p_2)}$.

For the wavefunction $\psi_{ee}(\ell_1,\ell_2)$, we can therefore combine the two solutions with general coefficients α, β

$$\psi_{ee}(\ell_1,\ell_2) = \alpha\ \psi^A_{ee}(\ell_1,\ell_2) + \beta\ \psi^B_{ee}(\ell_1,\ell_2), \tag{3.60}$$

where the notation is that ψ^A_{ee} has the A-coefficients and ψ^B_{ee} has the B-coefficients. Note that A, B are not indices, just different labels for the different wavefunctions. The even-odd, odd-even and odd-odd parts of the wavefunction are as above but with appropriate placements of $r(p)$. As we will show later, combining ψ^A and ψ^B in this way is necessary in order to get an eigenstate of the $\mathbb{Z}_2$ symmetry.

In summary, the total eigenstate that solves the two magnon problem is given by

$$|\psi\rangle_{\text{tot}} = \alpha\ |p_1,p_2,k_1,k_2\rangle_A + \beta\ |p_1,p_2,k_1,k_2\rangle_B\ . \tag{3.61}$$

Let us note that the structure of the solution bears a strong similarity to the approach of [47]. As discussed in Section 2.2.3, an extra set of momenta was used to solve

the three spin deviation problem for a spin-1 non-integrable system (for which there exists a scattering channel that exhibits diffractive scattering) by introducing a finite number of extra *discrete diffractive terms* to the usual Bethe ansatz. The main difference here is that the additional set of momenta already appears at the two magnon level. Writing, for example, $\psi^A_{ee}(\ell_1, \ell_2)$ as

$$\psi^A_{ee}(\ell_1, \ell_2) = \Psi(k_1, k_2)\Omega^A(p_1, p_2; \ell_1, \ell_2) - \Psi(p_1, p_2)\Omega^A(k_1, k_2; \ell_1, \ell_2), \quad (3.62)$$

where (here q_i stands for either p_i or k_i)

$$\Psi(q_1, q_2) = a(q_2, q_1)b(q_1, q_2) - b(q_2, q_1)a(q_1, q_2), \quad (3.63)$$

and

$$\Omega^A(q_1, q_2; \ell_1, \ell_2) = a(q_1, q_2)e^{iq_1\ell_1 + iq_2\ell_2} - a(q_2, q_1)e^{iq_2\ell_1 + iq_1\ell_2}\ , \quad (3.64)$$

the similarity to equation (2.104) is apparent.

Properties of the S-matrices

Factoring $A_{ee}(p_1, p_2)$ out from the above wavefunctions, we have

$$\begin{aligned}
\psi_{ee}(\ell_1, \ell_2) &= e^{ip_1\ell_1 + ip_2\ell_2} + S(p_1, p_2)e^{ip_2\ell_1 + ip_1\ell_2} \\
&\quad + T(p_1, p_2, k_1, k_2)e^{ik_1\ell_1 + ik_2\ell_2} + T(p_1, p_2, k_1, k_2)S(k_1, k_2)e^{ik_2\ell_1 + ik_1\ell_2}\ , \\
\psi_{eo}(\ell_1, \ell_2) &= r(p_2)e^{ip_1\ell_1 + ip_2\ell_2} + r(p_1)S(p_1, p_2)e^{ip_2\ell_1 + ip_1\ell_2} \\
&\quad + r(k_2)T(p_1, p_2, k_1, k_2)e^{ik_1\ell_1 + ik_2\ell_2} \\
&\quad + r(k_1)T(p_1, p_2, k_1, k_2)S(k_1, k_2)e^{ik_2\ell_1 + ik_1\ell_2}\ , \\
\psi_{oe}(\ell_1, \ell_2) &= r(p_1)e^{ip_1\ell_1 + ip_2\ell_2} + r(p_2)S(p_1, p_2)e^{ip_2\ell_1 + ip_1\ell_2} \\
&\quad + r(k_1)T(p_1, p_2, k_1, k_2)e^{ik_1\ell_1 + ik_2\ell_2} \\
&\quad + r(k_2)T(p_1, p_2, k_1, k_2)S(k_1, k_2)e^{ik_2\ell_1 + ik_1\ell_2}\ , \\
\psi_{oo}(\ell_1, \ell_2) &= r(p_1)r(p_2)e^{ip_1\ell_1 + ip_2\ell_2} + r(p_1)r(p_2)S(p_1, p_2)e^{ip_2\ell_1 + ip_1\ell_2} \\
&\quad + r(k_1)r(k_2)T(p_1, p_2, k_1, k_2)e^{ik_1\ell_1 + ik_2\ell_2} \\
&\quad + r(k_1)r(k_2)T(p_1, p_2, k_1, k_2)S(k_1, k_2)e^{ik_2\ell_1 + ik_1\ell_2},
\end{aligned} \quad (3.65)$$

where we have defined three S-matrices:

$$S(p_1, p_2) = \frac{A_{ee}(p_2, p_1)}{A_{ee}(p_1, p_2)}\ ,\ S(k_1, k_2) = \frac{A_{ee}(k_2, k_1)}{A_{ee}(k_1, k_2)}\ ,\ T(p_1, p_2, k_1, k_2) = \frac{A_{ee}(k_1, k_2)}{A_{ee}(p_1, p_2)}. \quad (3.66)$$

The S-matrix $S(p_1, p_2)$ is the usual Bethe ansatz S-matrix, while $S(k_1, k_2)$ plays the same role for the k momenta. However $T(p_1, p_2, k_1, k_2)$ is a new object, which

describes the scattering where an initial state with momenta $\{p_1, p_2\}$ becomes a final state with momenta $\{k_1, k_2\}$.

For the A solution, these S-matrices take the form

$$S^A(p_1, p_2; \kappa) = -\frac{a(p_2, p_1)}{a(p_1, p_2)}, \quad S^A(k_1, k_2; \kappa) = -\frac{a(k_2, k_1)}{a(k_1, k_2)}. \tag{3.67}$$

while T is

$$T^A(p_1, p_2; k_1, k_2, \kappa) = -\frac{a(p_2, p_1)b(p_1, p_2) - b(p_2, p_1)a(p_1, p_2)}{a(k_2, k_1)b(k_1, k_2) - b(k_2, k_1)a(k_1, k_2)} \frac{a(k_1, k_2)}{a(p_1, p_2)}. \tag{3.68}$$

Similarly, for the solution with B coefficients we have,

$$S^B(p_1, p_2; \kappa) = -\frac{b(p_2, p_1)}{b(p_1, p_2)}, \quad S^B(k_1, k_2; \kappa) = -\frac{b(k_2, k_1)}{b(k_1, k_2)}, \tag{3.69}$$

and

$$T^B(p_1, p_2; k_1, k_2; \kappa) = -\frac{a(p_2, p_1)b(p_1, p_2) - b(p_2, p_1)a(p_1, p_2)}{a(k_2, k_1)b(k_1, k_2) - b(k_2, k_1)a(k_1, k_2)} \frac{b(k_1, k_2)}{b(p_1, p_2)}. \tag{3.70}$$

It is intriguing to note that we can write all the S-matrices above (3.67), (3.69), (3.68) and (3.70) in a unified form by including the ratio of the Wronskian-type terms even for the S^A, S^B where the Wronskian-type factor becomes trivial. Using generic momenta $q_1, q_2 \to q_1', q_2'$ for the scattering process, we obtain the unifying formula:

$$\boxed{S(q_1, q_2; q_1', q_2') = -\frac{a(q_2, q_1)b(q_1, q_2) - b(q_2, q_1)a(q_1, q_2)}{a(q_2', q_1')b(q_1', q_2') - b(q_2', q_1')a(q_1', q_2')} \frac{b(q_1', q_2')}{b(q_1, q_2)}} \tag{3.71}$$

and we see that $S(p_1, p_2; p_2, p_1) = -S(p_1, p_2), S(k_1, k_2; k_2, k_1) = -S(k_1, k_2)$ and $S(p_1, p_2; k_1, k_2) = T(p_1, p_2; k_1, k_2)$.

The S matrices for the p and k momenta satisfy the unitary condition

$$S^A(p_1, p_2)S^A(p_2, p_1) = 1 \quad , \quad S^B(p_1, p_2)S^B(p_2, p_1) = 1 \tag{3.72}$$

as well as

$$S^A(p, p) = -1 \quad , \quad S^B(p, p) = -1. \tag{3.73}$$

They also smoothly reduce to the XXX S-matrix as $\kappa \to 1$, e.g

$$S^A(p_1, p_2) = -\frac{e^{i(p_1+p_2)} - 2e^{ip_2}r(p_1, \kappa) + r(p_1, \kappa)r(p_2, \kappa)}{e^{i(p_1+p_2)} - 2e^{ip_1}r(p_2, \kappa) + r(p_1, \kappa)r(p_2, \kappa)} \xrightarrow{\kappa \to 1} -\frac{e^{i(p_1+p_2)} - 2e^{ip_2} + 1}{e^{i(p_1+p_2)} - 2e^{ip_1} + 1}. \tag{3.74}$$

Using that $r(0,\kappa)=1$, it can also be easily seen that

$$S^{A,B}(0,p)=S^{A,B}(p,0)=1, \tag{3.75}$$

a property it shares with the XXX-model S-matrix.

On the other hand, $|T|\neq 1$ and therefore it is not a phase [11]. There is an interesting identity that one can derive by thinking physically about scattering from $\{p_1,p_2\}$ to $\{k_2,k_1\}$: one can first send $\{p_1,p_2\}\to\{k_1,k_2\}$ and then $\{k_1,k_2\}\to\{k_2,k_1\}$ or one can first send $\{p_1,p_2\}\to\{p_2,p_1\}$ and then $\{p_2,p_1\}\to\{k_2,k_1\}$. This gives

$$S^A(k_1,k_2)T^A(p_1,p_2,k_1,k_2)=T^A(p_2,p_1,k_2,k_1)S^A(p_1,p_2), \tag{3.76}$$

and a similar identity for the B coefficient solutions.

Symmetries

The two solutions $|p_1,p_2,k_1,k_2\rangle_A$ and $|p_1,p_2,k_1,k_2\rangle_B$ are related by $\mathbb{Z}_2$ symmetry. Recalling that $r(p,1/\kappa)=1/r(p,\kappa)$, we can see that

$$\begin{aligned} a(p_1,p_2,1/\kappa)&=\frac{1}{r(p_1)r(p_2)}b(p_1,p_2,\kappa),\\ b(p_1,p_2,1/\kappa)&=\frac{1}{r(p_1)r(p_2)}a(p_1,p_2,\kappa)\ , \end{aligned} \tag{3.77}$$

from which we find for the S-matrices ($\{x,y\}=\{p_1,p_2\}$ or $\{k_1,k_2\}$, similar for $\{w,z\}$)

$$S^A(x,y,1/\kappa)=S^B(x,y,\kappa),\quad T^A(x,y,w,z,1/\kappa)=\frac{r(k_1)r(k_2)}{r(p_1)r(p_2)}T^B(x,y,w,z,\kappa). \tag{3.78}$$

Using (3.77) one can check that the total action of $\mathbb{Z}_2$ on say ψ^A_{ee} is

$$\psi^A_{ee}\to -r(p_1)^{-2}r(p_2)^{-2}r(k_1)^{-2}r(k_2)^{-2}\psi^B_{oo}. \tag{3.79}$$

The other wavefunctions work similarly, with even and odd sites being exchanged by the $\mathbb{Z}_2$ action. Therefore, if we want the general solution (3.61) to also be an eigenstate of $\mathbb{Z}_2$ we need to impose $\alpha(1/\kappa)=\pm\beta(\kappa)$ and we find

$$\mathbb{Z}_2\,|\psi\rangle_{\text{tot}}=\mp\big(r(p_1)r(p_2)r(k_1)r(k_2)\big)^{-2}\,|\psi\rangle_{\text{tot}}. \tag{3.80}$$

[11] However we expect that a process where $p_1+p_2\to k_1+k_2$ is compensated by the inverse process.

It is also useful to study the symmetries related to permutations between the p and k momenta. Let us define the transformations:

$$\sigma_p : \{p_1, p_2\} \leftrightarrow \{p_2, p_1\} \, , \sigma_k : \{k_1, k_2\} \leftrightarrow \{k_2, k_1\} \, , \sigma_{pk,1} : \{p_1, p_2\} \leftrightarrow \{k_1, k_2\} \, , \tag{3.81}$$

and where the additional map $\sigma_{pk,2} : \{p_1, p_2\} \leftrightarrow \{k_2, k_1\}$ is a composition, e.g. $\sigma_{pk,2} = \sigma_k \circ \sigma_{pk,1} \circ \sigma_p$. We can now consider how these maps act on different parts of the wavefunctions, for example:

$$\begin{aligned} \sigma_p \psi_{oe}(\ell_1, \ell_2) &= -\psi_{oe}(\ell_1, \ell_2) \\ \sigma_k \psi_{oe}(\ell_1, \ell_2) &= -\psi_{oe}(\ell_1, \ell_2) \\ \sigma_{pk,1} \psi_{oe}(\ell_1, \ell_2) &= -\psi_{oe}(\ell_1, \ell_2) \\ \sigma_{pk,2} \psi_{oe}(\ell_1, \ell_2) &= -\psi_{oe}(\ell_1, \ell_2). \end{aligned} \tag{3.82}$$

In Table 3.1, we summarise the action of the $\mathbb{Z}_2$ maps, as well as the momentum permutation maps, on the A and B solutions.

Transformation	**Wavefunction**		
	$\|\psi\rangle_{(r)}$	$\|\psi\rangle_{(A)}$	$\|\psi\rangle_{(B)}$
$\mathbb{Z}_2$	$-z_{(r)}\|\psi\rangle_{(r)}$	$-z_{(g)}\|\psi\rangle_{(B)}$	$-z_{(g)}\|\psi\rangle_{(A)}$
σ_p	$-\|\psi\rangle_{(r)}$	$-\|\psi\rangle_{(A)}$	$-\|\psi\rangle_{(B)}$
σ_k	$\cdot$	$-\|\psi\rangle_{(A)}$	$-\|\psi\rangle_{(B)}$
$\sigma_{pk,1}$	$\cdot$	$-\|\psi\rangle_{(A)}$	$-\|\psi\rangle_{(B)}$
$\sigma_{pk,2}$	$\cdot$	$-\|\psi\rangle_{(A)}$	$-\|\psi\rangle_{(B)}$
$\sigma_p \circ \sigma_k$	$\cdot$	$+\|\psi\rangle_{(A)}$	$+\|\psi\rangle_{(B)}$
$\sigma_p \circ \sigma_{pk,1}$	$\cdot$	$+\|\psi\rangle_{(A)}$	$+\|\psi\rangle_{(B)}$
$\sigma_p \circ \sigma_{pk,2}$	$\cdot$	$+\|\psi\rangle_{(A)}$	$+\|\psi\rangle_{(B)}$
σ^n		$(-1)^n\|\psi\rangle_{(A)}$	$(-1)^n\|\psi\rangle_{(B)}$

Table 3.1: *A summary of the transformations of the wavefunctions considered in the text under the discrete symmetries of the problem. Here $|\psi\rangle_{(r)}$ is the restricted solution (3.84) while the two general solutions are as given in (3.52) with the coefficients in (3.57),(3.58) respectively. The respective $\mathbb{Z}_2$ eigenvalues are $z_r = (r(p_1)r(p_2))^{-2}(r(k_1)r(k_2))^{-1}$ and $z_g = (r(p_1)r(p_2))^{-2}(r(k_1)r(k_2))^{-2}$. The momentum maps are as defined in (3.81). (σ^n means any n-composition of the sigma operators).*

To conclude this section, we have exhibited the solution of the 2-magnon problem for the alternating Hamiltonian (3.1). The general solution includes scattering of the original momenta to another set of momenta which are not related by permutations. This feature, which is characteristic of staggered-type chains, can be thought of in

terms of the *discrete* diffractive framework discussed in Section 2.2.3 and, at least for the cases discussed there, is not by itself an impediment to solvability. Therefore, even though our system does exhibit diffractive scattering, and would on the surface appear to fail Sutherland's criterion of quantum integrability [46] (see also [48] and the discussion in Section 2.2.2), we believe that it is important to understand how far one can extend the Bethe ansatz framework for the study of the three- and higher-magnon problem, and in particular whether a discrete-diffractive ansatz can play a role in its solution.[12]

3.2.3 Restricted solution

As mentioned in the previous section, the k-momenta are generally complex-valued. This can lead to divergences coming from the exponents $\exp(ik_1\ell_1 + ik_2\ell_2)$ and $\exp(ik_2\ell_1 + ik_1\ell_2)$ in the wavefunctions. In fact, there are two ways this can happen: in the case of an infinite length spin chain, one of these terms will exponentially increase as the relative distance $|\ell_2 - \ell_1| \to \infty$; and, when considering the CoM case $K = 0$, the imaginary parts of k_1, k_2 diverge to complex infinity which again leads to exponentially increasing/decaying terms even for finite length chains. Thus, in these cases, the four term solution that we found in Section 3.2.2 is not applicable. However, it is possible to take an appropriate linear combination of the two $\mathbb{Z}_2$ conjugate solutions which removes the unwanted term.

Let us write $k_1 = K/2 + \pi/2 - iv$, $k_2 = K/2 - \pi/2 + iv$, $v \geq 0$. Since in the wavefunction we have $\ell_2 > \ell_1$, the term with swapped k-momenta is the one leading to the divergence in the cases described above: $|\exp(ik_2\ell_1 + ik_1\ell_2)| \sim |e^{v(\ell_2-\ell_1)}| \to \infty$.

Therefore, let us try to solve the eigenvalue problem while imposing the boundary condition that there are no divergences at infinite relative distance or $K = 0$. This requires that the swapped k coefficients be set to zero. The ansatz will still be of the

[12] Sutherland's criterion, discussed in Section 2.2.2, applies to the three- and higher-magnon problem, while here we already see additional momenta at the two magnon level. We can expect, of course, that the additional momenta will be a feature of the higher-magnon problems as well.

form (3.52), however now each Bethe wavefunction will consist of just three terms[13]

$$\begin{aligned}
\psi^{(r)}_{ee}(\ell_1,\ell_2) &= A_{ee}(p_1,p_2)e^{ip_1\ell_1+ip_2\ell_2} + A_{ee}(p_2,p_1)e^{ip_2\ell_1+ip_1\ell_2} \\
&\quad + A_{ee}(k_1,k_2)e^{ik_1\ell_1+ik_2\ell_2}, \\
\psi^{(r)}_{oe}(\ell_1,\ell_2) &= A_{oe}(p_1,p_2)e^{ip_1\ell_1+ip_2\ell_2} + A_{oe}(p_2,p_1)e^{ip_2\ell_1+ip_1\ell_2} \\
&\quad + A_{oe}(k_1,k_2)e^{ik_1\ell_1+ik_2\ell_2}, \\
\psi^{(r)}_{eo}(\ell_1,\ell_2) &= A_{eo}(p_1,p_2)e^{ip_1\ell_1+ip_2\ell_2} + A_{eo}(p_2,p_1)e^{ip_2\ell_1+ip_1\ell_2} \\
&\quad + A_{eo}(k_1,k_2)e^{ik_1\ell_1+ik_2\ell_2}, \\
\psi^{(r)}_{oo}(\ell_1,\ell_2) &= A_{oo}(p_1,p_2)e^{ip_1\ell_1+ip_2\ell_2} + A_{oo}(p_2,p_1)e^{ip_2\ell_1+ip_1\ell_2} \\
&\quad + A_{oo}(k_1,k_2)e^{ik_1\ell_1+ik_2\ell_2}.
\end{aligned} \tag{3.83}$$

We will call this the *restricted* solution, and we will see that it is still possible to solve all the equations with this restriction.[14]. The solution is as follows:

$$\begin{aligned}
A_{ee}(p_1,p_2) &= a(k_2,k_1)b(p_1,p_2) - b(k_2,k_1)a(p_1,p_2)\ , \\
A_{ee}(p_2,p_1) &= -\big(a(k_2,k_1)b(p_2,p_1) - b(k_2,k_1)a(p_2,p_1)\big)\ , \\
A_{ee}(k_1,k_2) &= -\big(a(p_2,p_1)b(p_1,p_2) - b(p_2,p_1)a(p_1,p_2)\big).
\end{aligned} \tag{3.84}$$

We observe that the A's here are quadratic in the a, b-coefficients, unlike the general (3.57), (3.58) which are cubic.

Let us call $|\psi\rangle_{(r)} = |p_1,p_2;k_1,k_2\rangle_{(r)}$ the solution obtained by substituting (3.84) in (3.52). For the above equations, we found this solution by directly solving the interacting equations with the restriction of no swapped k momenta. We should, of course, be able to recover this result from the four-term solution in equation (3.61) by tuning the $\alpha,\ \beta$ coefficients in such a way that the swapped k-momenta terms vanish. To show how this works, we set $\alpha = \alpha'/a(k_1,k_2)$ and $\beta = \beta'/b(k_1,k_2)$ in

[13]To be clear, we could have chosen to remove any one of the four momentum pairs $\{p_1,p_2\},\{p_2,p_1\},\{k_1,k_2\},\{k_2,k_1\}$ from the ansatz. The specific choice of removing $\{k_2,k_1\}$ is the one that is relevant when we start with real $\{p_1,p_2\}$ and demand $p_1+p_2\to 0$.

[14]Since we have established that, apart from the CoM case, there is no solution if we drop the k momenta completely, this ansatz also contains the *minimal* number of terms needed to solve the interacting equations.

(3.61). Then, for instance for ψ_{ee}, we can write

$$\begin{aligned}
&\alpha\,\psi^A_{ee}(\ell_1,\ell_2)+\beta\,\psi^B_{ee}(\ell_1,\ell_2)\\
&=[a(k_2,k_1)b(k_1,k_2)-b(k_2,k_1)a(k_1,k_2)]\\
&\times(\frac{\alpha'}{a(k_1,k_2)}a(p_1,p_2)+\frac{\beta'}{b(k_1,k_2)}b(p_1,p_2))e^{ip_1\ell_1+ip_2\ell_2}\\
&-[a(k_2,k_1)b(k_1,k_2)-b(k_2,k_1)a(k_1,k_2)]\\
&\times(\frac{\alpha'}{a(k_1,k_2)}a(p_2,p_1)+\frac{\beta'}{b(k_1,k_2)}b(p_2,p_1))e^{ip_2\ell_1+ip_1\ell_2}\\
&-[a(p_2,p_1)b(p_1,p_2)-b(p_2,p_1)a(p_1,p_2)]\\
&\times(\frac{\alpha'}{a(k_1,k_2)}a(k_1,k_2)+\frac{\beta'}{b(k_1,k_2)}b(k_1,k_2))e^{ik_1\ell_1+ik_2\ell_2}\\
&+[a(p_2,p_1)b(p_1,p_2)-b(p_2,p_1)a(p_1,p_2)]\\
&\times(\frac{\alpha'}{a(k_1,k_2)}a(k_2,k_1)+\frac{\beta'}{b(k_1,k_2)}b(k_2,k_1))e^{ik_2\ell_1+ik_1\ell_2}
\end{aligned}\tag{3.85}$$

.

The swapped k-momenta term vanishes if we take

$$\frac{\alpha'}{\beta'}=-\frac{a(k_1,k_2)}{a(k_2,k_1)}\frac{b(k_2,k_1)}{b(k_1,k_2)}.\tag{3.86}$$

For the coefficient in the first line above, we can substitute and rearrange as follows

$$\begin{aligned}
&[a(k_2,k_1)b(k_1,k_2)-b(k_2,k_1)a(k_1,k_2)](\frac{\alpha'}{a(k_1,k_2)}a(p_1,p_2)+\frac{\beta'}{b(k_1,k_2)}b(p_1,p_2))\\
&=\alpha'\left[\frac{a(k_2,k_1)}{a(k_1,k_2)}b(k_1,k_2)-b(k_2,k_1)\right]a(p_1,p_2)\\
&+\beta'\left[a(k_2,k_1)-\frac{b(k_2,k_1)}{b(k_1,k_2)}a(k_1,k_2)\right]b(p_1,p_2)\\
&=\beta'\Big(-\frac{a(k_1,k_2)}{a(k_2,k_1)}\frac{b(k_2,k_1)}{b(k_1,k_2)}\left[\frac{a(k_2,k_1)}{a(k_1,k_2)}b(k_1,k_2)-b(k_2,k_1)\right]a(p_1,p_2)\\
&+\left[a(k_2,k_1)-\frac{b(k_2,k_1)}{b(k_1,k_2)}a(k_1,k_2)\right]b(p_1,p_2)\Big)\\
&=\beta'\Big([a(k_2,k_1)b(p_1,p_2)-b(k_2,k_1)a(p_1,p_2)]\\
&+\left[\frac{a(k_1,k_2)}{a(k_2,k_1)}\frac{b(k_2,k_1)}{b(k_1,k_2)}b(k_2,k_1)a(p_1,p_2)-\frac{b(k_2,k_1)}{b(k_1,k_2)}a(k_1,k_2)b(p_1,p_2)\right]\Big)\\
&=\beta'\big([a(k_2,k_1)b(p_1,p_2)-b(k_2,k_1)a(p_1,p_2)]\\
&+\frac{\alpha'}{\beta'}\,[a(k_2,k_1)b(p_1,p_2)-b(k_2,k_1)a(p_1,p_2)]\big)\\
&=\beta'(1+\frac{\alpha'}{\beta'})\,[a(k_2,k_1)b(p_1,p_2)-b(k_2,k_1)a(p_1,p_2)]\,.
\end{aligned}\tag{3.87}$$

For the other terms in the second and third line, we find the same overall factor. Thus,

$$\alpha\, \psi^{A}_{ee}(\ell_1, \ell_2) + \beta\, \psi^{B}_{ee}(\ell_1, \ell_2) = \beta'(1 + \frac{\alpha'}{\beta'})\psi^{(r)}_{ee}(\ell_1, \ell_2). \tag{3.88}$$

The same is true for the eo, oe and oo wavefunctions. We can therefore express the restricted solution as

$$|\psi\rangle_{(r)} = \frac{1}{a(k_1, k_2)} \frac{c}{1+c}\, |\psi\rangle_A + \frac{1}{b(k_1, k_2)} \frac{1}{1+c}\, |\psi\rangle_B, \tag{3.89}$$

where

$$c = -\frac{b(k_2, k_1)}{b(k_1, k_2)} \frac{a(k_1, k_2)}{a(k_2, k_1)}. \tag{3.90}$$

As mentioned, this is the solution that we expect to describe the two magnon problem for infinite chains. In addition, it will play an important role in in Section 3.2.4 as it will be the starting point for taking the centre-of-mass frame limit $K \to 0$.

Let us take a closer look at the S-matrices appearing in the restricted solution, which we call $S^{(r)}$ and $T^{(r)}$. They are

$$S^{(r)}(p_1, p_2; k_1, k_2; \kappa) = \frac{A_{ee}(p_2, p_1)}{A_{ee}(p_1, p_2)} = -\frac{a(k_2, k_1)b(p_2, p_1) - b(k_2, k_1)a(p_2, p_1)}{a(k_2, k_1)b(p_1, p_2) - b(k_2, k_1)a(p_1, p_2)}\,, \tag{3.91}$$

and

$$T^{(r)}(p_1, p_2; k_1, k_2; \kappa) = \frac{A_{ee}(k_1, k_2)}{A_{ee}(p_1, p_2)} = -\frac{a(p_2, p_1)b(p_1, p_2) - b(p_2, p_1)a(p_1, p_2)}{a(k_2, k_1)b(p_1, p_2) - b(k_2, k_1)a(p_1, p_2)}\,. \tag{3.92}$$

Note in particular that the S-matrix $S^{(r)}$ swapping $p_1 \leftrightarrow p_2$ now also depends on the k momenta. It still satisfies the unitary condition

$$S^{(r)}(p_1, p_2, k_1, k_2)S^{(r)}(p_2, p_1, k_1, k_2) = 1, \tag{3.93}$$

as well as the condition $S^{(r)}(p_1, p_1, k_1, k_2) = -1$. (Note that $p_2 = p_1$ does not imply that $k_2 = k_1$). It also smoothly reduces to the XXX S-matrix as $\kappa \to 1$. Importantly, it is $\mathbb{Z}_2$ invariant

$$S^{(r)}(p_1, p_2; k_1, k_2; 1/\kappa) = S^{(r)}(p_1, p_2; k_1, k_2; \kappa). \tag{3.94}$$

The importance of this is that, as we will see in Section 3.2.4, in the limit $K \to 0$ $S^{(r)}$ will become the centre-of-mass S-matrix (3.36), which determines the CoM spectrum of our system and thus needs to be $\mathbb{Z}_2$ invariant.

Similarly to the analysis carried out for the general solution, it can be shown that the full restricted solution $|\psi\rangle_{(r)}$ is a $\mathbb{Z}_2$ eigenstate

$$\mathbb{Z}_2|\psi\rangle_{(r)} = -\big(r(p_1)r(p_2)\big)^{-2}\big(r(k_1)r(k_2)\big)^{-1}|\psi\rangle_{(r)}. \tag{3.95}$$

Of course, unlike the general solution, the restricted solution only has the σ_p momentum exchange symmetry, as the boundary condition has broken the symmetry between the four sets of momenta $\{p_1, p_2\}, \{p_2, p_1\}, \{k_1, k_2\}, \{k_2, k_1\}$.

3.2.4 Restricted solution in the CoM limit

In this section, we show how the generalised Bethe ansatz (3.54) for the XY sector, which involves a second set of momenta, reduces to the more standard Bethe ansatz (3.43) in the centre-of-mass frame $K = 0$. Understanding this limit will also clarify the origin of the contact terms that appear in the CoM frame.

To start, note (as can be seen from inspection of (3.51) that as $K \to 0$, the k momenta scale as $k_1 \to \pi/2 - i\infty$ and $k_2 \to \pi/2 + i\infty$. So the centre-of-mass limit needs to be taken very carefully.

As discussed, the relevant wavefunction on which to take the limit is the restricted solution (3.84), which contains only the direct k momenta k_1, k_2 (and not the swapped ones k_2, k_1 which leads to a divergent term). Let us write the S and T matrices arising in that solution, as found in section 3.2.3 (for general $\{p_1, p_2\}$), as follows

$$\begin{aligned} S^{(r)}(p_1, p_2, k_1, k_2) &= -\frac{a(k_2, k_1)b(p_2, p_1) - b(k_2, k_1)a(p_2, p_1)}{a(k_2, k_1)b(p_1, p_2) - b(k_2, k_1)a(p_1, p_2)} \\ &= -\frac{f\, b(p_2, p_1) - a(p_2, p_1)}{f\, b(p_1, p_2) - a(p_1, p_2)}, \end{aligned} \tag{3.96}$$

and

$$\begin{aligned} T^{(r)}(p_1, p_2, k_1, k_2) &= -\frac{a(p_2, p_1)b(p_1, p_2) - b(p_2, p_1)a(p_1, p_2)}{a(k_2, k_1)b(p_1, p_2) - b(k_2, k_1)a(p_1, p_2)} \\ &= -\frac{1}{b(k_2, k_1)}\frac{a(p_2, p_1)b(p_1, p_2) - b(p_2, p_1)a(p_1, p_2)}{f\, b(p_1, p_2) - a(p_1, p_2)}, \end{aligned} \tag{3.97}$$

where we have defined

$$f = \frac{a(k_2, k_1)}{b(k_2, k_1)}\ . \tag{3.98}$$

Now, we choose k_1, k_2 to be of the form $k_1 = K/2 + \pi/2 - iv,\ k_2 = K/2 - \pi/2 + iv$, where $v \geq 0$, since this leads to a decaying exponential in the wavefunctions. Noting the $1/\sin^2(K)$ term in (3.51), it is clear that for K sufficiently small the argument

of the arccos will eventually exceed 1 and the arccos term will become (positive) imaginary. As K is further decreased towards zero, $v \to \infty$.

What we will now show is that, in the limit where $p_2 \to -p_1$,

$$\begin{aligned} &1) \quad S^{(r)}(p_1, p_2, k_1, k_2) \longrightarrow S_{CoM}(p, -p), \\ &2) \quad r(k_1)T^{(r)}(p_1, p_2, k_1, k_2)e^{-ik_1} \longrightarrow r(p)e^{-ip}\mathcal{G}(-p). \end{aligned} \tag{3.99}$$

We will thus completely recover the centre-of-mass wavefunctions that were originally found using the contact term method in Section 3.2.1. For point 2, which we show later in this section, note that this comes from the fact that only nearest-neighbour terms for the $\{k_1, k_2\}$-term survive the limit. Consequently, looking at the wavefunctions in equation (3.83), the $\{k_1, k_2\}$-terms for even-even and odd-odd completely vanish (as they do not have nearest neighbour terms); for the odd-even and even-odd terms, only $(2\ell - 1, 2\ell)$ and $(2\ell, 2\ell + 1)$ survives, thus generating the δ_{ℓ_1+1,ℓ_2} which was entered by hand in the CoM wavefunctions.[15]

Recovering the centre-of-mass S-matrix:

To take the limits of the S matrix, it is clearly important to understand the limit of the function f in (3.98) as $p_2 \to -p_1$, as the other terms remain finite and non-zero in the limit. An important result concerns the limits of the ratio functions appearing in the a and b coefficients. They are

$$r(k_1) = -\frac{1}{\kappa}, \quad r(k_2) = \kappa \ , \quad \text{as} \ \ p_2 \to -p_1 \ . \tag{3.100}$$

We note the minus sign appearing in $r(k_1)$, which is important to get the right limit. Using this result, and also recalling that $r(-p) = 1/r(p)$, we find in the limit

$$f = -\frac{-\kappa + 2e^{ik_2} + \kappa e^{i(p_1+p_2)}}{\kappa(2\kappa e^{ik_2} + e^{i(p_1+p_2)} - 1)} \ . \tag{3.101}$$

Here we have taken the $K \to 0$ limit only of the ratio functions, and still need to take it in the exponents. The naive limit of this expression gives $0/0$, so to obtain a definite limit, we first express k_2 in terms of p_1, p_2 using (3.51) and then set $p_2 = -p_1 + \epsilon$, so that the limit becomes $\epsilon \to 0$. Since the equations for k_1, k_2 contain an arccos, we are able to remove the exponents using the formula

$$\arccos(z) = -i \ln\left(z + \sqrt{z^2 - 1}\right) \ . \tag{3.102}$$

[15] We note that this behaviour resembles that of bound states for the spin-1/2 XXX chain whose imaginary part can diverge and lead to localised interactions (see e.g. the introduction to the Bethe ansatz [41]).

After some analysis, we can extract the divergent terms $\csc(\epsilon)$ from both the numerator and denominator of equation (3.101). To take the limit $\epsilon \to 0$, we apply l'Hopital's rule to finally obtain the complete limit for f:

$$f(p,-p) = \frac{-1+\sqrt{1+\kappa^2 e^{-2ip_1}}\sqrt{1+\kappa^2 e^{2ip_1}}}{\kappa^2 - \sqrt{1+\kappa^2 e^{-2ip_1}}\sqrt{1+\kappa^2 e^{2ip_1}}}. \tag{3.103}$$

Substituting this back into $S(p_1,p_2,k_1,k_2)$ and setting $p_2 \to -p_1$ for the other terms (which are harmless), we find that

$$S(p_1,p_2,k_1,k_2) \longrightarrow S_{\text{CoM}}(p,-p)\ , \tag{3.104}$$

where $S_{\text{CoM}}(p,-p)$ is given in (3.36). We have thus confirmed that the CoM S-matrix obtained using the contact-term approach is a limiting case of the S-matrix for the restricted solution.

Recovering the contact term

The final step to confirm that the full centre-of-mass solution arises as a limit of the restricted solution is to check that the contact term $\mathcal{G}$ arises from one of the terms with additional momenta. Let us focus on the following term for the odd-even part of the wavefunction (3.84)

$$r(k_1)T(p_1,p_2,k_1,k_2)e^{ik_1\ell_1+ik_2\ell_2}. \tag{3.105}$$

We set $\ell_2 = 2\ell$ and $\ell_1 = 2\ell - (2m+1)$ where $m \geq 0$. Therefore, $m = 0$ corresponds to the nearest-neighbour case. After using that $k_1 + k_2 \to 0$ in the limit, we are left with

$$\begin{aligned} &r(k_1)T(p_1,p_2,k_1,k_2)e^{-ik_1(2m+1)} \\ &= -r(k_1)\frac{e^{-ik_1(2m+1)}}{b(k_2,k_1)}\frac{a(p_2,p_1)b(p_1,p_2) - b(p_2,p_1)a(p_1,p_2)}{f\ b(p_1,p_2) - \ a(p_1,p_2)}\ . \end{aligned} \tag{3.106}$$

The factor f was determined above. Proceeding in a similar manner as before, we find that the term

$$\frac{e^{-ik_1(2m+1)}}{b(k_2,k_1)} \xrightarrow{\epsilon\to 0} \frac{e^{-ik_1(2m+1)}}{-2\kappa e^{ik_2} - e^{i(p_1+p_2)} + 1}\ , \tag{3.107}$$

where we have again taken a partial limit. This factor vanishes in the full $\epsilon \to 0$ limit when $m > 0$. However, $m = 0$ gives a non-zero result, which is the nearest-neighbour term and produces the δ_{ℓ_1,ℓ_1+1} contact term that we originally inserted

by hand in the CoM method. More precisely, upon taking $\epsilon \to 0$ the $m = 0$ term reduces to:

$$\frac{\kappa}{-2\kappa^2 + 2\sqrt{1+\kappa^2 e^{-2ip}}\sqrt{1+\kappa^2 e^{2ip}}} \,. \tag{3.108}$$

Putting everything together we conclude that out of all the $\{k_1, k_2\}$-dependent terms in the odd-even part of (3.84), the only one that survives the centre-of-mass limit is

$$r(k_1)T(p_1, p_2, k_1, k_2)e^{i\ell_1 k_1 + i(\ell_1+1)k_2} \xrightarrow{\epsilon\to 0} r(p)e^{-ip}\mathcal{G}(-p). \tag{3.109}$$

which is precisely the centre-of-mass contact term appearing in the odd-even part of (3.84). A similar procedure applies to the even-odd part. We have thus shown how the general method of [52, 51, 47] of adding additional momenta also applies in the centre-of-mass frame, as long as the limit is taken carefully. All terms containing k momenta in the wavefunction vanish, apart from the nearest-neighbour term which produces the centre-of-mass contact term. This explains the physical origin of the contact terms. We end by noting that in the standard XXX Bethe ansatz at $\kappa = 1$, the momenta diverge in the limit $K \to \pi$. Moving slightly away from $\kappa = 1$, we see that the k momenta are finite in the CoM limit at $K = \pi$. So in a sense the role of the p and k momenta is exchanged at $K = \pi$ and this might allow us to think of the $\kappa \neq 1$ theory and the additional-momenta Bethe ansatz as a regularisation of the XXX Bethe ansatz at $K = \pi$.[16]

3.3 Bethe Ansatz for the XY Sector

In this section we show how our two magnon solution can be used to find the spectrum for closed chains. Note that in the XY sector only even-length closed chains are allowed, as otherwise the gauge indices of the first and last sites cannot be matched.[17]

As explained, we are not only interested in solutions satisfying the zero-momentum constraint, $K = 0$, but also in solutions with nonzero K. This is because we wish to think of our solutions as part of an eventual multi-magnon solution, which does satisfy the momentum constraint.

Starting with the one magnon momenta, in the untwisted sector, they are simply obtained by imposing periodicity, $e^{iLp} = 1$ (see also Section 2.2.2). Even though

[16] Recall that one always obtains a better understanding of the Bethe roots by regularising the Bethe ansatz. A more standard way of doing this is by introducing a phase that changes the periodicity properties (see e.g. [42] for a discussion).

[17] Also L needs to be larger than 2, as for $L = 2$ double-trace contributions, which are otherwise subleading in the planar limit, become important [18].

they are of course equal to their corresponding values for the XXX limit at $\kappa = 1$, the energies are different due to the dispersion relation (3.14). Since the S-matrices of the general two magnon solution (3.67),(3.69) satisfy $S(p, 0) = 1$, we can always construct periodic two magnon wavefunctions by taking e.g. $p_2 = 0$ and p_1 to be a one magnon momentum. Thus the one magnon energies are two magnon energies as well.

Proceeding to "true" two magnon energies, we saw in Section 3.2.2 that the solution of the two magnon problem for our alternating chain requires the addition of a second set of momenta, $\{k_1, k_2\}$, on top of the original set of momenta $\{p_1, p_2\}$. These momenta are uniquely defined by the relations

$$p_1 + p_2 = k_1 + k_2 = K \quad \text{and} \quad E(p_1) + E(p_2) = E(k_1) + E(k_2) = E_2 \ , \tag{3.110}$$

with $E(p)$ the one magnon dispersion relation (which can belong to either the upper or lower branch).

We also saw that when going to the centre-of-mass frame where $K = 0$, the k momenta diverge and one needs to take a subtle limit to keep the wavefunction finite. However, once the limit is taken (the details are in Section 3.2.4), one is left with the centre-of-mass S-matrix (3.36) for the p momenta which allows us to write a standard two magnon Bethe ansatz.[18] For the untwisted sector, the periodicity equation coming from the Bethe ansatz is much like the usual one and reads

$$e^{ipL} = 1/S(p, -p) \ , \tag{3.111}$$

with S as in (3.36).

Now, in the orbifold limit we also need to consider the twisted sector states [71, 17, 14, 13]. These are spin chains which include the twist matrix γ (see Section 2.4) somewhere on the chain. Without loss of generality, it can be taken to be the first or last site, and its effect is to modify the periodicity condition by a phase. In the $\mathbb{Z}_2$ case this phase is just -1 (see equation (2.153)), which means that to get the full spectrum (still at the orbifold limit) one needs to consider also antiperiodic chains. Precisely the same is true in the interpolating theory. For one magnon states we simply impose $e^{ipL} = -1$, which gives the correct one magnon energies (and trivially some two magnon energies where one of the momenta is zero). For the two

[18] We emphasise that the p and k momenta appear symmetrically in the wavefunction so which ones we call p and k is a matter of notation. We call p the solutions of (3.110) which stay finite in the CoM limit.

magnon twisted sector states we use the ansatz

$$e^{ipL} = -1/S(p,-p) \ , \tag{3.112}$$

with S again as in (3.36).

However, to get the full set of two magnon energies we also need to consider the case where $K \neq 0$. In this case our two magnon wavefunction is a linear combination of Bethe-like states, some of which depend on the p momenta and some on the k momenta. Imposing periodicity on such a wavefunction requires additional steps which we outline below.

First of all, it is clear that one cannot impose periodicity on the A or B solutions (3.57,3.58) separately. As in the CoM case, one needs to combine them. We will thus write

$$|\psi\rangle_{\text{tot}} = A(p_1,p_2,k_1,k_2) + xB(p_1,p_2,k_1,k_2) \ , \tag{3.113}$$

with x a function which, in principle, depends on all the momenta. For the XXX case, reviewed in Section 2.2.2, where we just have

$$|l_1,l_2\rangle = A_{12}(p)e^{il_1p_1+il_2p_2} + A_{21}(p)e^{il_1p_2+il_2p_1} \ , \tag{3.114}$$

the periodicity requirement ($|l_1+L,l_2\rangle = |l_1,l_2\rangle$) is imposed as

$$A_{12}(p)e^{il_1p_1+il_2p_2} = A_{21}(p)e^{il_2p_2+i(l_1+L)p_1} \ \Rightarrow \ e^{iLp_1} = \frac{A_{12}(p)}{A_{21}(p)} \ , \tag{3.115}$$

leading to the usual S-matrix $S_{12} = A_{21}/A_{12}$. For our case, it turns out that the only modification required is the introduction of the ratio x. In particular, we will impose periodicity separately on the p and k momenta as

$$\begin{aligned}(A_{12}^{\text{ee},p} + xB_{12}^{\text{ee},p})e^{i(l_1p_1+l_2p_2)} &= (A_{21}^{\text{ee},p} + xB_{21}^{\text{ee},p})e^{i(l_2p_2+(l_1+L)p_1)} \ , \\ (A_{12}^{\text{ee},k} + xB_{12}^{\text{ee},k})e^{i(l_1k_1+l_2k_2)} &= (A_{21}^{\text{ee},k} + xB_{21}^{\text{ee},k})e^{i(l_2k_2+(l_1+L)k_1)} \ ,\end{aligned} \tag{3.116}$$

for the even-even parts. We also impose the same condition on the odd-odd parts, while for the even-odd and odd-even ones we have

$$\begin{aligned}(A_{12}^{\text{eo},p} + xB_{12}^{\text{eo},p})e^{i(l_1p_1+l_2p_2)} &= (A_{21}^{\text{oe},p} + xB_{21}^{\text{oe},p})e^{i(l_2p_2+(l_1+L)p_1)} \ , \\ (A_{12}^{\text{eo},k} + xB_{12}^{\text{eo},k})e^{i(l_1k_1+l_2k_2)} &= (A_{21}^{\text{oe},k} + xB_{21}^{\text{oe},k})e^{i(l_2k_2+(l_1+L)k_1)} \ .\end{aligned} \tag{3.117}$$

Periodicity of the wavefunction hinges on the x factor in all of these relations being the same. Focusing on the even-even sector for now,we can simplify (3.116) as

$$e^{iLp_1} = -\frac{a(p_1,p_2)+x\ b(p_1,p_2)}{a(p_2,p_1)+x\ b(p_2,p_1)} \quad \text{and} \quad e^{iLk_1} = -\frac{a(k_1,k_2)+x\ b(k_1,k_2)}{a(k_2,k_1)+x\ b(k_2,k_1)} \ , \tag{3.118}$$

where we have used the explicit expressions of $A_{12}, A_{21}, B_{12}, B_{21}$ in terms of the a and b functions defined in (3.59). We can now solve for x in terms of one set of momenta (the k's, for instance), to write

$$\bar{x}(k_1, k_2) = -\frac{a(k_1, k_2) + a(k_2, k_1)e^{iLk_1}}{b(k_1, k_2) + b(k_2, k_1)e^{iLk_1}} \ . \tag{3.119}$$

Substituting this specific solution for x (which we call $\bar{x}$) into the p periodicity condition gives us the final form of the 2-magnon Bethe equation for the untwisted XY sector

$$e^{iLp_1} = -\frac{a(p_1, p_2) + \bar{x}(k_1, k_2)b(p_1, p_2)}{a(p_2, p_1) + \bar{x}(k_1, k_2)b(p_2, p_1)} \ . \tag{3.120}$$

The above was for the even-even part but similar considerations apply to the other parts of the wavefunction and lead to the same equation. Now recall that the k momenta are algebraically defined in terms of the p momenta by solving (3.110), which is a quartic relation between $z(p_i) = e^{2ip_i}$ and $z(k_i) = e^{2ik_i}$ and can be straightforwardly solved. Equation (3.120) can thus be expressed purely in terms of the p momenta, and its roots found numerically for given L and κ.

For the twisted sector everything works very similarly, apart from the fact that we need to impose antiperiodicity. This leads to the ratio between the two wavefunctions being

$$\bar{x}(k_1, k_2) = -\frac{a(k_1, k_2) - a(k_2, k_1)e^{iLk_1}}{b(k_1, k_2) - b(k_2, k_1)e^{iLk_1}} \ , \tag{3.121}$$

and the corresponding two magnon Bethe ansatz is now written in terms of this $\bar{x}$ as

$$e^{iLp_1} = \frac{a(p_1, p_2) + \bar{x}(k_1, k_2)b(p_1, p_2)}{a(p_2, p_1) + \bar{x}(k_1, k_2)b(p_2, p_1)} \ . \tag{3.122}$$

This is again a function only of the p momenta which can be solved numerically to obtain the required Bethe momenta.

It is worth noting that since the $\mathbb{Z}_2$ operation $\kappa \to 1/\kappa$ exchanges the a and b factors, it takes $\bar{x}(k_1, k_2) \to 1/\bar{x}(k_1, k_2)$. This is what is required for the full wavefunction $|\psi\rangle_{\text{tot}}$ to be invariant under $\mathbb{Z}_2$, which should be the case since the Hamiltonian is also $\mathbb{Z}_2$ invariant in the periodic/antiperiodic case[19].

In [27], the Bethe ansatz result for short chains are numerically compared to results from explicit diagonalisation of the Hamiltonian for both the twisted and untwisted sectors. The results show good agreement with the wavefunctions computed in this

[19]The $\kappa \to 1/\kappa$ operation can be undone by shifting the origin from an even to an odd site, which does not have an effect for a closed chain.

chapter as well as the approach to imposing periodicity discussed in this section. This provides excellent confirmation that the XY sector wavefunctions and the periodic Bethe ansatz for the twisted/untwisted sectors are indeed correct.

Chapter 4

SPIN CHAINS IN THE DILUTE XZ SECTOR

In this chapter, we will study the "SU(2)-like" sector composed of the X and Z fields. Unlike the XY sector discussed previously, in the XZ sector the two fields belong to different representations of the gauge groups (X being bifundamental while Z is in the adjoint of each of the groups) so we expect the theory to be less symmetric than the XY sector.

From Section 2.4.3, recall the Hamiltonian in this sector is given by (2.170)

$$\mathcal{H}(\lambda) = \begin{pmatrix} 0 & 0 & 0 & 0 \\ 0 & \kappa & -1 & 0 \\ 0 & -1 & 1/\kappa & 0 \\ 0 & 0 & 0 & 0 \end{pmatrix} \ , \ \mathcal{H}(\lambda') = \begin{pmatrix} 0 & 0 & 0 & 0 \\ 0 & 1/\kappa & -1 & 0 \\ 0 & -1 & \kappa & 0 \\ 0 & 0 & 0 & 0 \end{pmatrix} \text{ in the basis } \begin{pmatrix} XX \\ XZ \\ ZX \\ ZZ \end{pmatrix}, \tag{4.1}$$

where λ, λ' indicate whether the gauge group immediately to the left of the site where the Hamiltonian acts is the first or second gauge group respectively. Since Z does not change the gauge group, the Hamiltonian also does not change when crossing a Z field, however it will switch from $\mathcal{H}(\lambda)$ to $\mathcal{H}(\lambda')$ and vice versa when crossing an X field (see Figure 4.1 for an illustration).

A consequence of the XZ sector being less symmetric than the XY sector is that there are two inequivalent vacua, namely, one made up of X fields and the other of Z fields. The Z vacuum[1] belongs to the 1/2-BPS supermultiplet $\mathcal{E}_{-r(0,0)}$ discussed in Section 2.1.1 with $\Delta = -r$ (see Table 2.1 for the $U(1)_r$ charges). Spin chains with the Z fields as a vacuum were studied in [18]. The dispersion relation, with the X fields as excitations, is trigonometric and the S-matrices arising in the two magnon problem are similar to those of the XXZ chain. However, the dynamical nature of the chain becomes evident when considering the three magnon problem, due to the fact that there are two two-magnon S-matrices S and $\tilde{S}$ (mapped to each other by $\mathbb{Z}_2$). This leads to two possible sequences of two-body scatterings (particles 1+2 first, or particles 2+3 first) which lead to incompatible equations

$$S_{12}\tilde{S}_{13}S_{23} \neq \tilde{S}_{23}S_{13}\tilde{S}_{12}. \tag{4.2}$$

[1] Which is really two vacua, depending on λ. That is, either $|\cdots\phi_1\phi_1\phi_1\cdots\rangle$ or $|\cdots\phi_2\phi_2\phi_2\cdots\rangle$.

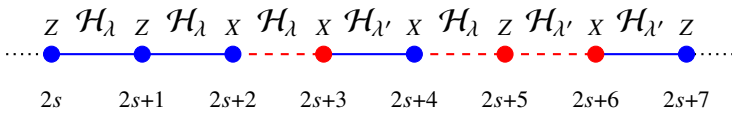

Figure 4.1: *A section of the dilute spin chain for the XZ sector, for a specific configuration of states. We have chosen the gauge group to the left of site* $2s$ *to be the first one (depicted by a blue solid line). To make it easier to read off the relevant gauge group for each Hamiltonian, we have also coloured the first of each two sites on which the Hamiltonian acts the same as the region to the left of that site. Unlike the alternating chain depicted in (3.1), here the choice of which Hamiltonian acts on each pair of sites is not related to the even-odd nature of the site but rather to the number of Z and X fields that have been crossed until that point.*

Thus, the standard Yang-Baxter equation is not satisfied. We can therefore think of excitations around the Z-vacuum as being described by a dynamical XXZ model.

In this thesis, we will consider the alternative X-vacuum, with the Z fields as excitations, which were not considered in [18]. In $\mathcal{N} = 2$ language, they will be of the type $|\cdots Q_{12}Q_{21}\phi_1 Q_{12}\phi_2 Q_{21}\cdots\rangle$. Even though the XZ-sector Hamiltonian (4.1) is rather different to the XY-sector Hamiltonian (3.1), it will turn out that the dispersion relation for Z excitations on the X vacuum is identical to that of the XY sector. Furthermore, even though the details of the wavefunctions (such as the ratio functions) will be different, the overall approach to solving the one and two magnon problem and the final form of the solutions will be almost identical as well. In particular, for the two magnon problem, both the contact-term approach in the centre-of-mass frame and the more general additional-momenta approach will apply, as we will show in the following sections.

Finally, it is interesting to rewrite the Hamiltonians slightly to compare to the alternating-bond model. These Hamiltonians are Temperley-Lieb type, which can be clearly seen, for instance, by comparing to equation (3.137) in [40]

$$e_\ell = \begin{pmatrix} 0 & 0 & 0 & 0 \\ 0 & q^{-1} & -1 & 0 \\ 0 & -1 & q & 0 \\ 0 & 0 & 0 & 0 \end{pmatrix}, \quad q = \kappa \text{ or } q = 1/\kappa, \tag{4.3}$$

where e_ℓ acts on sites $(\ell, \ell+1)$ and satisfies the Temperley-Lieb-Jones algebra

$$e_\ell^2 = e_\ell, \quad e_\ell e_{\ell\pm1} e_\ell = e_\ell, \quad e_{\ell_1} e_{\ell_2} = e_{\ell_2} e_{\ell_1}, \ |\ell_2 - \ell_1| \geq 2. \tag{4.4}$$

To compare with the XY sector alternating-bond Hamiltonian in equation (3.7), first note that we can write $H(\lambda)$ and $H(\lambda')$ in terms of the permutation matrix P and the κ-deformed identity matrix as $I(\kappa)$

$$H(\lambda) = I(1/\kappa) - P, \tag{4.5}$$

$$H(\lambda') = I(\kappa) - P, \tag{4.6}$$

where

$$P = \begin{pmatrix} 1 & 0 & 0 & 0 \\ 0 & 0 & 1 & 0 \\ 0 & 1 & 0 & 0 \\ 0 & 0 & 0 & 1 \end{pmatrix}, \quad I(\kappa) = \begin{pmatrix} 1 & 0 & 0 & 0 \\ 0 & 1/\kappa & 0 & 0 \\ 0 & 0 & \kappa & 0 \\ 0 & 0 & 0 & 1 \end{pmatrix}. \tag{4.7}$$

Note that $P^2 = \mathbb{1}$, the undeformed identity $I(1)$, as it should. Interestingly, $I(\kappa)^2 \neq I(1)$ but rather $I(\kappa)I(1/\kappa) = I(1) = \mathbb{1}$.

Next, we consider the most general XXZ Hamiltonian that preserves the total spin (see equation (2.2) in [75])

$$\begin{aligned} H^{XXZ}_{\ell,\ell+1} = {} & J_0 \mathbb{1}_{\ell,\ell+1} - J\sigma^x_\ell \sigma^x_{\ell+1} - J\sigma^y_\ell \sigma^y_{\ell+1} - J_z \sigma^z_\ell \sigma^z_{\ell+1} \\ & - h_1(\sigma^z_\ell \otimes \mathbb{1}_{\ell+1} + \mathbb{1}_\ell \otimes \sigma^z_{\ell+1}) - h_2(\mathbb{1}_\ell \otimes \sigma^z_{\ell+1} - \sigma^z_\ell \otimes \mathbb{1}_{\ell+1}), \end{aligned} \tag{4.8}$$

where $\mathbb{1}_{\ell,\ell+1} = \mathbb{1}_\ell \otimes \mathbb{1}_{\ell+1}$ and $\mathbb{1}_\ell$ is the 2×2 identity matrix acting at site ℓ on the lattice. Also, σ^i_ℓ is the i-th Pauli matrix acting on site ℓ, where $i = \{x, y, z\}$. In terms of matrices, the above Hamiltonian takes the form

$$H^{XXZ}_{\ell,\ell+1} = \begin{pmatrix} -2h_1 + J_0 - J_z & 0 & 0 & 0 \\ 0 & 2h_2 + J_0 + J_z & -2J & 0 \\ 0 & -2J & -2h_2 + J_0 + J_z & 0 \\ 0 & 0 & 0 & 2h_1 + J_0 - J_z \end{pmatrix}. \tag{4.9}$$

We can match this matrix to $H(\lambda), H(\lambda')$ as follows: first, we clearly must have $J = 1/2$. Furthermore, for $H(\lambda')$, we have the following system of equations

$$\begin{aligned} -2h_1 + J_0 - J_z &= 0, \\ 2h_2 + J_0 + J_z &= 1/\kappa, \\ -2h_2 + J_0 + J_z &= \kappa, \\ 2h_1 + J_0 - J_z &= 0. \end{aligned} \tag{4.10}$$

For $J_0 = J_z$, we must have $h_1 = 0$. This satisfies the first and fourth equations. For the second and third equations, we can solve to find $J_0 = \frac{1}{4}(\kappa + \kappa^{-1})$ and

$h_2 = -\frac{1}{4}(\kappa - \kappa^{-1})$. In a similar fashion, we find for $H(\lambda)$: $J_0 = J_z = \frac{1}{4}(\kappa + \kappa^{-1})$ and $h_2 = \frac{1}{4}(\kappa - \kappa^{-1})$.

Thus, in summary, we can write $H(\lambda), H(\lambda)$ as XXZ spin chains with the following couplings:

$$\begin{aligned} H(\lambda) = &\frac{1}{4}(\kappa + \kappa^{-1})\big(\mathbb{1}_{\ell,\ell+1} - \sigma^z_\ell \sigma^z_{\ell+1}\big) - \frac{1}{2}\big(\sigma^x_\ell \sigma^x_{\ell+1} + \sigma^y_\ell \sigma^y_{\ell+1}\big) \\ &- \frac{1}{4}(\kappa - \kappa^{-1})(\mathbb{1}_\ell \otimes \sigma^z_{\ell+1} - \sigma^z_\ell \otimes \mathbb{1}_{\ell+1}), \end{aligned} \tag{4.11}$$

$$\begin{aligned} H(\lambda') = &\frac{1}{4}(\kappa + \kappa^{-1})\big(\mathbb{1}_{\ell,\ell+1} - \sigma^z_\ell \sigma^z_{\ell+1}\big) - \frac{1}{2}\big(\sigma^x_\ell \sigma^x_{\ell+1} + \sigma^y_\ell \sigma^y_{\ell+1}\big) \\ &+ \frac{1}{4}(\kappa - \kappa^{-1})(\mathbb{1}_\ell \otimes \sigma^z_{\ell+1} - \sigma^z_\ell \otimes \mathbb{1}_{\ell+1}). \end{aligned} \tag{4.12}$$

Comparing these Hamiltonians to the Hamiltonians (3.7) in the XY sector, one can clearly see that the XZ sector is not an alternating bond spin chain of the form given in [51, 52].

4.1 One magnon

We start with the one magnon problem $H|p\rangle = E_1(p)|p\rangle$, where $|p\,\rangle$ indicates a Z magnon. Due to the dynamical nature of the spin chain, there will be two equations to solve, since a Z excitation on an arbitrary site ℓ can see either the parameter λ or λ' to its left. Specifically, we have

$$\begin{aligned} 2/\kappa\,|\ell\,\rangle_\lambda - |\ell-1\,\rangle_{\lambda'} - |\ell+1\,\rangle_{\lambda'} &= E_1\,|\ell\,\rangle_\lambda\ , \\ 2\kappa\,|\ell\,\rangle_{\lambda'} - |\ell-1\,\rangle_\lambda - |\ell+1\,\rangle_\lambda &= E_1\,|\ell\,\rangle_{\lambda'}\ . \end{aligned} \tag{4.13}$$

Here, we use the fact that if a Z field at site ℓ sees λ to its left, the states with a Z field at site $\ell - 1$ and $\ell + 1$ necessarily see a λ' to their left (since one needs to cross one less or more X field to get to that site). The argument is similar for a Z that sees λ' at some different site ℓ. Of course, for a single Z magnon, and given a reference point with fixed λ, the above equations can also be written in term of even and odd sites. However this is not general so we will avoid using this notation.

We therefore take for our ansatz a superposition of a single excitation on sites that see λ or λ'

$$|p\rangle = \sum_\ell\ \psi_\lambda(\ell)|\ell\rangle_\lambda + \sum_\ell\ \psi_{\lambda'}(\ell)|\ell\rangle_{\lambda'}\ , \tag{4.14}$$

where

$$\psi_\lambda(\ell) = A_\lambda(p)e^{ip\ell}, \quad \psi_{\lambda'}(\ell) = A_{\lambda'}(p)e^{ip\ell}. \tag{4.15}$$

In (4.14) the summations are over the sites corresponding to each value of λ.

Substituting this ansatz in the equations (4.13) we find

$$2/\kappa A_\lambda e^{ips} - A_{\lambda'} e^{ip(s-1)} - A_{\lambda'} e^{ip(s+1)} = E_1(p) A_\lambda e^{ips} \,, \tag{4.16}$$

and

$$2\kappa A_{\lambda'} e^{ipt} - A_\lambda e^{ip(t-1)} - A_\lambda e^{ip(t+1)} = E_1(p) A_{\lambda'} e^{ipt} \,. \tag{4.17}$$

From these equations, we find that the ratio between λ' and λ sites is

$$r(p;\kappa) := \frac{A_{\lambda'}(p)}{A_\lambda(p)} = \frac{1-\kappa^2 \mp \sqrt{\kappa^4 + 2\kappa^2\cos(2p)+1}}{2\kappa\cos(p)}, \tag{4.18}$$

and the eigenvalue is

$$E_1(p;\kappa) = \kappa + \frac{1}{\kappa} \pm \frac{1}{\kappa}\sqrt{\kappa^4 + 2\kappa^2\cos(2p)+1} \,. \tag{4.19}$$

We see that the dispersion relation is precisely the same as for the XY sector, however the ratio function $r(p)$ is different from the ratio between the odd and even sites defined in equation (3.13).

As in the XY sector, the one magnon wavefunction has a $\mathbb{Z}_2$ symmetry. First, note that under $\kappa \leftrightarrow 1/\kappa$,

$$E(1/\kappa) = E(\kappa) \quad \text{and} \quad r(p;1/\kappa) = 1/r(p;\kappa)\,, \tag{4.20}$$

which again implies that the two coefficients A_λ, $A_{\lambda'}$ in our wavefunction are exchanged and that

$$\mathbb{Z}_2|p\rangle = \frac{1}{r(p;\kappa)}|p\rangle \,. \tag{4.21}$$

4.2 Two magnons

Moving on to two magnons, we will again treat separately the non-interacting equations (those where the Z magnons are separated by at least one X field) and the interacting equations (those where the Z magnons are next to each other). There will again be four non-interacting equations as each magnon can see either λ or λ'

$$\begin{aligned}
&4\kappa^{-1}\,|\ell_1,\ell_2\rangle_{\lambda\lambda} - |\ell_1-1,\ell_2\rangle_{\lambda'\lambda} - |\ell_1+1,\ell_2\rangle_{\lambda'\lambda} - |\ell_1,\ell_2-1\rangle_{\lambda\lambda'} - |\ell_1,\ell_2+1\rangle_{\lambda\lambda'} = E_2\,|\ell_1,\ell_2\rangle_{\lambda\lambda}\,,\\
&2(\kappa+\kappa^{-1})\,|\ell_1,\ell_2\rangle_{\lambda\lambda'} - |\ell_1-1,\ell_2\rangle_{\lambda'\lambda'} - |\ell_1+1,\ell_2\rangle_{\lambda'\lambda'} - |\ell_1,\ell_2-1\rangle_{\lambda\lambda} - |\ell_1,\ell_2+1\rangle_{\lambda\lambda} = E_2\,|\ell_1,\ell_2\rangle_{\lambda\lambda'}\,,\\
&2(\kappa+\kappa^{-1})\,|\ell_1,\ell_2\rangle_{\lambda'\lambda} - |\ell_1-1,\ell_2\rangle_{\lambda\lambda} - |\ell_1+1,\ell_2\rangle_{\lambda\lambda} - |\ell_1,\ell_2-1\rangle_{\lambda'\lambda'} - |\ell_1,\ell_2+1\rangle_{\lambda'\lambda'} = E_2\,|\ell_1,\ell_2\rangle_{\lambda'\lambda}\,,\\
&4\kappa\,|\ell_1,\ell_2\rangle_{\lambda'\lambda'} - |\ell_1-1,\ell_2\rangle_{\lambda\lambda'} - |\ell_1+1,\ell_2\rangle_{\lambda\lambda'} - |\ell_1,\ell_2-1\rangle_{\lambda'\lambda} - |\ell_1,\ell_2+1\rangle_{\lambda'\lambda} = E_2\,|\ell_1,\ell_2\rangle_{\lambda'\lambda'}\,.
\end{aligned} \tag{4.22}$$

For the interacting equations, note that two consecutive Z magnons necessarily have the same value of λ. We therefore find

$$\begin{aligned} 2\kappa^{-1}\,|\ell,\ell+1\rangle_{\lambda\lambda} - |\ell-1,\ell+1\rangle_{\lambda'\lambda} - |\ell,\ell+2\rangle_{\lambda\lambda'} &= E_2\,|\ell,\ell+1\rangle_{\lambda\lambda}\ , \\ 2\kappa\,|\ell,\ell+1\rangle_{\lambda'\lambda'} - |\ell-1,\ell+1\rangle_{\lambda\lambda'} - |\ell,\ell+2\rangle_{\lambda'\lambda} &= E_2\,|\ell,\ell+1\rangle_{\lambda'\lambda'}\ . \end{aligned} \tag{4.23}$$

To solve these equations, we will proceed by direct analogy with Chapter 3. The main difference is that the eigenvalue equations are slightly different, and that we do not use even-odd notation in the wavefunction, but λ, λ' notation. We will start with the following ansatz

$$\begin{aligned} |p_1,p_2\rangle = &\sum_{\ell_1<\ell_2} \psi_{\lambda\lambda}(\ell_1,\ell_2)|\ell_1\ell_2\rangle + \sum_{\ell_1<\ell_2} \psi_{\lambda\lambda'}(\ell_1,\ell_2)|\ell_1\ell_2\rangle \\ &+ \sum_{\ell_1<\ell_2} \psi_{\lambda'\lambda}(\ell_1,\ell_2)|\ell_1\ell_2\rangle + \sum_{\ell_1<\ell_2} \psi_{\lambda'\lambda'}(\ell_1,\ell_2)|\ell_1\ell_2\rangle, \end{aligned} \tag{4.24}$$

where

$$\begin{aligned} \psi_{\lambda\lambda}(\ell_1,\ell_2) &= A_{\lambda\lambda}(p_1,p_2)e^{ip_1\ell_1+ip_2\ell_2}, \\ \psi_{\lambda\lambda'}(\ell_1,\ell_2) &= A_{\lambda\lambda'}(p_1,p_2)e^{ip_1\ell_1+ip_2\ell_2}, \\ \psi_{\lambda'\lambda}(\ell_1,\ell_2) &= A_{\lambda'\lambda}(p_1,p_2)e^{ip_1\ell_1+ip_2\ell_2}, \\ \psi_{\lambda'\lambda'}(\ell_1,\ell_2) &= A_{\lambda'\lambda'}(p_1,p_2)e^{ip_1\ell_1+ip_2\ell_2}. \end{aligned} \tag{4.25}$$

Here the sites ℓ_1, ℓ_2 are assumed to be such that the λ dependence is correct. For instance, if $\ell_2 = \ell_1 + 3$ then the only options are $\psi_{\lambda\lambda}(\ell_1, \ell_1+3)$ or $\psi_{\lambda'\lambda'}(\ell_1, \ell_1+3)$, since there are two X fields between the Z's. Fixing λ at a given site (e.g. $\ell = 1$) will resolve the remaining ambiguity.

Substituting in the non-interacting equations (4.22), we find that the eigenvalue is additive,

$$E_2(p_1,p_2) = E_1(p_1) + E_1(p_2), \tag{4.26}$$

with the coefficients having the ratios

$$\frac{A_{\lambda'\lambda'}(p_1,p_2)}{A_{\lambda\lambda}(p_1,p_2)} = r(p_1)r(p_2)\ \ , \quad \frac{A_{\lambda'\lambda}(p_1,p_2)}{A_{\lambda\lambda}(p_1,p_2)} = r(p_1)\ \ , \quad \frac{A_{\lambda\lambda'}(p_1,p_2)}{A_{\lambda\lambda}(p_1,p_2)} = r(p_2). \tag{4.27}$$

As in the XY sector, the usual Bethe approach of just adding the swapped momenta $\{p_1,p_2\} \leftrightarrow \{p_2,p_1\}$ does not lead to a solution of the interacting equations (4.23). In the next section we will improve the Bethe ansatz by adding contact terms, which as we will see, gives a solution in the centre-of-mass frame $K = 0$. To obtain more general solutions (for $K \neq 0$) we will need to add a second set of momenta, which we will do in Section 4.2.2. Since the steps are very similar to that of Chapter 3, we will provide fewer details in this chapter.

4.2.1 Centre-of-mass solution

Similar to Section 3.2.1, we will start by improving the ansatz (4.24) by adding the swapped momenta as well as contact terms

$$\begin{aligned}\psi_{\lambda\lambda'}(\ell_1,\ell_2) &= A_{\lambda\lambda'}(p_1,p_2)e^{ip_1\ell_1+ip_2\ell_2} + A_{\lambda\lambda'}(p_2,p_1)e^{ip_2\ell_1+ip_1\ell_2},\\ \psi_{\lambda'\lambda}(\ell_1,\ell_2) &= A_{\lambda'\lambda}(p_1,p_2)e^{ip_1\ell_1+ip_2\ell_2} + A_{\lambda'\lambda}(p_2,p_1)e^{ip_2\ell_1+ip_1\ell_2},\end{aligned} \tag{4.28}$$

$$\begin{aligned}\psi_{\lambda\lambda}(\ell_1,\ell_2) &= A_{\lambda\lambda}(p_1,p_2)\big(1+\delta_{\ell_2,\ell_1+1}\mathcal{A}(p_1,p_2)\big)e^{ip_1\ell_1+ip_2\ell_2}\\ &\quad + A_{\lambda\lambda}(p_2,p_1)\big(1+\delta_{\ell_2,\ell_1+1}\mathcal{A}(p_2,p_1)\big)e^{ip_2\ell_1+ip_1\ell_2},\\ \psi_{\lambda'\lambda'}(\ell_1,\ell_2) &= A_{\lambda'\lambda'}(p_1,p_2)\big(1+\delta_{\ell_2,\ell_1+1}\mathcal{B}(p_1,p_2)\big)e^{ip_1\ell_1+ip_2\ell_2}\\ &\quad + A_{\lambda'\lambda'}(p_2,p_1)\big(1+\delta_{\ell_2,\ell_1+1}\mathcal{B}(p_2,p_1)\big)e^{ip_2\ell_1+ip_1\ell_2}.\end{aligned} \tag{4.29}$$

Note that in this case two neighbouring Z fields have the same value of λ, so the contact terms enter in the $\psi_{\lambda\lambda}$ and $\psi_{\lambda'\lambda'}$ parts of the wavefunction. This is unlike the XY sector, where two neighbouring Y fields are necessarily at even-odd or odd-even sites, so in that case we modified the ψ_{eo} and ψ_{oe} terms.

Next-to-nearest neighbour magnons

The first step is to ensure that the contact terms do not spoil the non-interacting equations. There are two non-interacting equations where the contact terms enter, the $\lambda\lambda$ and $\lambda'\lambda'$ equations when $\ell_2 = \ell_1 + 2$. Cancelling the contact terms in these equations requires

$$\begin{aligned}\mathcal{A}(p_1,p_2) &= -r(p_1)r(p_2)e^{i(p_1+p_2)}\mathcal{B}(p_1,p_2)\\ \mathcal{A}(p_1,p_2) &= -r(p_1)r(p_2)e^{-i(p_1+p_2)}\mathcal{B}(p_1,p_2).\end{aligned} \tag{4.30}$$

and the same relations for the swapped terms. These are only consistent when $K = p_1 + p_2 = n\pi,\ n \in \mathbb{Z}$. We will focus on $K = 0$ since this is in the first Brillouin zone $(-\pi/2, \pi/2]$. Thus, in the rest of this section, we will be in the centre-of-mass frame. Our constraints are

$$\begin{aligned}\mathcal{A}(p_1,p_2) &= -r(p_1)r(p_2)\mathcal{B}(p_1,p_2),\\ \mathcal{A}(p_2,p_1) &= -r(p_1)r(p_2)\mathcal{B}(p_2,p_1).\end{aligned} \tag{4.31}$$

Interacting equations

We will temporarily keep p_2 as a placeholder, since it allows us to clearly show how the equations below factorise, and then set $p_2 = -p_1$ at the end. Substituting (4.31) in the (λ,λ) and (λ',λ') interacting equations (4.23), we obtain two S-matrices,

defined as $S^{\lambda\lambda} = A_{\lambda\lambda}(p_2, p_1)/A_{\lambda\lambda}(p_1, p_2)$ and $S^{\lambda'\lambda'} = A_{\lambda'\lambda'}(p_2, p_1)/A_{\lambda'\lambda'}(p_1, p_2)$. Explicitly, they are given by

$$S^{\lambda\lambda} = -\frac{e^{-2i(p_1-p_2)}\left(\kappa r\left(p_1\right) + e^{ip_1}\left(\left(\mathcal{A}(p_1,p_2)+1\right)\left(\mathrm{E}_2\kappa-2\right)+\kappa e^{ip_2} r\left(p_2\right)\right)\right)}{\left(\mathcal{A}(p_2,p_1)+1\right)e^{ip_2}\left(\mathrm{E}_2\kappa-2\right)+\kappa e^{i(p_1+p_2)} r\left(p_1\right)+\kappa r\left(p_2\right)}, \tag{4.32}$$

and

$$S^{\lambda'\lambda'} = -\frac{e^{-2i(p_1-p_2)}\left(r\left(p_2\right) + e^{ip_1} r\left(p_1\right)\left(\left(\mathcal{B}(p_1,p_2)+1\right)\left(E_2-2\kappa\right) r\left(p_2\right) + e^{ip_2}\right)\right)}{r\left(p_1\right)\left(1+\left(\mathcal{B}(p_2,p_1)+1\right)e^{ip_2}\left(E_2-2\kappa\right) r\left(p_2\right)\right) + e^{i(p_1+p_2)} r\left(p_2\right)}. \tag{4.33}$$

Equating these two S-matrices, we obtain a relation between $\mathcal{B}(p_2, p_1)$ and $\mathcal{B}(p_1, p_2)$. It is given by

$$\mathcal{B}(p_2, p_1) = F(p_1, p_2)\mathcal{B}(p_1, p_2) + \mathcal{G}(p_1, p_2), \tag{4.34}$$

where the functions F and $\mathcal{G}$ factorise as

$$F(p_1, p_2) = e^{i(p_1-p_2)}\frac{f(p_2, p_1)}{f(p_1, p_2)}, \quad \mathcal{G}(p_1, p_2) = -\frac{1}{r(p_1)r(p_2)e^{ip_2}}\frac{g(p_1, p_2)}{f(p_1, p_2)}, \tag{4.35}$$

with

$$\begin{aligned} f(p_1,p_2) = {} & \kappa\left(-e^{i(p_1+p_2)}\right)\left(\mathrm{E}_2-2\kappa\right) r\left(p_2\right) - \left(\mathrm{E}_2\kappa-2\right)\left(r\left(p_2\right) + e^{ip_1}\left(\mathrm{E}_2-2\kappa\right)\right) \\ & + r\left(p_1\right)\left(e^{i(p_1+p_2)}\left(2-\mathrm{E}_2\kappa\right) - \left(\mathrm{E}_2-2\kappa\right)\left(\kappa + e^{ip_1}\left(\mathrm{E}_2\kappa-2\right) r\left(p_2\right)\right)\right), \end{aligned} \tag{4.36}$$

and

$$\begin{aligned} g(p_1,p_2) = {} & -\kappa r\left(p_1\right)^2\left(-e^{ip_2}\left(-1+e^{2ip_1}\right)\left(\mathrm{E}_2-2\kappa\right) r\left(p_2\right) - e^{2i(p_1+p_2)} + 1\right) \\ & - e^{ip_1}\left(-1+e^{2ip_2}\right) r\left(p_1\right)\left(-\mathrm{E}_2\kappa + \kappa\left(\mathrm{E}_2-2\kappa\right) r\left(p_2\right)^2 + 2\right) \\ & - r\left(p_2\right)\left(e^{ip_2}\left(-1+e^{2ip_1}\right)\left(\mathrm{E}_2\kappa-2\right) + \kappa\left(-1+e^{2i(p_1+p_2)}\right) r\left(p_2\right)\right). \end{aligned} \tag{4.37}$$

Substituting these expressions back into one of the equations for the S-matrix and setting $p_2 = -p_1$, we find that the contact terms again cancel to give

$$S_{\mathrm{CoM}}(p) = -\frac{4\left(\kappa\left(\mathrm{E}_2-\kappa\right)-1\right) r(p) + e^{ip}\left(\mathrm{E}_2-2\kappa\right)\left(\mathrm{E}_2\kappa-2\right)\left(r(p)^2+1\right)}{e^{3ip}\left(\mathrm{E}_2-2\kappa\right)\left(\mathrm{E}_2\kappa-2\right)\left(r(p)^2+1\right) + 4e^{4ip}\left(\kappa\left(\mathrm{E}_2-\kappa\right)-1\right) r(p)}. \tag{4.38}$$

This S-matrix obeys unitarity $S_{\mathrm{CoM}}(-p)S_{\mathrm{CoM}}(p) = 1$ and in the orbifold limit $\kappa \to 1$, $S_{\mathrm{CoM}}(p) = e^{-ip}$ which matches the $\mathfrak{su}(2)$-sector S-matrix for $\mathcal{N} = 4$ super Yang-Mills in the CoM case.

Final form of the contact terms

The last step in finalising our wavefunction is to substitute the solution for $\mathcal{B}(p_2, p_1)$ (4.41) into the ansatz (4.29). As in the XY sector, we find that it leaves a single remaining contact term $\mathcal{G}(p)$.

First, we note that

$$F(p) = -e^{-2ip} S_{\text{CoM}}(p, -p)^{-1} \ , \tag{4.39}$$

and that

$$\mathcal{G}(p) = -F(p)\mathcal{G}(p) = e^{-2ip} S_{\text{CoM}}(p, -p)^{-1} \mathcal{G}(-p) \ . \tag{4.40}$$

Therefore, we can write

$$\mathcal{B}(-p, p) = -e^{-2ip} S_{\text{CoM}}(p, -p)^{-1} \mathcal{B}(p, -p) + e^{-2ip} S_{\text{CoM}}(p, -p)^{-1} \mathcal{G}(-p). \tag{4.41}$$

We see that the $\mathcal{B}(-p, p)$ term in the swapped part of the wavefunctions contains a $\mathcal{B}(p, -p)$ term which cancels the one from the direct part, leaving only $\mathcal{G}(p)$ as a contact term. As we saw in the XY sector, we have the option of keeping $\mathcal{G}(p)$ in the swapped part, bringing it to the direct part using (4.41), or distributing it in any other way. Choosing to move the contact term to the direct part, and factoring out an overall factor of $A_{\lambda'\lambda'}$, we can write our final centre-of-mass wavefunction as

$$\begin{aligned} \psi_{\lambda\lambda'}(\ell_1, \ell_2) &= r(p) e^{ip\ell_1 + i(-p)\ell_2} + r(p) S_{\text{CoM}}(p) e^{i(-p)\ell_1 + ip\ell_2}, \\ \psi_{\lambda'\lambda}(\ell_1, \ell_2) &= r(p) e^{ip_1\ell_1 + i(-p)\ell_2} + r(p) S_{\text{CoM}}(p) e^{i(-p)\ell_1 + ip\ell_2}, \end{aligned} \tag{4.42}$$

and

$$\begin{aligned} \psi_{\lambda\lambda}(\ell_1, \ell_2) &= \big(1 - r(p)^2 \delta_{\ell_2, \ell_1+1} \mathcal{G}(-p)\big) e^{ip\ell_1 + i(-p)\ell_2} \\ &\quad + S_{\text{CoM}}(p) e^{i(-p)\ell_1 + ip\ell_2} \ , \\ \psi_{\lambda'\lambda'}(\ell_1, \ell_2) &= r(p)^2 \big(1 + \delta_{\ell_2, \ell_1+1} \mathcal{G}(-p)\big) e^{ip\ell_1 + i(-p)\ell_2} \\ &\quad + r(p)^2 S_{\text{CoM}}(p) e^{i(-p)\ell_1 + ip\ell_2}, \end{aligned} \tag{4.43}$$

where $S_{\text{CoM}}(p)$ is given by equation (4.38) and $\mathcal{G}(-p)$ is given by $\mathcal{G}(-p, p)$ in equation (4.35). Also, to be clear, the $r(p)^2$ factor in front of $\mathcal{G}(-p)$ in the $\lambda\lambda$ wavefunction comes from equation (4.31).

4.2.2 General solution

Having found the centre-of-mass solution for two Z excitations in the X vacuum, we now proceed to study the case $K \neq 0$. As in Section 3.2.2, and still following the approach of [52, 51], we introduce a second set of momenta $\{k_1, k_2\}$ and its

permutation

$$\begin{aligned}
\psi_{\lambda\lambda}(\ell_1,\ell_2) &= A_{\lambda\lambda}(p_1,p_2)e^{ip_1\ell_1+ip_2\ell_2} + A_{\lambda\lambda}(p_2,p_1)e^{ip_2\ell_1+ip_1\ell_2} \\
&\quad + A_{\lambda\lambda}(k_1,k_2)e^{ik_1\ell_1+ik_2\ell_2} + A_{\lambda\lambda}(k_2,k_1)e^{ik_2\ell_1+ik_1\ell_2}, \\
\psi_{\lambda\lambda'}(\ell_1,\ell_2) &= A_{\lambda\lambda'}(p_1,p_2)e^{ip_1\ell_1+ip_2\ell_2} + A_{\lambda\lambda'}(p_2,p_1)e^{ip_2\ell_1+ip_1\ell_2} \\
&\quad + A_{\lambda\lambda'}(k_1,k_2)e^{ik_1\ell_1+ik_2\ell_2} + A_{\lambda\lambda'}(k_2,k_1)e^{ik_2\ell_1+ik_1\ell_2}, \\
\psi_{\lambda'\lambda}(\ell_1,\ell_2) &= A_{\lambda'\lambda}(p_1,p_2)e^{ip_1\ell_1+ip_2\ell_2} + A_{\lambda'\lambda}(p_2,p_1)e^{ip_2\ell_1+ip_1\ell_2} \\
&\quad + A_{\lambda'\lambda}(k_1,k_2)e^{ik_1\ell_1+ik_2\ell_2} + A_{\lambda'\lambda}(k_2,k_1)e^{ik_2\ell_1+ik_1\ell_2}, \\
\psi_{\lambda'\lambda'}(\ell_1,\ell_2) &= A_{\lambda'\lambda'}(p_1,p_2)e^{ip_1\ell_1+ip_2\ell_2} + A_{\lambda'\lambda'}(p_2,p_1)e^{ip_2\ell_1+ip_1\ell_2} \\
&\quad + A_{\lambda'\lambda'}(k_1,k_2)e^{ik_1\ell_1+ik_2\ell_2} + A_{\lambda'\lambda'}(k_2,k_1)e^{ik_2\ell_1+ik_1\ell_2}.
\end{aligned} \tag{4.44}$$

The k momenta are such that $k_1+k_2 = p_1+p_2$ and $E(k_1)+E(k_2) = E(p_1)+E(p_2)$. Since the dispersion relation in the XZ sector is the same as that of the XY sector, they are also given in terms of the energy and the p-momenta by equation (3.51).

Each of the four terms (in other words, the direct p, swapped p, direct k and swapped k terms) are solutions of the non-interacting equations if the appropriate version of (4.27) holds. Substituting those relations, there will be four remaining coefficients $A_{\lambda\lambda}(p_1,p_2)$, $A_{\lambda\lambda}(p_2,p_1)$, $A_{\lambda\lambda}(k_1,k_2)$ and $A_{\lambda\lambda}(k_2,k_1)$. Through the interacting equations, we will fix these coefficients in terms of just $A_{\lambda\lambda}(p_1,p_2)$ and thus obtain a solution.

Interacting equations

As before, it is convenient to simplify the interacting equations by combining them with the non-interacting equations which, although unphysical, are still satisfied for $\ell_2 = \ell_1 + 1$. In this way obtain the equations

$$2/\kappa\, \psi_{\lambda\lambda}(s,s+1) - \psi_{\lambda'\lambda}(s+1,s+1) - \psi_{\lambda\lambda'}(s,s) = 0, \tag{4.45}$$

and

$$2\kappa\, \psi_{\lambda'\lambda'}(t,t+1) - \psi_{\lambda\lambda'}(t+1,t+1) - \psi_{\lambda'\lambda}(t,t) = 0. \tag{4.46}$$

Solving these one obtains two $\mathbb{Z}_2$-conjugate solutions for the remaining coefficients. The first one is

$$\begin{aligned}
A_{\lambda\lambda}(p_1,p_2) &= \big(a(k_2,k_1)b(k_1,k_2) - b(k_2,k_1)a(k_1,k_2)\big)a(p_1,p_2) \\
A_{\lambda\lambda}(p_2,p_1) &= -\big(a(k_2,k_1)b(k_1,k_2) - b(k_2,k_1)a(k_1,k_2)\big)a(p_2,p_1) \\
A_{\lambda\lambda}(k_1,k_2) &= -\big(a(p_2,p_1)b(p_1,p_2) - b(p_2,p_1)a(p_1,p_2)\big)a(k_1,k_2) \\
A_{\lambda\lambda}(k_2,k_1) &= -\big(a(p_1,p_2)b(p_2,p_1) - b(p_1,p_2)a(p_2,p_1)\big)a(k_2,k_1)\ ,
\end{aligned} \tag{4.47}$$

and the second solution is given by

$$\begin{aligned}
B_{\lambda\lambda}(p_1,p_2) &= \big(a(k_2,k_1)b(k_1,k_2) - b(k_2,k_1)a(k_1,k_2)\big)b(p_1,p_2)\\
B_{\lambda\lambda}(p_2,p_1) &= -\big(a(k_2,k_1)b(k_1,k_2) - b(k_2,k_1)a(k_1,k_2)\big)b(p_2,p_1)\\
B_{\lambda\lambda}(k_1,k_2) &= -\big(a(p_2,p_1)b(p_1,p_2) - b(p_2,p_1)a(p_1,p_2)\big)b(k_1,k_2)\\
B_{\lambda\lambda}(k_2,k_1) &= -\big(a(p_1,p_2)b(p_2,p_1) - b(p_1,p_2)a(p_2,p_1)\big)b(k_2,k_1)\ ,
\end{aligned} \tag{4.48}$$

where a, b are the coefficients

$$\boxed{\begin{aligned}
a(p_1,p_2,\kappa) &= e^{i(p_1+p_2)}r(p_1) - 2\kappa\, e^{ip_1}r(p_1)r(p_2) + r(p_2)\ ,\\
b(p_1,p_2,\kappa) &= \kappa\, e^{i(p_1+p_2)}r(p_2) - 2e^{ip_1} + \kappa\, r(p_1),
\end{aligned}} \tag{4.49}$$

where the ratio $r(p,\kappa)$ is defined in equation (4.18). These coefficients clearly reduce to the standard XXX form $1 - 2e^{ip_1} + e^{i(p_1+p_2)}$ as $\kappa \to 1$. Note, however, that they are different from the equivalent ones for the XY sector in (3.59). To avoid cluttering the notation we use the same labels as in Chapter 3, it being understood that all instances of these coefficients in this section refer to (4.49). We will also drop the explicit dependence on κ unless required for clarity.

The most general solution will be a linear combination of these two solutions:

$$\psi_{\lambda\lambda}(\ell_1,\ell_2) = \alpha\, \psi^A_{\lambda\lambda}(\ell_1,\ell_2) + \beta\, \psi^B_{\lambda\lambda}(\ell_1,\ell_2), \tag{4.50}$$

where $\psi^A_{\lambda\lambda}$ and $\psi^B_{\lambda\lambda}$ are of the form in (4.44) with the A and B coefficients, respectively. The same holds true for the other wavefunctions but with appropriate placements of $r(p)$.

In summary, the total eigenstate that solves the two magnon problem is given by

$$|\psi\rangle_{\text{tot}} = \alpha\, |p_1,p_2,k_1,k_2\rangle_A + \beta\, |p_1,p_2,k_1,k_2\rangle_B, \tag{4.51}$$

where

$$\begin{aligned}
|p_1,p_2,k_1,k_2\rangle_i = \sum_{\ell_1<\ell_2} \big(&\psi^i_{\lambda\lambda}(\ell_1,\ell_2)|\ell_1\ell_2\rangle + \psi^i_{\lambda\lambda'}(\ell_1,\ell_2)|\ell_1\ell_2\rangle\\
&+ \psi^i_{\lambda'\lambda}(\ell_1,\ell_2)|\ell_1\ell_2\rangle + \psi^i_{\lambda'\lambda'}(\ell_1,\ell_2)|\ell_1\ell_2\rangle\big)\ , \quad i = A,B.
\end{aligned} \tag{4.52}$$

Finally, similar to the XY sector, we note that we can rewrite the wavefunctions as in equation (3.62) where (the result is similar for the B coefficients)

$$\psi^A_{ee}(\ell_1,\ell_2) = \Psi(k_1,k_2)\Omega^A(p_1,p_2;\ell_1,\ell_2) - \Psi(p_1,p_2)\Omega^A(k_1,k_2;\ell_1,\ell_2), \tag{4.53}$$

where (here q_i stands for either p_i or k_i)

$$\Psi(q_1, q_2) = a(q_2, q_1)b(q_1, q_2) - b(q_2, q_1)a(q_1, q_2), \tag{4.54}$$

and

$$\Omega^A(q_1, q_2; \ell_1, \ell_2) = a(q_1, q_2)e^{iq_1\ell_1 + iq_2\ell_2} - a(q_2, q_1)e^{iq_2\ell_1 + iq_1\ell_2}. \tag{4.55}$$

Properties of the S-matrices

Similar to the XY sector, since each of the two general solutions contains four Bethe-like terms, we can again define three S-matrices. Two of them refer to scattering of the p or k momenta among themselves

$$\begin{aligned} S^A(p_1, p_2, \kappa) &= \frac{A_{\lambda\lambda}(p_2, p_1)}{A_{\lambda\lambda}(p_1, p_2)} = -\frac{a(p_2, p_1)}{a(p_1, p_2)}, \\ S^A(k_1, k_2, \kappa) &= \frac{A_{\lambda\lambda}(k_2, k_1)}{A_{\lambda\lambda}(k_1, k_2)} = -\frac{a(k_2, k_1)}{a(k_1, k_2)}. \end{aligned} \tag{4.56}$$

There is also an S-matrix scattering the p momenta to the k momenta, which we call T

$$\begin{aligned} T^A(p_1, p_2, k_1, k_2, \kappa) &= \frac{A_{\lambda\lambda}(k_1, k_2)}{A_{\lambda\lambda}(p_1, p_2)} \\ &= -\frac{a(p_2, p_1)b(p_1, p_2) - b(p_2, p_1)a(p_1, p_2)}{a(k_2, k_1)b(k_1, k_2) - b(k_2, k_1)a(k_1, k_2)} \frac{a(k_1, k_2)}{a(p_1, p_2)}. \end{aligned} \tag{4.57}$$

Similarly, for the solution with B coefficients,

$$\begin{aligned} S^B(p_1, p_2, \kappa) &= \frac{B_{\lambda\lambda}(p_2, p_1)}{B_{\lambda\lambda}(p_1, p_2)} = -\frac{b(p_2, p_1)}{b(p_1, p_2)}, \\ S^B(k_1, k_2, \kappa) &= \frac{B_{\lambda\lambda}(k_2, k_1)}{B_{\lambda\lambda}(k_1, k_2)} = -\frac{b(k_2, k_1)}{b(k_1, k_2)}, \end{aligned} \tag{4.58}$$

and

$$\begin{aligned} T^B(p_1, p_2, k_1, k_2, \kappa) &= \frac{B_{\lambda\lambda}(k_1, k_2)}{B_{\lambda\lambda}(p_1, p_2)} \\ &= -\frac{a(p_2, p_1)b(p_1, p_2) - b(p_2, p_1)a(p_1, p_2)}{a(k_2, k_1)b(k_1, k_2) - b(k_2, k_1)a(k_1, k_2)} \frac{b(k_1, k_2)}{b(p_1, p_2)}. \end{aligned} \tag{4.59}$$

These two solutions are related by $\mathbb{Z}_2$ symmetry. More precisely, recalling that $r(p, 1/\kappa) = 1/r(p, \kappa)$, one finds

$$\begin{aligned} a(p_1, p_2, 1/\kappa) &= \frac{1}{\kappa} \frac{1}{r(p_1)r(p_2)} b(p_1, p_2, \kappa), \\ b(p_1, p_2, 1/\kappa) &= \frac{1}{\kappa} \frac{1}{r(p_1)r(p_2)} a(p_1, p_2, \kappa). \end{aligned} \tag{4.60}$$

From this, we find that

$$\begin{aligned} S^A(x,y,1/\kappa) &= S^B(x,y,\kappa), \\ T^A(x,y,w,z,1/\kappa) &= \frac{r(k_1)r(k_2)}{r(p_1)r(p_2)} T^B(x,y,w,z,\kappa), \end{aligned} \tag{4.61}$$

where $\{x,y\} = \{p_1,p_2\}$ or $\{k_1,k_2\}$ and similarly for $\{w,z\}$. The S-matrices satisfy unitarity and reduce to -1 for equal momenta

$$S^A(x,y)S^A(y,x) = 1\ ,\ S^B(x,y)S^B(y,x) = 1\ ,\ S^A(p,p) = -1\ , S^B(p,p) = -1\ . \tag{4.62}$$

They also smoothly reduce to the XXX S-matrix as $\kappa \to 1$. However, unlike the XXX S-matrix and the corresponding XY-sector S-matrices, $S^{A,B}(0,p) \neq 1$. Note that the T-matrix is again not a phase.

Finally, we note that we have the same relation as given in equation (3.76)

$$S^A(k_1,k_2)T^A(p_1,p_2,k_1,k_2) = T^A(p_2,p_1,k_2,k_1)S^A(p_1,p_2), \tag{4.63}$$

and similar for the B coefficient solutions.

Symmetries

Since $\mathbb{Z}_2$ maps the A coefficient solutions to the B coefficient solutions and vice versa, to obtain a $\mathbb{Z}_2$-invariant solution we need to combine them as

$$|\psi\rangle_{(gen)} = \alpha\ |p_1,p_2,k_1,k_2\rangle_A + \beta\ |p_1,p_2,k_1,k_2\rangle_B\ , \tag{4.64}$$

where we must have $\alpha(1/\kappa) = \pm\beta(\kappa)$. Then we have

$$\mathbb{Z}_2|\psi\rangle_{(gen)} = \mp\frac{1}{\kappa^3}\big(r(p_1)r(p_2)r(k_1)r(k_2)\big)^{-2}|\psi\rangle_{(gen)}. \tag{4.65}$$

Note that the eigenvalue is slightly different from the one of the XY sector (see Table 3.1).

One can also apply the momentum permutation maps (3.81) to the A and B solutions. The eigenvalues are exactly the same as those in Table 3.1.

4.2.3 Restricted Solution

Similar to the XY case, the presence of additional k momenta, which can take complex values (for real values of the original p momenta), is problematic when considering large distances $\ell_2 - \ell_1 \gg 1$ on the spin chain since one of the two k

momenta Bethe wavefunctions will diverge. In addition, even for short chains, the k momenta diverge as we take the centre-of-mass limit $K = 0$. For these reasons, we would like to restrict the general solution to remove one of the two k wavefunctions. Expressing $k_1 = K/2+\pi/2-iv$, $k_2 = K/2-\pi/2+iv$, with $v \geq 0$, the term we need to remove is the swapped k-momenta term $\{p_2, p_1\}$. We make an ansatz simply consisting of three terms

$$\begin{aligned}
\psi^{(r)}_{\lambda\lambda}(\ell_1,\ell_2) &= A_{\lambda\lambda}(p_1,p_2)e^{ip_1\ell_1+ip_2\ell_2} + A_{\lambda\lambda}(p_2,p_1)e^{ip_2\ell_1+ip_1\ell_2} \\
&\quad + A_{\lambda\lambda}(k_1,k_2)e^{ik_1\ell_1+ik_2\ell_2}, \\
\psi^{(r)}_{\lambda\lambda'}(\ell_1,\ell_2) &= A_{\lambda\lambda'}(p_1,p_2)e^{ip_1\ell_1+ip_2\ell_2} + A_{\lambda\lambda'}(p_2,p_1)e^{ip_2\ell_1+ip_1\ell_2} \\
&\quad + A_{\lambda\lambda'}(k_1,k_2)e^{ik_1\ell_1+ik_2\ell_2}, \\
\psi^{(r)}_{\lambda'\lambda}(\ell_1,\ell_2) &= A_{\lambda'\lambda}(p_1,p_2)e^{ip_1\ell_1+ip_2\ell_2} + A_{\lambda'\lambda}(p_2,p_1)e^{ip_2\ell_1+ip_1\ell_2} \\
&\quad + A_{\lambda'\lambda}(k_1,k_2)e^{ik_1\ell_1+ik_2\ell_2}, \\
\psi^{(r)}_{\lambda'\lambda'}(\ell_1,\ell_2) &= A_{\lambda'\lambda'}(p_1,p_2)e^{ip_1\ell_1+ip_2\ell_2} + A_{\lambda'\lambda'}(p_2,p_1)e^{ip_2\ell_1+ip_1\ell_2} \\
&\quad + A_{\lambda'\lambda'}(k_1,k_2)e^{ik_1\ell_1+ik_2\ell_2}.
\end{aligned} \tag{4.66}$$

This is the minimal number of terms needed to solve the interacting equations. We find the following solution

$$\begin{aligned}
A_{\lambda\lambda}(p_1,p_2) &= a(k_2,k_1)b(p_1,p_2) - b(k_2,k_1)a(p_1,p_2)\ , \\
A_{\lambda\lambda}(p_2,p_1) &= -\big(a(k_2,k_1)b(p_2,p_1) - b(k_2,k_1)a(p_2,p_1)\big)\ , \\
A_{\lambda\lambda}(k_1,k_2) &= -\big(a(p_2,p_1)b(p_1,p_2) - b(p_2,p_1)a(p_1,p_2)\big)\ .
\end{aligned} \tag{4.67}$$

with the other coefficients related to these three via (4.27). We observe that the A's here are quadratic in the a, b-coefficients unlike the general solution which is cubic. On the other hand, the a and b terms with p and k dependence are mixed in the restricted solution, while they appear in a more factorised form in the general one.

One can of course also recover this result by suitably combining the A and B solutions as

$$|\psi\rangle_{(r)} = \frac{1}{a(k_1,k_2)}\frac{c}{1+c}\,|\psi\rangle_A + \frac{1}{b(k_1,k_2)}\frac{1}{1+c}\,|\psi\rangle_B, \tag{4.68}$$

where

$$c = -\frac{b(k_2,k_1)}{b(k_1,k_2)}\frac{a(k_1,k_2)}{a(k_2,k_1)}. \tag{4.69}$$

The details are precisely the same as for the XY case (see Section 3.2.3), so we do not repeat them here.

The restricted solution (4.67) will be our starting point in Section 4.2.4, where we will carefully take the $p_2 \to -p_1$ limit and show how it leads to the centre-of-mass solution (4.43).

Symmetries

Factoring out the $A_{\lambda\lambda}$ coefficient, we can define two S-matrices:

$$S^{(r)}(p_1, p_2, k_1, k_2) = \frac{A_{\lambda\lambda}(p_2, p_1)}{A_{\lambda\lambda}(p_1, p_2)} = -\frac{a(k_2, k_1)b(p_2, p_1) - b(k_2, k_1)a(p_2, p_1)}{a(k_2, k_1)b(p_1, p_2) - b(k_2, k_1)a(p_1, p_2)} , \tag{4.70}$$

and

$$T^{(r)}(p_1, p_2, k_1, k_2) = \frac{A_{\lambda\lambda}(k_1, k_2)}{A_{\lambda\lambda}(p_1, p_2)} = -\frac{a(p_2, p_1)b(p_1, p_2) - b(p_2, p_1)a(p_1, p_2)}{a(k_2, k_1)b(p_1, p_2) - b(k_2, k_1)a(p_1, p_2)} . \tag{4.71}$$

The $S^{(r)}$ matrix satisfies the unitarity and fermionic property

$$S^{(r)}(p_1, p_2, k_1, k_2)S^{(r)}(p_2, p_1, k_1, k_2) = 1 \quad , \quad S^{(r)}(p_1, p_1, k_1, k_2) = -1 , \tag{4.72}$$

and smoothly reduces to the XXX S-matrix in the $\kappa \to 1$ limit. It is also $\mathbb{Z}_2$ invariant:

$$S^{(r)}(p_1, p_2, k_1, k_2, 1/\kappa) = S^{(r)}(p_1, p_2, k_1, k_2, \kappa) . \tag{4.73}$$

As before, the $T^{(r)}$ matrix is not a phase.

It can also be shown that $|\psi\rangle_{(r)}$ is a $\mathbb{Z}_2$ eigenstate, with a slightly different eigenvalue to the XY sector restricted solution, where

$$\mathbb{Z}_2|\psi\rangle_{(r)} = -\frac{1}{\kappa^2}\big(r(p_1)r(p_2)\big)^{-2}\big(r(k_1)r(k_2)\big)^{-1}|\psi\rangle_{(r)}. \tag{4.74}$$

Apart from this difference, all the transformations for $|\psi\rangle_{(r)}$ tabulated in Table 3.1 apply to the XZ restricted solution.

4.2.4 Restricted solution in the CoM limit

In our study of the X vacuum of the XZ sector we also applied two, superficially very different, methods to solve the two magnon problem: A contact-term method which required the centre-of-mass condition $K = 0$ (Section 4.2.1) and the approach with additional momenta (sections 4.2.2 and 4.2.3). As in the XY sector, in this section we show how the two methods are related, and in particular that the CoM S-matrix (4.38) arises as a limit of the restricted XZ-sector S-matrix (4.70). As most features are exactly parallel to the XY case in Section 3.2.4, we will just show the main points.

Recovering the centre-of-mass S-matrix:

Recall the restricted solution S-matrix in this sector is

$$\begin{aligned} S^{(r)}(p_1,p_2,k_1,k_2) &= -\frac{a(k_2,k_1)b(p_2,p_1)-b(k_2,k_1)a(p_2,p_1)}{a(k_2,k_1)b(p_1,p_2)-b(k_2,k_1)a(p_1,p_2)} \\ &= -\frac{f\cdot b(p_2,p_1)-a(p_2,p_1)}{f\cdot b(p_1,p_2)-a(p_1,p_2)}, \end{aligned} \tag{4.75}$$

where

$$f=\frac{a(k_2,k_1)}{b(k_2,k_1)}=\frac{e^{i(p_1+p_2)}r\left(k_2\right)+r\left(k_1\right)\left(1-2\kappa e^{ik_2}r\left(k_2\right)\right)}{\kappa e^{i(p_1+p_2)}r\left(k_1\right)+\kappa r\left(k_2\right)-2e^{ik_2}}. \tag{4.76}$$

Due to the divergence of the k momenta as $p_2\to -p_1$, the limit needs to be taken carefully. We start by simplifying the ratio functions $r(k_1)$, $r(k_2)$ by taking the partial limit in some of their terms

$$\begin{aligned} r(k_1) &\to \frac{e^{-ik_1}\left(-\kappa^2+\sqrt{\kappa^4+\kappa^2e^{2ik_1}+1}+1\right)}{\kappa}, \\ r(k_2) &\to \frac{e^{ik_2}\left(-\kappa^2+\sqrt{\kappa^4+\kappa^2e^{-2ik_2}+1}+1\right)}{\kappa}. \end{aligned} \tag{4.77}$$

We then substitute these expressions into f and set $k_1=p_1+p_2-k_2$. Next, to remove the divergent parts from k_2, we set $p_2=-p_1+\epsilon$. After some manipulation, we find that we can write

$$e^{2ik_2}=\frac{\sin^2(\epsilon)}{x}\text{ , where }\lim_{\epsilon\to 0}x=-\frac{4\left(\kappa^4+2\kappa^2\cos(2p)+1\right)}{\kappa^2}. \tag{4.78}$$

Substituting back into f and taking the limit $\epsilon\to 0$, we find that

$$f\to\frac{f_{\mathrm{n}}(p,\kappa)}{f_{\mathrm{d}}(p,\kappa)}, \tag{4.79}$$

where

$$\begin{aligned} f_{\mathrm{n}}(p,\kappa) &= \kappa^4+2\kappa^2\cos(2p)+\kappa^2\left(-\sqrt{\kappa^4+2\kappa^2\cos(2p)+1}-i\sqrt{-\kappa^4-2\kappa^2\cos(2p)-1}\right) \\ &\quad+\sqrt{\kappa^4+2\kappa^2\cos(2p)+1}+2i\sqrt{-\left(\kappa^4+2\kappa^2\cos(2p)+1\right)^2}+1, \end{aligned} \tag{4.80}$$

and

$$f_{\mathrm{d}}(p,\kappa)=\kappa^5+\kappa+2\kappa^3\cos(2p)-\kappa^3\sqrt{\kappa^4+2\kappa^2\cos(2p)+1}. \tag{4.81}$$

Then, substituting f into (4.70) and taking the remaining limits $p_2\to -p_1$, we find precisely S_{CoM} as in (4.38).

Recovering the contact term

To complete the matching of the solutions, we need to also recover the contact term $\mathcal{G}(-p)$ (where $\mathcal{G}(-p) = \mathcal{G}(-p, p)$ in (4.35)). We will focus on the (λ, λ) and (λ', λ') terms in the restricted wavefunction, as there are no neighbouring Z magnons in the $\psi^{(r)}_{\lambda\lambda'}, \psi^{(r)}_{\lambda'\lambda}$ wavefunctions. As in the previous case, we set $\ell_2 = \ell_1 + 2m + 1$, where $m \geq 0$ (in $\psi_{\lambda\lambda}, \psi_{\lambda',\lambda'}$, for a Z excitation at site ℓ_1, the excitation at ℓ_2 is an odd number of sites away). We will show that for $m = 0$ (in other words, the nearest-neighbour case), we have a finite non-zero result in the $K = 0$ limit, while the terms with $m > 0$ vanish. We will thus recover the required contact terms.

Recalling the form of T from (4.71), a generic term in $\psi^{(r)}_{\lambda\lambda}$ will be

$$\begin{aligned} &r(k_1)r(k_2)T^{(r)}(p_1, p_2, k_1, k_2)e^{ik_1\ell_1 + ik_2(\ell_1+2m+1)} \\ &= -r(k_1)r(k_2)\frac{e^{ik_2(2m+1)}}{b(k_2, k_1)}\frac{a(p_2, p_1)b(p_1, p_2) - b(p_2, p_1)a(p_1, p_2)}{f \cdot b(p_1, p_2) - a(p_1, p_2)}e^{i(k_1+k_2)\ell_1}\,. \end{aligned} \tag{4.82}$$

where we used that $k_1 + k_2 = 0$ in the limit. We have already determined the limit for f, and $r(k_1)r(k_2) \to -1$ in the limit, so it just remains to study the behaviour of the prefactor (for which will use the symbol t)

$$t = \frac{e^{ik_2(2m+1)}}{b(k_2, k_1)}. \tag{4.83}$$

Setting $p_2 = -p_1 + \epsilon$ and using equation (4.78), we find that t reduces to

$$t = \frac{\left(\frac{\sin^2(\epsilon)}{x}\right)^m}{\frac{-\kappa^2+\sqrt{\kappa^4+\kappa^2\left(\frac{\sin^2(\epsilon)}{x}+x\csc^2(\epsilon)\right)+1}+1}{\frac{\sin^2(\epsilon)}{x}+1} + \frac{e^{2i\epsilon}\left(-\kappa^2+\sqrt{\kappa^4+\kappa^2\left(\frac{e^{-2i\epsilon}\sin^2(\epsilon)}{x}+xe^{2i\epsilon}\csc^2(\epsilon)\right)+1}+1\right)}{\frac{\sin^2(\epsilon)}{x}+e^{2i\epsilon}} - 2}. \tag{4.84}$$

We then perform a series expansion to find

$$\begin{aligned} t = &\left(\frac{4^{-m}}{2\sqrt{\kappa^4 + 2\cos(2p)\kappa^2 + 1} - 2\kappa^2} - \frac{4^{-m}\left(\frac{-\kappa^4 - 8\cos(2p)\kappa^2 - 6\kappa^2 - 1}{12\sqrt{-\kappa^4 - 2\cos(2p)\kappa^2 - 1}} + \frac{i\left(11\kappa^4 + 16\cos(2p)\kappa^2 - 6\kappa^2 + 11\right)}{12\sqrt{\kappa^4 + 2\cos(2p)\kappa^2 + 1}}\right)\epsilon}{\left(2\sqrt{\kappa^4 + 2\cos(2p)\kappa^2 + 1} - 2\kappa^2\right)^2} + O\left(\epsilon^2\right)\right) \\ &\times\left(-\frac{\kappa^2\sin^2(\epsilon)}{\kappa^4 + 2\kappa^2\cos(2p) + 1}\right)^m \end{aligned} \tag{4.85}$$

It is straightforward to confirm that for $m > 0$, the above expression vanishes as we send $\epsilon \to 0$. However, if $m = 0$ we find

$$t = \frac{e^{ik_2}}{b(k_2, k_1)} \to \frac{1}{2\sqrt{\kappa^4 + 2\kappa^2\cos(2p) + 1} - 2\kappa^2}\,. \tag{4.86}$$

Substituting this (and f) back into (4.82), we find a precise match with the term

$$-r(p)^2 e^{-ip}\mathcal{G}(-p), \tag{4.87}$$

which arises in the solution (4.43). The case of $\psi^{(r)}_{\lambda'\lambda'}$ works similarly. Thus, as in the XY sector, we conclude that the contact term wavefunction (4.43) is a limiting case of the restricted wavefunction (4.66),(4.67) in the centre-of-mass limit.

4.3 Bethe Ansatz for the XZ Sector

In this section we will consider closed chains in the XZ sector using the two-Z magnon solution around the X vacuum constructed above. It should be noted that due to the dilute nature of these chains, not all configurations of magnons are possible. For instance, odd-Z-magnon states on an even-length closed chain are not allowed, as there is no way to match the gauge indices, or alternatively guarantee that the value of λ to the left of the first site is the same as that to the right of the last site. Let us, for example, consider the state $|XXZX\rangle$. If the value of the dynamical parameter is λ to the left of the first site, making that X a Q_{12}, then its value is λ' to the right of the last site, making that X a Q_{12} again. The gauge indices of these fields cannot be contracted to create a closed chain. However if we consider a state with two Z magnons, such as $|XZZX\rangle$, the last field is a Q_{21} and we now can contract the gauge indices. Therefore, the two-Z magnon problem is restricted to closed chains of even length.

Another difference to the XZ sector is that the length-L Hamiltonian is not just a direct product of the (alternately) $\mathcal{H}_{eo}$ and $\mathcal{H}_{oe}$ Hamiltonians acting on each pair of sites, and it is not possible to choose a reference site (e.g. the first one) with a fixed λ, as the action of the Hamiltonian on sites $(L, 1)$ can change that value. Therefore, we work on the full basis of two-Z excitations, with both possibilities for λ on the first site[2].

Despite these differences, it is clear that the solution of the two magnon problem in the X vacuum of the XZ sector is very similar to that of the alternating XY sector. It also requires two sets of momenta, p_i and k_i, giving the same total momentum K and energy E_2. The main differences stem from the fact that the a and b coefficients (4.49) entering the S matrices are different from (3.59). Also, as we will focus on even-length chains, there is no one magnon problem, and thus also no "trivial" two

[2]For example, for the length-6 examples studied in [27], this basis is 30-dimensional

magnon energies just obtained by periodicity.[3]

In the CoM frame, we will again have, for the untwisted and twisted sectors respectively:

$$e^{ipL} = 1/S(p,-p) \quad \text{and} \quad e^{ipL} = -1/S(p,-p) \ , \tag{4.88}$$

with S now as in (4.38). Since $S \to e^{-ip}$ in the limit $\kappa \to 1$, the momenta reduce to those of the standard XXX model as they should.

Periodicity for the general (non-CoM) solution is also easy to impose by suitably combining the two wavefunctions related by $\mathbb{Z}_2$

$$|\psi\rangle_{\text{tot}} = A(p_1,p_2,k_1,k_2) + xB(p_1,p_2,k_1,k_2) \ , \tag{4.89}$$

where now

$$\begin{aligned} (A_{12}^{\lambda\lambda,p} + xB_{12}^{\lambda\lambda,p})e^{i(l_1p_1+l_2p_2)} &= (A_{21}^{\lambda\lambda,p} + xB_{21}^{\lambda\lambda,p})e^{i(l_2p_2+(l_1+L)p_1)} \ , \\ (A_{12}^{\lambda\lambda,k} + xB_{12}^{\lambda\lambda,k})e^{i(l_1k_1+l_2k_2)} &= (A_{21}^{\lambda\lambda,k} + xB_{21}^{\lambda\lambda,k})e^{i(l_2k_2+(l_1+L)k_1)} \ , \end{aligned} \tag{4.90}$$

and similarly for the $\lambda'\lambda'$ parts. For the $\lambda\lambda'$ parts we have

$$\begin{aligned} (A_{12}^{\lambda\lambda',p} + xB_{12}^{\lambda\lambda',p})e^{i(l_1p_1+l_2p_2)} &= (A_{21}^{\lambda'\lambda,p} + xB_{21}^{\lambda'\lambda,p})e^{i(l_2p_2+(l_1+L)p_1)} \ , \\ (A_{12}^{\lambda\lambda',k} + xB_{12}^{\lambda\lambda',k})e^{i(l_1k_1+l_2k_2)} &= (A_{21}^{\lambda'\lambda,k} + xB_{21}^{\lambda'\lambda,k})e^{i(l_2k_2+(l_1+L)k_1)} \ , \end{aligned} \tag{4.91}$$

which all lead to

$$\bar{x}(k_1,k_2) = -\frac{a(k_1,k_2) + a(k_2,k_1)e^{iLk_1}}{b(k_1,k_2) + b(k_2,k_1)e^{iLk_1}} \ , \tag{4.92}$$

in terms of which the Bethe ansatz is

$$e^{iLp_1} = -\frac{a(p_1,p_2) + \bar{x}(k_1,k_2)b(p_1,p_2)}{a(p_2,p_1) + \bar{x}(k_1,k_2)b(p_2,p_1)} \ . \tag{4.93}$$

This is the same expression as for the XY sector, however now the a, b functions are those in (4.49).

Analogously, we can study the twisted sector by imposing antiperiodicity on (4.89). The Bethe ansatz is now

$$e^{iLp_1} = \frac{a(p_1,p_2) + \bar{x}(k_1,k_2)b(p_1,p_2)}{a(p_2,p_1) + \bar{x}(k_1,k_2)b(p_2,p_1)} \ , \tag{4.94}$$

with $\bar{x}$ defined by

$$\bar{x}(k_1,k_2) = -\frac{a(k_1,k_2) - a(k_2,k_1)e^{iLk_1}}{b(k_1,k_2) - b(k_2,k_1)e^{iLk_1}} \ . \tag{4.95}$$

[3] Accordingly, the S-matrices of the XZ sector general solution (4.56),(4.58) do not reduce to 1 as one of the momenta becomes zero.

In [27], similar to the XY sector, the Bethe ansatz result is numerically compared to results from explicit diagonalisation of the Hamiltonian for both the twisted and untwisted sectors and show good agreement. Thus, the numerical results provide excellent confirmation that the XZ sector wavefunctions and the periodic Bethe ansatz for the twisted/untwisted sectors are indeed correct.

Chapter 5

ELLIPTIC PARAMETRISATION

The motivation of this chapter is to understand the most appropriate parametrisation for each of our sectors. The dispersion relation appearing in the XY sector and the X-vacuum of the XZ sector is naturally uniformised by elliptic functions. In this chapter, we provide more details of this parametrisation and show how it allows us to uncover an interesting relation between these two sectors.

XY sector

Let us start with the dispersion relation (3.15) in the upper branch

$$E(p) = \kappa + \frac{1}{\kappa} + \frac{1}{\kappa}\sqrt{1+\kappa^2 e^{-2ip}}\sqrt{1+\kappa^2 e^{2ip}} \ . \tag{5.1}$$

Recall that the rapidity variable v which uniformises the dispersion relation should be such that

$$\frac{\partial p(v)}{\partial v} = E(p) \ \Rightarrow \ v(p) = \int \frac{\mathrm{d}p}{E(p)} \ . \tag{5.2}$$

The solutions of this equation are not very easy to work with, so we shift the energy temporarily to $E' = E - \frac{1}{\kappa} - \kappa$. It should be pointed out that, although this shift is by a constant, it is not completely harmless since it brings the dispersion relation to an XY-model/free-fermion form, effectively dropping the contribution from the $\sigma^z \otimes \sigma^z$ terms in the Hamiltonian which are responsible for the $1/\kappa + \kappa$ term. We can now follow the treatment in [45], which is in the context of the XY model, to express this relation using Jacobi elliptic functions with modular parameter $m = \kappa^4$. We find

$$e^{ip} = i\kappa \mathrm{sn}(v/\kappa|m_{XY}) \ , \tag{5.3}$$

in terms of which the energy is expressed as

$$E'(v) = \frac{\mathrm{d}p}{\mathrm{d}v} = \frac{i}{\kappa}\frac{\mathrm{cn}(v/\kappa|m)\mathrm{dn}(v/\kappa|m)}{\mathrm{sn}(v/\kappa|m)} \ . \tag{5.4}$$

We note that in the above parametrisation $p = 0$ corresponds to $v_0 = -i\kappa K(1-m)/2$, with $K(m)$ the elliptic integral of the first kind with modular parameter m. One could thus have shifted the rapidity as $v \to v + v_0$ so that $v = 0$ corresponds to

$p = 0$ [45]. Another important quantity entering our wavefunctions in Chapter 3 is the ratio function, which for this sector is

$$r_{XY}(p) = \frac{e^{ip}\sqrt{1+\kappa^2 e^{-2ip}}}{\sqrt{1+\kappa^2 e^{2ip}}} \to r_{XY}(v) = \frac{\kappa \mathrm{cn}(v/\kappa, m)}{\mathrm{dn}(v/\kappa, m)} \ . \tag{5.5}$$

XZ sector

The dispersion relation of the XZ sector is the same as the XY sector. However, for reasons to be clear momentarily, for this sector we will choose not to split the square root and instead write the dispersion relation as (3.14)

$$E(p) = \frac{1}{\kappa} + \kappa + \frac{1}{\kappa}\sqrt{(1+\kappa^2)^2 - 4\kappa^2 \sin^2 p} \ . \tag{5.6}$$

Then the natural modular parameter that presents itself is $\tilde{m} = \frac{4\kappa^2}{(1+\kappa^2)^2}$. Consequently, we will parametrise equation (5.6) using elliptic functions depending on this parameter.[1] Subtracting the constant and using (5.2) we find

$$\sin(p) = \mathrm{sn}((\kappa + \kappa^{-1})v|\tilde{m}) \ , \tag{5.7}$$

and the energy is now

$$E'(v) = (\kappa + \kappa^{-1})\mathrm{dn}((\kappa + \kappa^{-1})v|\tilde{m}) \ . \tag{5.8}$$

The ratio function for the XZ sector is expressed as

$$r_{XZ}(v) = \frac{(\kappa - \kappa^{-1}) - (\kappa + \kappa^{-1})\mathrm{dn}(-(\kappa + \kappa^{-1})v|\tilde{m})}{2\mathrm{cn}(-(\kappa + \kappa^{-1})v|\tilde{m})} \ . \tag{5.9}$$

An interesting relation between the ratio functions arises if we use the Gauss transformation (or descending Landen transformation) (e.g. [76])[2]

$$\begin{aligned} \mathrm{cn}\left((1+\sqrt{m})v\Big|\frac{4\sqrt{m}}{(1+\sqrt{m})^2}\right) &= \frac{\mathrm{cn}(v|m)\mathrm{dn}(v|m)}{1+\sqrt{m}\mathrm{sn}(v|m)^2} \ , \\ \mathrm{dn}\left((1+\sqrt{m})v\Big|\frac{4\sqrt{m}}{(1+\sqrt{m})^2}\right) &= \frac{1-\sqrt{m}\mathrm{sn}(v|m)^2}{1+\sqrt{m}\mathrm{sn}(v|m)^2} \ . \end{aligned} \tag{5.10}$$

It can then be straightforwardly shown that

$$r_{XZ}((\kappa + \kappa^{-1})v|\tilde{m}) = \frac{1}{r_{XY}(v/\kappa|m)} \ . \tag{5.11}$$

[1] This approach is closer to the standard elliptic function parametrisation of the higher-loop $\mathcal{N} = 4$ dispersion relation, where the elliptic parameter is $m = -4g_{YM}^2$ with g_{YM} the Yang-Mills coupling (see e.g. [8, 9])

[2] In the $\mathcal{N} = 4$ higher-loop context, Landen transformations were used in [77].

Thus, despite being quite different functions of the momentum, the ratio functions of the two sectors can be mapped to each other by a modular identity, for the same value of the rapidity.[3]. This mapping hints that there exists a unifying form of the Bethe ansatz equations in the two sectors, which should become evident with the correct elliptic uniformisation.

Theta function parametrisation

It is also instructive to switch to a theta function parametrisation. We will only show this explicitly for the choice of modular parameter $m = \kappa^4$ as in the XY sector. Using standard relations (e.g. [40]), we can write

$$e^{ip} = i\sqrt{k}\,\mathrm{sn}(v/\kappa) = i\sqrt{k}\frac{1}{\sqrt{k}}\frac{\theta_1(u)}{\theta_4(u)} = i\frac{\theta_1(u)}{\theta_4(u)}\ , \tag{5.12}$$

where the arguments of the Jacobi and theta functions are related as $v/\kappa = 2K(m)u$. For the XY sector ratio function we have

$$r(u) = \frac{\sqrt{k}\,\mathrm{cn}(v/\kappa)}{\mathrm{dn}(v/\kappa)} = \sqrt{k}\left(\sqrt{\frac{k'}{k}}\frac{\theta_2(u)}{\theta_4(u)}\right)\left(\frac{1}{\sqrt{k'}}\frac{\theta_4(u)}{\theta_3(u)}\right) = \frac{\theta_2(u)}{\theta_3(u)}\ . \tag{5.13}$$

Here we use the nome

$$q = e^{i\pi\tau}\ ,\ \text{where}\ \ \tau = i\frac{K'(m)}{K(m)}\ , \tag{5.14}$$

with $m = \kappa^4$, $K'(m) = K(1-m)$ and our theta function conventions as in [40, 78]. In particular we have

$$\theta_1(u+1) = -\theta_1(u)\ ,\ \ \theta_1(u+\tau) = -e^{\pi i(2u+\tau)}\theta_1(u)\ . \tag{5.15}$$

The zeroes of $\theta_1(u)$ are at $u = m + n\tau$ with m, n integer. As above, it is usually convenient to shift the rapidity u by $\tau/4$ in order to get that $u = 0$ gives $p = 0$, and that real rapidities correspond to real momenta.

It is intriguing that e^{ip} and the ratio function $r(p)$, (which both appear in the $a(p_1, p_2)$ and $b(p_1, p_2)$ terms entering the S-matrices) can be exchanged by the simple shift $u \to u + \frac{1}{2}$, given that $\theta_{1,3,4}(u+\frac{1}{2}) = \theta_{2,4,3}(u)$ and $\theta_2(u+\frac{1}{2}) = -\theta_1(u)$

$$e^{ip} \overset{u\to u+1/2}{\longrightarrow} ir(p;\kappa) \overset{u\to u+1/2}{\longrightarrow} -e^{ip} \overset{u\to u+1/2}{\longrightarrow} -ir(p;\kappa) \overset{u\to u+1/2}{\longrightarrow} e^{ip}. \tag{5.16}$$

[3] One could of course have redefined the ratio in one of the sectors to be the opposite ratio, so as to get precise matching.

Also, under shifts $u \to u+\tau/2$, given the transformations $\theta_{1,4}(u+\tau/2) = ie^{-\pi i(u+\tau/4)}\theta_{4,1}(u)$ and $\theta_{2,3}(u+\tau/2) = e^{-\pi i(u+\tau/4)}\theta_{3,2}(u)$, we have

$$e^{ip} \overset{u\to u+\tau/2}{\longrightarrow} -e^{-ip} = e^{i(\pi-p)} \quad \text{and} \quad r(p;\kappa) \overset{u\to u+\tau/2}{\longrightarrow} \frac{1}{r(p;\kappa)} \,. \tag{5.17}$$

We can put the above components together to write the one magnon wavefunction as

$$\begin{aligned} |p\rangle &= \sum_{\ell\in 2\mathbb{Z}} e^{ip\ell}|\ell\rangle + \sum_{\ell\in 2\mathbb{Z}+1} r(p;\kappa)e^{ip\ell}|\ell\rangle \\ &= \sum_{\ell\in 2\mathbb{Z}} \left(i\frac{\theta_1(u)}{\theta_4(u)}\right)^{\ell} |\ell\rangle + \sum_{\ell\in 2\mathbb{Z}+1} \frac{\theta_2(u)}{\theta_3(u)} \left(i\frac{\theta_1(u)}{\theta_4(u)}\right)^{\ell} |\ell\rangle \,. \end{aligned} \tag{5.18}$$

The reduced energy is also rather simple to express in terms of theta functions

$$E'(u) = -i\frac{\theta_4(0)^2}{\theta_2(0)\theta_3(0)}\frac{\theta_2(u)\theta_3(u)}{\theta_1(u)\theta_4(u)} \,, \tag{5.19}$$

and given the relation

$$\kappa^2 = k = \sqrt{m} = \left(\frac{\theta_2(0)}{\theta_3(0)}\right)^2 \,, \tag{5.20}$$

the energy shift $E(0)-E'(0) = \kappa+1/\kappa$ of the total energy $E(u)$ can also be expressed in terms of theta functions. Finally, the $\mathbb{Z}_2$ eigenvalue of the 1-magnon solution is (3.18)

$$\mathbb{Z}_2\,|p\,\rangle = \frac{\theta_3(u)}{\theta_2(u)}\,|p\,\rangle. \tag{5.21}$$

Similarly, for the two magnon eigenproblem, we can express the wavefunctions (for the CoM, general and restricted solutions) and their energy and $\mathbb{Z}_2$ eigenvalues (summarised in Table 3.1) in terms of theta functions. Even though we derived these solutions by explicitly solving the coordinate Bethe ansatz, we could have attempted to guess the wavefunctions simply by knowing their eigenvalues and modular properties. It is possible that this point of view will be helpful in the solution of the multi-magnon problem and also in the study of more general quiver orbifold eigenproblems, which is a future research topic.

Chapter 6

TOWARDS THE THREE MAGNON SOLUTION

In this chapter, we will discuss the three magnon problem. Even though its solution has not yet been constructed, we can make several interesting comments that may be useful towards eventually constructing the wavefunctions. Being able to solve this problem is one way to answer the question of integrability (see the definition around equation (2.75)) for the $\mathcal{N} = 2$ scalar sectors that we studied in previous chapters.

Generalising the methods for the two magnon case, one can easily show that the non-interacting equations for three magnons are solved by $E(p_1, p_2, p_3) = E(p_1) + E(p_2) + E(p_3)$.

Momenta

In order to construct wavefunctions that solve the system of two magnon equations for both the XY sector and the XZ sector, we required an extra set of momenta $\{k_1, k_2\}$ and its permutation. Most importantly, the construction of the two magnon solution is achievable due to the existence of two conserved charges

$$\mathfrak{M}_1 = K, \quad \mathfrak{M}_2 = E. \tag{6.1}$$

In the case of Section 2.2.2 and Section 2.2.3, the quadratic nature of E_2 leads to the only possible two magnon momenta being $\{p_1, p_2\}$ and $\{p_2, p_1\}$. In the case of the XY and XZ sectors of this thesis, the square root nature of E_2 leads to the momenta described above and permutations: $\{p_1, p_2\}$, $\{p_2, p_1\}$, $\{k_1, k_2\}$, $\{k_2, k_1\}$. Importantly, up to periodicities in equation (3.51), these new sets of momenta are completely specified by an initial set of momenta thanks to the conserved charges $\mathfrak{M}_1, \mathfrak{M}_2$. In other words, given an initial set of real momenta $\{p_1, p_2\}$, we were able to explicitly determine $\{k_1, k_2\}$ through equation (3.51) such that $k_1 = k_1(p_1, p_2, \kappa)$ and $k_2 = k_2(p_1, p_2, \kappa)$.

For the three magnon case, things can be more complicated. In the case of the ferromagnetic Heisenberg model of Section 2.2.2, a higher third charge $\mathfrak{M}_3$ exists (in fact, a tower of higher conserved charges exist due to quantum integrability (2.75); for an explicit construction see [49]). Together, the three conserved charges constrain an initial set of incoming momenta $\{p_1, p_2, p_3\}$ to a set of outgoing

momenta that is only a permutation of the initial set. This solves the system of equations for the three magnon case. In contrast, the spin-1 model of Section 2.2.3 was not integrable since it exhibits diffractive scattering. Consequently, there is no higher conserved charge and an initial incoming set of momenta can lead to an outgoing set of momenta that is not a permutation of the initial set. Most notably, unlike the description of the extra momenta given in the previous paragraph, this new set of momenta is not uniquely determined by the initial set of momenta $\{p_1, p_2, p_3\}$ since it is only constrained by $\mathfrak{M}_1$ and $\mathfrak{M}_2$.

For our case for the XY and XZ sectors, without knowledge of the existence of a higher order charge, we cannot determine whether new extra sets of momenta, unique to the three magnon case (in other words, momenta not determined by two magnon data), are needed to solve the system of three magnon equations (at least in terms of using the same approach as in the two magnon case). However, a first step towards a solution is to try and write down all legal sets of three momenta, permitted by $\mathfrak{M}_1$ and $\mathfrak{M}_2$, using two magnon interactions. Then, using the compact notation $k_i(p_j, p_k) \equiv k_i^{jk},\ i = 1, 2,\ j, k = 1, 2, 3$, the allowed sets of momenta are (we suppress the κ dependence of the k-momenta)

$$\begin{aligned} &1)\ \{p_1, p_2, p_3\}, \\ &2)\ \{k_1^{12}, k_2^{12}, p_3\}, \\ &3)\ \{k_1^{13}, p_2, k_2^{13}\}, \\ &4)\ \{p_1, k_1^{23}, k_2^{23}\}, \end{aligned} \tag{6.2}$$

and their permutations, in other words, $\{k_1^{12}, k_2^{12}, p_3\},\ \{k_2^{12}, k_1^{12}, p_3\},\ \{k_1^{12}, p_3, k_2^{12}\}$ and so forth. Note that the $k-$momenta are symmetric: $k_i^{jk} = k_i^{kj}$. In total, this brings the number of possible terms in the wavefunctions to 24. Physically, all the $k-$momenta can be accounted for by two body scattering processes as shown in Figure 6.1. Considering the left hand side of the figure which exhibits the sequence $(12) - (13) - (23)$ for example (see also Figure 2.3), we can scatter $\{p_1, p_2, p_3\}$ to give the two sets $\{p_2, p_1, p_3\}$ and $\{k_1^{12}, k_2^{12}, p_3\}$. Then, we can scatter $\{p_2, p_1, p_3\}$ to give the sets $\{p_2, p_3, p_1\}$ and $\{p_1, k_1^{13}, k_2^{13}\}$. Finally, we can scatter $\{p_2, p_3, p_1\}$ to give the sets $\{p_3, p_2, p_1\}$ and $\{k_1^{23}, k_2^{23}, p_1\}$. The right hand side of the figure is similar.

From the process described in the previous paragraph, we still need to consider the scattering of the $k-$momenta with p_3 for the set $\{k_1^{12}, k_2^{12}, p_3\}$ (and similar for the sets $\{p_2, k_1^{13}, k_2^{13}\}$ and $\{k_1^{23}, k_2^{23}, p_1\}$). One may notice that scattering two momenta

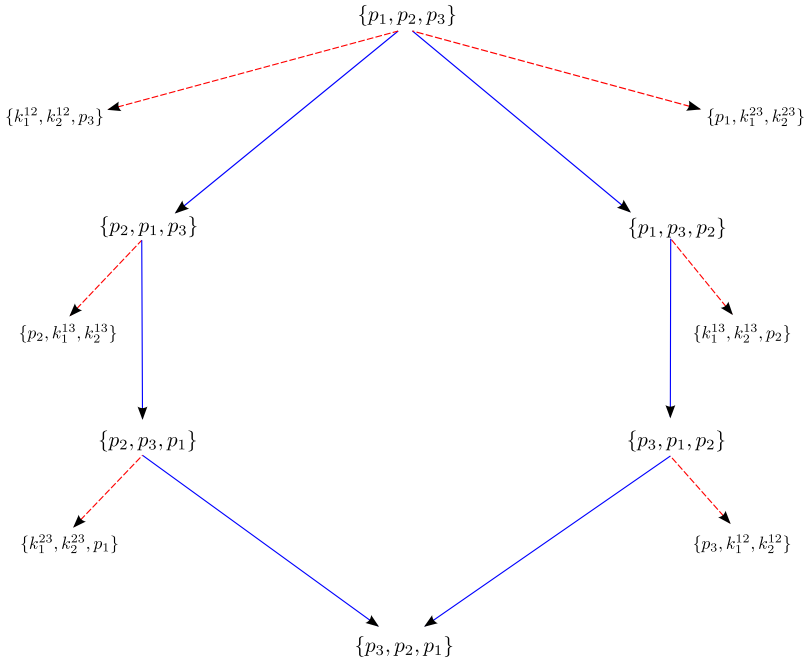

Figure 6.1: *A subset of the possible sets of momenta for the three magnon case. Each set will correspond to a Bethe-term in the wavefunctions. Each scattering of two momenta produces a complementary set of $k-$momenta.*

is always complemented with an extra set of momenta. If we consider scattering k_2^{12} with p_3, we may write the extra set of momenta as

$$\{k_1^{12}, k_1(k_2^{12}, p_3), k_2(k_2^{12}, p_3)\}. \tag{6.3}$$

If k_2^{12} is real-valued (see the discussion in Section 3.2.2), then $k_1(k_2^{12}, p_3)$ and $k_2(k_2^{12}, p_3)$ yields momenta that satisfy $\mathfrak{M}_1$ and $\mathfrak{M}_2$. If k_2^{12} is complex-valued, one finds that $E_A(k_1^{12}) + E_A\left(k_1(k_2^{12}, p_3)\right) + E_A\left(k_2(k_2^{12}, p_3)\right) \neq E_A(p_1) + E_A(p_2) + E_A(p_3)$ where A denotes the acoustic branch. This can be resolved by considering, instead of the acoustic branch, the optical branch for one of the $k-$momenta. One can then continue iterating this process and checking if the momenta satisfy $\mathfrak{M}_1$ and $\mathfrak{M}_2$. It is an ongoing research question whether this iteration eventually terminates, in other words, one starts generating the same sets of momenta and one needs to add a finite number of Bethe-terms to each wavefunction; or, if it carries on indefinitely and one has to add a countably infinite number of Bethe-terms to each wavefunction. Note that this approach will also yield the remaining permutation terms mentioned above (for example, terms such as $\{k_1^{13}, p_2, k_2^{13}\}$).

Interestingly, there is another approach in terms of generating new momenta for the three magnon case using two magnon data. Starting with an initial set $\{p_1, p_2, p_3\}$,

we can generate a new set of $k-$momenta as follows

$$p_1 + p_2 + p_3 = k_1(p_1 + p_2, p_3) + k_2(p_1 + p_2, p_3). \tag{6.4}$$

We can decompose $k_1(p_1 + p_2, p_3)$ into two momenta by forcing energy conservation. More precisely, for a fixed $E(p_1, p_2, p_3)$,

$$\begin{aligned}
&E(p_1, p_2, p_3) \\
&= E(p_1) + E(p_2) + E(p_3) \\
&= E\left(k_1(p_1 + p_2, p_3)\right) + E\left(k_2(p_1 + p_2, p_3)\right) \\
&= \left[E(k_+) + E(k_-)\right]|_{k_+ + k_- = k_1(p_1+p_2,p_3)} + E(k_2(p_1 + p_2, p_3)) \\
&\Rightarrow \left[E(k_+) + E(k_-)\right]|_{k_+ + k_- = k_1(p_1+p_2,p_3)} = E(p_1, p_2, p_3) - E\left(k_2(p_1 + p_2, p_3)\right).
\end{aligned} \tag{6.5}$$

Here, k_+, k_- are the decompositions of $k_1(p_1 + p_2, p_3)$, in other words, $k_1(p_1 + p_2, p_3) = k_+ + k_-$. The sum of their energies are constrained by the last line, which is known for a given $\{p_1, p_2, p_3\}$. To get k_+, k_-, we can use equation (3.48). We substitute $K = k_+ + k_- = k_1(p_1 + p_2, p_3)$ and $E_2 = E(k_+) + E(k_-) = E(p_1, p_2, p_3) - E\left(k_2(p_1 + p_2, p_3)\right)$. Then, we find $k_+ = (1/2)K + q = (1/2)k_1(p_1 + p_2, p_3) + q$ and $k_- = (1/2)K - q = (1/2)k_1(p_1 + p_2, p_3) - q$. As before, because of the $\pm$ in the equation (3.48), we actually find four solutions for q. In addition to these new momenta, one may also permute the p-momenta to combine $p_1 + p_3$ with p_2 and $p_2 + p_3$ with p_1 to generate more k_+, k_--momenta.

Thus, we have found new sets of new momenta that are given by $\{k_+, k_-, k_3\}$ where $k_3 = k_2(p_1 + p_2, p_3)$. Unlike the $k_1(p_i, p_j)$ and $k_2(p_i, p_j)$ momenta, the $k_\pm, k_3$ momenta are functions of all three initial momenta. It is interesting to perform a numerical comparison of all the momenta: for $p_1 = 0.8, p_2 = 0.6, p_3 = 0.3, \kappa = 0.7$, we find

$$\begin{array}{lll}
p_1 = 0.800000, & p_2 = 0.600000, & p_3 = 0.300000, \\
k_1^{12} = 2.2708 - 0.652047i, & k_2^{12} = -0.870796 + 0.652047i, & p_3 = 0.300000, \\
k_1^{13} = 2.1208 - 1.10513i, & k_2^{13} = -1.0208 + 1.10513i, & p_2 = 0.600000, \\
k_1^{23} = 2.0208 - 1.4125i, & k_2^{23} = -1.1208 + 1.4125i, & p_1 = 0.800000, \\
k_+^a = 2.36896 - 0.28928i, & k_-^a = -0.772636 + 0.28928i, & k_3^a = 0.103679, \\
k_+^b = 0.798161 + 0.38501i, & k_-^b = 0.798161 - 0.38501i, & k_3^b = 0.103679.
\end{array}$$

All the above numbers satisfy momentum and energy conservation in the acoustic-acoustic-acoustic continuum (in other words, we used the lower branch of the three magnon energy dispersion relation to compute these results). The new momenta are given by the sets $\{k_+^a, k_-^a, k_3^a\}$, $\{k_+^b, k_-^b, k_3^b\}$. Observe that the set $\{k_+^b, k_-^b, k_3^b\}$

appears as a bound state between k_+^b and k_-^b (with the momentum k_3^b being a magnon) since it has the same real parts (unlike the resonant states whose real parts differ by π). The appearance of a bound state in the continuum (BIC) [79, 80, 81, 82, 83] is fascinating and warrants further investigation [1]. The above numerical results clearly show that $\{k_+^a, k_-^a, k_3^a\}$ and $\{k_+^b, k_-^b, k_3^b\}$ are new sets of momenta.

It is clear that, apart from the 24 sets of momenta listed above, one may generate a large amount of new sets of momenta that satisfy $\mathfrak{M}_1$ and $\mathfrak{M}_2$. As mentioned, one would need to determine if these extra sets of momenta terminate after iterations by returning to an already generated set of momenta. This leads to technical difficulties when trying to solve the two-particle scattering sector (which is the sector consisting of scattering two particles with the third particle being free) of the three magnon system.

Quantum Integrability

In Section 2.2.2 following [46], we presented the definition of quantum integrability through equation (2.75). The definition is a statement made at the three spin deviation level. We presented two examples of spin chain models in Sections 2.2.2, 2.2.3 that are, respectively, integrable and non-integrable, by solving their three spin deviation problem. In particular, the spin-1 model of Section 2.2.3 exhibited diffractive scattering where the incoming set of momenta $\{p_1, p_2, p_3\}$ is scattered to an outgoing set of momenta $\{k_1, k_2, k_3\}$ that is not a permutation of the original set.

In the XY and XZ sectors studied in this thesis, we already have diffractive terms appearing at the two spin deviation level. As mentioned in the discussion around equation (2.75), the two spin deviation problem is insensitive to integrability as it can always be solved. The three magnon wavefunctions, as discussed in the previous paragraphs, already have many different sets of diffractive momenta coming from the two magnon data and not from true three-particle diffractive scattering. This makes it more difficult to use Sutherland's definition [46] for integrability which is a statement about three-particle diffraction.

Due to the interesting similarities in equations (3.62), (4.53) and the non-integrable spin-1 model of [47] studied in Section 2.2.3, one may hope to generalise the method

[1] It is also interesting to note that for the Hubbard model studied in [80, 81, 82], it is found that the model's Hilbert space decomposes into two sectors, with one sector constructed out of Bethe-terms and the other sector constructed out of diffractive terms. The two sectors are related by $\mathbb{Z}_2$ symmetry.

used in [47] to our three magnon case. However, there is evidence that associativity is lost for spin chains that appear in our $\mathcal{N} = 2$ interpolating theory. For the spin chains studied in [18], using the Z fields as the vacua with X fields as excitations, it was found that the Yang-Baxter equation was not satisfied for the interpolating theory due to the existence of two XXZ S-matrices S and $\tilde{S}$ (related by $\mathbb{Z}_2$ symmetry). More precisely, the scattering sequence $(12) - (13) - (23)$ and $(23) - (13) - (12)$ leads to a violation of the Yang-Baxter equation for the interpolating $\mathcal{N} = 2$ theory

$$S\tilde{S}S \neq \tilde{S}S\tilde{S}. \tag{6.6}$$

This is indicative of broken associativity since the scattering order matters. Consequently, this leads to the two-particle scattering sector of the three magnon system already not being satisfied (for example, a solution of the first scattering sequence will not be a solution for the second scattering sequence and vice versa). In contrast, in the case of [47], the two-particle scattering sector of the three magnon case was already solved by the Bethe-terms in equation (2.100) and only failed when considering the three-particle equations (which is where three-particle diffractive scattering is needed). Thus, the method of [47] is difficult to generalise to our case until we can find a solution for our two-particle/one-free scattering sector.

Now, in terms of Sutherland's definition for integrability given by equation (2.75), an important fact to note is that the three spin deviation solution (and the general spin deviation solution) can be solved completely in terms of the data (such as the S-matrices) from the two spin deviation solution. For a non-integrable system, the three spin deviation problem needs to be solved on its own merit. Adding more spin deviations would mean one has to solve the system again to compute the new diffractive terms. The fact that, for integrable spin chains, one can solve the general spin deviation problem by two spin deviation data is a strong sign of integrability and it has the benefit that it momentarily avoids the discussion of diffractive scattering.

Therefore, despite the subtleties discussed in the previous paragraphs for our spin chains concerning diffractive scattering and loss of associativity, a first step for checking evidence of integrability in our system using the coordinate Bethe ansatz, is to check whether the three spin deviation solution can be solved completely in terms of two spin deviation data (which would include different factorised products of the two S-matrices and the application of equation (3.48)). More precisely, if a complete solution of the two-particle/one-free scattering sector can be found which is also a solution of the three-particle scattering sector, then this will provide some positive evidence of integrability.

Supposing a solution of this form can be found (if not, the system would be non-integrable), one can then compare the solution to the definition given by equation (2.75) in terms of diffractive scattering. In this chapter, we have shown that one can generate valid Bethe terms with sets of three momenta that are different from an initial set of three momenta using equation (3.48)). If one considers three-particle diffraction to be the case where an incoming set of three momenta is scattered to an outgoing set of different three momenta (in other words, not a permutation of the original set), then the solution would violate Sutherland's definition and the system would not be integrable (despite the three spin deviation system hypothetically being solved by the two spin deviation data). Alternatively, if one considers diffraction as a true three-particle process (and similar for higher spin deviations), in the sense that the diffractive term in equation (2.75) cannot be decomposed to a process of two-particle interactions (which in our case would include two-particle diffraction) and that scatters an incoming set of three momenta to an outgoing set of different three momenta, then the system would be integrable under Sutherland's definition.

For the problem of associativity, it is also possible that the three spin deviation wave-functions will need to include extra terms, which may be additive or multiplicative, to account for the loss of associativity and that these terms are unique to the three spin deviation case (in other words, it is not information from the two spin deviation solution). These terms will be non-local information about the three spin deviation scattering and are of course different from the scattering condition in Sutherland's definition. Thus, if these terms are needed, it is an interesting research question as to how these terms affect Sutherland's definition for integrability.

For further checks of integrability for our spin chains, it also worth mentioning the techniques used in [84, 85]. The construction of higher conserved charges provides good evidence of integrability. In [84, 85], one can start with a Hamiltonian, which is the sum of nearest-neighbour interactions, and use a boosting procedure to try to generate a conserved charge with next-to-nearest neighbour interaction range. In particular, their procedure has the benefit of using the Hamiltonian instead of the R-matrix (which may or may not be known) to generate higher conserved charges. This approach is particularly attractive for the XY sector which has a simple alternating-bond structure. Another possible approach is given in [86], in which integrable models with longer range interactions are studied. There is some early tentative evidence that the XZ sector's dynamical Hamiltonian may be written as a non-dynamical next-to-nearest neighbour Hamiltonian. It may therefore be possible

to apply the conjecture given in [86] to check for evidence of integrability.

Finally, a very promising approach using the algebraic Bethe ansatz is discussed in [27]. In particular, there is some evidence that a special class of elliptic R-matrices, that satisfies a dynamical Yang-Baxter equation (see (4.11) in [27] as well as [24, 25]), have an important role to play in our system. These structures, and more broadly quasitriangular quasi-Hopf algebras, are well-suited to deal with spin chain models that have lost associativity by using an algebraic structure called a coassociator (see the review [87] as well as [21, 22, 23]) that relaxes associativity in a controlled manner. Constructing the correct elliptic R-matrix that yields the Hamiltonians for our sectors in the quantum plane limit may shed light on the technical issues concerning the construction of the three magnon wavefunctions for the coordinate Bethe ansatz.

Chapter 7

CONCLUSION

As shown in this thesis, the scalar sector of orbifold $\mathcal{N} = 2$ quiver theories yields spin chain models that exhibits rich physics through the coordinate Bethe ansatz. We have studied two scalar sectors constructed out of fields from the $\mathcal{N} = 2$ vector multiplet and the $\mathcal{N} = 2$ hypermultiplet. Unlike the $\mathfrak{su}(2)$ subsector in $\mathcal{N} = 4$ SYM, their is no symmetry that rotates the fields from one multiplet to another multiplet as they are in different representations of the quiver gauge groups.

The XY sector, constructed out of scalar fields in the bifundamental of each gauge sector, can be mapped to an alternating-bond spin chain with Heisenberg-type Hamiltonian. This is due to the fact that it is considered dense, since the dynamical parameter is shifted as one moves from one site to the next. The one magnon problem is easily solved using a superposition of even and odd site wavefunctions. The dispersion relation has the interesting form given by equation (3.14). In addition, the XY sector is characterized by its ratio function which is given by equation (3.13).

The two magnon problem was first solved for the CoM case using contact terms for nearest-neighbour sites. When solving the interacting equations, the contact terms vanish from the CoM S-matrix, which is given in equation (3.36). However, to be able to ultimately construct three magnon wavefunctions, one needs the two magnon solution for general values of the total momenta. In addition, the origin of the contact terms needed to solve the interacting equations was mysterious. In order to solve the two magnon problem for the general case, we made use of the techniques used in [52, 67, 68]. Using equation (3.50), we are able to show that, given an initial set of momenta $\{p_1, p_2\}$, there exists another set of momenta $\{k_1, k_2\}$ that satisfies the same momentum and energy conserved charges (6.1). This enhanced the usual two magnon Bethe wavefunction from two terms to four terms, which was sufficient to solve the system of equations for the two magnon problem. Since these new momenta are not a permutation of the original set of momenta, the two magnon system already exhibits diffractive scattering. Furthermore, the wavefunctions contains two S-matrices, namely, S for scattering inside the p-momenta sector or the k-momenta sector and T for scattering a set of $p-$momenta to a set of $k-$momenta. The properties and the limits of the $S-$matrices were studied in detail. Due to the extra

set of momenta, the wavefunctions was also shown to have extra symmetry as stated in Table 3.1. The general wavefunctions have to be restricted when imposing the infinite length spin chain boundary condition or when considering the CoM case. This is due to the fact that the $k-$momenta are generically complex-valued. This resulted in the restricted solution given in Section 3.2.3, which is also the minimal number of terms needed to solve the two magnon system of equations. The restricted wavefunctions was shown to reduce precisely to the contact term solutions for the CoM case we originally found, thus, clarifying the origin of the contact terms. Finally, we stated the Bethe ansatz for a closed spin chain for the untwisted sector given in equation (3.120) and the twisted sector given in equation (3.122).

We then studied the XZ sector which is constructed out of scalar fields in the adjoint of one of the gauge groups and scalar fields in the bifundamental of each gauge group. The resulting Hamiltonians are of Temperley-Lieb type. In contrast to the XY sector, the XZ sector is dilute since crossing a Z field does not shift the dynamical parameter and, thus, the sector cannot be mapped to an alternating-bond spin chain model. Remarkably, despite the difference, the dispersion relation is exactly the same as the XY sector's dispersion relation. The ratio function, given in equation (4.18), is also different to the analogous ratio function of the XY sector. However, we showed in equation (5.11) that these functions are related by a modular transformation. The fact that the two sectors share the same dispersion relation and have ratio functions related by a modular transformation warrants further investigation. Furthermore, given these facts, we were able to solve the two magnon problem for the XZ sector in exactly the same manner as the XY sector.

The *shifted* dispersion relation E' in Chapter 5, shared by the two scalar sectors, can be naturally parametrised using elliptic functions. There are two choices for the modular parameter. For the XY sector, a natural choice is given by $m = \kappa^4$. For the XZ sector, a natural choice is given by $\tilde{m} = 4\kappa^2/(1+\kappa^2)^2$. Using these modular parameters, we showed how the ratios and the dispersion relations simplified when using Jacobi functions as well as theta functions. However, it should be noted that the parametrisation we used was more appropriate for an XX-model [45] since we considered the shifted dispersion relation E'. We expect better simplification, especially when considering the elliptic version of the S-matrices, once we compute the appropriate parametrisation for E.

The three magnon wavefunction was discussed in Chapter 6. Using the two magnon solution, we argued that the amount of possible terms one could add to the three

magnon wavefunctions can in principle grow very large. We also showed that we can generate a three magnon set of $k-$momenta $\{k_+, k_-, k_3\}$, using only two magnon data from equation (3.50), that contributes a new solution. In its spectrum, we also find a bound state in the continuum which warrants deeper investigation.

Finally, we provided a discussion around the notion of quantum integrability for these sectors. Constructing the correct three magnon wavefunctions is a possible approach to determining if quantum integrability is present for these theories, despite the appearance of diffractive scattering terms already at the two magnon level.

A promising alternative is the algebraic Bethe ansatz approach discussed in [27], where it is argued that an elliptic quantum group captures the symmetry behaviour of the interpolating theory and that the quantum Yang-Baxter equation is enhanced to a dynamical Yang-Baxter equation. More precisely, the $SU(3)$ scalar holomorphic sector can be mapped to a dynamical 15 vertex model which can also be written as a class of restricted solid-on-solid (RSOS) type statistical models. This fact hints at a general link between quiver theories and statistical models which, regardless of any integrable/solvable structures, is worth understanding in more detail since it may provide deeper insights into SCFTs. Furthermore, through the algebraic Bethe ansatz, the R-matrix must lead to the same eigenvectors and eigenvalues that were determined through the coordinate Bethe ansatz in this thesis. Thus, the results in this thesis provides some of the groundwork and guidance for constructing the correct R-matrix for the algebraic Bethe ansatz.

From a more general perspective, since we have only studied scalar fields in two closed subsectors of the theory, it would be interesting to attempt to extend our results to larger subsectors and even to the full scalar sector. Similar to the $SU(2|3)$ subsector of $\mathcal{N} = 4$ SYM [43], for example, the Cartan charges for larger subsectors could involve the addition of fermionic fields. Furthermore, a fascinating avenue of research is to continue beyond the $\mathbb{Z}_2$ quiver theory and study the spin chains that appear in more general $\mathbb{Z}_k$ orbifolds. In terms of extending our spin chain results, an interesting topic would be to determine how much additional momenta are needed for the analogous spin chains. For example, the $\mathbb{Z}_3$ orbifold will, of course, have three gauge couplings g_1, g_2, g_3 (see Section 2.4). In this case, for a Z excitation in the X vacuum, the dispersion relation is cubic

$$E^3 - 2E^2\left(g_1^2 + g_2^2 + g_3^2\right) + 3E\left(g_1^2 g_2^2 + g_1^2 g_3^2 + g_2^2 g_3^2\right) + 2g_1^2 g_2^2 g_3^2\left(\cos(3p) - 1\right) = 0, \tag{7.1}$$

compared to equation (4.19) which is the solution of a quadratic equation. Finally, since the work in this thesis is at one-loop, it would also be interesting to study the resulting spin chains at higher loops which would lead to longer range (such as next-to-nearest neighbour) Hamiltonians.

Ultimately, we hope that, by unraveling some of the structures that appear in our study of the spin chain models that arise in $\mathcal{N} = 2$ quiver theories, our results could be a stepping stone towards a better understanding of the spectral problem in a much larger class of theories than $\mathcal{N} = 4$ super Yang-Mills theory.

Appendix A

SUPERCONFORMAL ALGEBRA

In this appendix, we state the superconformal algebra in (1+3)-dimensions following the conventions in [33]. The Minkowski metric has signature $\eta_{\mu\nu}$ = diag(-1,1,1,1) where $\mu, \nu = 0, 1, 2, 3$. The conformal algebra is generated by the Poincare generators $\{P_\mu, M_{\mu\nu}\}$ (where P_μ generates spacetime translations and the antisymmetric Lorentz generator $M_{\mu\nu}$ generates rotations and boosts) enhanced with the conformal generators $\{K_\mu, D\}$. The K_μ, called the special conformal generator, generates a spacetime translation, preceded and followed by an inversion (see [56]). The generator D, called the dilatation generator, generates scalings. Together, these generators form the following algebra [33]

$$\begin{aligned}
&[M_{\mu\nu}, P_\rho] = i\eta_{\mu\rho}P_\nu - i\eta_{\nu\rho}P_\mu, \quad [M_{\mu\nu}, K_\rho] = i\eta_{\mu\rho}K_\nu - i\eta_{\nu\rho}K_\mu, \\
&[M_{\mu\nu}, M_{\rho\sigma}] = i\eta_{\mu\rho}M_{\nu\sigma} - i\eta_{\nu\rho}M_{\mu\sigma} + i\eta_{\nu\sigma}M_{\mu\rho} - i\eta_{\mu\sigma}M_{\nu\rho}, \\
&[D, P_\mu] = iP_\mu, \quad [D, K_\mu] = -iK_\mu, \quad [K_\mu, P_\nu] = -2iM_{\mu\nu} - 2i\eta_{\mu\nu}D.
\end{aligned} \tag{A.1}$$

By increasing the spacetime dimension to (2+3)-dimensions (in other words, adding another time dimension), we can write the conformal algebra more compactly. The metric becomes $\eta_{\mathcal{I}\mathcal{J}}$ = diag$(-1, 1, 1, 1, -1)$ where $\mathcal{I}, \mathcal{J} = 0, 1, 2, 3, 4$. Defining the antisymmetric generator $L_{\mathcal{I}\mathcal{J}}$ by

$$L_{\mu\nu} = M_{\mu\nu}, \quad L_{\mu d} = -\frac{1}{2}\left(P_\mu - K_\mu\right), \quad L_{\mu d+1} = -\frac{1}{2}\left(P_\mu + K_\mu\right), \quad L_{dd+1} = D, \tag{A.2}$$

or in matrix form,

$$L_{\mathcal{I}\mathcal{J}} = \begin{pmatrix} M_{\mu\nu} & -\frac{1}{2}\left(P_\mu - K_\mu\right) & -\frac{1}{2}\left(P_\mu + K_\mu\right) \\ \frac{1}{2}\left(P_\nu - K_\nu\right) & 0 & D \\ \frac{1}{2}\left(P_\nu + K_\nu\right) & -D & 0 \end{pmatrix}. \tag{A.3}$$

This mapping satisfies the algebra

$$[L_{\mathcal{I}\mathcal{J}}, L_{\mathcal{M}\mathcal{N}}] = i\eta_{\mathcal{I}\mathcal{M}}M_{\mathcal{J}\mathcal{N}} - i\eta_{\mathcal{J}\mathcal{M}}M_{\mathcal{I}\mathcal{N}} + i\eta_{\mathcal{J}\mathcal{N}}M_{\mathcal{I}\mathcal{M}} - i\eta_{\mathcal{I}\mathcal{N}}M_{\mathcal{J}\mathcal{M}}, \tag{A.4}$$

which implies that the conformal algebra corresponds to $\mathfrak{so}(3, 2)$ [33][56].

The conformal algebra is enhanced with a set of fermionic supergenerators

$$\{Q^A_{\ \alpha}, \bar{Q}_{A\dot{\alpha}}, \mathcal{S}_B^{\ \alpha}, \bar{\mathcal{S}}^{B\dot{\alpha}}\}, \tag{A.5}$$

where $A, B = 1, .., \mathcal{N}$ and spinor indices $\alpha, \dot{\alpha}$ take values $\alpha, \dot{\alpha} = \pm$. The superconformal algebra $\mathfrak{su}(2,2|\mathcal{N})$ is given by

$$
\begin{aligned}
&\left[M_\alpha^{\ \beta}, M_\gamma^{\ \delta}\right] = \delta_\gamma^{\ \beta} M_\alpha^{\ \delta} - \delta_\alpha^{\ \delta} M_\gamma^{\ \beta}, \quad \left[\bar{M}_{\dot\beta}^{\ \dot\alpha}, \bar{M}_{\dot\delta}^{\ \dot\gamma}\right] = -\delta_{\dot\delta}^{\ \dot\alpha}\bar{M}_{\dot\beta}^{\ \dot\gamma} + \delta_{\dot\beta}^{\ \dot\gamma}\bar{M}_{\dot\delta}^{\ \dot\alpha} \\
&\left[M_\alpha^{\ \beta}, Q_\gamma^A\right] = \delta_\gamma^{\ \beta} Q_\alpha^A - \frac{1}{2}\delta_\alpha^{\ \beta} Q_\gamma^A, \quad \left[\bar{M}_{\dot\beta}^{\ \dot\alpha}, \bar{Q}_{A\gamma}\right] = -\delta_{\dot\gamma}^{\ \dot\alpha}\bar{Q}_{A\dot\beta} + \frac{1}{2}\delta_{\dot\beta}^{\ \dot\alpha}\bar{Q}_{A\dot\gamma}, \\
&\left[M_\alpha^{\ \beta}, \mathcal{S}_A^{\ \gamma}\right] = -\delta_\alpha^{\ \gamma}\mathcal{S}_A^{\ \beta} + \frac{1}{2}\delta_\alpha^{\ \beta}\mathcal{S}_A^{\ \gamma}, \quad \left[\bar{M}_{\dot\beta}^{\ \dot\alpha}, \bar{\mathcal{S}}^{A\dot\gamma}\right] = \delta_{\dot\beta}^{\ \dot\gamma}\bar{\mathcal{S}}^{A\dot\alpha} - \frac{1}{2}\delta_{\dot\beta}^{\ \dot\alpha}\bar{\mathcal{S}}^{A\dot\gamma}, \\
&\left[D, Q_\alpha^A\right] = \frac{i}{2}Q_\alpha^A, \quad \left[D, \bar{Q}_{A\dot\alpha}\right] = \frac{i}{2}\bar{Q}_{A\dot\alpha}, \quad \left[D, \mathcal{S}_A^{\ \alpha}\right] = -\frac{i}{2}\mathcal{S}_A^{\ \alpha}, \\
&\left[D, \bar{\mathcal{S}}^{A\dot\alpha}\right] = -\frac{i}{2}\bar{\mathcal{S}}^{A\dot\alpha}, \quad \left[K_\mu, Q_\alpha^A\right] = -\sigma_{\mu\alpha\dot\alpha}\bar{\mathcal{S}}^{A\dot\alpha}, \\
&\left[K_\mu, \bar{Q}_{A\dot\alpha}\right] = \mathcal{S}_A^{\ \alpha}\sigma_{\mu\alpha\dot\alpha}, \quad \left[P_\mu, \bar{\mathcal{S}}^{A\dot\alpha}\right] = -\bar{\sigma}_\mu^{\ \dot\alpha\alpha} Q_\alpha^A, \\
&\left[P_\mu, \bar{\mathcal{S}}^{A\dot\alpha}\right] = \bar{Q}_{A\dot\alpha}\bar{\sigma}_\mu^{\ \dot\alpha\alpha}, \quad \{Q_\alpha^A, \bar{Q}_{B\dot\alpha}\} = 2\delta_B^A P_{\alpha\dot\alpha}, \\
&\{Q_\alpha^A, Q_\beta^B\} = \{\bar{Q}_{A\dot\alpha}, \bar{Q}_{B\dot\beta}\} = 0, \quad \{\bar{\mathcal{S}}^{A\dot\alpha}, \mathcal{S}_B^{\ \alpha}\} = 2\delta_B^A K^{\dot\alpha\alpha}, \\
&\{\bar{\mathcal{S}}^{A\dot\alpha}, \bar{\mathcal{S}}^{B\dot\beta}\} = \{\mathcal{S}_A^{\ \alpha}, \mathcal{S}_B^{\ \beta}\} = 0, \quad \{Q_\alpha^A, \bar{\mathcal{S}}^{A\dot\alpha}\} = 0, \\
&\{\mathcal{S}_A^{\ \alpha}, \bar{Q}_{B\dot\alpha}\} = 0, \quad \{Q_\alpha^A, \mathcal{S}_B^{\ \beta}\} = 4\left(\delta_B^A\left(M_\alpha^{\ \beta} - \frac{1}{2}i\delta_\alpha^{\ \beta}D\right) - \delta_\alpha^{\ \beta}R_\beta^{\ A}\right), \\
&\{\bar{\mathcal{S}}^{A\dot\alpha}, \bar{Q}_{B\dot\alpha}\} = 4\left(\delta_B^A\left(\bar{M}_{\dot\beta}^{\ \dot\alpha} + \frac{1}{2}i\delta_{\dot\beta}^{\ \dot\alpha}D\right) - \delta_{\dot\beta}^{\ \dot\alpha}R_\beta^{\ A}\right),
\end{aligned}
\tag{A.6}
$$

where we have used the bispinorial basis which maps objects with spacetime indices to $\mathfrak{sl}(2)$ matrices [88]

$$
\begin{aligned}
&P_{\alpha\dot\alpha} = \sigma_{\alpha\dot\alpha}^{\ \mu} P_\mu, \quad K^{\dot\alpha\alpha} = \bar{\sigma}^{\mu\dot\alpha\alpha} K_\mu, \\
&M_\alpha^{\ \beta} = -\frac{i}{4}(\sigma^\mu\bar{\sigma}^\nu)_\alpha^{\ \beta} M_{\mu\nu}, \quad \bar{M}_{\dot\beta}^{\ \dot\alpha} = -\frac{i}{4}(\bar{\sigma}^\mu\sigma^\nu)_{\dot\beta}^{\ \dot\alpha} M_{\mu\nu}.
\end{aligned}
\tag{A.7}
$$

Explicitly, the basis is given by

$$
\begin{aligned}
&\sigma_{\alpha\dot\alpha}^{\ \mu} = \left(-\mathbb{1}, \sigma^i\right), \\
&\bar{\sigma}^{\mu\dot\alpha\alpha} := \epsilon^{\dot\alpha\dot\beta}\epsilon^{\alpha\beta}\sigma_{\beta\dot\beta}^{\ \mu} = \left(-\mathbb{1}, -\sigma^i\right), \quad i = 1, 2, 3,
\end{aligned}
\tag{A.8}
$$

where $\epsilon^{\alpha\beta}$ and $\epsilon^{\dot\alpha\dot\beta}$ are the totally antisymmetric tensors with $\epsilon_{21} = \epsilon^{12} = 1$ and $\epsilon_{\dot2\dot1} = \epsilon^{\dot1\dot2} = 1$.

In addition, we have the $U(\mathcal{N})$ R-symmetry

$$
\left[R_B^{\ A}, R_D^{\ C}\right] = \delta_B^{\ C} R_D^{\ A} - \delta_D^{\ A} R_B^{\ C},
\tag{A.9}
$$

which rotates the supergenerators into each other

$$
\begin{aligned}
&\left[R_B^{\ A}, Q_\alpha^C\right] = \delta_B^{\ C} Q_\alpha^A - \frac{1}{4}\delta_B^{\ A} Q_\alpha^C, \quad \left[R_B^{\ A}, \bar{Q}_{C\dot\alpha}\right] = -\delta_C^{\ A}\bar{Q}_{B\dot\alpha} + \frac{1}{4}\delta_B^{\ A}\bar{Q}_{C\dot\alpha} \\
&\left[R_B^{\ A}, \mathcal{S}_C^{\ \alpha}\right] = -\delta_C^{\ A}\mathcal{S}_B^{\ \alpha} + \frac{1}{4}\delta_B^{\ A}\mathcal{S}_C^{\ \alpha}, \quad \left[R_B^{\ A}, \bar{\mathcal{S}}^{C\dot\alpha}\right] = \delta_B^{\ C}\bar{\mathcal{S}}^{A\dot\alpha} - \frac{1}{4}\delta_B^{\ A}\bar{\mathcal{S}}^{C\dot\alpha}.
\end{aligned}
\tag{A.10}
$$

For the $\mathcal{N} = 4$ case, one can clearly see that the $\mathfrak{u}(1)_r$ (where $\mathfrak{su}(\mathcal{N})_R \oplus \mathfrak{u}(1)_r \subset \mathfrak{u}(\mathcal{N})$) generator $R^A_{\ A}$ commutes with all other generators (in other words, it is central). We can thus quotient this $\mathfrak{u}(1)_r$ out to give the algebra $\mathfrak{psu}(2,2|4) \cong \mathfrak{su}(2,2|4)/\mathfrak{u}(1)_r$ [33][35][89]. The resulting R-symmetry is therefore given by $\mathfrak{su}(4)_R$.

The supergenerators $Q, \bar{Q}$ have conformal dimension $1/2$ and the supergenerators $\mathcal{S}, \bar{\mathcal{S}}$ have conformal dimension $-1/2$. Descendent states are generated by acting with Q and/or $\bar{Q}$ on the highest weight state $|\Delta, R, r\rangle^{hw}_{(j,\bar{j})}$. Using the shorthand notation $R_{(j,\bar{j})}$, for $\mathcal{N} = 2$, the supergenerators have the following charges [33]

$$Q^1_{\ \alpha} \sim \frac{1}{2}_{(\pm\frac{1}{2},0)}, \quad Q^2_{\ \alpha} \sim (-\frac{1}{2})_{(\pm\frac{1}{2},0)}, \quad \bar{Q}_{1\dot{\alpha}} \sim \frac{1}{2}_{(0,\pm\frac{1}{2})}, \quad \bar{Q}_{2\dot{\alpha}} \sim (-\frac{1}{2})_{(0,\pm\frac{1}{2})}. \tag{A.11}$$

The charges of descendent states are determined by adding the charges of the above supergenerators to the highest weight state.

Appendix B

HAMILTONIAN OF THE INTERPOLATING $\mathcal{N} = 2$ QUIVER THEORY

In this section, we will calculate the Hamiltonian for the $\mathcal{N} = 2$ interpolating theory at one-loop order. We will work in the "downstairs" $\mathcal{N} = 2$ picture using the fields shown in Table 2.1. The "upstairs" $\mathcal{N} = 4$ picture (using the projected chiral fields) is discussed in Section 2.4. We will use the conventions of [18].

The computation is very similar to the $\mathcal{N} = 4$ case discussed in Section 2.3. Thus, we will only derive the Hamiltonian itself. An apparent difference, however, is the fact that we now have two gauge groups. This leads to a truncated basis when considering single trace operators since we cannot color contract indices from different gauge groups. Furthermore, for the same reason, interaction vertices can only be contracted in accordance with the gauge structure of the single trace operator.

The $\mathcal{N} = 2$ quiver Lagrangian was computed in [18]. As in the case for $\mathcal{N} = 4$ SYM, we will only consider scalar fields. The scalar interaction Lagrangian is given by

$$\begin{aligned}\mathcal{L}(g_1, g_2) = {} & g_1^2 \,\mathrm{Tr}\left[\frac{1}{2}\left[\bar{\phi}, \phi\right]^2 + \mathcal{M}_{\mathcal{I}}^{\mathcal{I}}\left(\phi\bar{\phi} + \bar{\phi}\phi\right) + \mathcal{M}_{\mathcal{I}}^{\mathcal{J}}\mathcal{M}_{\mathcal{J}}^{\mathcal{I}} - \frac{1}{2}\mathcal{M}_{\mathcal{I}}^{\mathcal{I}}\mathcal{M}_{\mathcal{J}}^{\mathcal{J}}\right] \\ & + g_2^2 \,\mathrm{Tr}\left[\frac{1}{2}\left[\check{\bar{\phi}}, \check{\phi}\right]^2 + \check{\mathcal{M}}^{\mathcal{I}}{}_{\mathcal{I}}\left(\check{\phi}\check{\bar{\phi}} + \check{\bar{\phi}}\check{\phi}\right) + \check{\mathcal{M}}^{\mathcal{I}}{}_{\mathcal{J}}\check{\mathcal{M}}^{\mathcal{J}}{}_{\mathcal{I}} - \frac{1}{2}\check{\mathcal{M}}^{\mathcal{I}}{}_{\mathcal{I}}\check{\mathcal{M}}^{\mathcal{J}}{}_{\mathcal{J}}\right] \\ & + g_1 g_2 \,\mathrm{Tr}\left[-2Q_{\mathcal{I}\hat{\mathcal{I}}}\check{\phi}\bar{Q}^{\hat{\mathcal{I}}\mathcal{I}}\bar{\phi} + \mathrm{h.c}\right] - \frac{1}{N}\mathcal{L}_{\mathrm{d.t.}},\end{aligned} \tag{B.1}$$

where the mesonic operators are given by

$$\mathcal{M}_{\mathcal{J}}^{\mathcal{I}a}{}_{b} = \frac{1}{\sqrt{2}}Q^{a}_{\mathcal{J}\hat{\mathcal{J}}\check{a}}\bar{Q}^{\hat{\mathcal{J}}\mathcal{I}\check{a}}{}_{b}, \quad \check{\mathcal{M}}^{\mathcal{I}\check{a}}{}_{\mathcal{J}\check{b}} = \frac{1}{\sqrt{2}}\bar{Q}^{\hat{\mathcal{J}}\mathcal{I}\check{a}}{}_{a}Q^{a}_{\mathcal{J}\hat{\mathcal{J}}\check{b}}. \tag{B.2}$$

The double-trace terms are given by

$$\begin{aligned}\mathcal{L}_{\mathrm{d.t.}} = {} & g_1^2\left(\mathrm{Tr}\left[\mathcal{M}_{\mathcal{I}}^{\mathcal{J}}\right]\mathrm{Tr}\left[\mathcal{M}_{\mathcal{J}}^{\mathcal{I}}\right] - \frac{1}{2}\mathrm{Tr}\left[\mathcal{M}_{\mathcal{I}}^{\mathcal{I}}\right]\mathrm{Tr}\left[\mathcal{M}_{\mathcal{J}}^{\mathcal{J}}\right]\right) \\ & + g_2^2\left(\mathrm{Tr}\left[\check{\mathcal{M}}^{\mathcal{I}}{}_{\mathcal{J}}\right]\mathrm{Tr}\left[\check{\mathcal{M}}^{\mathcal{J}}{}_{\mathcal{I}}\right] - \frac{1}{2}\mathrm{Tr}\left[\check{\mathcal{M}}^{\mathcal{I}}{}_{\mathcal{I}}\right]\mathrm{Tr}\left[\check{\mathcal{M}}^{\mathcal{J}}{}_{\mathcal{J}}\right]\right).\end{aligned} \tag{B.3}$$

However, since we are working in the planar limit, the double-trace terms are subleading and therefore do not contribute for spin chains with length $L > 2$ [1]. In this thesis, we only consider length $L > 2$ spin chains and thus we will not use the double-trace terms. Furthermore, additional identity pieces will be contributed by similar Feynman diagrams as shown in Figure 2.8; however, we can again use matching arguments to determine these contributions without explicitly computing them.

Single trace scalar operators are constructed from the set

$$V_{\mathcal{N}=2}^{\text{scalar}} = \{\phi, \bar{\phi}, \check{\phi}, \bar{\check{\phi}}, Q_{\mathcal{I}\hat{\mathcal{I}}}, \bar{Q}^{\hat{\mathcal{J}}\mathcal{J}}\}, \quad \mathcal{J}, \mathcal{I} = \pm,\ \hat{\mathcal{I}}, \hat{\mathcal{J}} = \hat{\pm}, \tag{B.4}$$

and we may act on the fields with covariant derivatives. However, as previously mentioned, one needs to consider a truncated tensor product due to gauge structure. As in Section 2.3, we will consider subcorrelators at sites $\ell, \ell+1$. We will also use the ket notation $|\mathcal{V}\mathcal{V}'\rangle$ to mean any $\mathcal{V}, \mathcal{V}' \in V_{\mathcal{N}=2}^{\text{scalar}}$ (with appropriate index contraction) at sites $\ell, \ell+1$ of the single trace operator. We will use the analogous Feynman graphs used in Section 2.3. Since we have two gauge groups, we will represent the index a (of gauge group $SU(N_1)$) with a solid blue line and the index $\check{a}$ (of gauge group $SU(N_2)$) with a dashed red line.

Finally, we will work in the large $N_1 \equiv N_2$ (planar) limit while keeping fixed the 't Hooft couplings

$$\lambda = g_1^2 N_1, \quad \check{\lambda} = g_2^2 N_2. \tag{B.5}$$

We will also use the deformation parameter $\kappa = g_2/g_1$ defined in Section 2.4.

ϕ^4 and $\check{\phi}^4$ Vertex

Following [18], we will make use the following definitions $\phi^{\mathfrak{p}}, \mathfrak{p} = \pm$, where

$$\phi^+ \equiv \bar{\phi}, \quad \phi^- \equiv \phi, \quad g_{\mathfrak{pq}} = g^{\mathfrak{pq}} = \begin{pmatrix} 0 & 1 \\ 1 & 0 \end{pmatrix}. \tag{B.6}$$

In particular, note that $g_{\mathfrak{pq}} g^{\mathfrak{qr}} = \delta_{\mathfrak{p}}^{\mathfrak{r}}$. Thus $\mathfrak{p}$ labels the $U(1)_r$ charge of $\phi, \bar{\phi}$ (see Table 2.1).

We consider $\langle \phi_{\mathfrak{p}'} \phi_{\mathfrak{q}'} | H | \phi^{\mathfrak{p}} \phi^{\mathfrak{q}} \rangle_{\phi^4}$. The relevant part of the interaction Lagrangian comes from the scalar potential term

$$\mathcal{L}_{\phi^4} = g_1^2 \text{Tr}[\frac{1}{2}\left[\bar{\phi}, \phi\right]^2]. \tag{B.7}$$

[1] For the case $L = 2$, the double-trace terms do contribute and are needed for the protection of certain special operators. See the discussion in [18].

Now, using the cyclicity of the trace,

$$\begin{aligned}\mathcal{L}_{\phi^4} &= g_1^2 \mathrm{Tr}[\frac{1}{2}\left[\bar{\phi},\phi\right]^2] \\ &= \frac{g_1^2}{2}\mathrm{Tr}\left[\bar{\phi}\phi\bar{\phi}\phi - \bar{\phi}\phi\phi\bar{\phi} - \phi\bar{\phi}\bar{\phi}\phi + \phi\bar{\phi}\phi\bar{\phi}\right] \\ &= \frac{g_1^2}{2}\mathrm{Tr}\left[2\phi^+\phi^-\phi^+\phi^- - 2\phi^+\phi^-\phi^-\phi^+\right] \\ &= \frac{g_1^2}{2}\mathrm{Tr}\left[g_{\mathfrak{p}\mathfrak{q}}g_{\mathfrak{a}\mathfrak{b}}\phi^{\mathfrak{p}}\phi^{\mathfrak{q}}\phi^{\mathfrak{a}}\phi^{\mathfrak{b}} - g_{\mathfrak{p}\mathfrak{q}}g_{\mathfrak{a}\mathfrak{b}}\phi^{\mathfrak{p}}\phi^{\mathfrak{a}}\phi^{\mathfrak{q}}\phi^{\mathfrak{b}}\right].\end{aligned} \tag{B.8}$$

We thus have two vertices, which is analogous to equation (2.126) in Section 2.3. Figure B.1 shows the first vertex used in the subcorrelator (the diagram for the second vertex is similar). Note that we have assumed that the overall trace of the operator closes over gauge group 1 but we could also have chosen gauge group 2 (in which case, we would have red dashed lines at the top and bottom of the diagram instead).

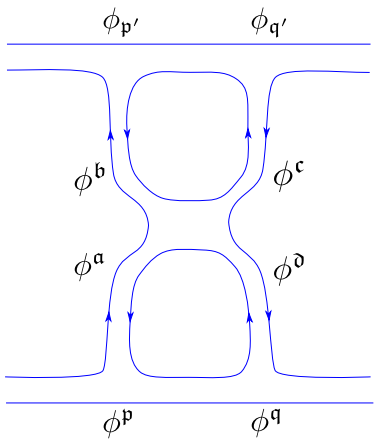

Figure B.1: *The ϕ^4 vertex. The solid blue line denotes the first gauge group. Note, we have assumed that the overall trace of the operator closes over gauge group 1.*

With incoming $(\phi^{\mathfrak{p}}\phi^{\mathfrak{q}})^a_c$ to outgoing $(\phi_{\mathfrak{q}'}\phi_{\mathfrak{p}'})^{c'}_{a'}$, the first vertex contributes four terms

$$\frac{N^2}{2}\delta^a_{a'}\delta^{c'}_c\left(2\delta^{\mathfrak{p}}_{\mathfrak{p}'}\delta^{\mathfrak{q}}_{\mathfrak{q}'} + 2g^{\mathfrak{p}\mathfrak{q}}g_{\mathfrak{p}'\mathfrak{q}'}\right), \tag{B.9}$$

and the second vertex also contributes four terms

$$\frac{N^2}{2}\delta^a_{a'}\delta^{c'}_c\left(4\delta^{\mathfrak{p}}_{\mathfrak{q}'}\delta^{\mathfrak{q}}_{\mathfrak{p}'}\right). \tag{B.10}$$

Combining these results, we find that $\mathcal{L}_{\phi^4}$ contributes (factoring out g_1^2)

$$\langle\phi_{\mathfrak{p}'}\phi_{\mathfrak{q}'}|H|\phi^{\mathfrak{p}}\phi^{\mathfrak{q}}\rangle_{\phi^4} = \delta^{\mathfrak{p}}_{\mathfrak{p}'}\delta^{\mathfrak{q}}_{\mathfrak{q}'} + g^{\mathfrak{p}\mathfrak{q}}g_{\mathfrak{p}'\mathfrak{q}'} - 2\delta^{\mathfrak{p}}_{\mathfrak{q}'}\delta^{\mathfrak{q}}_{\mathfrak{p}'}, \tag{B.11}$$

In exactly the same manner, for $\langle \check{\phi}_{\mathfrak{p}'} \check{\phi}_{\mathfrak{q}'} | H | \check{\phi}^{\mathfrak{p}} \check{\phi}^{\mathfrak{q}} \rangle_{\check{\phi}^4}$, we find that

$$\langle \check{\phi}_{\mathfrak{p}'} \check{\phi}_{\mathfrak{q}'} | H | \check{\phi}^{\mathfrak{p}} \check{\phi}^{\mathfrak{q}} \rangle_{\check{\phi}^4} = \kappa^2 \left(\delta^{\mathfrak{p}}_{\mathfrak{p}'} \delta^{\mathfrak{q}}_{\mathfrak{q}'} + g^{\mathfrak{p}\mathfrak{q}} g_{\mathfrak{p}'\mathfrak{q}'} - 2\delta^{\mathfrak{p}}_{\mathfrak{q}'} \delta^{\mathfrak{q}}_{\mathfrak{p}'} \right). \tag{B.12}$$

Q^4 Vertex

We next consider $\langle \bar{Q}^{\hat{\mathcal{L}}\mathcal{L}} Q_{\mathcal{K}\hat{\mathcal{K}}} | H | Q_{\mathcal{I}\hat{\mathcal{I}}} \bar{Q}^{\hat{\mathcal{J}}\mathcal{J}} \rangle_{Q^4}$. The relevant potential terms are

$$\mathcal{L}_{Q^4} = g_1^2 \mathrm{Tr}\left[\mathcal{M}_{\mathcal{I}}^{\ \mathcal{J}} \mathcal{M}_{\mathcal{J}}^{\ \mathcal{I}} - \frac{1}{2} \mathcal{M}_{\mathcal{I}}^{\ \mathcal{I}} \mathcal{M}_{\mathcal{J}}^{\ \mathcal{J}} \right] + \check{g}_2^2 \mathrm{Tr}\left[\check{\mathcal{M}}^{\mathcal{I}}_{\ \mathcal{J}} \check{\mathcal{M}}^{\mathcal{J}}_{\ \mathcal{I}} - \frac{1}{2} \check{\mathcal{M}}^{\mathcal{I}}_{\ \mathcal{I}} \check{\mathcal{M}}^{\mathcal{J}}_{\ \mathcal{J}} \right]. \tag{B.13}$$

The incoming and outgoing terms in the subcorrelator is given by $(Q_{\mathcal{I}\hat{\mathcal{I}}} \bar{Q}^{\hat{\mathcal{J}}\mathcal{J}})^a_{\ c}$ and $(Q_{\mathcal{K}\hat{\mathcal{K}}} \bar{Q}^{\hat{\mathcal{L}}\mathcal{L}})^{c'}_{\ a'}$, respectively.

Consider the first term in $\mathcal{L}_{Q^4}$

$$\begin{aligned} g_1^2 \mathrm{Tr}\left[\mathcal{M}_{\mathcal{I}}^{\ \mathcal{J}} \mathcal{M}_{\mathcal{J}}^{\ \mathcal{I}} - \frac{1}{2} \mathcal{M}_{\mathcal{I}}^{\ \mathcal{I}} \mathcal{M}_{\mathcal{J}}^{\ \mathcal{J}} \right] \sim g_1^2 \big(& Q^a_{\ \mathcal{I}\hat{\mathcal{J}}\check{a}} \bar{Q}^{\hat{\mathcal{J}}\mathcal{J}\check{a}}_{\ \ \ b} Q^b_{\ \mathcal{J}\hat{\mathcal{I}}\check{b}} \bar{Q}^{\hat{\mathcal{I}}\mathcal{I}\check{b}}_{\ \ \ a} \\ & - \frac{1}{2} Q^a_{\ \mathcal{I}\hat{\mathcal{I}}\check{a}} \bar{Q}^{\hat{\mathcal{I}}\mathcal{I}\check{a}}_{\ \ \ b} Q^b_{\ \mathcal{J}\hat{\mathcal{J}}\check{b}} \bar{Q}^{\hat{\mathcal{J}}\mathcal{J}\check{b}}_{\ \ \ a} \big). \end{aligned} \tag{B.14}$$

Thus, this term contributes two vertices. The first term is shown in Figure B.2 (the second term is similar). Notice, due to the gauge indices, there are only two ways we can contract the vertex with the incoming and outgoing legs of the diagram.

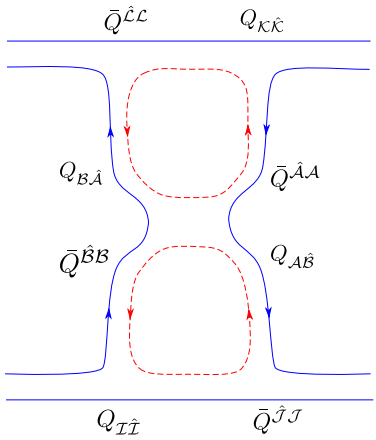

Figure B.2: *The Q^4 vertex. The solid blue line denotes the first gauge group and the red dashed line denotes the second gauge group. Note, we have assumed that the overall trace of the operator closes over gauge group 1.*

The first vertex thus contributes

$$N^2 \delta^a_{a'} \delta^{c'}_c \left(2\delta^{\mathcal{L}}_{\mathcal{I}} \delta^{\hat{\mathcal{J}}}_{\hat{\mathcal{I}}} \delta^{\mathcal{J}}_{\mathcal{K}} \delta^{\hat{\mathcal{L}}}_{\hat{\mathcal{K}}} \right). \tag{B.15}$$

Similarly, for the second vertex, we find

$$-\frac{N^2}{2}\delta^a_{a'}\delta^{c'}_{c}\left(2\delta^{\mathcal{J}}_{\mathcal{I}}\delta^{\hat{\mathcal{J}}}_{\hat{\mathcal{I}}}\delta^{\mathcal{L}}_{\mathcal{K}}\delta^{\hat{\mathcal{L}}}_{\hat{\mathcal{K}}}\right). \tag{B.16}$$

For the analogous interaction term in $\mathcal{L}_{Q^4}$ with the check notation, the procedure is identical with an overall factor of κ^2.

Combining these results, we find the total contribution to be

$$\begin{aligned}\langle\bar{Q}^{\hat{\mathcal{L}}\mathcal{L}}Q_{\mathcal{K}\hat{\mathcal{K}}}|H|Q_{\mathcal{I}\hat{\mathcal{I}}}\bar{Q}^{\hat{\mathcal{J}}\mathcal{J}}\rangle_{Q^4} &= 2\delta^{\mathcal{L}}_{\mathcal{I}}\delta^{\hat{\mathcal{J}}}_{\hat{\mathcal{I}}}\delta^{\mathcal{J}}_{\mathcal{K}}\delta^{\hat{\mathcal{L}}}_{\hat{\mathcal{K}}}-\delta^{\mathcal{J}}_{\mathcal{I}}\delta^{\hat{\mathcal{J}}}_{\hat{\mathcal{I}}}\delta^{\mathcal{L}}_{\mathcal{K}}\delta^{\hat{\mathcal{L}}}_{\hat{\mathcal{K}}}\\ &\quad+\kappa^2\left(2\delta^{\mathcal{J}}_{\mathcal{I}}\delta^{\hat{\mathcal{L}}}_{\hat{\mathcal{I}}}\delta^{\mathcal{L}}_{\mathcal{K}}\delta^{\hat{\mathcal{J}}}_{\hat{\mathcal{K}}}-\delta^{\mathcal{L}}_{\mathcal{I}}\delta^{\hat{\mathcal{J}}}_{\hat{\mathcal{K}}}\delta^{\mathcal{J}}_{\mathcal{K}}\delta^{\hat{\mathcal{L}}}_{\hat{\mathcal{I}}}\right).\end{aligned} \tag{B.17}$$

In the same manner, but with the opposite gauge indices (in other words, exchanging the blue solid line with the red dashed line in Figure B.2, with the vertex appropriately contracted with the incoming and outgoing legs), we find the contribution

$$\begin{aligned}\langle Q_{\mathcal{I}\hat{\mathcal{I}}}\bar{Q}^{\hat{\mathcal{J}}\mathcal{J}}|H|\bar{Q}^{\hat{\mathcal{L}}\mathcal{L}}Q_{\mathcal{K}\hat{\mathcal{K}}}\rangle_{Q^4} &= \kappa^2\left(2\delta^{\mathcal{L}}_{\mathcal{I}}\delta^{\hat{\mathcal{J}}}_{\hat{\mathcal{I}}}\delta^{\mathcal{J}}_{\mathcal{K}}\delta^{\hat{\mathcal{L}}}_{\hat{\mathcal{K}}}-\delta^{\mathcal{J}}_{\mathcal{I}}\delta^{\hat{\mathcal{J}}}_{\hat{\mathcal{I}}}\delta^{\mathcal{L}}_{\mathcal{K}}\delta^{\hat{\mathcal{L}}}_{\hat{\mathcal{K}}}\right)\\ &\quad+2\delta^{\mathcal{J}}_{\mathcal{I}}\delta^{\hat{\mathcal{L}}}_{\hat{\mathcal{I}}}\delta^{\mathcal{L}}_{\mathcal{K}}\delta^{\hat{\mathcal{J}}}_{\hat{\mathcal{K}}}-\delta^{\mathcal{L}}_{\mathcal{I}}\delta^{\hat{\mathcal{J}}}_{\hat{\mathcal{K}}}\delta^{\mathcal{J}}_{\mathcal{K}}\delta^{\hat{\mathcal{L}}}_{\hat{\mathcal{I}}}.\end{aligned} \tag{B.18}$$

$Q^2\phi^2$ and $Q^2\check{\phi}^2$ Vertex

Finally, we consider $\langle\phi_{\mathfrak{p}'}\phi_{\mathfrak{q}'}|H|Q_{\mathcal{I}\hat{\mathcal{I}}}\bar{Q}^{\hat{\mathcal{J}}\mathcal{J}}\rangle_{Q^2\phi^2}$.

The relevant interaction is given by

$$\begin{aligned}\mathcal{L}_{Q^2\phi^2} &= g_1^2\mathrm{Tr}\left[\mathcal{M}^{\mathcal{I}}_{\mathcal{I}}\left(\phi\bar{\phi}+\bar{\phi}\phi\right)\right]\\ &\sim g_1^2 g_{\mathfrak{p}\mathfrak{q}}\,Q^{e}_{\mathcal{I}\hat{\mathcal{I}}\check{e}}\bar{Q}^{\hat{\mathcal{I}}\mathcal{I}\check{e}}{}_{f}\phi^{\mathfrak{p}f}{}_{g}\phi^{\mathfrak{q}g}{}_{e}.\end{aligned} \tag{B.19}$$

Inserting the vertex into the subcorrelator, we find the Feynman graph in Figure B.3.

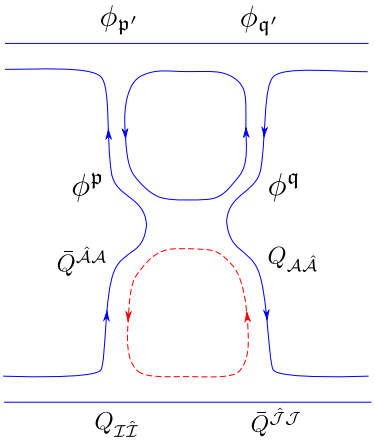

Figure B.3: *The $Q^2\phi^2$ vertex. The solid blue line denotes the first gauge group and the red dashed line denotes the second gauge group. Note, we have assumed that the overall trace of the operator closes over gauge group 1.*

Clearly, due to the gauge structure, there is only one way to attach the vertex to the incoming and outgoing legs. The resulting contribution is therefore given by

$$\langle \phi_{\mathfrak{p}'}\phi_{\mathfrak{q}'}|H|Q_{\mathcal{I}\hat{\mathcal{I}}}\bar{Q}^{\hat{\mathcal{J}}\mathcal{J}}\rangle_{Q^2\phi^2} = \delta^{\mathcal{J}}_{\mathcal{I}}\delta^{\hat{\mathcal{J}}}_{\hat{\mathcal{I}}}\, g_{\mathfrak{p}'\mathfrak{q}'}. \tag{B.20}$$

In precisely the same manner, we find the result

$$\langle \check{\phi}_{\mathfrak{p}'}\check{\phi}_{\mathfrak{q}'}|H|Q_{\mathcal{I}\hat{\mathcal{I}}}\bar{Q}^{\hat{\mathcal{J}}\mathcal{J}}\rangle_{Q^2\check{\phi}^2} = \kappa^2\delta^{\mathcal{J}}_{\mathcal{I}}\delta^{\hat{\mathcal{J}}}_{\hat{\mathcal{I}}}\, g_{\mathfrak{p}'\mathfrak{q}'}. \tag{B.21}$$

Finally, equation (B.19) also acts on $\langle \phi_{\mathfrak{q}}\bar{Q}^{\hat{\mathcal{J}}\mathcal{J}}|H|\phi^{\mathfrak{p}}Q_{\mathcal{I}\hat{\mathcal{I}}}\rangle_{\phi Q\check{\phi}\bar{Q}}$ to give

$$\langle \phi_{\mathfrak{q}}\bar{Q}^{\hat{\mathcal{J}}\mathcal{J}}|H|\phi^{\mathfrak{p}}Q_{\mathcal{I}\hat{\mathcal{I}}}\rangle_{\phi Q\check{\phi}\bar{Q}} = 2\,\delta^{\mathcal{J}}_{\mathcal{I}}\delta^{\hat{\mathcal{J}}}_{\hat{\mathcal{I}}}\delta^{\mathfrak{p}}_{\mathfrak{q}}, \tag{B.22}$$

and, analogously, on $\langle \bar{Q}^{\hat{\mathcal{J}}\mathcal{J}}\check{\phi}_{\mathfrak{q}}|H|Q_{\mathcal{I}\hat{\mathcal{I}}}\check{\phi}^{\mathfrak{p}}\rangle_{\phi Q\check{\phi}\bar{Q}}$ to give

$$\langle \bar{Q}^{\hat{\mathcal{J}}\mathcal{J}}\check{\phi}_{\mathfrak{q}}|H|Q_{\mathcal{I}\hat{\mathcal{I}}}\check{\phi}^{\mathfrak{p}}\rangle_{\phi Q\check{\phi}\bar{Q}} = 2\kappa^2\,\delta^{\mathcal{J}}_{\mathcal{I}}\delta^{\hat{\mathcal{J}}}_{\hat{\mathcal{I}}}\delta^{\mathfrak{p}}_{\mathfrak{q}}. \tag{B.23}$$

$\phi Q\check{\phi}\bar{Q}$ Vertex

We next determine $\langle \bar{Q}^{\hat{\mathcal{J}}\mathcal{J}}\check{\phi}_{\mathfrak{q}}|H|\phi^{\mathfrak{p}}Q_{\mathcal{I}\hat{\mathcal{I}}}\rangle_{\phi Q\check{\phi}\bar{Q}}$ and $\langle \phi^{\mathfrak{p}}\bar{Q}^{\hat{\mathcal{J}}\mathcal{J}}|H|Q_{\mathcal{I}\hat{\mathcal{I}}}\check{\phi}_{\mathfrak{q}}\rangle_{\phi Q\check{\phi}\bar{Q}}$.

Consider $\langle \bar{Q}^{\hat{\mathcal{J}}\mathcal{J}}\check{\phi}_{\mathfrak{q}}|H|\phi^{\mathfrak{p}}Q_{\mathcal{I}\hat{\mathcal{I}}}\rangle_{\phi Q\check{\phi}\bar{Q}}$. Our index structure is $(\phi^{\mathfrak{p}}Q_{\mathcal{I}\hat{\mathcal{I}}})^{a}_{\check{c}}$. For the bra term, note that $Q^{a}_{\mathcal{I}\hat{\mathcal{I}}\check{a}}\check{\phi}^{\mathfrak{p}\check{a}}_{\check{c}}$ conjugated gives $Q_{a}^{\hat{\mathcal{I}}\mathcal{I}\check{a}}\check{\phi}_{\mathfrak{p}\check{a}}{}^{\check{c}}$. The relevant interaction term is

$$\mathcal{L}_{\phi Q\check{\phi}\bar{Q}} = g_1 g_2 \mathrm{Tr}\big[-2Q_{\mathcal{I}\hat{\mathcal{I}}}\check{\phi}\bar{Q}^{\hat{\mathcal{I}}\mathcal{I}}\bar{\phi} + \mathrm{h.c}\big]. \tag{B.24}$$

The hermitian conjugate term (h.c.) is given by

$$(Q^{a}_{\mathcal{I}\hat{\mathcal{I}}\check{a}}\check{\phi}^{\check{a}}_{\check{b}}\bar{Q}^{\hat{\mathcal{I}}\mathcal{I}\check{b}}{}_{c}\bar{\phi}^{c}{}_{a})^{\dagger} = (\bar{\phi}^{c}{}_{a})^{\dagger}(\bar{Q}^{\hat{\mathcal{I}}\mathcal{I}\check{b}}{}_{c})^{\dagger}(\check{\phi}^{\check{a}}_{\check{b}})^{\dagger}(Q^{a}_{\mathcal{I}\hat{\mathcal{I}}\check{a}})^{\dagger} = \phi^{a}{}_{c}Q^{c}_{\mathcal{I}\hat{\mathcal{I}}\check{b}}\bar{\check{\phi}}^{\check{b}}_{\check{a}}\bar{Q}^{\hat{\mathcal{I}}\mathcal{I}\check{a}}{}_{a}. \tag{B.25}$$

Using this expression, and the cyclicity of the trace, $\mathcal{L}_{\phi Q\check{\phi}\bar{Q}}$ becomes (with $g_2 = \kappa g_1$)

$$\mathcal{L}_{\phi Q\check{\phi}\bar{Q}} = -2\kappa\, g_1^2 g_{\mathfrak{p}\mathfrak{q}}\, \mathrm{Tr}\big[\phi^{\mathfrak{p}}Q_{\mathcal{I}\hat{\mathcal{I}}}\check{\phi}^{\mathfrak{q}}\bar{Q}^{\hat{\mathcal{I}}\mathcal{I}}\big]. \tag{B.26}$$

Figure B.4 shows the vertex inserted into the subcorrelator.

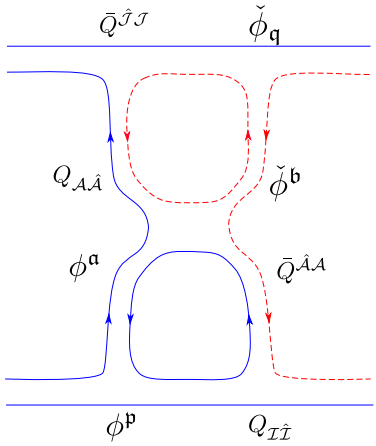

Figure B.4: *The $\phi Q\phi Q$ vertex. The solid blue line denotes the first gauge group and the red dashed line denotes the second gauge group. Note, we have assumed that the overall trace of the operator closes over gauge group 1.*

As in the previous case, notice that there is again only one possible way to insert the vertex. This gives

$$-2\kappa\, N^2\delta^{a}_{a'}\delta^{\check{c}'}_{\check{c}}\delta^{\mathcal{J}}_{\mathcal{I}}\delta^{\hat{\mathcal{J}}}_{\hat{\mathcal{I}}}g^{\mathfrak{p}\mathfrak{a}}\delta^{\mathfrak{b}}_{\mathfrak{q}}g_{\mathfrak{a}\mathfrak{b}} = -2\kappa\, N^2\delta^{a}_{a'}\delta^{\check{c}'}_{\check{c}}\delta^{\mathcal{J}}_{\mathcal{I}}\delta^{\hat{\mathcal{J}}}_{\hat{\mathcal{I}}}\delta^{\mathfrak{p}}_{\mathfrak{q}}. \tag{B.27}$$

Thus, we find that

$$\langle\bar{Q}^{\hat{\mathcal{J}}\mathcal{J}}\check{\phi}_{\mathfrak{q}}|H|\phi^{\mathfrak{p}}Q_{\mathcal{I}\hat{\mathcal{I}}}\rangle_{\phi Q\check{\phi}\bar{Q}} = -2\kappa\,\delta^{\mathcal{J}}_{\mathcal{I}}\delta^{\hat{\mathcal{J}}}_{\hat{\mathcal{I}}}\delta^{\mathfrak{p}}_{\mathfrak{q}}. \tag{B.28}$$

In precisely the same manner,

$$\langle\phi^{\mathfrak{p}}\bar{Q}^{\hat{\mathcal{J}}\mathcal{J}}|H|Q_{\mathcal{I}\hat{\mathcal{I}}}\check{\phi}_{\mathfrak{q}}\rangle_{\phi Q\check{\phi}\bar{Q}} = -2\kappa\,\delta^{\mathcal{J}}_{\mathcal{I}}\delta^{\hat{\mathcal{J}}}_{\hat{\mathcal{I}}}\delta^{\mathfrak{p}}_{\mathfrak{q}}. \tag{B.29}$$

Identity Terms

In summary, we find a match in terms of the equations given in Appendix A.2 of [18]

$$\langle \phi_{\mathfrak{p}'}\phi_{\mathfrak{q}'}|H|\phi^{\mathfrak{p}}\phi^{\mathfrak{q}}\rangle_{\phi^4} = \delta^{\mathfrak{p}}_{\mathfrak{p}'}\delta^{\mathfrak{q}}_{\mathfrak{q}'} + g^{\mathfrak{p}\mathfrak{q}}g_{\mathfrak{p}'\mathfrak{q}'} - 2\delta^{\mathfrak{p}}_{\mathfrak{q}'}\delta^{\mathfrak{q}}_{\mathfrak{p}'}, \tag{B.30}$$

$$\langle \check{\phi}_{\mathfrak{p}'}\check{\phi}_{\mathfrak{q}'}|H|\check{\phi}^{\mathfrak{p}}\check{\phi}^{\mathfrak{q}}\rangle_{\check{\phi}^4} = \kappa^2\big(\delta^{\mathfrak{p}}_{\mathfrak{p}'}\delta^{\mathfrak{q}}_{\mathfrak{q}'} + g^{\mathfrak{p}\mathfrak{q}}g_{\mathfrak{p}'\mathfrak{q}'} - 2\delta^{\mathfrak{p}}_{\mathfrak{q}'}\delta^{\mathfrak{q}}_{\mathfrak{p}'}\big), \tag{B.31}$$

$$\begin{aligned}\langle \bar{Q}^{\hat{\mathcal{L}}\mathcal{L}}Q_{\mathcal{K}\hat{\mathcal{K}}}|H|Q_{\mathcal{I}\hat{\mathcal{I}}}\bar{Q}^{\hat{\mathcal{J}}\mathcal{J}}\rangle_{Q^4} &= 2\delta^{\mathcal{L}}_{\mathcal{I}}\delta^{\hat{\mathcal{J}}}_{\hat{\mathcal{I}}}\delta^{\mathcal{J}}_{\mathcal{K}}\delta^{\hat{\mathcal{L}}}_{\hat{\mathcal{K}}} - \delta^{\mathcal{J}}_{\mathcal{I}}\delta^{\hat{\mathcal{J}}}_{\hat{\mathcal{I}}}\delta^{\mathcal{L}}_{\mathcal{K}}\delta^{\hat{\mathcal{L}}}_{\hat{\mathcal{K}}} \\ &\quad + \kappa^2\big(2\delta^{\mathcal{J}}_{\mathcal{I}}\delta^{\hat{\mathcal{L}}}_{\hat{\mathcal{I}}}\delta^{\mathcal{L}}_{\mathcal{K}}\delta^{\hat{\mathcal{J}}}_{\hat{\mathcal{K}}} - \delta^{\mathcal{L}}_{\mathcal{I}}\delta^{\hat{\mathcal{J}}}_{\hat{\mathcal{K}}}\delta^{\mathcal{J}}_{\mathcal{K}}\delta^{\hat{\mathcal{L}}}_{\hat{\mathcal{I}}}\big),\end{aligned} \tag{B.32}$$

$$\begin{aligned}\langle Q_{\mathcal{I}\hat{\mathcal{I}}}\bar{Q}^{\hat{\mathcal{J}}\mathcal{J}}|H|\bar{Q}^{\hat{\mathcal{L}}\mathcal{L}}Q_{\mathcal{K}\hat{\mathcal{K}}}\rangle_{Q^4} &= \kappa^2\big(2\delta^{\mathcal{L}}_{\mathcal{I}}\delta^{\hat{\mathcal{J}}}_{\hat{\mathcal{I}}}\delta^{\mathcal{J}}_{\mathcal{K}}\delta^{\hat{\mathcal{L}}}_{\hat{\mathcal{K}}} - \delta^{\mathcal{J}}_{\mathcal{I}}\delta^{\hat{\mathcal{J}}}_{\hat{\mathcal{I}}}\delta^{\mathcal{L}}_{\mathcal{K}}\delta^{\hat{\mathcal{L}}}_{\hat{\mathcal{K}}}\big) \\ &\quad + 2\delta^{\mathcal{J}}_{\mathcal{I}}\delta^{\hat{\mathcal{L}}}_{\hat{\mathcal{I}}}\delta^{\mathcal{L}}_{\mathcal{K}}\delta^{\hat{\mathcal{J}}}_{\hat{\mathcal{K}}} - \delta^{\mathcal{L}}_{\mathcal{I}}\delta^{\hat{\mathcal{J}}}_{\hat{\mathcal{K}}}\delta^{\mathcal{J}}_{\mathcal{K}}\delta^{\hat{\mathcal{L}}}_{\hat{\mathcal{I}}},\end{aligned} \tag{B.33}$$

$$\langle \phi_{\mathfrak{p}'}\phi_{\mathfrak{q}'}|H|Q_{\mathcal{I}\hat{\mathcal{I}}}\bar{Q}^{\hat{\mathcal{J}}\mathcal{J}}\rangle_{Q^2\phi^2} = \delta^{\mathcal{J}}_{\mathcal{I}}\delta^{\hat{\mathcal{J}}}_{\hat{\mathcal{I}}}g_{\mathfrak{p}'\mathfrak{q}'},\ \langle \check{\phi}_{\mathfrak{p}'}\check{\phi}_{\mathfrak{q}'}|H|\bar{Q}^{\hat{\mathcal{J}}\mathcal{J}}Q_{\mathcal{I}\hat{\mathcal{I}}}\rangle_{Q^2\check{\phi}^2} = \kappa^2\delta^{\mathcal{J}}_{\mathcal{I}}\delta^{\hat{\mathcal{J}}}_{\hat{\mathcal{I}}}g_{\mathfrak{p}'\mathfrak{q}'}, \tag{B.34}$$

$$\langle \bar{Q}^{\hat{\mathcal{J}}\mathcal{J}}\check{\phi}_{\mathfrak{q}}|H|\phi^{\mathfrak{p}}Q_{\mathcal{I}\hat{\mathcal{I}}}\rangle_{\phi Q\check{\phi}\bar{Q}} = -2\kappa\,\delta^{\mathcal{J}}_{\mathcal{I}}\delta^{\hat{\mathcal{J}}}_{\hat{\mathcal{I}}}\delta^{\mathfrak{p}}_{\mathfrak{q}},\ \langle \phi^{\mathfrak{p}}\bar{Q}^{\hat{\mathcal{J}}\mathcal{J}}|H|Q_{\mathcal{I}\hat{\mathcal{I}}}\check{\phi}_{\mathfrak{q}}\rangle_{\phi Q\check{\phi}\bar{Q}} = -2\kappa\,\delta^{\mathcal{J}}_{\mathcal{I}}\delta^{\hat{\mathcal{J}}}_{\hat{\mathcal{I}}}\delta^{\mathfrak{p}}_{\mathfrak{q}}, \tag{B.35}$$

$$\langle \phi_{\mathfrak{q}}\bar{Q}^{\hat{\mathcal{J}}\mathcal{J}}|H|\phi^{\mathfrak{p}}Q_{\mathcal{I}\hat{\mathcal{I}}}\rangle_{\phi Q\check{\phi}\bar{Q}} = 2\,\delta^{\mathcal{J}}_{\mathcal{I}}\delta^{\hat{\mathcal{J}}}_{\hat{\mathcal{I}}}\delta^{\mathfrak{p}}_{\mathfrak{q}},\ \langle \bar{Q}^{\hat{\mathcal{J}}\mathcal{J}}\check{\phi}_{\mathfrak{q}}|H|Q_{\mathcal{I}\hat{\mathcal{I}}}\check{\phi}^{\mathfrak{p}}\rangle_{\phi Q\check{\phi}\bar{Q}} = 2\kappa^2\,\delta^{\mathcal{J}}_{\mathcal{I}}\delta^{\hat{\mathcal{J}}}_{\hat{\mathcal{I}}}\delta^{\mathfrak{p}}_{\mathfrak{q}}. \tag{B.36}$$

The first four equations will pick up identity terms from diagrams analogous to the diagrams shown in Figure 2.8. Similar to Section 2.3, we can use an indirect matching argument to determine their contributions without computing these terms directly.

For the interpolating $\mathcal{N} = 2$ quiver theory, the procedure is outlined in Appendix A.2 of [18] (see also A.1). We will use the $\mathbb{Z}_2$ symmetry which sends $\kappa \leftrightarrow 1/\kappa$ (equivalently, $g_1 \leftrightarrow g_2$) and exchanges fields with their $\mathbb{Z}_2$ conjugate $Q \leftrightarrow \bar{Q}$, $\phi \leftrightarrow \check{\phi}$. In addition, we will also match to terms in the Hamiltonian for $\mathcal{N} = 2$ SCQCD (computed in [18] in equation (3.3)) by taking the limit $\kappa \to 0$. Only the first four terms above receive contributions.

For the first two terms, we add

$$\langle \phi_{\mathfrak{p}'}\phi_{\mathfrak{q}'}|H|\phi^{\mathfrak{p}}\phi^{\mathfrak{q}}\rangle_{\phi^4} = \alpha\delta^{\mathfrak{p}}_{\mathfrak{p}'}\delta^{\mathfrak{q}}_{\mathfrak{q}'} + g^{\mathfrak{p}\mathfrak{q}}g_{\mathfrak{p}'\mathfrak{q}'} - 2\delta^{\mathfrak{p}}_{\mathfrak{q}'}\delta^{\mathfrak{q}}_{\mathfrak{p}'}, \tag{B.37}$$

$$\langle \check{\phi}_{\mathfrak{p}'}\check{\phi}_{\mathfrak{q}'}|H|\check{\phi}^{\mathfrak{p}}\check{\phi}^{\mathfrak{q}}\rangle_{\check{\phi}^4} = \kappa^2\big(\beta\delta^{\mathfrak{p}}_{\mathfrak{p}'}\delta^{\mathfrak{q}}_{\mathfrak{q}'} + g^{\mathfrak{p}\mathfrak{q}}g_{\mathfrak{p}'\mathfrak{q}'} - 2\delta^{\mathfrak{p}}_{\mathfrak{q}'}\delta^{\mathfrak{q}}_{\mathfrak{p}'}\big), \tag{B.38}$$

Performing $\mathbb{Z}_2$ conjugation, the two terms match provided that $\alpha = \beta$. Taking the $\kappa \to 0$ limit, the second term of course uncouples from the theory. Then, to match with equation (3.3) in [18], we clearly need to take $\alpha = 2$.

For the remaining two terms, it is convenient to use the identity, trace and permutation operators $\mathbb{1}, \mathbb{K}, \mathbb{P}$ defined in [18] which can be determined by looking at the indices in the previous equation. We can then compactly write

$$\begin{aligned}\langle \bar{Q}^{\hat{\mathcal{L}}\mathcal{L}} Q_{\mathcal{K}\hat{\mathcal{K}}} | H | Q_{\mathcal{I}\hat{\mathcal{I}}} \bar{Q}^{\hat{\mathcal{J}}\mathcal{J}} \rangle_{Q^4} &= 2\alpha \mathbb{1}\hat{\mathbb{K}} - \mathbb{K}\hat{\mathbb{K}} \\ &\quad + \kappa^2 \big(2\beta \mathbb{K}\hat{\mathbb{1}} - \gamma \mathbb{1}\hat{\mathbb{1}}\big),\end{aligned} \tag{B.39}$$

$$\begin{aligned}\langle Q_{\mathcal{I}\hat{\mathcal{I}}} \bar{Q}^{\hat{\mathcal{J}}\mathcal{J}} | H | \bar{Q}^{\hat{\mathcal{L}}\mathcal{L}} Q_{\mathcal{K}\hat{\mathcal{K}}} \rangle_{Q^4} &= \kappa^2 \big(2\alpha \mathbb{1}\hat{\mathbb{K}} - \mathbb{K}\hat{\mathbb{K}}\big) \\ &\quad + 2\beta \mathbb{K}\hat{\mathbb{1}} - \gamma \mathbb{1}\hat{\mathbb{1}},\end{aligned} \tag{B.40}$$

where the unhatted operators act on $SU(2)_R$ indices and the hatted operators act on the $SU(2)_L$ indices. As in the previous case, $\mathbb{Z}_2$ symmetry implies that they have the same identity coefficients. Taking the $\kappa \to 0$ limit and comparing with equation (3.4) in A.2 of [18], we clearly need

$$\alpha = \beta = 1, \quad \gamma = 0. \tag{B.41}$$

Combining these results, we find the one-loop Hamiltonian for the interpolating $\mathcal{N} = 2$ quiver theory[2]

$$\begin{aligned} H_{\ell,\ell+1} = &\\ &\begin{array}{cc} & \phi^{\mathfrak{p}}\phi^{\mathfrak{q}} \qquad\qquad\qquad\qquad Q_{\mathcal{I}\hat{\mathcal{I}}}\bar{Q}^{\hat{\mathcal{J}}\mathcal{J}} \\ \phi_{\mathfrak{p}'}\phi_{\mathfrak{q}'} & \begin{pmatrix} 2\delta^{\mathfrak{p}}_{\mathfrak{p}'}\delta^{\mathfrak{q}}_{\mathfrak{q}'} + g^{\mathfrak{p}\mathfrak{q}}g_{\mathfrak{p}'\mathfrak{q}'} - 2\delta^{\mathfrak{p}}_{\mathfrak{q}'}\delta^{\mathfrak{q}}_{\mathfrak{p}'} & \delta^{\mathcal{J}}_{\mathcal{I}}\delta^{\hat{\mathcal{J}}}_{\hat{\mathcal{I}}} g_{\mathfrak{p}'\mathfrak{q}'} \\ \delta^{\mathcal{L}}_{\mathcal{K}}\delta^{\hat{\mathcal{L}}}_{\hat{\mathcal{K}}} g^{\mathfrak{p}\mathfrak{q}} & (2\delta^{\mathcal{L}}_{\mathcal{I}}\delta^{\mathcal{J}}_{\mathcal{K}} - \delta^{\mathcal{J}}_{\mathcal{I}}\delta^{\mathcal{L}}_{\mathcal{K}})\delta^{\hat{\mathcal{J}}}_{\hat{\mathcal{I}}}\delta^{\hat{\mathcal{L}}}_{\hat{\mathcal{K}}} + 2\kappa^2\delta^{\mathcal{J}}_{\mathcal{I}}\delta^{\hat{\mathcal{L}}}_{\hat{\mathcal{I}}}\delta^{\mathcal{L}}_{\mathcal{K}}\delta^{\hat{\mathcal{J}}}_{\hat{\mathcal{K}}} \end{pmatrix} \end{array} \\ \oplus &\begin{array}{cc} & \check{\phi}^{\mathfrak{p}}\check{\phi}^{\mathfrak{q}} \qquad\qquad\qquad\qquad \bar{Q}^{\hat{\mathcal{J}}\mathcal{J}}Q_{\mathcal{I}\hat{\mathcal{I}}} \\ \check{\phi}_{\mathfrak{p}'}\check{\phi}_{\mathfrak{q}'} & \begin{pmatrix} \kappa^2(2\delta^{\mathfrak{p}}_{\mathfrak{p}'}\delta^{\mathfrak{q}}_{\mathfrak{q}'} + g^{\mathfrak{p}\mathfrak{q}}g_{\mathfrak{p}'\mathfrak{q}'} - 2\delta^{\mathfrak{p}}_{\mathfrak{q}'}\delta^{\mathfrak{q}}_{\mathfrak{p}'}) & \kappa^2\delta^{\mathcal{J}}_{\mathcal{I}}\delta^{\hat{\mathcal{J}}}_{\hat{\mathcal{I}}} g_{\mathfrak{p}'\mathfrak{q}'} \\ \kappa^2\delta^{\mathcal{L}}_{\mathcal{K}}\delta^{\hat{\mathcal{L}}}_{\hat{\mathcal{K}}} g^{\mathfrak{p}\mathfrak{q}} & \kappa^2(2\delta^{\mathcal{L}}_{\mathcal{I}}\delta^{\mathcal{J}}_{\mathcal{K}} - \delta^{\mathcal{J}}_{\mathcal{I}}\delta^{\mathcal{L}}_{\mathcal{K}})\delta^{\hat{\mathcal{J}}}_{\hat{\mathcal{I}}}\delta^{\hat{\mathcal{L}}}_{\hat{\mathcal{K}}} + 2\delta^{\mathcal{J}}_{\mathcal{I}}\delta^{\hat{\mathcal{L}}}_{\hat{\mathcal{I}}}\delta^{\mathcal{L}}_{\mathcal{K}}\delta^{\hat{\mathcal{J}}}_{\hat{\mathcal{K}}} \end{pmatrix} \end{array} \\ \oplus &\begin{array}{cc} & \phi^{\mathfrak{p}}Q_{\mathcal{I}\hat{\mathcal{I}}} \qquad\qquad Q_{\mathcal{I}\hat{\mathcal{I}}}\check{\phi}^{\mathfrak{p}} \\ \phi_{\mathfrak{p}'}\bar{Q}^{\hat{\mathcal{L}}\mathcal{L}} & \begin{pmatrix} 2\,\delta^{\mathcal{L}}_{\mathcal{I}}\delta^{\hat{\mathcal{L}}}_{\hat{\mathcal{I}}}\delta^{\mathfrak{p}}_{\mathfrak{p}'} & -2\kappa\,\delta^{\mathcal{L}}_{\mathcal{I}}\delta^{\hat{\mathcal{L}}}_{\hat{\mathcal{I}}}\delta^{\mathfrak{p}}_{\mathfrak{p}'} \\ -2\kappa\,\delta^{\mathcal{L}}_{\mathcal{I}}\delta^{\hat{\mathcal{L}}}_{\hat{\mathcal{I}}}\delta^{\mathfrak{p}}_{\mathfrak{p}'} & 2\kappa^2\,\delta^{\mathcal{L}}_{\mathcal{I}}\delta^{\hat{\mathcal{L}}}_{\hat{\mathcal{I}}}\delta^{\mathfrak{p}}_{\mathfrak{p}'} \end{pmatrix} \end{array} \\ \oplus &\begin{array}{cc} & \check{\phi}^{\mathfrak{p}}\bar{Q}^{\hat{\mathcal{J}}\mathcal{J}} \qquad\qquad \bar{Q}^{\hat{\mathcal{J}}\mathcal{J}}\phi^{\mathfrak{p}} \\ \check{\phi}_{\mathfrak{p}'}Q_{\mathcal{K}\hat{\mathcal{K}}} & \begin{pmatrix} 2\kappa^2\,\delta^{\mathcal{J}}_{\mathcal{K}}\delta^{\hat{\mathcal{J}}}_{\hat{\mathcal{K}}}\delta^{\mathfrak{p}}_{\mathfrak{p}'} & -2\kappa\,\delta^{\mathcal{J}}_{\mathcal{K}}\delta^{\hat{\mathcal{J}}}_{\hat{\mathcal{K}}}\delta^{\mathfrak{p}}_{\mathfrak{p}'} \\ -2\kappa\,\delta^{\mathcal{J}}_{\mathcal{K}}\delta^{\hat{\mathcal{J}}}_{\hat{\mathcal{K}}}\delta^{\mathfrak{p}}_{\mathfrak{p}'} & 2\,\delta^{\mathcal{J}}_{\mathcal{K}}\delta^{\hat{\mathcal{J}}}_{\hat{\mathcal{K}}}\delta^{\mathfrak{p}}_{\mathfrak{p}'} \end{pmatrix} \end{array}, \end{aligned} \tag{B.42}$$

[2]Here, we use the basis specified in [18] which is different to the basis we use in Section 2.4.

or, more compactly in terms of the permutation and trace operators (as in [18], we suppress the identity operator),

$$\mathcal{H}_{\ell,\ell+1} =$$

$$\begin{array}{c} \\ \phi\phi \\ \bar{Q}Q \\ \check{\phi}\check{\phi} \\ Q\bar{Q} \\ \phi Q \\ Q\check{\phi} \\ \check{\phi}\bar{Q} \\ \bar{Q}\phi \end{array} \begin{array}{c} \begin{array}{cccccccc} \phi\phi & Q\bar{Q} & \check{\phi}\check{\phi} & \bar{Q}Q & \phi Q & Q\check{\phi} & \check{\phi}\bar{Q} & \bar{Q}\check{\phi} \end{array} \\ \begin{pmatrix} 2+\mathbb{K}-2\mathbb{P} & \mathbb{K} & 0 & 0 & 0 & 0 & 0 & 0 \\ \mathbb{K} & (2-\mathbb{K})\hat{\mathbb{K}}+2\kappa^2\mathbb{K} & 0 & 0 & 0 & 0 & 0 & 0 \\ 0 & 0 & \kappa^2(2+\mathbb{K}-2\mathbb{P}) & \kappa^2\mathbb{K} & 0 & 0 & 0 & 0 \\ 0 & 0 & \kappa^2\mathbb{K} & \kappa^2(2-\mathbb{K})\hat{\mathbb{K}}+2\mathbb{K} & 0 & 0 & 0 & 0 \\ 0 & 0 & 0 & 0 & 2 & -2\kappa & 0 & 0 \\ 0 & 0 & 0 & 0 & -2\kappa & 2\kappa^2 & 0 & 0 \\ 0 & 0 & 0 & 0 & 0 & 0 & 2\kappa^2 & -2\kappa \\ 0 & 0 & 0 & 0 & 0 & 0 & -2\kappa & 2 \end{pmatrix} \end{array}. \tag{B.43}$$

We can, of course, recover our Hamiltonians from equation (B.42) for the XY and XZ sectors used in Section 2.4.

XY Sector

For the XY sector, first note that (see Section 2.4)

$$X = \chi_{+\hat{+}} = \begin{pmatrix} 0 & Q_{+\hat{+}} \\ -\bar{Q}^{\hat{-}-} & 0 \end{pmatrix}, \quad Y = \chi_{+\hat{-}} = \begin{pmatrix} 0 & Q_{+\hat{-}} \\ -\bar{Q}^{\hat{+}-} & 0 \end{pmatrix}, \tag{B.44}$$

and, therefore,

$$X^\dagger = (\chi_{+\hat{+}})^\dagger = -\epsilon^{+-}\epsilon^{\hat{+}\hat{-}}\chi_{-\hat{-}} = -\chi_{-\hat{-}}, \tag{B.45}$$

where

$$\chi_{-\hat{-}} = \begin{pmatrix} 0 & Q_{-\hat{-}} \\ -\bar{Q}^{\hat{+}+} & 0 \end{pmatrix}, \tag{B.46}$$

and

$$Y^\dagger = (\chi_{+\hat{-}})^\dagger = -\epsilon^{+-}\epsilon^{\hat{-}\hat{+}}\chi_{-\hat{+}} = \chi_{-\hat{+}}, \tag{B.47}$$

where

$$\chi_{-\hat{+}} = \begin{pmatrix} 0 & Q_{-\hat{+}} \\ -\bar{Q}^{\hat{-}+} & 0 \end{pmatrix}. \tag{B.48}$$

For $XX \to (XX)^\dagger$, which in matrix form is given by,

$$\begin{pmatrix} -Q_{+\hat{+}}\bar{Q}^{\hat{-}-} & 0 \\ 0 & -\bar{Q}^{\hat{-}-}Q_{+\hat{+}} \end{pmatrix} \to \begin{pmatrix} -\bar{Q}^{\hat{+}+}Q_{-\hat{-}} & 0 \\ 0 & -Q_{-\hat{-}}\bar{Q}^{\hat{+}+} \end{pmatrix} \tag{B.49}$$

and in particular looking at the term $\bar{Q}^{\hat{-}-}Q_{+\hat{+}} \to Q_{-\hat{-}}\bar{Q}^{\hat{+}+}$, we have from equation (B.42)

$$\bar{Q}^{\hat{-}-}Q_{+\hat{+}} \mapsto \left[\kappa^2(2\delta^+_+\delta^-_- - \delta^-_+\delta^+_-)\delta^{\hat{-}}_{\hat{+}}\delta^{\hat{+}}_{\hat{-}} + 2\delta^-_+\delta^{\hat{+}}_{\hat{+}}\delta^+_-\delta^{\hat{-}}_{\hat{-}}\right] Q_{-\hat{-}}\bar{Q}^{\hat{+}+} = 0. \tag{B.50}$$

In a similar manner, $Q_{+\hat{+}}\bar{Q}^{\hat{-}-} \mapsto 0$.

For $XY \to (XY+YX)^\dagger = -\chi_{-\hat{-}}\chi_{-\hat{+}} - \chi_{-\hat{+}}\chi_{-\hat{-}}$, we have in matrix form

$$\begin{pmatrix} Q_{+\hat{+}}\bar{Q}^{\hat{+}-} & 0 \\ 0 & -\bar{Q}^{\hat{-}-}Q_{+\hat{-}} \end{pmatrix} \to -\begin{pmatrix} -\bar{Q}^{\hat{+}+}Q_{-\hat{+}} & 0 \\ 0 & Q_{-\hat{-}}\bar{Q}^{\hat{-}+} \end{pmatrix} - \begin{pmatrix} \bar{Q}^{\hat{-}+}Q_{-\hat{-}} & 0 \\ 0 & -Q_{-\hat{+}}\bar{Q}^{\hat{+}+} \end{pmatrix}. \tag{B.51}$$

Looking, in particular, at the term $\bar{Q}^{\hat{-}-}Q_{+\hat{-}} \to Q_{-\hat{-}}\bar{Q}^{\hat{-}+}$, we find from equation B.42

$$\bar{Q}^{\hat{-}-}Q_{+\hat{-}} \mapsto \left[\kappa^2(2\delta^+_+\delta^-_- - \delta^-_+\delta^+_-)\delta^{\hat{-}}_{\hat{-}}\delta^{\hat{-}}_{\hat{-}} + 2\delta^-_+\delta^{\hat{-}}_{\hat{-}}\delta^+_-\delta^{\hat{-}}_{\hat{-}}\right] Q_{-\hat{-}}\bar{Q}^{\hat{-}+} = 2\kappa^2\, Q_{-\hat{-}}\bar{Q}^{\hat{-}+}. \tag{B.52}$$

Similarly, for $Q_{+\hat{+}}\bar{Q}^{\hat{+}-} \to \bar{Q}^{\hat{+}+}Q_{-\hat{+}}$ we find

$$Q_{+\hat{+}}\bar{Q}^{\hat{+}-} \mapsto \left[(2\delta^+_+\delta^-_- - \delta^-_+\delta^+_-)\delta^{\hat{+}}_{\hat{+}}\delta^{\hat{+}}_{\hat{+}} + 2\kappa^2\delta^-_+\delta^{\hat{+}}_{\hat{+}}\delta^+_-\delta^{\hat{+}}_{\hat{+}}\right]\bar{Q}^{\hat{+}+}Q_{-\hat{+}} = 2\,\bar{Q}^{\hat{+}+}Q_{-\hat{+}}. \tag{B.53}$$

Finally, for $\bar{Q}^{\hat{-}-}Q_{+\hat{-}} \to Q_{-\hat{+}}\bar{Q}^{\hat{+}+}$, we find

$$\bar{Q}^{\hat{-}-}Q_{+\hat{-}} \mapsto -\left[\kappa^2(2\delta^+_+\delta^-_- - \delta^-_+\delta^+_-)\delta^{\hat{-}}_{\hat{-}}\delta^{\hat{+}}_{\hat{+}} + 2\delta^-_+\delta^{\hat{+}}_{\hat{-}}\delta^+_-\delta^{\hat{-}}_{\hat{+}}\right] Q_{-\hat{+}}\bar{Q}^{\hat{+}+} = -2\kappa^2\, Q_{-\hat{+}}\bar{Q}^{\hat{+}+}, \tag{B.54}$$

and for $Q_{+\hat{+}}\bar{Q}^{\hat{+}-} \to \bar{Q}^{\hat{-}+}Q_{-\hat{-}}$, we find

$$Q_{+\hat{+}}\bar{Q}^{\hat{+}-} \mapsto -\left[(2\delta^+_+\delta^-_- - \delta^-_+\delta^+_-)\delta^{\hat{+}}_{\hat{+}}\delta^{\hat{-}}_{\hat{-}} + 2\kappa^2\delta^-_+\delta^{\hat{-}}_{\hat{+}}\delta^+_-\delta^{\hat{+}}_{\hat{-}}\right] \bar{Q}^{\hat{-}+}Q_{-\hat{-}} = -2\,\bar{Q}^{\hat{-}+}Q_{-\hat{-}}. \tag{B.55}$$

A similar computation holds for the case when $YX \to (YX+XY)^\dagger$.

For the case $YY \to (YY)^\dagger$, we find the same results as for the XX case: $YY \mapsto 0$. All other possible terms in equation (B.42) are zero.

We therefore, up to a rescaling of 2κ and ordering of basis, find the XY sector Hamiltonian.

XZ Sector

For the XZ sector, we follow a similar computation. For Z, we have

$$Z = \begin{pmatrix} \phi^- & 0 \\ 0 & \check{\phi}^- \end{pmatrix}, \tag{B.56}$$

and

$$Z^\dagger = \begin{pmatrix} \phi_- & 0 \\ 0 & \check{\phi}_- \end{pmatrix}. \tag{B.57}$$

We consider the term $XZ \to (XZ+ZX)^\dagger = -Z^\dagger \chi_{-\hat{-}} - \chi_{-\hat{-}} Z^\dagger$. In matrix form, this is given by

$$\begin{pmatrix} 0 & Q_{+\hat{+}}\check{\phi}^- \\ -\bar{Q}^{\hat{-}-}\phi^- & 0 \end{pmatrix} \to -\begin{pmatrix} 0 & -\bar{Q}^{\hat{+}+}\check{\phi}_- \\ Q_{-\hat{-}}\phi_- & 0 \end{pmatrix} - \begin{pmatrix} 0 & -\phi_-\bar{Q}^{\hat{+}+} \\ \check{\phi}_- Q_{-\hat{-}} & 0 \end{pmatrix}. \quad \text{(B.58)}$$

For the term $Q_{+\hat{+}}\check{\phi}^- \to \bar{Q}^{\hat{+}+}\check{\phi}_-$, equation (B.42) gives

$$Q_{+\hat{+}}\check{\phi}^- \mapsto 2\kappa^2\ \delta^+_+\delta^{\hat{+}}_{\hat{+}}\delta^-_-\ \ \bar{Q}^{\hat{+}+}\check{\phi}_- = 2\kappa^2\ \ \bar{Q}^{\hat{+}+}\check{\phi}_-, \quad \text{(B.59)}$$

where the δ^-_- comes from the $U(1)_r$ labels $\check{\phi}^- = \check{\phi}$ (see equation (B.6)). Similarly, for the term $Q_{+\hat{+}}\check{\phi}^- \to \phi_-\bar{Q}^{\hat{+}+}$, we find from equation (B.42)

$$Q_{+\hat{+}}\check{\phi}^- \mapsto -2\kappa\ \ \delta^+_+\delta^{\hat{+}}_{\hat{+}}\delta^-_-\ \ \phi_-\bar{Q}^{\hat{+}+} = -2\kappa\ \ \phi^-\bar{Q}^{\hat{+}+}. \quad \text{(B.60)}$$

The other term is similar, with $\bar{Q}^{\hat{-}-}\phi \mapsto 2\, Q_{-\hat{-}}\phi$ and $\bar{Q}^{\hat{-}-}\phi \mapsto -2\kappa\ \check{\phi}Q_{-\hat{-}}$. Furthermore, one finds similar results for the case $ZX \to (ZX+XZ)^\dagger$.

Finally, we consider the term $ZZ \to (ZZ)^\dagger$. These terms are

$$\phi^-\phi^- \mapsto \left[2\delta^-_-\delta^-_- + g^{--}g_{--} - 2\delta^-_-\delta^-_-\right]\phi_-\phi_- = 0, \quad \text{(B.61)}$$

and similarly $\check{\phi}^-\check{\phi}^- \mapsto 0$.

In a similar manner, all remaining terms in equation (B.42) give zero. The resulting Hamiltonian can be written in the compact form

$$\mathcal{H}_{\ell,\ell+1} =$$

$$\begin{array}{c} \\ \phi\phi \\ \bar{Q}Q \\ \check{\phi}\check{\phi} \\ Q\bar{Q} \\ \phi Q \\ Q\check{\phi} \\ \check{\phi}\bar{Q} \\ \bar{Q}\phi \end{array} \begin{array}{c} \begin{array}{cccccccc} \phi\phi & Q\bar{Q} & \check{\phi}\check{\phi} & \bar{Q}Q & \phi Q & Q\check{\phi} & \check{\phi}\bar{Q} & \bar{Q}\check{\phi} \end{array} \\ \begin{pmatrix} 0 & 0 & 0 & 0 & 0 & 0 & 0 & 0 \\ 0 & 0 & 0 & 0 & 0 & 0 & 0 & 0 \\ 0 & 0 & 0 & 0 & 0 & 0 & 0 & 0 \\ 0 & 0 & 0 & 0 & 0 & 0 & 0 & 0 \\ 0 & 0 & 0 & 0 & 2 & -2\kappa & 0 & 0 \\ 0 & 0 & 0 & 0 & -2\kappa & 2\kappa^2 & 0 & 0 \\ 0 & 0 & 0 & 0 & 0 & 0 & 2\kappa^2 & -2\kappa \\ 0 & 0 & 0 & 0 & 0 & 0 & -2\kappa & 2 \end{pmatrix} \end{array}, \quad \text{(B.62)}$$

which is our XZ Hamiltonian, up to a rescaling of 2κ and basis ordering.

Appendix C

DERIVATION OF TWO MAGNON CONTINUUM BOUNDARIES

In this appendix, we derive the two magnon boundaries that define the scattering continua shown in Figure 3.3 in Section 3.2.2. We follow the procedure outlined in [53].

First, we recall the $\cos(2q)$ formula derived in 3.2.2:

$$\cos(2q) = \frac{T_1}{32\kappa^4} \pm \frac{\sqrt{T_2}}{32\kappa^4}, \tag{C.1}$$

where

$$\begin{aligned} T_1 &= -8\kappa^2 \cot(K)\csc(K)\ \Omega^2, \\ T_2 &= 64\kappa^4 \sin^2(K)\ (-4\kappa^4\Omega^2 + \Omega^4 - 4\Omega^2 + 16\kappa^4\sin^2(K)) + 64\kappa^4\Omega^4\cos^2(K). \end{aligned} \tag{C.2}$$

and $\Omega = \kappa E_2 - 2\kappa(\kappa + 1/\kappa)$.

The boundaries and the continua they enclose can be determined by the following constraints [53]

$$\begin{aligned} &\text{Constraint 1:} \quad \cos(2q) = \pm 1, \\ &\text{Constraint 2:} \quad T_2 = 0 \quad \text{and} \quad |\cos(2q)| \leq 1. \end{aligned} \tag{C.3}$$

As discussed in Section 3.2.2, there are two types of solutions for q: the continua solutions where two q's are real-valued and two q's are generically complex-valued (but in certain special regions, can also be real), and the bound state solutions where all four q's are complex-valued. Of course, the boundary is where these two types of solutions are separated; in other words, the boundary is the "saturation" curve at which the four solutions of q, consisting of two real and two complex solutions, is just about to switch over to all complex-valued. This saturation clearly occurs when the first constraint is satisfied (since $|\cos(2q)| > 1 \Rightarrow q \in \mathbb{C}$). The second constraint comes from analysis of the square root since $\sqrt{T_2}$ for $T_2 < 0$ implies a complex-valued q. Thus, the saturation condition is when $T_2 = 0$. However, although this is necessary, this is not sufficient since we can still have the remaining term involving T_1 (in the $\cos(2q)$ formula above) have magnitude greater than 1. Thus, we need the additional condition $|\cos(2q)| \leq 1$ which guarantees sufficiency for constraint 2.

Constraint 1: To derive the curves for constraint 1, we set

$$\frac{T_1}{32\kappa^4} + \gamma\frac{\sqrt{T_2}}{32\kappa^4} = \lambda, \tag{C.4}$$

where $\gamma = \pm 1, \lambda = \pm 1$ keeps track of the signs. By rearranging to get the square root on one side, squaring and then solving for E (upon substituting $\Omega = \kappa E(p_1, p_2) - 2\kappa(\kappa + 1/\kappa)$), we find the following four curves $E_2 = W_i$ given by

$$\begin{aligned}
W_a &= \frac{2\left(\kappa^2 - \sqrt{\kappa^4 + 2\kappa^2\cos(K) + 1} + 1\right)}{\kappa}, \\
W_b &= \frac{2\left(\kappa^2 - \sqrt{\kappa^4 - 2\kappa^2\cos(K) + 1} + 1\right)}{\kappa}, \\
W_c &= \frac{2\left(\kappa^2 + \sqrt{\kappa^4 - 2\kappa^2\cos(K) + 1} + 1\right)}{\kappa}, \\
W_d &= \frac{2\left(\kappa^2 + \sqrt{\kappa^4 + 2\kappa^2\cos(K) + 1} + 1\right)}{\kappa},
\end{aligned} \tag{C.5}$$

which are arranged in increasing value for energy as in [53].

Constraint 2: First, we solve $T_2 = 0$ to get the following four curves $E_2 = Z_i$

$$\begin{aligned}
Z_a &= \frac{2\left(\kappa^2 - \sin(K) + 1\right)}{\kappa}, \\
Z_b &= \frac{2\left(\kappa^2 - \kappa^2\sin(K) + 1\right)}{\kappa}, \\
Z_c &= \frac{2\left(\kappa^2 + \kappa^2\sin(K) + 1\right)}{\kappa}, \\
Z_d &= \frac{2\left(\kappa^2 + \sin(K) + 1\right)}{\kappa},
\end{aligned} \tag{C.6}$$

again arranged in increasing energy. To satisfy the second condition of constraint 2, we substitute these results back into the $\cos(2q)$ formula (of course the square root vanishes) to find four expressions for $\cos(2q)$ corresponding to the four Z's above

$$\begin{aligned}
\cos(2q) &= -\frac{\cos(K)}{\kappa^2}, \quad (\text{from } Z_a), \\
\cos(2q) &= -\frac{\cos(K)}{\kappa^2}, \quad (\text{from } Z_d), \\
\cos(2q) &= -\kappa^2\cos(K), \quad (\text{from } Z_b), \\
\cos(2q) &= -\kappa^2\cos(K), \quad (\text{from } Z_c),
\end{aligned} \tag{C.7}$$

We observe that there are only two equations. For $0 \leq \kappa \leq 1$, we clearly have $|-\kappa^2\cos(K)| \leq 1$ since K is always real-valued. However, for the other equation,

we can see that for $K = 0$ and $\kappa < 1$ we clearly have $|-\cos(K)/\kappa^2| > 1$, thus violating the second condition. However, we can find a critical K_c such that for $K > K_c$, $|-\cos(K)/\kappa^2| \leq 1$. We choose K_c to saturate the inequality for the second condition which we set to -1 (since $\cos(K)$ is positive for $0 \leq K \leq \pi/2$ so that $-\cos(K)$ is negative) and solve to find

$$-\frac{\cos(K_c)}{\kappa^2} = -1 \quad \Rightarrow \quad K_c = \cos^{-1}(\kappa^2). \tag{C.8}$$

To summarize, the curves $Z_b,\ Z_c$ are boundaries for all values of K. The curves $Z_a,\ Z_d$ are boundaries <u>only</u> for $K > K_c$.

As discussed in [53], an interesting observation can also be made about the critical point K_c. Here, we have $W_b = Z_a$ and $W_c = Z_d$. For $K > K_c$, Z_a is a continuum boundary and $Z_a > W_b$ which means that W_b is no longer a boundary as it is inside the continuum. The same situation occurs for W_c and Z_d for $K > K_c$ where W_c is a curve inside the continuum and $Z_d < W_c$ is the boundary. The curves $E = W_b$ and $E = W_c$ are called *internal van Hove singularities*. Crossing these van Hove singularities in the continuum changes the nature of the q's.

In summary, we have [53]

1. AA Lower Boundary: $E = W_a$
2. AA Upper Boundary:
$$E = \begin{cases} W_b, & K < K_c \\ W_b = Z_a, & K = K_c \\ Z_a, & K > K_c \end{cases}$$
3. AO or Mixed-Mode Lower Boundary: $E = Z_b$
4. AO or Mixed-Mode Upper Boundary: $E = Z_c$
5. OO Lower Boundary:
$$E = \begin{cases} W_c, & K < K_c \\ W_c = Z_d, & K = K_c \\ Z_d, & K > K_c \end{cases}$$
6. OO Upper Boundary: $E = W_d$

These curves are plotted in Figure 3.3 and further discussed in Section 3.2.2.

BIBLIOGRAPHY

[1] N. Seiberg and E. Witten. "Electric-magnetic duality, monopole condensation, and confinement in $N = 2$ supersymmetric Yang-Mills theory". In: *Nuclear Physics B* 426.1 (Sept. 1994), pp. 19–52. ISSN: 0550-3213. DOI: 10.1016/0550-3213(94)90124-4. arXiv: hep-th/9407087 [hep-th].

[2] S. Mandelstam. "Light-cone superspace and the ultraviolet finiteness of the N=4 model". In: *Nuclear Physics B* 213.1 (1983), pp. 149–168. ISSN: 0550-3213. DOI: 10.1016/0550-3213(83)90179-7.

[3] L. Brink, O. Lindgren, and B.E.W. Nilsson. "The ultra-violet finiteness of the $N = 4$ Yang-Mills theory". In: *Physics Letters B* 123.5 (1983), pp. 323–328. ISSN: 0370-2693. DOI: https://doi.org/10.1016/0370-2693(83)91210-8.

[4] J. Maldacena. "The Large-N Limit of Superconformal Field Theories and Supergravity". In: *International Journal of Theoretical Physics* 38 (Jan. 1999), pp. 1113–1133. DOI: 10.1023/A:1026654312961. arXiv: hep-th/9711200 [hep-th].

[5] J.A. Minahan and K. Zarembo. "The Bethe-ansatz for $\mathcal{N} = 4$ super Yang-Mills". In: *Journal of High Energy Physics* 2003.03 (Mar. 2003), pp. 013–013. ISSN: 1029-8479. DOI: 10.1088/1126-6708/2003/03/013. arXiv: hep-th/0212208.

[6] N. Beisert. "The complete one-loop dilatation operator of $N = 4$ super-Yang–Mills theory". In: *Nuclear Physics B* 676.1-2 (Jan. 2004), pp. 3–42. ISSN: 0550-3213. DOI: 10.1016/j.nuclphysb.2003.10.019. arXiv: hep-th/0307015 [hep-th].

[7] N. Beisert et al. "Review of AdS/CFT Integrability: An Overview". In: *Letters in Mathematical Physics* 99.1-3 (Oct. 2011), pp. 3–32. ISSN: 1573-0530. DOI: 10.1007/s11005-011-0529-2. arXiv: 1012.3982 [hep-th].

[8] N. Beisert. "The analytic Bethe ansatz for a chain with centrally extended $\mathfrak{su}(2|2)$ symmetry". In: *Journal of Statistical Mechanics: Theory and Experiment* 2007.01 (Jan. 2007), P01017–P01017. ISSN: 1742-5468. DOI: 10.1088/1742-5468/2007/01/p01017. arXiv: nlin/0610017 [nlin.SI].

[9] G. Arutyunov and S. Frolov. "On string S-matrix, bound states and TBA". In: *Journal of High Energy Physics* 2007.12 (Dec. 2007), pp. 024–024. ISSN: 1029-8479. DOI: 10.1088/1126-6708/2007/12/024. arXiv: 0710.1568 [hep-th].

[10] G. Arutyunov, S. Frolov, and M. Zamaklar. "The Zamolodchikov–Faddeev Algebra for $AdS_5 \times S^5$superstring". In: *Journal of High Energy Physics*

2007.04 (Apr. 2007), pp. 002–002. ISSN: 1029-8479. DOI: 10.1088/1126-6708/2007/04/002. arXiv: hep-th/0612229 [hep-th].

[11] G. Arutyunov and S. Frolov. "Foundations of the AdS_5S^5 superstring: I". In: *Journal of Physics A: Mathematical and Theoretical* 42.25 (June 2009), p. 254003. ISSN: 1751-8121. DOI: 10.1088/1751-8113/42/25/254003. arXiv: 0901.4937 [hep-th].

[12] M.R. Douglas and G.W. Moore. "D-branes, quivers, and ALE instantons". In: (Mar. 1996). arXiv: hep-th/9603167.

[13] A. Solovyov. "Bethe ansatz equations for general orbifolds of $\mathcal{N} = 4$ SYM". In: *Journal of High Energy Physics* 2008.04 (Apr. 2008), pp. 013–013. ISSN: 1029-8479. DOI: 10.1088/1126-6708/2008/04/013. arXiv: 0711.1697 [hep-th].

[14] N. Beisert and R. Roiban. "The Bethe ansatz for $\mathbb{Z}_S$ orbifolds of $\mathcal{N} = 4$ super Yang-Mills theory". In: *Journal of High Energy Physics* 2005.11 (Nov. 2005), pp. 037–037. ISSN: 1029-8479. DOI: 10.1088/1126-6708/2005/11/037. arXiv: hep-th/0510209 [hep-th].

[15] S. Kachru and E. Silverstein. "4D Conformal Field Theories and Strings on Orbifolds". In: *Physical Review Letters* 80.22 (June 1998), pp. 4855–4858. ISSN: 1079-7114. DOI: 10.1103/physrevlett.80.4855. arXiv: hep-th/9802183 [hep-th].

[16] L. Dixon et al. "Strings on orbifolds". In: *Nuclear Physics B* 261 (1985), pp. 678–686. ISSN: 0550-3213. DOI: 10.1016/0550-3213(85)90593-0.

[17] K. Ideguchi. "Semiclassical Strings on $AdS(5) \times S(5)/Z(M)$ and Operators in Orbifold Field Theories". In: *Journal of High Energy Physics* 2004.09 (Sept. 2004), pp. 008–008. ISSN: 1029-8479. DOI: 10.1088/1126-6708/2004/09/008. arXiv: hep-th/0408014 [hep-th].

[18] A. Gadde, E. Pomoni, and L. Rastelli. "Spin chains in $\mathcal{N} = 2$ superconformal theories: from the $\mathbb{Z}_2$ quiver to superconformal QCD". en. In: *Journal of High Energy Physics* 2012.6 (June 2012), p. 107. ISSN: 1029-8479. DOI: 10.1007/JHEP06(2012)107. arXiv: 1006.0015 [hep-th].

[19] P. Liendo, E. Pomoni, and L. Rastelli. "The complete one-loop dilation operator of $\mathcal{N} = 2$ SuperConformal QCD". In: *Journal of High Energy Physics* 2012.7 (July 2012). ISSN: 1029-8479. DOI: 10.1007/jhep07(2012)003. arXiv: 1105.3972 [hep-th].

[20] J.S. Caux and J. Mossel. "Remarks on the notion of quantum integrability". In: *Journal of Statistical Mechanics: Theory and Experiment* 2011.02 (Feb. 2011), P02023. ISSN: 1742-5468. DOI: 10.1088/1742-5468/2011/02/p02023. arXiv: 1012.3587 [cond-mat.str-el].

[21] T. Månsson and K. Zoubos. "Quantum symmetries and marginal deformations". In: *Journal of High Energy Physics* 2010.10 (Oct. 2010). ISSN: 1029-8479. DOI: 10.1007/jhep10(2010)043. arXiv: 0811.3755 [hep-th].

[22] H. Dlamini and K. Zoubos. *Integrable Hopf twists, marginal deformations and generalised geometry*. 2016. arXiv: 1602.08061 [hep-th].

[23] H. Dlamini and K. Zoubos. "Marginal deformations and quasi-Hopf algebras". In: *Journal of Physics A: Mathematical and Theoretical* 52.37 (Aug. 2019), p. 375402. ISSN: 1751-8121. DOI: 10.1088/1751-8121/ab370f. arXiv: 1902.08166 [hep-th].

[24] G. Felder and A. Varchenko. "On representations of the elliptic quantum group $E_{\tau,\eta}(sl_2)$". In: *Communications in Mathematical Physics* 181.3 (Dec. 1996), pp. 741–761. ISSN: 1432-0916. DOI: 10.1007/bf02101296. arXiv: q-alg/9601003 [math.QA].

[25] T. Deguchi. "Construction of some missing eigenvectors of the XYZ spin chain at the discrete coupling constants and the exponentially large spectral degeneracy of the transfer matrix". In: *Journal of Physics A: Mathematical and General* 35.4 (Jan. 2002), pp. 879–895. ISSN: 1361-6447. DOI: 10.1088/0305-4470/35/4/303. arXiv: cond-mat/0109078 [cond-mat.stat-mech].

[26] E. Pomoni. "Integrability in $N = 2$ superconformal gauge theories". In: *Nuclear Physics B* 893 (Apr. 2015), pp. 21–53. ISSN: 0550-3213. DOI: 10.1016/j.nuclphysb.2015.01.006. arXiv: 1310.5709 [hep-th].

[27] E. Pomoni, R. Rabe, and K. Zoubos. "Dynamical spin chains in 4D $\mathcal{N} = 2$ SCFTs". In: *Journal of High Energy Physics* 2021.8 (Aug. 2021), p. 127. ISSN: 1029-8479. DOI: 10.1007/JHEP08(2021)127. arXiv: 2106.08449 [hep-th].

[28] E. Pomoni. *4D $\mathcal{N} = 2$ SCFTs and spin chains*. 2019. arXiv: 1912.00870 [hep-th].

[29] D. Gaiotto. "$N = 2$ dualities". In: *Journal of High Energy Physics* 2012.8 (Aug. 2012). ISSN: 1029-8479. DOI: 10.1007/jhep08(2012)034. arXiv: 0904.2715 [hep-th].

[30] D. Gaiotto. *Families of N=2 field theories*. 2014. arXiv: 1412.7118 [hep-th].

[31] P.C. Argyres and M.R. Douglas. "New phenomena in $SU(3)$ supersymmetric gauge theory". In: *Nuclear Physics B* 448.1-2 (Aug. 1995), pp. 93–126. ISSN: 0550-3213. DOI: 10.1016/0550-3213(95)00281-v. arXiv: hep-th/9505062 [hep-th].

[32] H. Bethe. "Zur Theorie der Metalle: I. Eigenwerte und Eigenfunktionen der linearen Atomkette". de. In: *Zeitschrift fur Physik* 71.3-4 (Mar. 1931), pp. 205–226. ISSN: 1434-6001, 1434-601X. DOI: 10.1007/BF01341708.

[33] F.A. Dolan and H. Osborn. "On short and semi-short representations for four-dimensional superconformal symmetry". In: *Annals of Physics* 307.1 (Sept. 2003), pp. 41–89. ISSN: 0003-4916. DOI: 10.1016/s0003-4916(03)00074-5. arXiv: hep-th/0209056 [hep-th].

[34] L. Eberhardt. *Superconformal symmetry and representations*. 2020. arXiv: 2006.13280 [hep-th].

[35] M. Ammon and J. Erdmenger. *Gauge/Gravity Duality: Foundations and Applications*. Cambridge University Press, 2015. DOI: 10.1017/CBO9780511846373.

[36] N. Beisert. "Review of AdS/CFT Integrability, Chapter VI.1: Superconformal Symmetry". In: *Letters in Mathematical Physics* 99.1-3 (May 2011), pp. 529–545. ISSN: 1573-0530. DOI: 10.1007/s11005-011-0479-8. arXiv: 1012.4004 [hep-th].

[37] J. Lamers. "A pedagogical introduction to quantum integrability, with a view towards theoretical high-energy physics". In: *Proceedings of 10th Modave Summer School in Mathematical Physics — PoS(Modave2014)* (Feb. 2015). DOI: 10.22323/1.232.0001. arXiv: 1501.06805 [math-ph].

[38] J. Fuchs and C. Schweigert. *Symmetries, Lie algebras and representations: A graduate course for physicists*. Cambridge University Press, Oct. 2003. ISBN: 978-0-521-54119-0.

[39] H.M. Babujian. "Exact solution of the one-dimensional isotropic Heisenberg chain with arbitrary spins S". In: *Physics Letters A* 90.9 (1982), pp. 479–482. ISSN: 0375-9601. DOI: 10.1016/0375-9601(82)90403-0.

[40] C. Gómez, M. Ruiz-Altaba, and G. Sierra. *Quantum Groups in Two-Dimensional Physics*. Cambridge Monographs on Mathematical Physics. Cambridge University Press, 1996. DOI: 10.1017/CBO9780511628825.

[41] M. Karabach and G. Müller. "Introduction to the Bethe Ansatz I". In: *Comput. Phys.* 11.1 (Jan. 1997), pp. 36–43. ISSN: 0894-1866. DOI: 10.1063/1.4822511.

[42] M. Staudacher. "Review of AdS/CFT Integrability, Chapter III.1: Bethe Ansätze and the R-Matrix Formalism". In: *Letters in Mathematical Physics* 99.1-3 (Sept. 2011), pp. 191–208. ISSN: 1573-0530. DOI: 10.1007/s11005-011-0530-9. arXiv: 1012.3990 [hep-th].

[43] J.A. Minahan. "Review of AdS/CFT Integrability, Chapter I.1: Spin Chains in $\mathcal{N} = 4$ Super Yang-Mills". In: *Letters in Mathematical Physics* 99.1-3 (Aug. 2011), pp. 33–58. ISSN: 1573-0530. DOI: 10.1007/s11005-011-0522-9. arXiv: 1012.3983 [hep-th].

[44] R.I. Nepomechie. "A spin chain primer". In: *International Journal of Modern Physics B* 13.24n25 (Oct. 1999), pp. 2973–2985. ISSN: 1793-6578. DOI: 10.1142/s0217979299002800. arXiv: hep-th/9810032 [hep-th].

[45] H. B. Thacker. "Continuous space-time symmetries in a lattice field theory". In: *arXiv e-prints*, hep-lat/9809141 (Sept. 1998), hep–lat/9809141. arXiv: hep-lat/9809141 [hep-lat].

[46] B. Sutherland. *Beautiful Models*. World Scientific, 2004. DOI: 10.1142/5552. eprint: https://www.worldscientific.com/doi/pdf/10.1142/5552.

[47] P.N. Bibikov. "Three magnons in an isotropic $S = 1$ ferromagnetic chain as an exactly solvable non-integrable system". In: *Journal of Statistical Mechanics: Theory and Experiment* 2016.3 (Mar. 2016), p. 033109. DOI: 10.1088/1742-5468/2016/03/033109. arXiv: 1506.01554 [cond-mat.str-el].

[48] A. Lamacraft. "Diffractive scattering of three particles in one dimension: A simple result for weak violations of the Yang-Baxter equation". In: *Physical Review A* 87.1 (Jan. 2013). ISSN: 1094-1622. DOI: 10.1103/physreva.87.012707. arXiv: 1211.4110 [cond-mat.quant-gas].

[49] M.P. Grabowski and P. Mathieu. "Quantum integrals of motion for the Heisenberg spin chain". In: *Modern Physics Letters A* 09.24 (Aug. 1994), pp. 2197–2206. ISSN: 1793-6632. DOI: 10.1142/s0217732394002057. arXiv: hep-th/9403149 [hep-th].

[50] S. T. Chiu-Tsao, P.M. Levy, and C. Paulson. "Elementary excitations of high-degree pair interactions: The two-spin—deviation spectra for a spin-1 ferromagnet". In: *Phys. Rev. B* 12 (5 Sept. 1975), pp. 1819–1838. DOI: 10.1103/PhysRevB.12.1819.

[51] A. J. M. Medved, B. W. Southern, and D. A. Lavis. "Two-magnon states of the alternating-bond ferrimagnetic chain". In: *Phys. Rev. B* 43 (1 Jan. 1991), pp. 816–824. DOI: 10.1103/PhysRevB.43.816.

[52] S. C. Bell et al. "Two-magnon states of the alternating ferromagnetic Heisenberg chain". In: *J Phys.: Condens. Matter* (1 1989).

[53] A.J.M. Medved. "Two-magnon states of alternating ferrimagnetic chains". en. In: (1990). URL: https://mspace.lib.umanitoba.ca/xmlui/handle/1993/17219.

[54] J.L. Martinez Cuellar. "Three magnon excitations in alternating quantum spin/bond chains". en_US. In: (June 1997). URL: https://mspace.lib.umanitoba.ca/xmlui/handle/1993/1039 (visited on 05/20/2021).

[55] S. Giombi. *TASI Lectures on the Higher Spin - CFT duality*. 2016. arXiv: 1607.02967 [hep-th].

[56] P. Di Francesco, P. Mathieu, and D. Sénéchal. *Conformal Field Theory*. Graduate texts in contemporary physics. Island Press, 1996. ISBN: 9781461222576.

[57] G. 't Hooft. "A planar diagram theory for strong interactions". In: *Nuclear Physics B* 72.3 (1974), pp. 461–473. ISSN: 0550-3213. DOI: 10.1016/0550-3213(74)90154-0.

[58] H. Năstase. *Introduction to the AdS/CFT Correspondence*. Cambridge University Press, 2015. DOI: 10.1017/CBO9781316090954.

[59] J. Plefka. "Spinning Strings and Integrable Spin Chains in the AdS/CFT Correspondence". In: *Living Reviews in Relativity* 8.1 (Nov. 2005). ISSN: 1433-8351. DOI: 10.12942/lrr-2005-9. arXiv: hep-th/0507136 [hep-th].

[60] D. Serban. "Integrability and the AdS/CFT correspondence". In: *Journal of Physics A Mathematical General* 44.12, 124001 (Mar. 2011), p. 124001. DOI: 10.1088/1751-8113/44/12/124001. arXiv: 1003.4214 [hep-th].

[61] A. Gadde, E. Pomoni, and L. Rastelli. *The Veneziano Limit of $N = 2$ Superconformal QCD: Towards the String Dual of $N = 2SU(N_c)$ SYM with $N_f = 2N_c$*. 2009. arXiv: 0912.4918 [hep-th].

[62] T.J. Hollowood and V.V. Khoze. "ADHM and D-instantons in orbifold AdS/CFT duality". In: *Nuclear Physics B* 575.1-2 (May 2000), pp. 78–106. ISSN: 0550-3213. DOI: 10.1016/s0550-3213(00)00086-9. arXiv: hep-th/9908035 [hep-th].

[63] N. Dorey et al. "Multi-instanton calculus and the AdS/CFT correspondence in superconformal field theory". In: *Nuclear Physics B* 552.1-2 (July 1999), pp. 88–168. ISSN: 0550-3213. DOI: 10.1016/s0550-3213(99)00193-5. arXiv: hep-th/9901128 [hep-th].

[64] R. Roiban. "On spin chains and field theories". In: *Journal of High Energy Physics* 2004.09 (Sept. 2004), pp. 023–023. ISSN: 1029-8479. DOI: 10.1088/1126-6708/2004/09/023. arXiv: hep-th/0312218 [hep-th].

[65] J. Sirker et al. "Thermally Activated Peierls Dimerization in Ferromagnetic Spin Chains". In: *Phys. Rev. Lett.* 101 (15 Oct. 2008), p. 157204. DOI: 10.1103/PhysRevLett.101.157204. arXiv: 0807.4693 [cond-mat.str-el].

[66] R. Feyerherm, C. Mathonière, and O. Kahn. "Magnetic anisotropy and metamagnetic behaviour of the bimetallic chain $MnNi(NO_2)_4(en)_2$ (en = ethylenediamine)". In: *Journal of Physics: Condensed Matter* 13.11 (Mar. 2001), pp. 2639–2650. DOI: 10.1088/0953-8984/13/11/319.

[67] B.W. Southern, R.J. Lee, and D.A. Lavis. "Three-magnon excitations in ferromagnetic spin-S chains". In: *Journal of Physics: Condensed Matter* 6.46 (Nov. 1994), pp. 10075–10092. DOI: 10.1088/0953-8984/6/46/024.

[68] B. W. Southern, J. L. Martınez Cuéllar, and D. A. Lavis. "Multimagnon excitations in alternating spin/bond chains". In: *Phys. Rev. B* 58 (14 Oct. 1998), pp. 9156–9165. DOI: 10.1103/PhysRevB.58.9156.

[69] V. S Viswanath and G. Müller. *The Recursion Method: Application to Many-Body Dynamics*. English. OCLC: 851841734. Berlin, Heidelberg: Springer Berlin Heidelberg, 1994. ISBN: 9783540583196 9783540486510.

[70] G. Huang et al. “Soliton excitations in the alternating ferromagnetic Heisenberg chain”. In: *Phys. Rev. B* 43 (13 May 1991), pp. 11197–11206. DOI: 10.1103/PhysRevB.43.11197.

[71] X.J. Wang and Y.S. Wu. “Integrable spin chain and operator mixing in $\mathcal{N} = 1, 2$ supersymmetric theories”. In: *Nuclear Physics B* 683.3 (Apr. 2004), pp. 363–386. ISSN: 0550-3213. DOI: 10.1016/j.nuclphysb.2003.12.040. arXiv: hep-th/0311073 [hep-th].

[72] V.I. Kukulin, V.M. Krasnopol’sky, and Horáček. J. *Theory of Resonances: Principles and Applications*. English. OCLC: 958542068. Dordrecht: Springer Netherlands, 2010. ISBN: 9789401578172.

[73] N. Moiseyev. *Non-Hermitian quantum mechanics*. English. OCLC: 1105412045. Cambridge; New York: Cambridge University Press, 2011. ISBN: 9780511993152 9780511976186.

[74] R. J. Baxter. *Exactly solved models in statistical mechanics*. 1982. ISBN: 978-0-486-46271-4.

[75] N. Beisert et al. “Integrable deformations of the XXZ spin chain”. In: *Journal of Statistical Mechanics: Theory and Experiment* 2013.09 (Sept. 2013), P09028. ISSN: 1742-5468. DOI: 10.1088/1742-5468/2013/09/p09028. arXiv: 1308.1584 [math-ph].

[76] M. Abramowitz and I.A. Stegun, eds. *Handbook of Mathematical Functions with Formulas, Graphs, and Mathematical Tables*. National Bureau of Standards Applied Mathematics Series 55. U.S. Government Printing Office, Washington, D.C., 1964, pp. xiv+1046.

[77] I. Kostov, D. Serban, and D. Volin. “Strong coupling limit of Bethe ansatz equations”. In: *Nuclear Physics B* 789.3 (Feb. 2008), pp. 413–451. ISSN: 0550-3213. DOI: 10.1016/j.nuclphysb.2007.06.017. arXiv: hep-th/0703031 [hep-th].

[78] S. Kharchev and A. Zabrodin. “Theta vocabulary I”. In: *Journal of Geometry and Physics* 94 (2015), pp. 19–31. ISSN: 0393-0440. DOI: https://doi.org/10.1016/j.geomphys.2015.03.010. arXiv: 1502.04603 [math.CA].

[79] C.W. Hsu et al. “Bound states in the continuum”. en. In: *Nature Reviews Materials* 1.9 (July 2016), pp. 1–13. ISSN: 2058-8437. DOI: 10.1038/natrevmats.2016.48.

[80] J.M. Zhang, D. Braak, and M. Kollar. “Bound States in the Continuum Realized in the One-Dimensional Two-Particle Hubbard Model with an Impurity”. In: *Physical Review Letters* 109.11 (Sept. 2012). ISSN: 1079-7114. DOI: 10.1103/physrevlett.109.116405. arXiv: 1205.6431 [cond-mat.dis-nn].

[81] J.M. Zhang, D. Braak, and M. Kollar. "Bound states in the one-dimensional two-particle Hubbard model with an impurity". In: *Physical Review A* 87.2 (Feb. 2013). ISSN: 1094-1622. DOI: 10.1103/physreva.87.023613. arXiv: 1210.6767 [cond-mat.quant-gas].

[82] D. Braak, J.M. Zhang, and M. Kollar. "Integrability and weak diffraction in a two-particle Bose–Hubbard model". In: *Journal of Physics A: Mathematical and Theoretical* 47.46 (Nov. 2014), p. 465303. ISSN: 1751-8121. DOI: 10.1088/1751-8113/47/46/465303. arXiv: 1403.6875 [quant-ph].

[83] S. Longhi and G. Della Valle. "Tamm–Hubbard surface states in the continuum". In: *Journal of Physics: Condensed Matter* 25.23 (May 2013), p. 235601. ISSN: 1361-648X. DOI: 10.1088/0953-8984/25/23/235601. arXiv: 1306.0658 [cond-mat.str-el].

[84] M. De Leeuw, A. Pribytok, and P. Ryan. "Classifying two-dimensional integrable spin chains". In: *J. Phys. A* 52.50 (2019), p. 505201. DOI: 10.1088/1751-8121/ab529f. arXiv: 1904.12005 [math-ph].

[85] M. de Leeuw et al. "Yang-Baxter and the Boost: splitting the difference". In: *SciPost Physics* 11.3 (Sept. 2021). ISSN: 2542-4653. DOI: 10.21468/scipostphys.11.3.069. arXiv: 2010.11231 [math-ph].

[86] T. Gombor and B. Pozsgay. "Integrable spin chains and cellular automata with medium-range interaction". In: *Phys. Rev. E* 104.5 (2021), p. 054123. DOI: 10.1103/PhysRevE.104.054123. arXiv: 2108.02053 [nlin.SI].

[87] K. Zoubos. "Review of AdS/CFT Integrability, Chapter IV.2: Deformations, Orbifolds and Open Boundaries". In: *Letters in Mathematical Physics* 99.1-3 (July 2011), pp. 375–400. ISSN: 1573-0530. DOI: 10.1007/s11005-011-0515-8. arXiv: 1012.3998 [hep-th].

[88] S. Krippendorf, F. Quevedo, and O. Schlotterer. *Cambridge Lectures on Supersymmetry and Extra Dimensions*. 2010. arXiv: 1011.1491 [hep-th].

[89] M. Bianchi. "(Non-)perturbative tests of the AdS/CFT correspondence". In: *Nuclear Physics B - Proceedings Supplements* 102-103 (Sept. 2001), pp. 56–64. ISSN: 0920-5632. DOI: 10.1016/s0920-5632(01)01536-5. arXiv: hep-th/0103112 [hep-th].